Shell Organic Matrices in some Pearl Oysters and other Bivalves.

Thesis submitted by

Barry James Aquinas Vance BSc (Vet.) (Hons.Physiology) U.of Qld.

for the degree of Doctor of Philosophy in
the Department of Marine Biology at
James Cook University of North Queensland
December 1994.

I, the undersigned, the author of this thesis, understand that James Cook University of North Queensland will make it available for use within the University Library and, by microfilm or other photographic means, allow access to users in other approved libraries. All users consulting this thesis will have to sign the following statement:

"In consulting this thesis I agree not to copy or closely paraphrase it in whole or in part without the written consent of the author; and to make proper written acknowledgement for any assistance which I have obtained from it."

Beyond this, I do not wish to place any restriction on access to this thesis.

26-11-1996

ACKNOWLEDGEMENTS

I wish to thank the Head of Department of Marine Biology, Professor J.H. Choat, for his efficient and dependable assistance and my supervisor Associate Professor C.G. Alexander for giving of his already overcommitted time and personal resources.

I am indebted to the entire staff of the Department of Marine Biology for assistance throughout this project. I should especially acknowledge the many hours spent by Dr. John Collins in converting a physiologist to a malacologist. My debt to him is of such an order as to almost warrant the statement that any mistakes are his responsibility - not mine.

The same level of thanks are due Ms. Heather Windsor for her unfailing helpfullness in teaching electron microscopy. To refer to her efforts as "discussions" and "assistance" is to misuse the language.

Numerous others supplied specimens or helped with my teaching.

Every request made to any person engaged in the pearling industry whether for specimens, accomodation, or use of boat or pearl farm facilities was graciously complied with.

I gratefully thank those from the industry in Queensland and the Torres Strait who have gone to considerable trouble on my behalf over the duration of the project.

More recently, the executive officer of the Australian Pearl

Producers Association Mr. M. Buckley and a number of members of that association in Western Australia and the Northern Territory have helped with proffered knowledge and advice and in other practical ways. Please accept my gratitude.

Many thanks to Ms. C. Gillman for typing this manuscript.

All the members of my family know more than they ever needed to about pearl oysters.

ABSTRACT

Pearl Oysters of twenty species belonging to four genera of the superfamily Pteriacea, and thirty eight other species of bivalves of thirty-one genera belonging to sixteen superfamilies have been examined to investigate the relationship between particular shell structures and the tissues which secrete the precursors of their organic matrices.

A strictly descriptive nomenclature to adequately describe the parts of the mantles, mantle margins, and shells of pearl oysters is suggested based on morphology and histology.

Inadequacy of taxonomy of the Australian pearl oysters has been revealed by this study. Shell ultrastructure and histology of the mantle and mantle margins are used to increase the number of species of the genus *Pinctada*.

A large number of the tissues and glands thought to be involved in the secretion of the precursors of the organic matrices of the different shell layers in the animals studied are described, and where known, the roles of their secretions discussed. In particular a detailed light and electron microcopic study of some pearl oysters from Australian waters is presented and forming organic matrices of their nacreous and prismatic layers are described and illustrated. The possible roles played by the pallial blood sinus and the rami of the circum-pallial nerve in pearl oyster shell production are discussed.

TABLE OF CONTENTS

INDEX TO FIGURES

CHAPTER 2.

CHAPTER 3.

CHAPTER 4.

CHAPTER 5.

DECLARATION

I declare that this thesis is my own work and has not been submitted in any form for another degree or diploma at any university or other institution of tertiary education. Information derived from the published or unpublished work of others is acknowledged in the text and a list of references is given.

26-11-1996
....

CHAPTER 1. - INTRODUCTION

CHAPTER 1. - CONTENTS.

Note. A capital will be used for the initial letter of all formal nomenclature. (for reasons, see page 38).

1.1.INITIAL AIM.

The initial aim of this project was to study growth and the control of growth in pearl oysters, their shells and cultured pearls.

1.2. THE BIVALVE SHELL

The bivalve shell is composed of a protein rubber Hinge (Shadwick and Gosline, 1983), joining two valves, each having one or more Shell Layers (Taylor, 1973).

Saleuddin and Petit (1983) state the "molluscan shell is covered externally by a thin, pliable, fibrous layer called the periostracum".

This outer Shell Layer or "periostracum" is allegedly produced by the Mantle Margin and reflected through nearly one hundred and eighty degrees and hence comes to lie, with what was its medial surface now lateral, on the outer surface of the shell (Stasek and McWilliams, (1973), Wilbur and Saleuddin, (1983), Saleuddin and Petit, (1983), Waite, (1983)). Thus produced, the outer shell layer necessarily covers the entire outer surface of the bivalve shell unless abraded or eroded or otherwise lost.

The inner Shell Layer of bivalve shells of more than one Shell Layer may be coextensive with the outer Shell Layer, or may terminate proximal to the shell periphery (Wilbur and Saleuddin 1983).

In a shell with more than two Shell Layers, the middle Shell Layer or Layers necessarily has or have a periphery somewhere between coextensive with the outer Shell Layer and coextensive with the inner Shell Layer, (Wilbur and Saleuddin 1983).

The Shell Layers inside the alleged periostracum of a multi-layered shell are said to be "composed of organic materials and calcium carbonate crystals occurring mostly as calcite or aragonite", (Watabe, 1984).

While the system of classification of these calcified Shell Layers varies slightly from author to author, the classification used in this work is that of Taylor, (1973). He used nine names to describe the calcareous Shell Layers of twenty six superfamilies of the Class Bivalvia.

Taylor, (1973) described a primitive ancestral bivalve shell type exemplified by the shells of several extant superfamilies including the Unionoidea. This primitive shell type has three calcareous Shell Layers - an outer simple aragonitic Prismatic Layer outside an Outer Nacreous Layer and an Inner Nacreous Layer (Figure 1.1.).

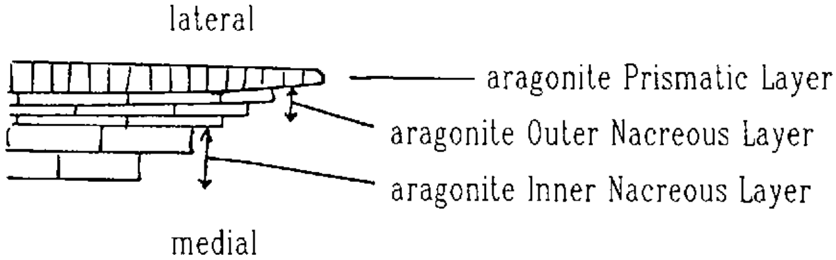

Figure 1.1. Shell Layers in Unionoidea.

According to Taylor, (1973), every known bivalve, whether extant or from the fossil record, has a shell which has "evolved" from this primitive type by the loss of, or alteration of, one or more of these three Shell Layers.

The bivalve used in this work as an example of Taylor's primitive shell type is *Velesunio ambiguus*, Iredale, 1934.

Taylor (1973) lists seven evolutionary trends away from the ancestral shell condition. All the superfamilies to which the species used in this investigation belong, apart from Unionoidea, are on Taylor's evolutionary trends 1, 5, 6, and 7.

Only trend 1 need be considered immediately. Trends 5, 6 and 7 will be given later in this Chapter. Taylor's work is fundamentally important to the present investigation and it will be reviewed at length in Chapter 6.

ANOMIOIDEA and PECTINOIDEA
(Lost Outer Shell Layer).

Foliated Structure (calcite).
Crossed Lamellar Structure

OSTREOIDEA
Simple Calcitic Prismatic Layer
Foliated Structure (calcite).
(Lost Inner Shell Layer).

MYTILOIDEA.
Mytilid Prismatic Layer
(or non-calcareous Layer)
Outer Nacreous Layer (aragonite).
Inner Nacreous Layer (aragonite).

PROPEAMUSSIUM
Outer Calcitic Prismatic Layer.

Foliated Structure (calcite).
Crossed Lamellar Structure.

PTERIOIDEA (pearl Oysters) and PINNOIDEA.
Simple Calcitic Prismatic Layer (calcite).
Outer Nacreous Layer (aragonite).
Inner Nacreous Layer (aragonite).

UNIONOIDEA
(Trilaminate Non-calcareous Layer)
Simple Aragonitic Prismatic Layer
(aragonite).
Outer Nacreous Layer (aragonite).
Inner Nacreous Layer (aragonite).

Figure 1.2. Taylor's (1973) trend 1. Taylor's diagram excludes the non-calcareous outer Shell Layers shown here.

According to Taylor, (1973) pearl oyster shells derive from the primitive condition by the alteration of the outer calcareous Shell Layer from aragonite to calcite Simple Prisms. The two medial Shell Layers, Outer Nacreous Layer and

Inner Nacreous Layer, remain the same from Unionoidea through Pterioidea and Pinnoidea to the Mytiloidea.

Taylor's (1973) trend 1, (Figure 1.2.) illustrates the development by alteration and loss of the three Shell Layers of the primitive Unionacean shell. Only the outer Shell Layer is altered to give the Shell Layer array of the Pterioidea and Pinnoidea, and through them it alters again to give that of the Mytilacea. On a side branch by way of a *Propeamussium* like shell, the Shell Layers of the Anomioidea and Pectinoidea develop by loss of the outer calcareous Shell Layer and alteration of the two inner calcareous Shell Layers. Conversely, according to Taylor (1973), the ostreacean shell type develops by loss of the inner Shell Layer and alteration of the middle Shell Layer from that seen in the Pterioidea (and Unionoidea).

1.3. THE PEARL SHELL.

The pearl oysters, being members of the Superfamily Pterioidea, are said to have shells composed of an external calcitic Prismatic Layer outside an Outer Nacreous Layer and, medial to this, an Inner Nacreous Layer, (Taylor, 1973). As above, according to this, the only alteration from the primitive condition of the bivalve shell to that of the pearl oysters is the development of an outer calcitic Prismatic Layer in place of an outer aragonitic Prismatic Layer. Taylor disregards the "periostracum" or any other outer fibrous layer in his publication "The structural evolution of the Bivalve shell" - a matter of great significance in this study, (Taylor, 1973).

lateral

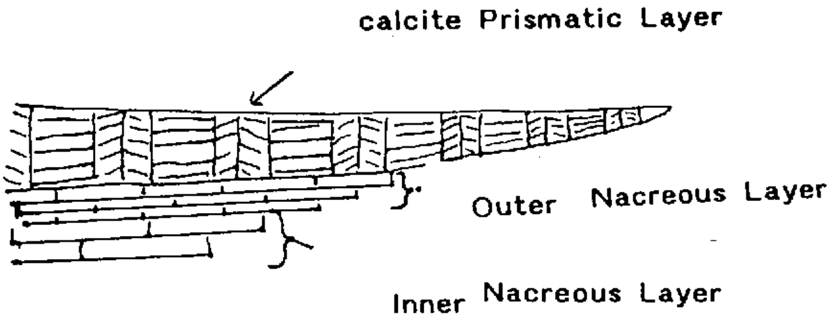

medial

Figure 1.3. The three Shell Layers of the pearl shell.

1.4. FORMATION OF THE BIVALVE SHELL.

Saleuddin and Petit (1983), discussing formation of periostracum in bivalves, describe an outer layer, middle layers and an inner layer. The outer layer is said to be "denser" than the other layers and is shown as a fibrous layer outside the forming Prismatic Layer. The "distended middle layer" is said to be "continuous with the matricial top and bottom of the prisms". These two layers are said to comprise all the periostracum emerging from the periostracal groove". The inner layer (of periostracum) is said to undergo morphological changes "related to the formation of layers of initial nacre" and is said to be added at the 'mantle edge'. Thus these authors have included as periostracum not only an outer uncalcified shell covering (Watabe 1984), but organic matrix structures of both the Prismatic Layer and the Nacreous Layer thus rendering the term a misnomer and inextricably confusing what it describes with a large part of what is also described by the term "conchiolin". This confusing terminology will be dealt with more fully in Chapter 2 - Nomenclature.

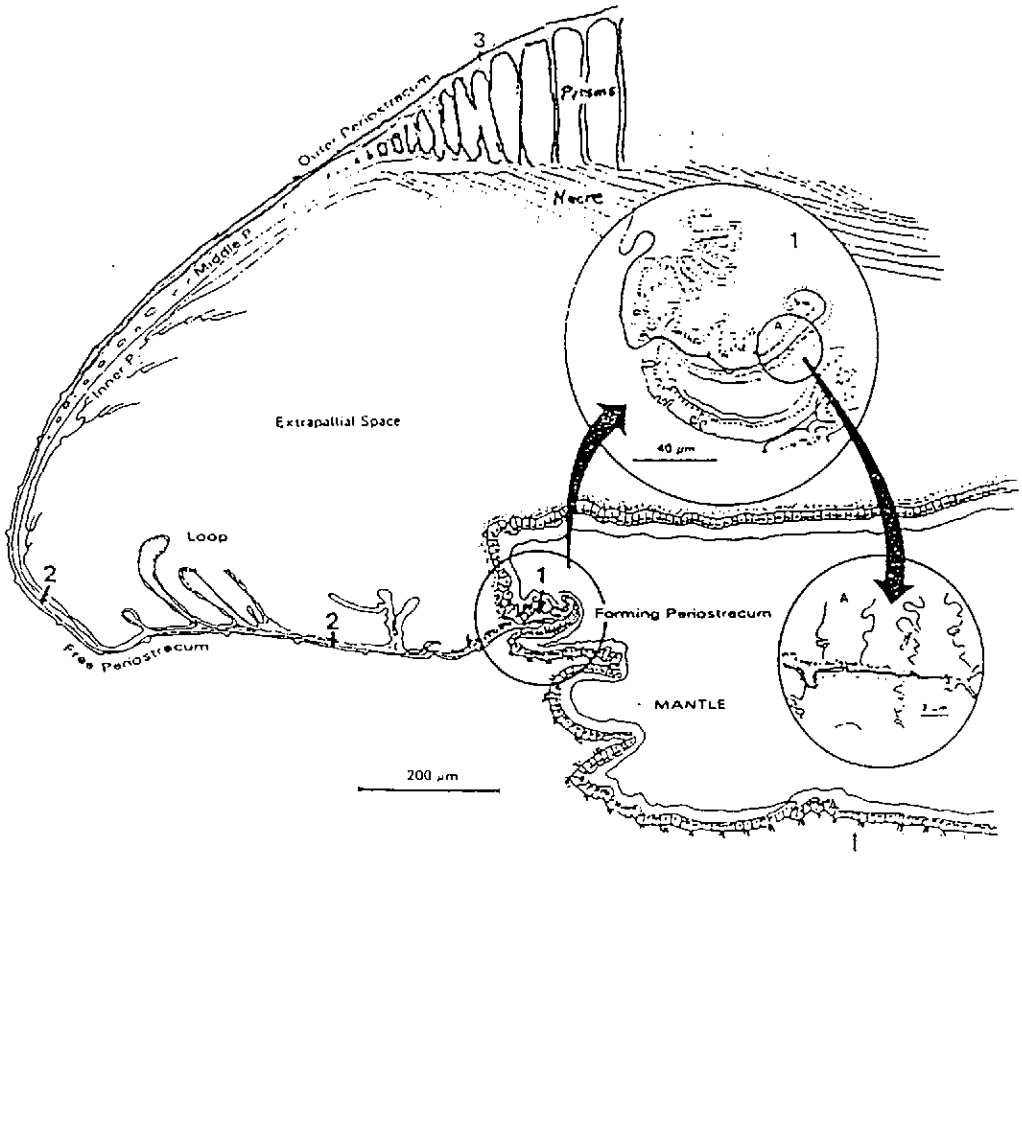

FIGURE 1.4. Mantle Margin and forming periostracum in Bivalves (after Saleuddin and Petit, 1983).

The generalised picture to illustrate the relationships between the shell and mantle in bivalves, as given by Wilbur and Saleuddin, (1983), is as follows:

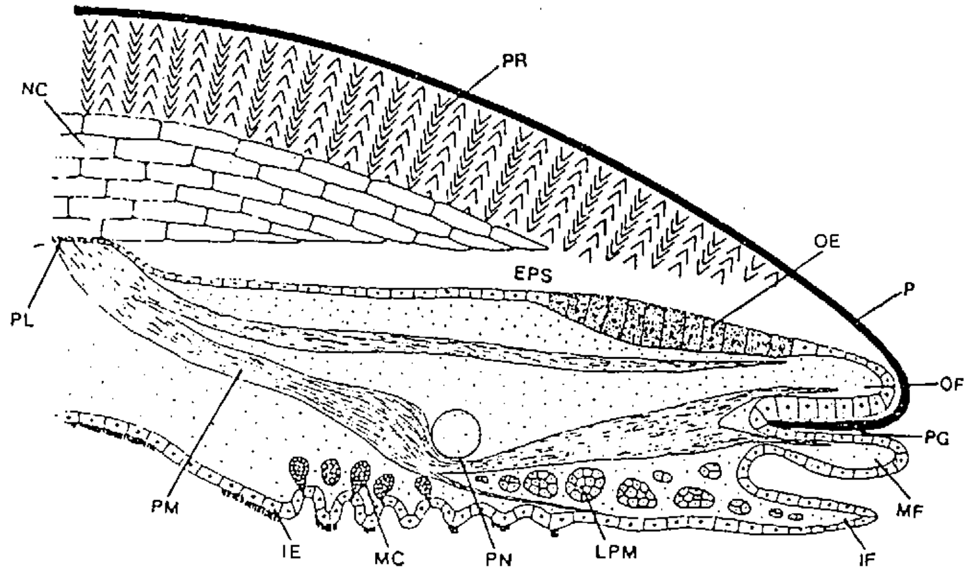

Fig. 1. Radial section of the mantle edge of a bivalve to show the relationship between the shell and mantle. (Not to scale.) EPS, Extrapallial space; IE, inner epithelium; IF, inner fold; LPM, longitudinal pallial muscle; MC, mucous cell; MF, middle fold; NC, nacreous shell layer; OE, outer epithelium; OF, outer fold; P, periostracum; PG, periostracal groove; PL, pallial line; PM, pallial muscle; PN, pallial nerve; PR, prismatic shell layer.

FIGURE 1.5. Bivalve Shell and Mantle Margin (Wilbur and Saleuddin, 1983).

Saleuddin and Petit's (1983) illustration for the mode of formation of the periostracum and its involvement in formation of the Prismatic Layer and Nacreous layer is given below:

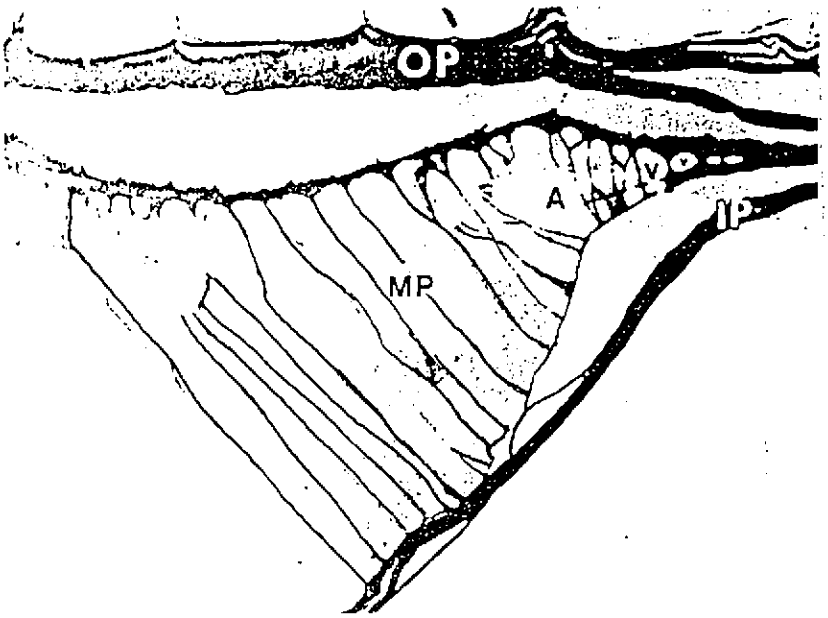

FIGURE 1.6. Formation of periostracum (Saleuddin and Petit, 1983). "*Amblema*. Light micrograph of the cleaving periostracum. Lying between the outer (OP) and inner (IP) periostracal layers is the distended middle layer (MP) which is continuous with the matricial top and bottom of the prisms. . . . The vacuoles (V) and antrum (A) formation precede prism formation."

Waite's (1983) illustration of the cells involved in periostracum formation is as follows.

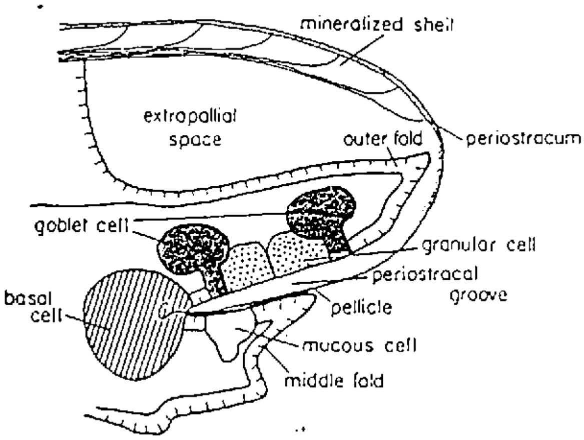

FIGURE 1.7. Cells involved in periostracum formation (after Waite, 1983).

All show a continuous layer of periostracum being formed in the most lateral of the Marginal Mantle Grooves which is then reflected around the distal extremity of the most lateral Marginal Mantle Fold to form a continuous sheath or outer layer of the bivalve shell. However whereas Saleuddin and Petit (1983) show the "periostracum" not only as an organic sheath on the lateral surface of the valve but also as the major if not sole component of the organic material of the Prismatic Layer and also as an organic component of the "initial nacre", no such roles as the latter two are afforded the "periostracum" in the diagrams taken from the other authors shown above.

However despite these apparent contradictions, the generalised picture from these publications of the structure of a bivalve shell and the relationship of the shell parts to the Mantle tissues that form them is as follows. The shell consists of two calcareous layers inside a non-calcareous layer. The Mantle Margin has three peripheral Marginal Mantle Folds and hence, between them, two Marginal Mantle Grooves. The outer non-calcareous layer, "periostracum", is formed in the more lateral of the two Marginal Mantle Grooves and reflected around the outer Marginal Mantle Fold to form the outer layer of the shell. The medial surface of the inner calcareous Shell Layer is joined to the External Mantle at the Pallial Line, thus enclosing the growing surfaces of the two calcareous Shell Layers in a physically confined space - the Extra-pallial Space. The growing surface of the outer calcareous Shell Layer, the Prismatic Layer, is opposed to the tissue lining the distal medial surface of the Extra-pallial Space, i.e. the Mantle Edge Gland. The growing surface of the Inner calcareous Shell Layer, Nacreous Layer, is opposed to the tissue lining the Proximal medial surface of the Extra-pallial Space. (Figure 1.8.).

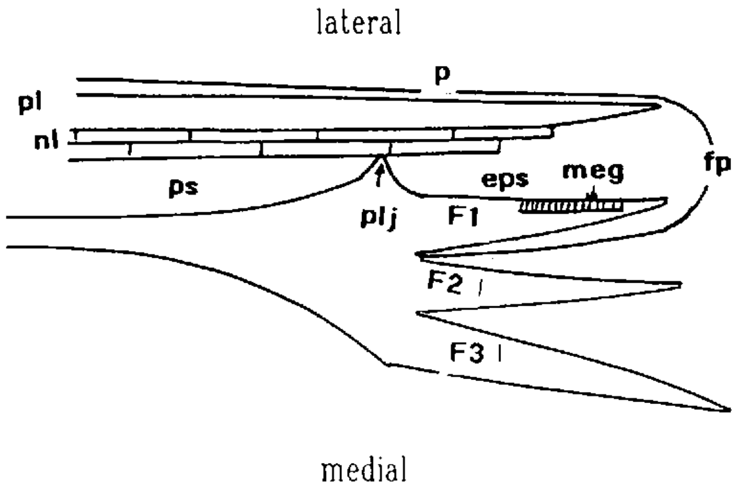

FIGURE 1.8. Generalised picture from above publications of formation of the bivalve shell. F1., F2. and F3. are the outer, middle and Inner Mantle Margin Folds respectively; fp = forming periostracum; p = periostracum; meg = Mantle Edge Gland; ps = Pallial Space; eps = Extra-pallial Space; plj = Pallial line Junction; nl = Nacreous Layer; P.L. = Prismatic Layer.

No extant Bivalve Superfamily as described by Taylor (1973) quite fits this picture. Further, the scenario is manifestly inadequate as there is no mechanism given for growth of the shell proximal to the Pallial Line. This matter will be discussed in Chapter 6.1.

1.5. FORMATION OF PEARL SHELLS.

Nakahara and Bevelander, (1971) described the formation of the Prismatic Layer of the shell of *Pinctada radiata* and unequivocally attributed it to the secretory functions of the "proximal region of the outer surface of the outer mantle fold in the pallial space bounded externally by the periostracum". Further these authors in a series of diagrams describe how they believe the layers of Prismatic Layer and also the Growth Processes (which they call "spurs") are formed by the extension and contraction of the outer Marginal Mantle Fold and secretion into the thus moulded periostracum of Prismatic Layer by the lateral surface of the outer Marginal Mantle Fold (Figure 1.9.).

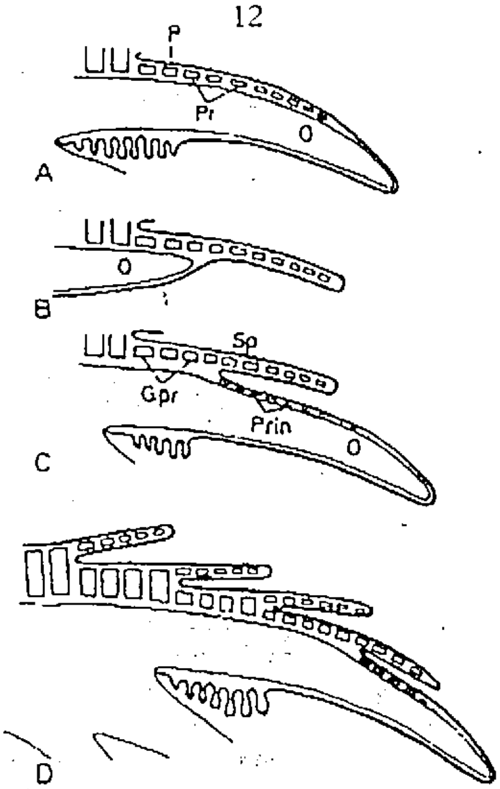

Fig. 16 A–D. This series of diagrams represents our interpretation of the important steps that occur in the formation of the prismatic layer (including spurs) of *P. radiata* and illustrates the relationship between the outer fold, the periostracum and the prisms. To simplify the illustrations, proportions of the structures were modified slightly. A. This diagram illustrates a completed single array of prisms located between the outer fold and the periostracum. Following the establishment of these prisms the mantle retracts. *P*, periostracum; *Pr*, prism array; *O*, outer fold. B. Showing new relation of the distal portion of the prism layer now enveloped on both upper and lower surfaces by the periostracum. *O*, outer fold. C. Mantle fold now in extended position again. The marginal portion of newly-formed array is enveloped by the periostracum to form a new spur. The proximal portion of the array is in continuous contact with the mantle epithelium and undergoes growth similar to proximal prisms previously formed. Also, prism formation is again initiated in the newly formed space between the margin of the outer fold and the periostracum. The formation of additional spurs consist of a repetition of the cycle A→B→C. *G.pr*, growing prisms; *O*, outer fold, *Pr in*, initiation of prisms; *Sp*, spur. D. Structure of shell and margin of the mantle following the formation of several spurs and additional prisms located proximally to the spurs. These prisms increase in height which results in a thickening of the prismatic layer. The periodic formation of additional proximal prisms also results in marginal growth

Figure 1.9. Formation of Prismatic Layer of Pinctada radiata (after Nakahara and Bevelander, 1971).

Dix, (1973), in *Pinctada maxima,* (Jameson, 1901), and Jabbour-Zahab et al, (1992), in *P. margaritifera* Linnaeus, 1758, and Garcia Gasca et al (1994) in *P. mazatlanica* Hanley, 1856, all describe the production of the "periostracum" in the "periostracal groove" essentially in accord with the picture given above for the formation of Prismatic Layer inside "periostracum" in *Pinctada radiata,* (Figure 1.9.), and the formation of shell in bivalves generally, (Figure 1.8.).

It has for many years been the basis of the cultured pearl industry that a piece of Pallial epithelium inserted into an appropriate place in the same or a different pearl oyster of the same species, along with a suitable nucleus, would result in the growth around the nucleus of a "pearl sac" and the secretion of nacre around the nucleus to form a cultured pearl, (Gervis and Sims, 1992).

From the foregoing it seems that Dix, (1973) in *Pinctada maxima*, Jabbour-Zahab et al. (1992) in *Pinctada margaritifera*, and Garcia Gasca et al. in *Pinctada mazatlanica* thought that the "periostracum" covered both the medial surface of the Prismatic Layer distal to the Nacreous Layer and the lateral surface of the entire Prismatic Layer. If this was the position then presumably it was believed that (as in Figure 1.10.) :

1, the Inner Nacreous Layer was produced by the Pallial Mantle;

2, "periostracum" was produced by the cells of the "periostracal groove";

3, the Prismatic Layer was produced by the cells of the lateral surface of the outer Marginal Mantle Fold; and

4, the Outer Nacreous Layer was produced by the equivalent in a pearl oyster of the cells lining the proximal Extrapallial Space of other bivalves.

lateral

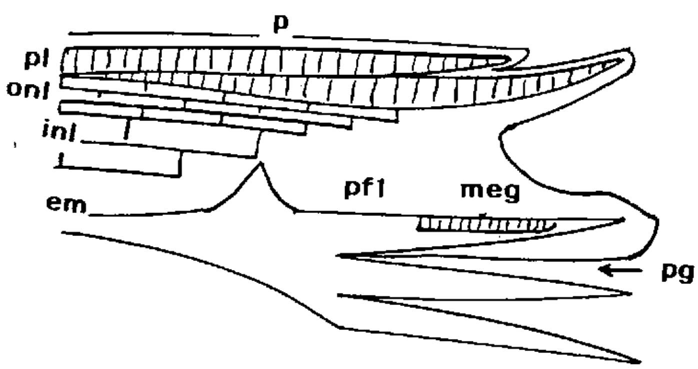

Figure 1.10. Relationships of pearl oyster and pearl shell as described by Dix,(1973), Jabbour-Zahab et al. (1992) and Garcia Gasca et al. (1994). p = periostracum, pg = periostracal groove. inl = Inner Nacreous Layer, em = External Pallial Mantle. onl = Outer Nacreous Layer, pF1 = Proximal part outer Marginal Mantle Fold. PL = Prismatic Layer, meg = Mantle Edge Gland.

Further, control of shell growth in Gastropods had been shown to be hormonal (Joosse and Geraerts, !983), and this was also thought to be the situation in Bivalves, (Waite, 1983).

The inherent contradictions in the usages of the terms "periostracum" and "conchiolin", and a preliminary examination of pearl oysters and their shells raised serious doubts concerning some of these beliefs. No "forming periostracum" could be seen joining the Mantle Margin of pearl oysters to the periphery of the valve. No "periostracum" as such could be discerned on the outer surface of a pearl shell. The surface of the Prismatic Layer visible on the medial surface of a pearl shell appeared to be different from the lateral surface of the same piece of Prismatic Layer. Finally, Dix (1973), in his study of the histology and histochemistry of the Mantle Margin of *Pinctada maxima* had not identified cells which could be readily equated with the "periostracum precursor" secreting cells of Saleuddin and Petit (1983), and Waite (1983).

1.6. NECESSARILY ALTERED AIM OF STUDY.

Growth and the control of growth in pearl oysters could not be properly studied until it was ascertained which tissues, cells and physiological systems were involved.

The more immediate aim of this work thus became an attempt to ascertain more certainly which tissues and glands were responsible for the secretion of the Organic Matrices precursors of the Shell Layers of pearl oysters, and the physiological control of them. Since peripheral growth of the pearl shell means, in essence, growth of the Prismatic Layer, this focussed attention on the tissues and glands responsible for the secretion of the Organic Matrices of the Prismatic Layer. Since increase in shell thickness is largely accomplished by an increase in the thickness of the nacre, and the valuable layer of cultured pearls is formed of nacre, these focused attention on the tissues and glands responsible for the formation of the Organic Matrices of the Nacreous Layers.

1.7. CLASSIFICATION OF BIVALVES BY SHELLS AND SHELL LAYERS.

Bivalves have historically and up to the present been classified largely on the basis of shell characters (Hynd, 1955). Following the work of Taylor et al., (1969), Taylor, et al., (1973) and Taylor, (1973), Waller, (1978) used types of Shell Layers as character states in the construction of a cladogram for a new classification of the Pteriomorphia.

1.8. CLASSIFICATION OF THE *PINCTADA* IN AUSTRALIAN WATERS.

Hynd, (1955) reviewed the taxonomy of the *Pinctada* in Australian waters and concluded that they all belonged to six species:
Pinctada maxima (Jameson 1901)the gold or silver lip pearl oyster;
P. margaritifera Linnaeus, 1758, the black lip pearl oyster;
P. fucata (Gould, 1850) a rather smaller species characterised by a relatively strongly convex shell and sharply pointed Growth Process;
P. chemnitzi (Philippi, 1849) which is a smallish pearl oyster with a light coloured prismatic layer and relatively insignificant growth processes;
P. maculata (Gould, 1850), which has whitish plaques on its external Prismatic layer; and
P. albina Lamarck, 1819, of which he, (Hynd) distinguished two sub-species -
P. albina carchariarum (Jameson, 1901) which he says occurs from Shark Bay to the Darwin area; and
P. albina sugillata (Reeve, 1857), which occurs from the vicinity of Darwin to the Southern New South Wales Coast.
P. albina is the "bastard shell" of the pearling industry where it is regarded as a fouling organism.

Hynd's review includes a "key" for establishing, almost totally on the basis of shell structures, the species of any pearl oyster in Australian waters. Hynd specifically dismisses soft tissues, with the exception of the Anal Funnel, as being of no importance in the classification of Australian pearl oysters.

1.9. RE HYND'S CLASSIFICATION OF THE *PINCTADA* AND SOFT TISSUES IN PEARL OYSTER CLASSIFICATION.

People working in the pearling industry on the North East coast of Queensland and in the Torres Straits have local common names for a number of medium sized pearl oysters, which, in some respects, are similar to *Pinctada fucata* but which they distinguish from them, and from "bastard shell" (which in this area is *Pinctada albina sugillata*). This suggests that there may be additional species whose shells are sufficiently similar to those of *P. fucata* for Hynd's key to fail to distinguish them.

Further, preliminary investigation of small pearl oysters from Balgal Beach fringing reef strongly suggested that specimens which Hynd's key placed in the species *Pinctada albina sugillata* might also belong to more than one species. In particular a type of pearl oyster with opaque silvery nacre, broad bands of radiating light and dark colouration of its Prismatic Layer and a deeply notched Byssal Groove was thought to be highly unlikely to be properly classified with *Pinctada albina sugillata* as this latter has a relatively very translucent nacre with a suffusion of gold colour, relatively more diffuse colouration of the Prismatic Layer and a shallow and indistinct Byssal Groove. It seemed likely that pearl oysters of similar sizes and ages grown in near proximity and displaying consistent shell differences of Nacre quality, Prismatic Layer colouration, and Byssal Groove structure belonged to different species.

It appeared that restricting the bases of classification to those shell characters used by Hynd was failing to classify, accurately, in the first case, middle sized pearl oysters similar to *Pinctada fucata*, and in the second, a group of smaller pearl oysters similar to *Pinctada albina sugillata*. Weiner et al. (1983), had found that not only the type of calcareous crystalline mineralisation but even the orientation of the crystallographic axes were determined by Organic

Matrices. Thus clear visual differences in Nacre may reflect chemical differences in Organic Matrices.

Further, if shell mineral structures are determined by Shell Organic Matrices and these are produced extracellularly by combination of secreted precursors (Waite, 1983), it seemed likely that particularity of shell structures would be reflected in an at least equivalent particularity of Shell Organic Matrices precursor secretory structures.

Thus both the adequacy of Hynd's classification and the exclusion of pearl oyster soft tissues from use in classification appeared questionable.

1.10. INITIAL OBSERVATIONS - MICROMORPHOLOGY OF ORGANIC MATRICES OF ACID DECALCIFIED PEARL SHELLS AND HISTOLOGY OF THE EXTERNAL MANTLES AND MANTLE MARGINS WHICH SECRETED THEM.

(Material presented here in summary form will be fully presented in Chapter 5 and discussed fully in Chapter 6. It is given here in summary form to give coherency to the experimental plan and to make the choice of animals intelligible).

1.10.1. Organic Matrices of Acid Decalcified Pearl Shells.

1.10.1.1. Micromorphological study of acid decalcified pearl shells of *Pinctada maxima*, *P.margaritifera*, *P. fucata*, two *P. albina sugillata* -like small pearl oysters, as well as *Pteria penguin* (Lamarck, 1819), and *Isognomon ephippium* (Linneaus, 1758), rendered the published description of pearl shell Prismatic Layer formation untenable for all these species, with the exception of *P. fucata* on geometrical grounds. Bands of aberrant staining in the specimens from *P. fucata* indicated that this species formed its prismatic layer in the same way as the other species listed.

1.10.1.2. No structure on acid-decalcified Organic Matrices of pearl shells could be identified as likely to have derived from a periostracum recurving from a Marginal Mantle Groove.

1.10.1.3. The Organic Matrices remaining after acid decalcification of pearl shells from the above species had many structural features in common. However these structural features and the overall micromorphology were species specific and complex, consisting of at least seven identifiable different scleroprotein structures in the Prismatic Layers of each species as well as the Organic Matrices remaining from the Nacreous Layers.

1.10.1.4. Separate Inner and Outer Nacreous Layers could not be discerned in acid decalcified pearl shell Organic Matrices.

1.10.2. Histological examination of the External Mantles and Mantle Margins.

1.10.2.1. The microanatomy was similar for all species of the *Pinctada* examined. Both *Pteria penguin* and *Isognomon ephippium* differed from the *Pinctada* in having four Marginal Mantle Folds rather than three.

1.10.2.2. Twenty one discrete tissues were identified on the External Mantle and Mantle Margin of any species of the *Pinctada* examined and analogous tissues occur at equivalent locations in all species of the Genus studied. Most of these tissues were replicated, some in the same and some in different loci, in the specimens from the other pearl oyster genera examined.

1.10.2.3. Where uniqueness and constancy of shell features made species identification certain, the detailed histology of each of these tissues was found to be rigidly species specific. This was true for all the species listed at 1.10.1.1. above except for the specimens of the two *P. albina sugillata* - like species. Their External Mantle and Mantle Margins histologies were as diverse as any two of the other species of *Pinctada*, indicating that they were different species.

1.10.2.4. The highly differentiated and complex tissues of the middle Marginal Mantle Fold and the lateral surface of the medial Marginal Mantle Fold of the *Pinctada*, and the equivalent loci on the third most lateral and fourth most lateral Marginal Mantle Folds of the other pearl oyster genera examined strongly suggested a role for these tissues in specific shell Organic Matrix scleroprotein formation. The function given to the secretion in the Marginal Mantle Groove lateral to them denied them any such role. If it was forming periostracum then after it had recurved around the terminus of the most lateral Marginal Mantle fold to form the lateral surface of the shell any material secreted medial to it would have been excluded from the shell. (Figure 1.11.).

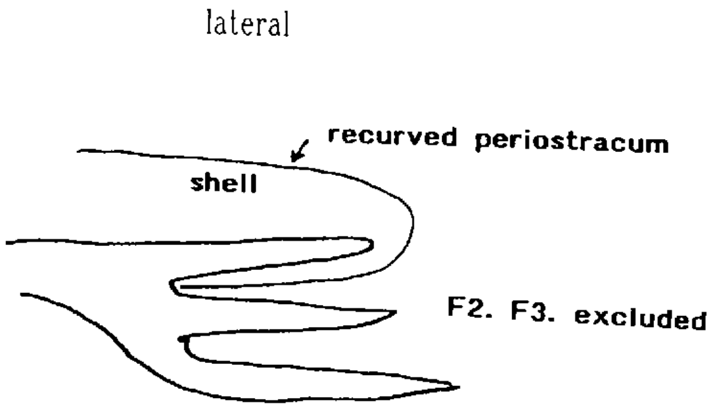

Figure 1.11. Exclusion of secretory structures of Middle and Medial Marginal Mantle Folds from a role in Shell Layer formation by recurving "forming periostracum".

1.10.2.5. No histological structures of the lateral surface of the outermost Marginal mantle Fold was of such a complexity so to give credence to its published role as the source of the precursors of the Prismatic Layer Organic Matrices scleroproteins. (Nakahera and Bevelander, 1971).

1.10.2.6. The Circumpallial Nerve was located just proximal to the apex of the most lateral Marginal Mantle Groove in the *Pinctada* and in the same locus relative to the second most lateral Marginal Mantle Groove in the other pearl oyster genera in all species examined, and supplied branches to the secretory tissues thoughout the Mantle Margin. The branches to the secretory tissues rivalled in size the branches to the Mantle musculature. What appeared to be concentrations of peripheral neurons occurred in the Circum-pallial Nerve trunk, especially near the origins of the large branches to the secretory tissues of the Marginal Mantle Folds. This, together with the destination of the branches suggested a major role for the nervous system in shell growth regulation. This contrasted with the current published material that shell growth was under hormonal regulation, (Joosse and Geraerts, 1983).

In summary these initial investigations suggested that the classification of the Australian *Pinctada* was deficient and the bases for their classification inadequate. There was no adequate nomenclature available to describe either the micromorphology of the shell Organic Matrices, nor for most of the discrete tissues and identifiable secretory structures and glands of the Mantle and Mantle Margin. Some existing nomenclature was both wrong and misleading. Published mechanisms of shell formation in pearl oysters, especially of Prismatic Layer formation, accorded with neither the micromorphology of the pearl shells, nor the histology of their Mantles and Mantle Margins. Physiological control of Mantle and Mantle Margin secretory structures appeared to be largely neural rather than exclusively hormonal.

The initial observations had shown many current ideas of pearl shell production to be wrong. However the evidence, while it suggested a role in shell formation for at least some of the secretory structures of the more medial two Marginal Mantle Folds, failed to add specifically to the evidence from production of cultured pearls, as to which tissues produced which precursors of which Organic Matrices of which Shell Layers.

1.11. RELATIONSHIPS OF SHELL LAYERS IN DIFFERENT SUPERFAMILIES IN THE BIVALVIA AND THE GEOMETRY OF SHELLS AND MANTLES.

A major source of difficulty in discerning the cellular sources of the pearl oyster Shell Layer Organic Matrices precursors was the lack of physically discrete compartments in which the growing surfaces of the Shell Layers and the tissues responsible for their growth were confined.

While no two Nacreous Layers as described by Taylor (1973) could be discerned in acid decalcified pearl shell Organic Matrices, the Nacreous Layers of *Velesunio ambiguus* clearly changed physical structure abruptly at the Pallial Line. Further this species has a junction of External Mantle and the medial surface of the Valve at the Pallial Line - thus there is a physically enclosed space - the Pallial Space - in which only one Shell Layer is generated. Necessarily the precursors of the Inner Nacreous Layer must be secreted into the Pallial Space by the External Mantle between the Isthmus and the Pallial Line. Further again, the periphery of the shell of this species is adherent to the Mantle Margin. There is thus another enclosed space, the Extra-pallial Space, into which the precursors of the outer two Shell Layers must be secreted, and hence the secretory structures responsible must be located in tissues open to this space.

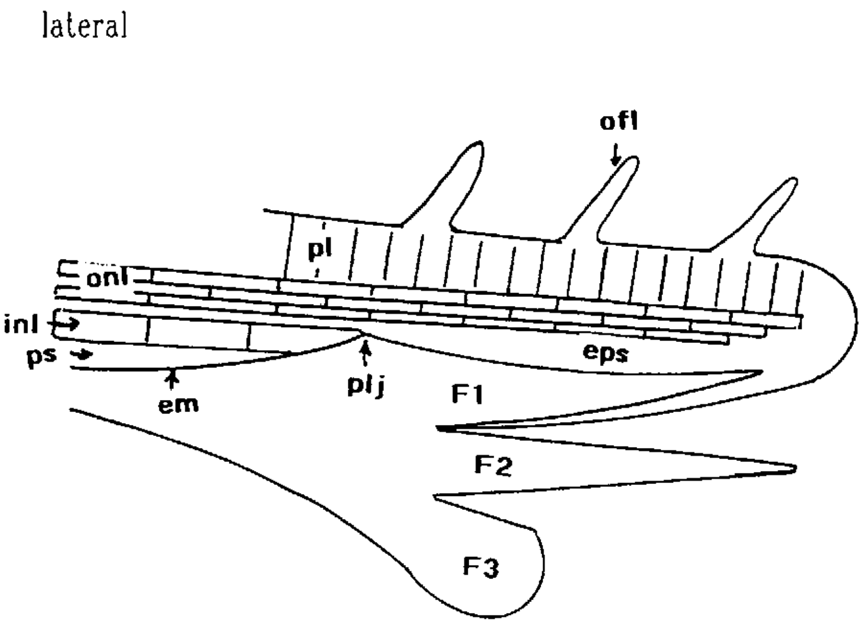

Figure 1.12. Relationships between the External Mantle, Mantle Margin and Shell Layers of the Valve of *Velesunio ambiguus*. F1., F2. and F3. = outer, middle and inner Mantle Margin Folds respectively; em = Pallial External Mantle; ps = Pallial Space; plj = Pallial Line Junction; eps = Extra-pallial Space; inl = Inner Nacreous Layer; onl = Outer Nacreous Layer; PL = Prismatic Layer; ofl = Outer Fibrous Layer.

Via Taylor's (1973) trend 1, the two Nacreous Layers of the Pterioidea are supposed to be derived from those of a primitive Bivalve such as the Unionoidea (Figure 1.2. above). In the Pterioidea, since on initial observations no connection between the Mantle and the Valve could be seen distal to the region of the Adductor Muscle, the geometrical relationships between the Mantle and the Valve in pearl oysters is as follows:-

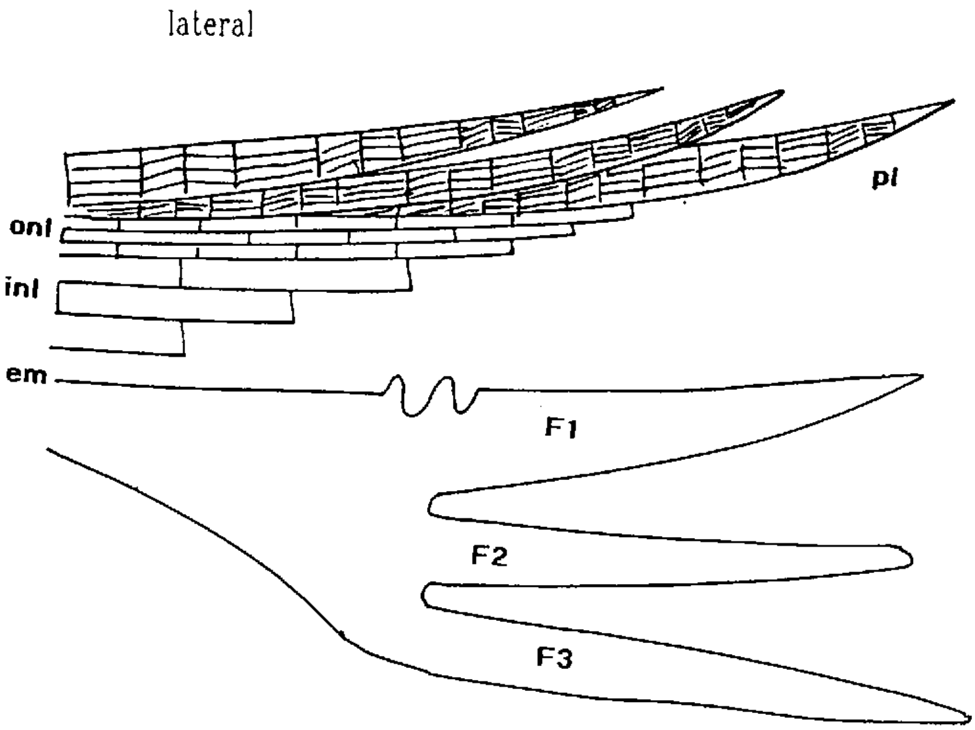

Figure 1.13. Relationships between the External Mantle, Mantle Margin and the Shell Layers of the Valve of a pearl oyster. F1., F2. and F3. are the outer, middle and inner Mantle Margin Folds respectively; em = External Pallial Mantle; inl = Inner Nacreous Layer; onl = Outer Nacreous Layer; P.L. = Prismatic Layer.

In Taylor's (1973) trend 5, the Outer calcareous Shell Layer of the Unionoidea, simple aragonite Prismatic Layer, is replaced by a composite Prismatic Layer. The two medial Shell Layers - both Nacreous Layers - remain the same as in the primitive condition.

	Composite Prismatic Layer, (calcite)
NUCULOIDEA	Outer Nacreous Layer, (aragonite).
	Inner Nacreous Layer, (aragonite).
	Aragonite Prismatic Layer.
UNIONOIDEA	Outer Nacreous Layer, (aragonite).
	Inner Nacreous Layer, (aragonite).

Figure 1.14. Taylor's (1973) trend 5.

In Taylor's (1973) trend 6, the sequence of alteration of the three calcareous Shell Layers of the Primitive Bivalve shell are first to a shell as in the Genus *Panopea* which has an outer aragonitic simple Prismatic Layer, the Outer Nacreous Layer is replaced by a middle Homogeneous Shell Layer, and within the Pallial Line, a Shell Layer which is sometimes like Complex Crossed Lamellar Layer, (Figure 1.15.). A further development to some Pholadoidea resulted in a shell with an outer Shell Layer of simple Aragonite Prisms, a middle Crossed Lamellar Shell Layer, and an inner Shell layer of Complex Crossed Lamellar Structure. The next step in this sequence is the loss of the outer Shell Layer to give the Gastrochaenoidean and Corbiculoidan shells with two calcareous Shell Layers (Figure 1.15.).

GASTROCHAENOIDEA	Crossed Lamellar Structure.
CORBULOIDEA	Complex Crossed Lamellar Structure.
↑	
	Simple Aragonite Prismatic Layer.
Some PHOLADOIDEA	Crossed Lamellar Structure.
↑	Complex Crossed Lamellar Structure.
	Simple Aragonite Prismatic Layer.
PANOPEA	Homogeneous Layer.
↑	Complex Crossed Lamellar Layer.
	Simple Aragonite Prismatic Layer
UNIONOIDEA	Outer Nacreous Layer, (aragonite).
	Inner Nacreous Layer, (aragonite).

Figure 1.15. Taylor's (1973) trend 6.

In Taylor's (1973) trend 7, which contains most of the Heterodont Bivalves the three calcareous Shell Layers of the primitive bivalve shell are altered to an outer Composite Prismatic Layer, a middle Crossed Lamellar Structure, and an

Inner Complex Crossed Lamellar Structure. These are the calcareous Shell Layers found in the Tellinoidea and some Veneroidea, (Figure 1.16). Further development in this trend sees the loss of the Outer Prismatic Layer resulting in the Shell Layers found in the Carditoidea and Mactroidea, (and also, according to Taylor, the Limopsoidea and Arcoidea, (Figure 1.16.). The next sequence in this Trend sees the degeneration of these two Shell Layers into Homogeneous Layers as in some Veneroidea, (Figure 1.16.).

VENEROIDEA	Homogeneous Structure. Homogeneous Structure.
↑	
CARDITOIDEA, MACTROIDEA, LIMOPSOIDEA, ARCOIDEA.	Crossed Lamellar Structure. Complex Crossed Lamellar Structure.
↑	
TELLINOIDEA, Some VENEROIDEA.	Composite Prismatic Layer. Crossed Lamellar Structure. Complex Crossed Lamellar Structure.
↑	
UNIONOIDEA	Simple Aragonite Prismatic Layer. Outer Nacreous Layer. Inner Nacreous Layer.

FIGURE 1.16. Taylor's (1973) Trend 7.

On preliminary investigations, those of the above Superfamilies involved in this study which, like *Velesunio ambiguus*, have both an enclosed Pallial Space and an enclosed Extra-pallial Space (Figure 1.12.), are the Mytiloideans in Trend 1, the Gastrochaenoideans and Corbiculoideans in Trend 6, and all the Superfamilies of Trend 7 - i.e. the Tellinoidea, Veneroidea, Carditoidea, Mactroidea, Limopsoidea, and Arcacea.

Those Superfamilies where the Pallial Space and Extra-pallial Space are, as in the pearl oysters, (Figure 1.13.), not physically confined are the Pterioidea, Ostreoidea, Anomioidea, and Pectinoidea, all belonging to Trend 1. The Nuculoidea of Trend 5 have a unique geometric configuration of Mantle Margin and valve occasioned by the reflection of the Mantle Margin, Taylor, (1973). They have a physically enclosed Pallial Space.

1.12. DECALCIFICATION AND ATTEMPTED SEPARATION OF SHELL LAYERS OF PEARL SHELLS AND SHELLS OF OTHER BIVALVES USING WEAK ACIDS.

It had been observed that the Nacreous Layers and Prismatic Layers of pearl shells maintained at least their visual integrity after decalcification with weak acids. Since Taylor had described a large number of Shell Layer assemblages in other bivalves with individual Shell Layers either similar to, derived from, or similarly derived as the Shell Layers in the Pterioidea it was decided to study their behaviour after decalcification with weak acids as well as the pearl shells. As above, various of these Shell Layers had been formed inside enclosed spaces as in *Velesunio ambiguus* and others under conditions similar to that in the Pteriacea.

The major outcomes of this work were a method for simultaneous acid decalcification of the shells and fixation of the tissues and Shell Layer Organic matrices of some bivalves, and some cautions concerning over-reliance on Shell Layers in taxonomy. Since these have more to do with planning the major part of this study than being a part of it, this work is described here.

Shells of the unionacean *Velesunio ambiguus*, the pinnacean *Pinna bicolor*, Gmelin, 1791, the pterioidean pearl oysters *Pinctada maxima*, *P. margaritifera*, *P. albina sugillata*, *Pteria penguin*, *Isognomon isognomon* and *I. ephippium*, (Linneaus, 1758), the mytiloidean *Trichomya hirsuta*, (Lamarck, 1819), the pectinoidean *Amusium pleuronectes* (Linneaus, 1758), the ostreoideans

Ostrea sp. and *Saccostrea echinata* (Quoy and Gaimard, 1835), the nuculoidean *Nucula superba* Hedley, 1902, a tellinoidean *Tellina sp.* the veneroidean *Gafrarium divaricatum* (Gmelin, 1791), the gastrochaenoidean *Gastrochaena cuneiformis*, Spengler, 1783, and the arcoideans *Anadara pilula* (Reeve 1844), and *Trisidos tortuosa* (Linneaus, 1758), were subjected to acid decalcification and attempted separation of Shell Layers using acetic acid added dropwise when bubble production on the shell surface ceased, with sucrose as a calcium removal agent.

1. Decalcification of all species of pearl shell tested from the Genera *Pinctada*, *Pteria* and *Isognomon* if performed very slowly, eg. in 2% acetic acid or weaker, with the careful release of the carbon dioxide bubbles which form between the lateral surface of the outer Nacreous Layer and the medial surface of the Prismatic Layer, results in a decalcified entity in which the major morphological features of the Shell Layer Organic Matrices appear intact visually. Hopes that simple acid hydrolysis could be of use in freeing precursors from the resultant organic matrices were abandoned when gradual increase in acid strength up to 10% acetic or hydrochloric acid failed to have any visually perceivable effect on the decalcified organic residue from the decalcification with 2% acetic acid.

2. A similar procedure used on the valves of the oyster *Saccostrea echinata* resulted in hydrolysis of the organic matrices of both valves - but the most resistant part of the shell was the lateral part (Prismatic Layer according to Taylor (1973)) of the upper (right) valve.

3. A similar procedure used on the upper and lower valves of the scallop *Amusium pleuronectes* but carried out very slowly over several weeks resulted in partial decalcification of the lower valve without total hydrolysis of the organic matrices, and a similar result with both the inner (white) and outer (brown) Shell Layers of the upper valve, which were parted by the process. An attempt to accelerate the process resulted in hydrolysis of the shell organic matrices. Other

results obtained with a similar procedure and the valves of different bivalve species ranged from results similar to those obtained with the Pterioidea to those obtained with the valves of *Trisidos tortuosa* - here the shell organic matrices hydrolysed under the gentlest conditions for effective decalcification.

4. In an attempt to prevent or slow down acid hydrolysis of the organic matrices of the shell layers while decalcification was attempted, they were first fixed in an acid fixative, Marine Bouin's fixative (see Materials and Methods Chapter 4). Acetic acid was then added very slowly until decalcification was complete. This procedure was very effective for maintaining at least a visual semblance of integrity of the Organic Matrices of some Shell Layers in some animals but failed to prevent disintegration or solubilization of others.

In summary, the results of these preliminary investigations into acid solubility of the Organic Matrices of Bivalve shells are:

1. Pre-fixation with Marine Bouins followed by gentle decalcification with acetic acid yielded a specimen of shell Organic Matrix capable of being used for light microscopy which at least visually maintained the integrity of the Shell Layers of pearl oysters and, to a similar or lesser extent, those of some other bivalves. This technique allowed for the fixation, sectioning and staining of the whole animal and at least the major outlines of its shell Organic Matrices *in situ* for small bivalves with some particular Shell Layers.

2. That types of shell layer should, on their own, be used with caution in assessing phylogenetic relationships was highlighted by the very different acid solubilities of the organic matrices of the Outer Prismatic Layers of *Saccostrea echinata* and those of the Pterioidea investigated; the different acid solubilities of the organic matrices of the Foliated Structure Shell Layers of the Ostreoideans from that of *Amusium pleuronectes*; and the differences in acid solubilities of the Organic Matrices of the Crossed Lamellar and Complex Crossed Lamellar Shell Layers of the shells of the Veneroidea, Tellinoidea and Arcoidea.

1.13. AVAILABLE AVENUES OF INVESTIGATION.

In pearl oysters, with the absence of physical compartments in which the growing surface of a Shell Layer and the tissues which secrete its Organic Matrix precursors are confined, the three possible direct lines of investigation are :

1. To observe the growth of the Shell Layers.

2. To study the components of the Shell Layer Organic Matrices and the histologies of the External Mantles and Mantle Margins which produced them.

3. To chemically split the Shell Organic Matrices of the Shell Layers to the secreted precursors.

No pearl oyster had been observed producing the Organic Matrices of their Prismatic Layer, and the third option was probably chemically, for all practical purposes, impossible.

Study of Shell layer components could indicate the degree of complexity likely to be found in the tissue source of the Shell Layer Organic Matrix Precursors. Study of the tissues of the Mantle and Mantle Margin could indicate the location of secretory tissues of sufficient complexity as to be considered likely to be involved in the production and/or the secretion of Shell Layer Organic Matrix scleroprotein precursors. This approach, on its own, had led to the erroneous interpretations indicated above. Initial observations had already indicated that the erroneous description of Prismatic Layer formation of Nakahara and Bevelander (1971), would have been avoided had these authors studied the micromorphology of a sufficiently wide array of other species of the Pterioidea. This led to a constraint on the design of this work - where the micromorphology of a Shell Layer was broadly consistent across a range of taxa, then the wider the spread of species for which the interpretation of the formation of the Shell Layer was tenable the more likely was it to be valid in a particular case. Thus the greater the number and variety of species of the Pterioidea included in the study the more likely were the conclusions from their study to be valid.

Taylor's (1973) work, while open to criticism in some respects, had shown that the Shell Layer assemblages found in Bivalves were largely similar in the groups into which they had been classified on other bases. This made it very likely that Taylor's proposals were fundamentally valid - that is, that there is an evolutionary relationship between the Shell Layers seen in the different Bivalve Superfamilies. However before this relationship could be used for determination of the sources of the Organic Matrix scleroprotein precursors of the Shell layers of the Pterioidea, it was necessary that this relationship be placed on a sounder evolutionary footing. That too glib a use of Shell Layer types on their own could be a source of error was highlighted by Taylor's placement of the Limopsoidea and Arcoidea in the Heterodonta via trend 7 - and then their replacement in the Pteriomorphia by Waller (1978), even though he used Taylor's Shell Layers in his classification of the Pteriomorphia. It thus seemed prudent that if Taylor's Shell Layers were to be used as a basis for a comparative study between species which secreted Shell Layers in discrete compartments and those with similar Shell Layers secreted without compartments, that the histology of the secretory tissues should also be demonstrably related as well as the Shell Layers, before too much reliance could be placed on the comparisons.

The major part of the problem of finding the tissues which produce the pearl shell's Shell Layer Organic Matrices can be reduced to finding the tissues which produce those of the Prismatic Layer, since the source of the precursors of the Organic Matrices of the Inner Nacreous Layer are known from the growing of cultured pearls, and the source of those of the Outer Nacreous Layer must in all likelihood occur on the Mantle or Mantle Margin in between the other two.

1.14. SPECIES AVAILABLE FOR A COMPARATIVE STUDY OF THE TISSUE ORIGINS OF SHELL LAYER ORGANIC MATRICES PRECURSORS IN PEARL OYSTERS AND OTHER BIVALVES.

Taylor had listed as a Bivalve Superfamily displaying the primitive condition of outer aragonite simple Prismatic Layer outside two Nacreous Layers the Unionoidea and from this Superfamily *Velesunio ambiguus* was available.

For comparison, representatives of two Superfamilies from Taylor's trend 6 which lacked Outer Prismatic Layers were available, the corbiculoidean *Geloina coaxans,* (Gmelin, 1791), and the gastrochaenoidean *Gastrochaena cuneiformis* Spengler, 1783.

Available from Taylor's (1973) trend 7 for comparison with the primitive condition of shell of *Velesunio ambiguus* were the members of Superfamilies where the Outer simple Prismatic Layer had been replaced by a Composite Prismatic Layer, the tellinoideans *Tellina sp.* and *Phylloda foliacea* Linnaeus, 1758, and also the veneroideans *Dosinia juvenilis* (Gmelin, 1791), *Circe trigona,* (Reeve, 1864), *Gafrarium divaricatum,* (Gmelin, 1791), *G. tumidum,* Roding, 1798, *Placamen calophyllum* Philippi, 1836, and *Globivenus embrithes,* (Melvill and Standen, 1899).

As examples of trend 7 taxa without outer Prismatic Layers the carditoidean *Cardita variegata* Bruguiere, 1792, was available as were the mactroideans *Mactra abbreviata,* Lamarck, 1819, and *Mactra dissimilis* Reeve, 1854, and the heterodont solenoideans *Solen grandis* Dunker, 1862, and *Solen vagina* Linnaeus, 1758.

Also placed by Taylor as part of trend 7 and also lacking an outer Prismatic Layer the limopsoidean *Melaxinaea vitrea* Lamasck, 1819, was available as were the arcoideans *Anadara antiquata*, (Linnaeus 1758) *Anadara pilula*, *Arca aladdin*, (Iredale, 1939 as *Navicula aladdin)*, *Barbatium amygdalumtostum*, (Roding 1798), *Mesocibota luana*, Iredale, 1939, and *Trisidos tortuosa*. As above this placement of these taxa amongst the heterodont Bivalves was in dispute (Waller, 1978), and so the Mantle and Mantle Margin histology of these groups as compared with that of the Superfamilies of trend 7 with the same Shell Layers, and more importantly, as compared with the Superfamilies of trends with and without the same Shell Layers was important both as a source of comparative data and as a check on the validity of the assumptions on which the comparisons were to be made.

In Taylor's (1973) trend 5 the nuculoideans are shown as having one change from the primitive condition - an outer Composite Prismatic Shell Layer instead of an outer Shell Layer of aragonite Simple Prisms. Live specimens of *Nucula superba* were available as well as formalin fixed specimens of an unidentified member of this genera - *Nucula sp.*.

In trend 1 the alteration of the primitive Bivalve Shell Layers to those of the Pinnoidea and the Pterioidea described by Taylor is that the outer aragonitic Simple Prismatic Layer changes to a calcitic one. Available from the Pinnoidea was *Pinna bicolor* Gmelin 1791, and from the Pterioidea the following; *Pinctada maxima*, *P. margaritifera*, *P. fucata*, two other *Pinctada* similar in size to *P. fucata* with very different growth processes and other features of their shells, presumed different species and termed *Pinctada sp.1* and *Pinctada sp.2*, two small purple shelled *Pinctada* again thought to be different species and termed *Pinctada sp.3* and *Pinctada sp.4*, *P. chemnitzi* a species which may be *P. maculata* but here termed *Pinctada sp.5*, *P. albina sugillata* and five pearl oysters which are somewhat similar to this last but distinctly different in various ways termed *Pinctada sp.6*, *Pinctada sp.7*, *Pinctada sp.8*, *Pinctada sp.9*, and *Pinctada sp.10* as well as *Pteria penguin* and *Pteria avicula* and the isognomons *Isognomon isognomon* and *Isognomon ephippium*, and *Malleus alba*.

In trend 1 the Mytiloidea are said by Taylor to have either Mytilid Prisms as an Outer Shell Layer or in some tropical mytilids the outer Prismatic Layer is said to be totally lost. Available from the Mytiloidea were *Trichomya hirsuta* (lamarck 1819) and the coral borers *Lithophaga teres* (Philippi 1846), and *Botulopa silicula infra* Iredale 1939.

On another branch of Trend 1 Taylor placed the Ostreoidea and the Anomioideaea and Pectinoidea. According to Taylor, the *Ostrea* have both valves consisting of Foliated Structure, a successor to the ancestral middle Shell Layer of outer Nacreous Layer having lost both the Outer Prismatic Layer and the Inner Nacreous Layer. *Hyotissa hyotis* (Linnaeus 1758) is alleged to have only one Shell Layer as for *Ostrea sp.* but *Saccostrea echinata* Quoy and Gaimard 1835, has an Outer calcitic Prismatic Layer on its Upper (Right) Valve and *S. cuccullata* (Born 1788) has this plus similar Prismatic Layer on the raised Posterior Border of the Bottom (Left) Valve as well. The anomiacean *Placuna placenta* (Linnaeus 1758), is said by Taylor to have a valve composed of an Outer Crossed Lamellar Shell Layer and an Inner Complex Crossed Lamellar Shell Layer. Taylor suggests that this is also the situation in the Pectinoidea but this is probably not so in the scallop *Amusium pleuronectes* (Linnaeus 1758) which while it has two outer Shell Layers in its Upper Valve appears to have only the Inner Complex Crossed Lamellar Layer represented in its Lower Valve. Another pectinoidean available for study was the spondylid *Spondylus lamarcki* (Chenu, 1845).

All the Superfamilies listed above in trends 6 and 7 have an inner Shell Layer of Complex Crossed Lamellar Structure which Taylor (1973) lists as a successor to the ancestral Inner Nacreous Layer and outside this a layer of Crossed Lamellar Structure - the alleged successor to the ancestral middle (nacreous) Shell Layer. The Middle and Inner Shell Layers of Nuculoidea (Trend 4) remain Nacreous Layers as in the ancestral condition.

In trend 1 the Middle and Inner Nacreous Layers of the Ancestral condition are maintained in the Pinnoidea and Pterioidea whose Mantles and Mantle Margins are free distal to the Adductor Muscle and also in the Mytiloiodea where the

Pallial Space and the Extrapallial Space are physically confined.

While it had already been established that the same Shell Layers in different Superfamilies may have chemically different Organic Matrices, it was thought that the overall similarities in Shell Layer assemblages in closely related taxa was indicative of an overall pattern of chemical similarity in similar Shell Layers. This in turn was thought likely to be related to an overall pattern in similarity of secreted precursors and the structures secreting them.

The group of Bivalves referred to above contained a wide variety of Superfamilies classified as fairly remote from the pearl oysters (Waller, 1978), as well as representatives of every available Superfamily in the Pteriomorphia where the Mantle and Mantle Margin were, like in the pearl oysters, free, distal to the Adductor Muscle. It also contained an allegedly primitive freshwater unionoidean for comparison. Further it contained species where outer aragonitic Prismatic Layer, outer Composite Prismatic Layer, the middle Shell Layer - Outer Nacreous Layer, the Inner Shell Layer - Inner Nacreous Layer, and the middle and inner Shell Layers allegedly derived from these were secreted in physically enclosed compartments. The Organic Matrices of these Shell Layers, the tissues which secreted their precursors, and the secretions, could be compared with the Organic Matrices of the calcitic outer Prismatic Layer, the Outer Nacreous Layer and Inner Nacreous Layer of pearl shells, and the secretory tissues and glands and their secretions on the External Mantle and Mantle Margin of pearl oysters.

1.15. PLAN OF EXPERIMENTS.

The External Mantle and Mantle Margin of twenty species of pearl oysters (i.e. every species available) were studied under light microscopy (L.M.) and the same tissues of eleven of these under transmission electron microscopy, (T.E.M.). The decalcified Shell Organic Matrices of these latter were sectioned, stained and studied under L.M., and the Nacreous Layers and Prismatic Layers of their valves studied with scanning electron microscopy, (S.E.M.).

The External Mantles, Mantle Margins and, where available, the decalcified shell

Organic Matrices of thirty eight species of non-pearl oyster bivalves were also studied under L.M..

For L.M., where considered necessary, and possible, entire animals together with their decalcified valves were serially sectioned. In other instances sufficient of each specimen was serially sectioned to allow of the building up of a three dimensional picture of the tissues and/or shell organic matrices.

1.16. ARRANGEMENT OF RESULTS.

This work is a comparative study of the tissues of the External Mantle and Mantle Margin of some pearl oysters and other bivalves - and an accompanying study of the micromorphology of the shell layers of the same animals. The aim is to determine the spatial, physical, chemical - and therefore likely physiological - relationships of the discrete tissues and the parts of the shell organic matrices scleroproteins resulting from the chemical combination of the precursors which the discrete tissues secrete. It is a direct extension of the work of Taylor (1973). He showed that the assemblage of shell layers found in bivalves allowed them to be grouped into what he called "evolutionary trends" away from an ancestral bivalve shell layer assemblage. This work extends this concept to the tissues which secrete the precursors of the scleroproteins of the shell layers. It is thus based on the notion that the array of shell layer assemblages seen in bivalves are a consequence of alteration away from an ancestral bivalve array of tissues which secrete the precursors of the ancestral shell layer assemblage. This dictates that the Results be presented, species by species in an order which the results themselves determine. Thus the first animal illustrated is the example used with Taylor's ancestral bivalve shell layer assemblage - *Velesunio ambiguus*. Then follows illustration of those non-pearl oyster species placed by Taylor in his "Trend 1". The Nuculoidea and Pinnoidea are interposed between these and the pearl oysters for ease of comparison of the salient features of each of these with the taxa on either side. These are followed by the pearl oysters, and beyond these, the oysters pectins arc clams and related taxa. This is so that the similarities and differences of the shells and mantles of those placed before and after the pearl oysters can be readily compared with them. After these are placed those animals more remote from the pearl oysters taxonomically, to illustrate the scope of shell layer, (especially outer shell layer), making strategies employed in the Bivalvia.

The work has seven major parts :-

1. A new and functional nomenclature, (see 1.18).
2. Species specificity of Mantle and Mantle Margin histologies of the Pinctada is suggested as a basis for classification. (see 1 19).
3. Current nacre production theories are shown to be untenable for pearl oysters.
4. A method of nacre production in accord with the evidence presented in the thesis is suggested.
5. The Pleated Secretion of Groove F1F2. is shown not to be "forming periostracum" and another function is suggested for it; and therefore
6. The various published mechanisms whereby Prismatic Layer is said to be formed in pearl oysters and some other bivalves are shown to be untenable for pearl oysters .
7. Tissues from which the precursors of the pearl shell Prismatic Layer organic matrix scleroproteins are likely to be secreted are identified together with evidence for the method of production of the Prismatic Layer Growth Processes.

The material presented in the Results has been selected so that, where possible, the same illustrations are useful for as many of the above as possible. Thus the detailed Mantle and Mantle Margin histologies of *Pinctada maxima* and *P. margaritifera* and the similarly detailed shell layer micromorphologies from the same regions of the same species serve as :-

1. Detailed examples of the species specificity of pearl oyster External Mantle and Mantle Margin histology;
2. The most thorough demonstrations of the relationship between regional differences in histology to regional differences in shell micromorphology.
3. The most thorough illustrations of the source and nature of the Pleated secretion of Groove F1F2..
4. The major part of the evidence re the mechanism of nacre production, as well as,
5. taking their place in the overall panorama of relationships of shell Organic

Matrix secreting tissues and the resultant shell layers seen in the bivalves studied. (on which all major features of this work are based).

This last requires that the results are presented species by species and these are arranged in an order which reflects the basis of this work in that of Taylor (1973) with some modifications determined by histological similarities in the groups studied.

Some of the more important comparisons available in the material presented are indicated in the appropriate sections of the Results.

1.17. ARRANGEMENT OF DISCUSSION.

The discussion is divided into six sections.

1. is a general consideration of the origin of Shell Layers in all the Bivalves studied.
2. considers the evidence for two Nacreous Layers in the Pterioidea.
3. relates morphology of the Inner Nacreous Layer to opposing External Mantle.
4. considers the morphology of the Outer Nacreous Layer and the Histology of the outer Marginal Mantle Fold.
5. considers current theories of formation of Nacreous Layers and suggests an alternative theory of Nacre Formation in accord with the data presented here.
6. In this section current ideas of pearl shell Prismatic layer origin are assessed in the light of the data presented here and a new theory which accords with these data is suggested.

1.18. NECESSITY FOR NEW NOMENCLATURE.

This study of the External Mantle and Mantle Margin of pearl oysters and other Bivalves and their relationship to the forming Shell Layers of these animals revealed numerous histological entities displaying particularity with respect to location, morphology and staining affinities which were either not previously described, inadequately described or assigned names which were either confusing, doubtfully appropriate, or wrongly implied a function. Similarly, the nomenclature available to describe the morphology and micromorphology of the shell parts was inadequate and in some cases seriously misleading. At its worst, e.g., in calling the secretory sheet ubiquitously seen in the lateral Marginal Mantle Groove of the *Pinctada* "forming periostracum", the commonly used nomenclature was not only wrong but its use was inextricably interwoven with long held and oft repeated wrong notions. Use of this nomenclature tended to preclude the understanding of the function of all the tissues of the Mantle Margin.

The reporting of this work therefore necessitated the generation of a nomenclature appropriate to the structures to be described. Previously used terms which still had validity have been retained. Names which imply a knowledge of function which is either wrong or in doubt have been eliminated and replaced with names which form part of a nomenclature which is rigidly and accurately descriptive of morphology, or location, or, where universally consistent, staining affinities, or a combination of these. As the functions of the tissues and glands are ascertained with certainty in the future, where appropriate, functional names can replace descriptive ones.

The arrangement of the Results, with only partial descriptions of the tissues and shell organic matrices of the species preceding the pearl oysters, and the coherency of the nomenclature, made it an absolute requirement for the presentation of the Results that the nomenclature be presented as a separate chapter preceding the Results.

Since repeated usage over a long period of erroneous and ambiguous nomenclature has played such a significant role in the perpetuation of erroneous notions of bivalve shell production, and since this thesis employs such a large number of proposed new terms, throughout this thesis upper case will be used for the first letter of all terms used as formal nomenclature.

Further, for clarity, anagrams will be used very sparingly and except as specifically noted in the text will be used only for light microscopy, scanning electron microscopy and transmission electron microscopy which are referred to as L.M., S.E.M. and T.E.M. respectively.

1.19. SPECIES SPECIFICITY OF THE MANTLE AND MANTLE MARGIN HISTOLOGY AS A BASIS FOR CLASSIFICATION OF THE GENUS PINCTADA.

The species specificity of the Mantle and Mantle Margin histology of those pearl oyster species, where uniqueness and constancy of shell features makes identification certain, is such that, where sufficiently detailed, the illustrations of the histology of *Pinctada maxima* given in the publications of Dix (1972,1973) would serve equally as well as the illustrations used in this thesis for a description of the histology of that species. Similarly, again where sufficiently detailed, the illustrations of the histology of *P. margaritifera* given by Fougeropuse - Tsing and Herbaut (1994) from specimens collected in French Polynesia would serve equally as well as those used in this thesis for illustrating the histology of the Mantle and Mantle Margin of *P. margaritifera*. The same differences in histology seen in the publications of Dix (1972, 1973) (*P. maxima*) and that of Fougerouse - Tsing and Herbaut (1994) (*P. margaritifera*) are demonstrated in the illustrations of the histologies of these two species in this thesis.

Again, the species specificity of the External Mantle and Mantle Margin histology with respect to sequences of tissues and staining affinities of the component secretory glands of these different tissues is illustrated for four different specimens of the pearl oyster *P. albina sugillata* in Fig. 5.141.

Thus species specificity of the histology of the Mantle and Mantle Margin of pearl oysters holds over decades in time and thousands of kilometres in distance.

This rigidity in species specificity in histology is to be expected in tissues which are involved in a function as intrinsically complex as the secretion of the precursors of scleroproteins (Waite, 1983), - especially where the chemical attributes of the resultant scleroproteins determine not only the types of calcareous mineralisation deposited, (e.g. calcite or aragonite), but even the allignment of the crystallographic axes, (Weiner et al. 1983), and therefore the success or otherwise of the resulting shell layer as part of a functional shell.

As a corollary, where there are gross differences in the histologies of the mantle and mantle margins of specimens of pearl oysters they must necessarily belong to different species. Otherwise the particularity of micromorphology of the shells of pearl oyster species would have to be held to result from the combination of secreted precursors from some mixture of secretory glands resulting from the heritability of not only the physiological control mechanisms but also the location, relative frequencies and chemical nature of the products of different types of secretory glands and/or different tissues such as those illustrated in Figure 5.142.

However the selection pressure in this case is not for any particular sequence or combination of secretory glands but for a functional shell. This being so, any genetic change which resulted in an altered Mantle and Mantle Margin histology which still produced an equally functional shell was selected for equally, from this point of view, with selection for lack of genetic change. Inevitably this has resulted in errors in classification in the pearl oysters where genetically very different animals with very different histologies have produced very similar shells, and gross shell morphology alone has been relied on, or given undue weight, in classification.

Thus while it was possible for the Australian members of the Genus *Pinctada* to be classified into six species from a study of their shell features, (Hynd, 1953), this classification is manifestly deficient following a study of the glands and tissues responsible for the secretion of the precursors of the Shell Organic Matrices.

CHAPTER 2.

MORPHOLOGICAL, ANATOMICAL AND HISTOLOGICAL NOMENCLATURE

INDEX

2.1. Introduction

Inevitably, matters will be referred to in this section which more properly belong in Results. They will be given here only in as far as is necessary for a full and coherent nomenclature and then formally presented in Results.

Previously used nomenclature of the morphology, anatomy and histology of pearl oysters was to some extent deficient and otherwise inaccurate or confusing. A nomenclature has been devised which is rigorously descriptive and, where appropriate, universally applicable throughout the Bivalvia. Many of the terms are in common use and are retained. Others have been devised to facilitate the reporting of this work. Where the author found terms in common usage to be inaccurate or wrong they have been dropped and replaced with accurate descriptive terms.

Where nomenclature appropriate to species of the genus *Pinclada* is inappropriate for species of *Pteria, Isognomon* or *Malleus* or bivalves other than pearl oysters in this study, a suitable nomenclature is given.

2.2. SHELL MORPHOLOGY NOMENCLATURE.

Here, the terminology used by Hynd (1955) is adopted and, where necessary, added to. The shell morphology described as a type for the *Pinctada* is that of a young adult *Pinctada margaritifera* The reasons for this choice are: It is a commercial species found over a large range of the Indo-Pacific thus is well known (Gervis and Sims, 1992); like most members of the *Pinctada* it has a byssus throughout its adult life (Hynd, 1955); and its Hinge, Prismatic Layer and Inner and Outer Nacreous Layers are moderate in morphology, (Hynd, 1955; Fougerouse-Tsing and Herbaut, 1994). Where necessary for clarification or comparison other species of pearl oysters will be referred to.

The orientation, by convention, of a bivalve, in this case *P. margaritifera*, is shown in Figure 2.1.. The periphery near the Hinge is the Dorsal Border. The Ventral Border is that opposite the Hinge. The Byssus projects to the Anterior and the opposite border is Posterior. Thus the Right Valve is the one on the right of any intact animal (or pair of joined Valves) held with the Hinge horizontal and Dorsal and the Anterior Periphery away from the holder. The opposite is the Left Valve, (Fougerouse-Tsing and Herebaut, 1994). The valves of *Pinctada margaritifera* are nearly equal in concavity, have relatively large and similar areas covered by nacre and are about equal in their antero-posterior and dorso-ventral axes, (Figures 2.1., 5.82). Other species are not so regular and the terminology used to describe their regularity or lack thereof is that used by Hynd (1955).

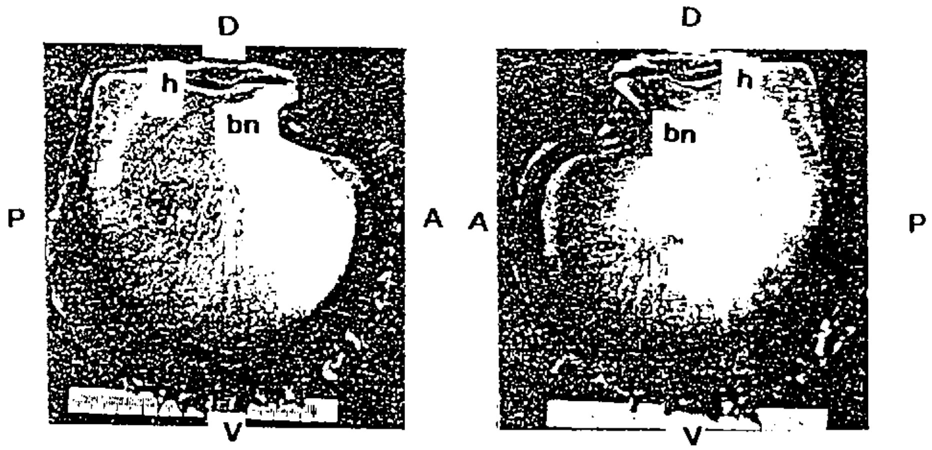

Figure 2.1. Valves of *P. margaritifera*. x 0.5. Left Valve on left, Right Valve on right. D = dorsal; V = ventral; A = anterior; P = posterior; h = Hinge; bn = Byssal Notch.

The shell consists of three parts. The Hinge is composed of protein rubber (Shadwick and Gosline, 1983) and joins the two **Valves** in about the dorsal midline. It consists itself of three parts - dorso-ventrally short **Anterior** and **Posterior** parts and a ventrally enlarged **Middle Part**. This latter occupies about the third and fourth sevenths of the hinge going antero-posteriorly (Figure 5.82).

The calcified valves are themselves comprised of three parts - an outer Prismatic Layer lateral to Outer and Inner Nacreous Layers, (Taylor, 1973).

Viewed laterally, the **Byssal Notch** in *Pinctada margaritifera* is a large almost right angle notch in the antero-dorsal part of the border of each **Valve**. In **Valves** with a hinge of 7cm. length the **Byssal Notch** measures approximately 3cm. x 3cm. (Figure 5.82).

The Prismatic **Layer** covers the entire lateral surface of a **Valve** unless worn away or broken off. It also constitutes the entire periphery of the **Valve** and forms a relatively wide band around the inner valve surface inside the periphery. This is because the Outer Nacreous Layer does not reach to the periphery of the medial surface (Figure 5.82).

Viewed laterally, the Prismatic Layer in a *Pinctada margaritifera* specimen of this size appears to be covered by about twenty more or less curvilinear (but occasionally branching or joining) radiating series of blunt distally pointing spines which are flattened latero-medially. These radiate from the Umbonal Region and the external spines of each series project beyond the rest of the border of the Valve for about 1cm. These spines termed Growth Processes are most prominent on the distal half of the border of the Valve, (Figure 5.82).

The width of the Prismatic Layer on the medial surface of the **Valves** of the specimen described ranges from about 1cm. Anteriorly and 1.5cm. **Ventrally** to about 0.5cm. on the Dorsal half of the Posterior Border, (Figure 5.82).

The Nacreous Layers, composed of medio-laterally flattened aragonitic Nacre Tiles surrounded by Organic Matrix, and arranged in Nacre Sheets, (Nakahara, 1991), cover the medial surface of the Valves with the exceptions of the periphery, that area covered by Hinge, and that covered by the Adductor Muscle Scars, (Figure 5.82).

In *Pinctada margaritifera* and the gold lip form of *Pinctada maxima* the Outer Nacreous Layer is more easily distinguishable from the Inner Nacreous Layer by eye than by light microscopy (L.M.) of the shell or sections of decalcified shell. The differences seen under scanning electron microscopy (S.E.M.) will be described in "Results", Chapter 5.

The Adductor Muscle Scar is kidney shaped, its concavity directed towards the byssal notch. It lies almost wholly in the posterior dorsal quarter of the shell medial surface, its most antero-ventral point being approximately the bisection of the dorso-ventral and antero-posterior axes of the shell (Figure 5.82).

The study of the shell of *Pinctada margaritifera* and indeed of all similar bivalve shells by L.M. and S.E.M. have presented major problems of interpretation and hence nomenclature which remain unresolved. In some cases S.E.M. of radial broken surfaces dramatically clarified what had been a blurred suggestion under L.M.. In other cases features commonly and clearly seen in an array of related species with stained radial sections of acid-decalcified shell Organic Matrices under L.M. have seldom been observed with S.E.M. of radial broken surfaces, (Figure 5.96 c.f. Figures 5.97-5.99). For this reason an appropriate nomenclature to describe features observed with stained sections of decalcified shell of a *Pinctada*, *(P. margaritifera)* under L.M. will be given, and then one applicable to those features seen under S.E.M.. Presumably the features seen with S.E.M. but not observed or of doubtful morphology with L.M. are either too fine structured for the latter technique or were solubilized or damaged by decalcification. Those features seen in L.M. of decalcified shells which have not been observed under S.E.M. are either hidden by the calcium carbonate crystals or obscured by other material which is removed in the process of decalcification.

2.2.1. LIGHT MICROSCOPY OF ORGANIC MATRICES FOLLOWING ACID DECALCIFICATION.

2.2.1.1. Nacreous Layers.

Under L.M. in radial section the decalcified and stained Inner and Outer Nacreous Layers of *Pinctada margaritifera* (or any species of the pearl oysters studied), are indistinguishable from each other. The entire thickness of the Nacre seen sagittally is divided into irregularly spaced and sometimes anastomosing strands of substance with a fine fibrous appearance, the fibres lying radially. (The decalcified and stained Inner and Outer Nacreous Layers of the Nuculoidea studied are physically separate; those of the Mytiloidea are physically distinct).

In *Pinctada margaritifera*, (as in nearly all specimens of all species with a calcitic simple Prismatic Layer outside Nacreous Layers), in radial section with L.M., small and sometimes isolated particles of Prismatic Layer material can be observed between thicknesses of Nacreous Layer. These almost invariably increase in size and frequency towards the distal extremity of the thicknesses of Nacre Sheets they lie between, (Figures 2.2 and e.g. in *Isognomon ephippium*, 5.152. a, b and c), until they form the most proximal prisms of the continuous proximal end of a layer of Prismatic Layer, i.e. a Growth Scale.

lateral

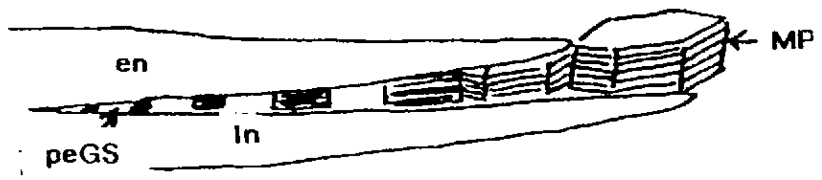

mediall

FIGURE 2.2. *P. margaritifera* - Radial section decalcified Valve. Proximal end of Growth Scale between distal extremities of successive depositions of Nacre. en = earlier nacre; ln = later nacre; peGS = proximal end of Growth Scale; MP = Major Prism.

2.2.1.2. Prismatic Layer.

The long axes of the Prisms of the Prismatic layer are normal to the shell surface, and being polygonal, (tending to hexagonal), in sagittal section, they form a honey-comb pattern viewed laterally or medially.

The morphologies of the calcitic simple Prismatic Layers of pearl oysters are species specific. The most obvious differences between the Prismatic Layers of different species viewing stained radial sections is the degree by which the successive Growth Scales are physically defined.

In *Pteria penguin*, viewed sagittally in radial section, the Prismatic Layer consists of a number of elongate distorted spindle shaped Growth Scales partly superimposed but with each successsive medial one partially displaced distally.

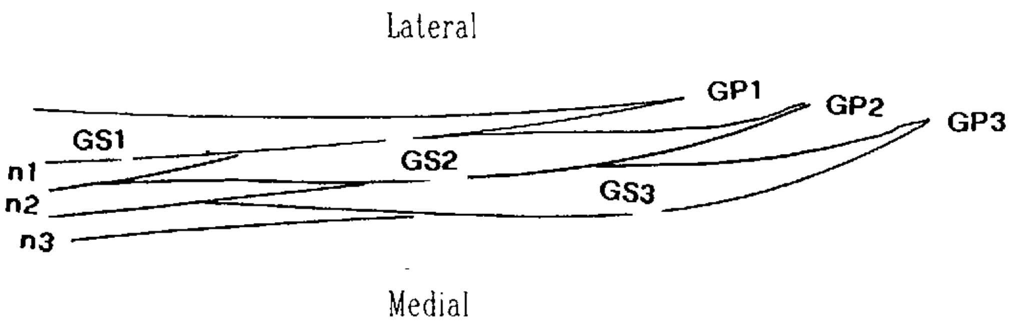

FIGURE 2.3. *Pteria penguin* - Distal extremities of successive depositions of nacre separating the proximal ends of successive Growth Scales. n1,n2,n3 = successively later depositions of nacre respectively; GS1, GS2, and GS3, GP1, GP2, and GP3 = Successively later laid down Growth Scales and Growth Processes respectively.

The proximal end of each spindle shape lies between the distal ends of two strands of nacre, (Figures 2.3. and 6.59). The spindles increase in width towards the middle and then taper toward their free, distal extremities where directed towards the Valve periphery and slightly laterally. The free extremity of the last laid down (or at least a recent) spindle forms the actual periphery of the Valve.

Viewed medially, (Figure 2.4.), (this distorted spindle is the radial section viewed sagitally), the Growth Scale, is a distorted horseshoe in the shape of the Anterior Ventral and Posterior Borders of the Valve at the time of it's deposition. As above, its proximal border lies between the two depositions of Outer Nacreous Layer immediately preceding and succeeding its deposition. The distal border is thrown into somewhat irregularly shaped and placed protruberances, the Growth Processes. The remainder of the distal border is termed the Distal Free Border of the Growth Scale, (Figures 2.4. and 5.142). Therefore the distal free extremity of the spindles seen in the sagittal view of a radial section may be either Growth Process or Distal Free Border of the Growth Scale depending on the location of the radial section.

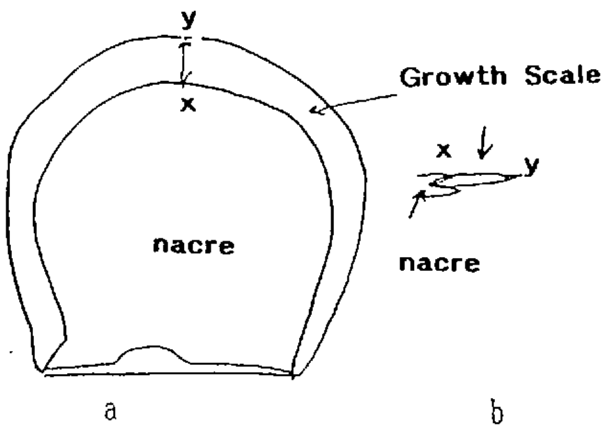

FIGURE 2.4. Growth Scale, a medial view. b, sagittal view of radial section.

Most Growth Scales of *Pteria penguin* are covered laterally for at least part of their length, by a continuous, relatively thick, strong staining layer of Organic Matrix - the Outer Fibrous Sheath of the Growth Scale, and where this is absent, by the Outer Prismatic End Plates. The Growth Scales of this species, as for all species studied with this type of Prismatic Layer, have the medial surface of their Growth Scales covered with an Inner Fibrous Sheath only for the distal part of the Growth Scale - i.e. on medial view of the last produced Growth Scale, this Inner Fibrous Sheath invariably terminates between the peripheral Nacreo-prismatic Junction and the distal edge of the Growth Scale. Because of the sometimes present continuous Outer Fibrous Sheath, and the normally present Inner and Outer Prismatic End Plates, Growth Scales in this species, in radial section viewed sagittally, usually appear as discrete well defined elongate spindles, (Figures 2.3 and 5.143).

In marked contrast, the Prismatic Layer of *Pinctada fucata* presents, in sagittal view of a radial section, as a single layer of Major Prisms (q.v.) covering the entire lateral surface of the valve (where not eroded). Structures analogous to the pointed free extremities of the spindles as seen in *Pteria penguin* (Growth Processes or Distal Free extremities of the Growth Scales), arise without apparent proximal physical continuation, (Figure 2.5.). That is, the Outer Fibrous Sheath terminates proximally at the junction of the lateral surface of a Growth Scale with the medial surface of the Growth Scale lateral to it, (Figure 2.5. and 5.127, a).

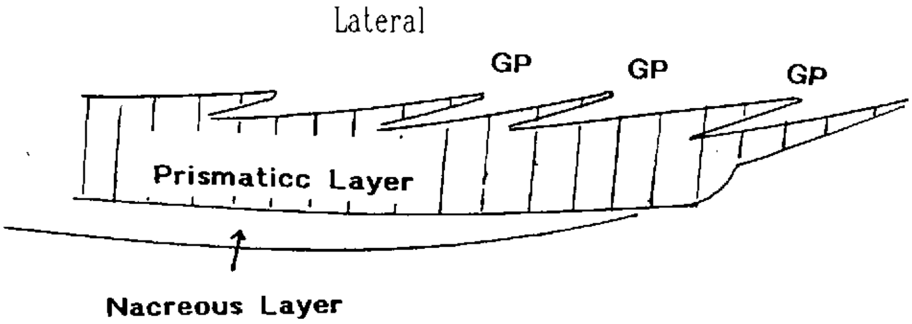

FIGURE 2.5. *Pinctada fucata* -Prismatic Layer. GP = Growth Processes.

All members of the genera *Pinctada*, *Pteria*, *Isognomon* and *Malleus* studied have Prismatic Layers whose overall structure falls in between the two extremes of *Pteria penguin* and *Pinctada fucata*.

The Growth Scales of *Pinctada margaritifera* have, like *Pteria penguin* but unlike *Pinctada fucata*, Proximal Borders which commence between the distal parts of two thicknesses of Outer Nacreous Layer (Figure 2.6).

Viewed radially, this may or may not continue distally as a discrete spindle bordered laterally by the Outer Fibrous Sheath, (Figure 5.93. b). Where there is no Outer Fibrous Sheath over Outer Prismatic End Plates, (Figure 5.97.a), on the lateral surface of any Growth Scale and the Major Prisms (q.v.) continue across the boundary of successive Growth Scales, the Prismatic Layer of *P. margaritifera* is analogous in structure to the Prismatic Layer of *Pinctada fucata* ; where each of the spindles has an Outer Fibrous Sheath or where the Major Prisms of a Growth Scale have Outer Prismatic End-plates it has the appearance of *Pteria penguin* (Figures 5.93. b. and 5.97. b and c).

The lateral surfaces of all Growth Processes of *Pinctada margaritifera* are covered by a thick fibrous sheath - the Outer Fibrous Sheath of the Growth Process, (Figure 5.95. d, e, f and g). The distal parts of the medial surfaces of the Growth Processes are also covered by a fibrous sheath which is less robust than that which covers the lateral surfaces. This is termed the Inner Fibrous Sheath of the Growth Process. (Figure 5.94 b. c and d).

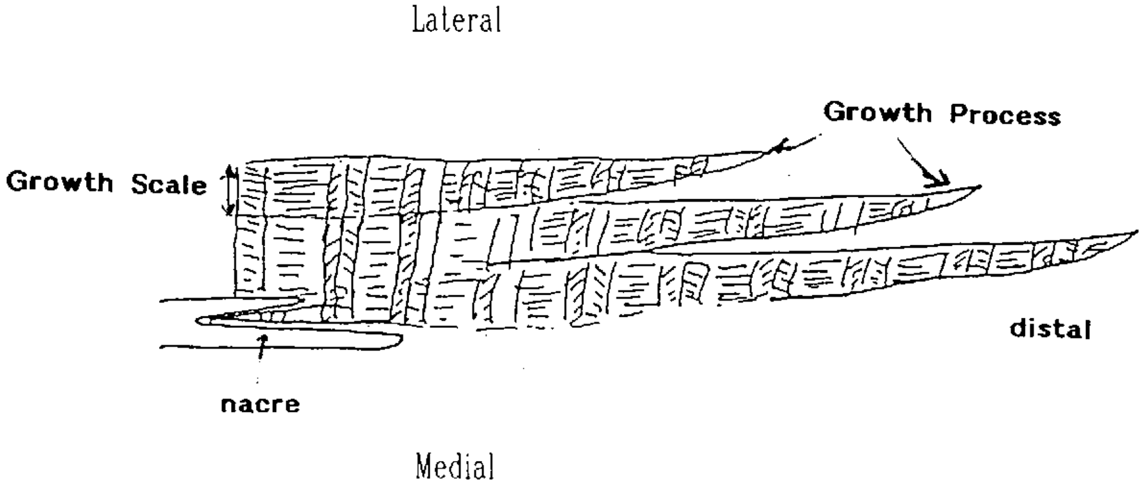

FIGURE 2.6. Prismatic Layer of *Pinctada Margaritifera.*

Prismatic Layers of the Pterioidea studied stain predominantly a certain colour, but bands of different colouration occur, invariably tracing out the shape of a Growth Scale lateral surface in a plane medial and parallel to the Outer Fibrous Sheath in Valves of *Pteria penguin* like construction. or to where the Outer Fibrous Sheath of a Growth Scale would have continued proximal to the Growth Process were the Valve of *Pteria penguin* like construction. (*Pinctada maxima* Figure 5.40 c; *P. margaritifera* Figure 5.97. a and b; *P. fucata* Figure 5.127 a; *Pteria penguin*, Figure 5.143).

A Major Prism is the single prismatic structure with polygonal. commonly hexagonal. outline in sagittal section which occupies the space between the Outer Fibrous Sheath of a Growth Scale and the medial physical termination of that prismatic structure. This medial termination may be the medial surface of that

Growth Scale, the lateral or medial surface of a Growth Scale medial to it, or the medial surface of the Prismatic Layer at the radial Nacreo-prismatic Junction, and whether fibrous or not.

A Major Prism (under L.M.) consists of an Outer Prismatic End Plate, Inner lateral Structure, Parallel Transverse Prismatic Side Walls, Intra-prismatic Organic Matrix, and sometimes an Inner Prismatic End Plate, (Figures 5.40, and 5.97-5.99).

Lateral

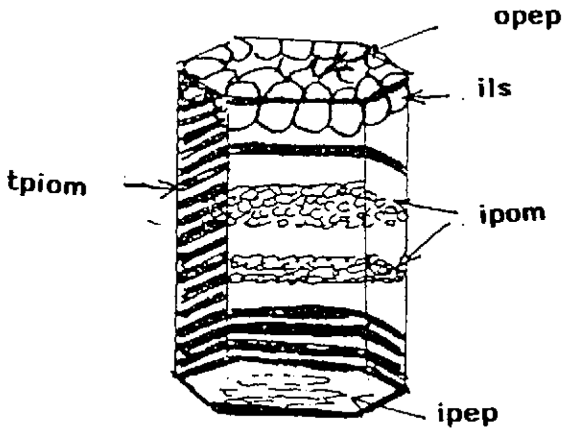

Figure 2.7. The Parts of a Major Prism with L.M.. opep = Outer Prismatic End Plate; ils = Inner Lateral Structure; ptiom = Parallel transverse Inter-prismatic Organic Matrix; ipom = Intra-prismatic Organic Matrix; ipep = Inner Prismatic End Plate.

An Outer Prismatic End Plate is a membranous structure covering the lateral end of a Major Prism or Growth Process Prism (Figure 5.99 d, and 5.97, b). The Inner Lateral Structure is an ill-defined Organic Matrix sub-structure in the lateral end of the Major Prism. Where the Organic Matrix of the Inner Lateral Structure joins the Outer Prismatic End Plate this results, in lateral view, in a lead-light window pattern, (Figure 5.99, a, b, c and d). The Transverse Parallel Side Walls, which are common to adjacent Prisms, are composed of touching parallel straps of Organic Matrix which join those of adjacent Prismatic Side Walls in a swelling. They predominantly stain one colour but bands of aberrant staining have occurred in any Prismatic Layer examined (Figures 5.97 - 5.99).

The Intra-prismatic organic matrix invariably exists as a wispy and usually collapsed structure lying within each Prism which stains distinctly differently - shades of blue to dark blue/grey - from the other remaining Prismatic Organic matrices, (Figures 5.97, d and 5.98, c and d). It will be described more fully under the section on Nomenclature of structures seen in the Prismatic Layer with S.E.M.

The Inner Prismatic End Plates differ from Outer Prismatic End Plates in structure in that they commonly have three or four lighter staining elliptical areas which lie so that the long axes of the ellipses are parallel, as distinct from the lead-light appearance of the Outer Prismatic End Plates.

2.2.2. SCANNING ELECTRON MICROSCOPY OF PEARL OYSTER SHELLS

2.2.2.1. Nacreous Layers.

S.E.M. of the Nacreous Layers shows them to consist of numerous individual medio-laterally flattened tablets, Nacre Tiles, which occur in more or less parallel Nacre Sheets. (Figures 5.85 - 5.91). The thickness of the Nacre Sheets may depend on species and position on the shell.

In medial view, although the Nacre Tiles in the Nacre Sheets tends to a rough hexagonal shape, (medio-laterally), they are in fact polygonal and usually irregular. The Nacre Tiles in the edges of the Nacre Sheets are less tightly opposed to each other than those further from the edge and tend to have an outline of some regular geometric shape. Depending on species, and to a lesser extent position on the Valve, these geometric shapes may be a regular hexagon, an elongate hexagon, diamond shape, truncated diamond shape or truncated orthorhombic shape. These are the Partly-bound Nacre Tiles. Beyond the Edge of the Nacre Sheet (and therefore resting on the Bound Nacre Tiles of the next most lateral Nacre Sheet) there are Free Nacre Tiles invariably of the same geometric shape as the Partly Bound Nacre Tiles adjacent to them. These Free Nacre Tiles decrease in size with distance from the Edge of the Nacre Sheet, Figure 2.8. and Figures 5.85 - 5.90).

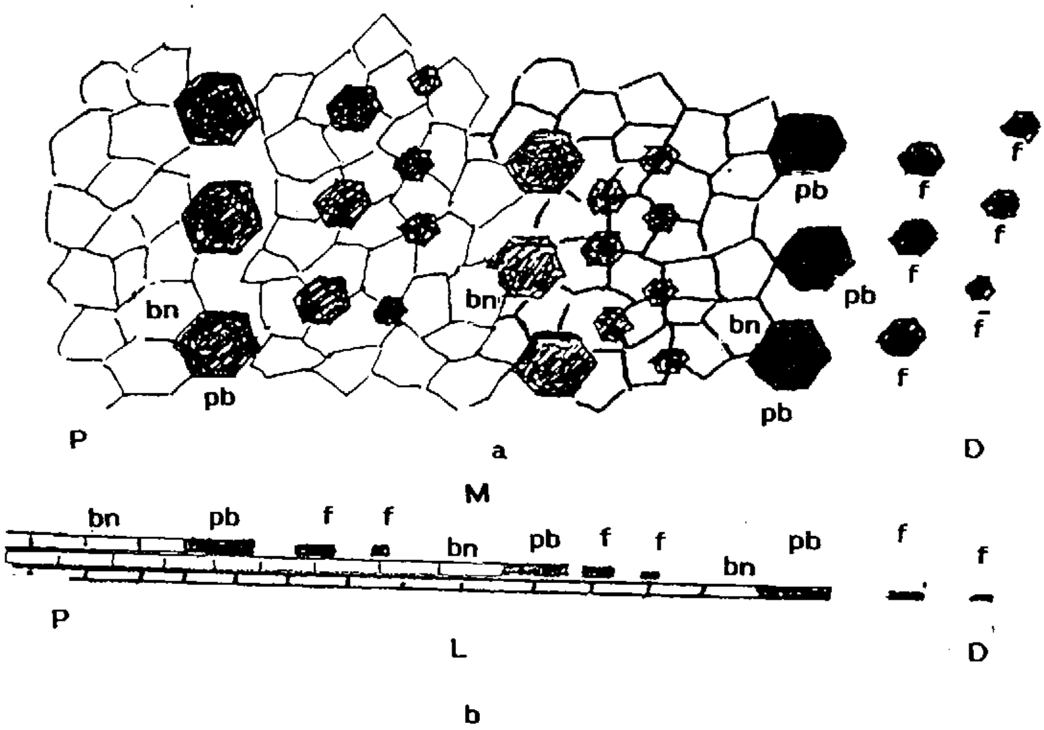

Figure 2.8. Diagrammitic representation of S.E.M. of Pearl Shell Nacre. Nacre Sheets and Bound, Partly-bound and Free Nacre Tiles.

2.8. a, medial view.

2.8. b, sagittal view of radial broken surface.

bn = Bound Nacre Tiles; pb = Partly Bound Nacre Tiles; f = Free Nacre Tiles; P = proximal; D = distal; M = medial; L = lateral.

Also depending on the species and the part of the Valve examined, the Edges of the Nacre Sheets may describe concentric circles, spiral structures, curvilinear structures or parallel lines, (Figures 2.9, and. 5.85 - 5.90).

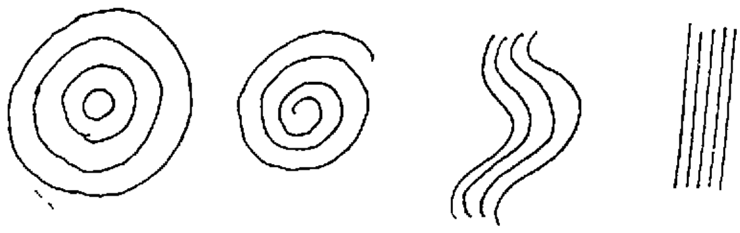

a b c d

Figure 2.9. Patterns of Edges of Nacre Sheets. a, concentric circles; b, spiral structure; c, curvilinear structure; d, parallel lines

Where radial broken sections are viewed sagittally, the Nacre Tiles in consecutive Nacre Sheets commonly are displaced distally similar distances from the equivalent Nacre Tile in each successive Nacre Sheet so that they appear to form a regular stepped pattern - a Nacre Stair (Figures 2.10, and 5.91, c and d)

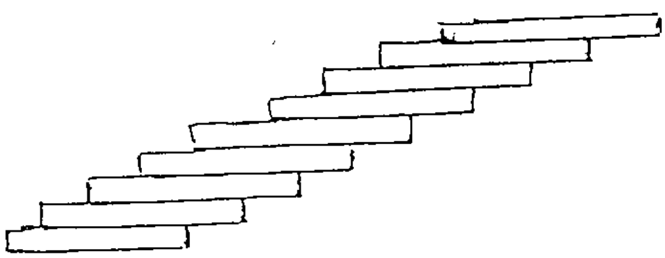

Figure 2.10. Pearl Oyster Nacreous Layer. Sagittal view of radial broken surface. Nacre Stair.

2.2.2.2. **Prismatic Layers.**

S.E.M. of the **Prismatic Layer** of pearl oysters confirms that the lateral surface of the **Growth Processes** and part or all of the **Growth Scales** proximal to the **Growth Processes** (depending on species) are covered by the **Outer Fibrous Sheath**. This demonstrates unique features in some species and may well prove to be species specific.

Medial to the **Outer Fibrous Sheath**, each **Prism**, whether of **Growth Process** or a **Major Prism**, is covered by the **Outer Prismatic End Plate**. These are of different patterns in at least some different species and again may be species specific. These patterns range from concentric circles in one species to, in another, a pattern of roughly isosceles triangles with their apices at about the geometric centre and their bases the sides of the polygon of which the prism end is made - a spider web like pattern, (Figure 2.11.).

Figure 2.11. S.E.M. of **Outer Prismatic End Plates.**

The **Inner Lateral Structure** which is clearly visible in all radial sections of **Prismatic Layer** of decalcified pearl shell is difficult to identify under S.E.M. (*Pteria penguin* Figure 5.145).

Similarly the **Transverse Parallel Side Walls**- the major feature of decalcified pearl shell **Prismatic Layer** (*Pinctada maxima* Figure 5.40, *P. margaritifera*, Figures 5. 97 - 5. 99) -have rarely been clearly identified with S.E.M. of radial broken surface of pearl shell **Prismatic Layer**. What appeared to be **Transverse Parallel Side Walls** was seen on the radial broken surface of a pearl shell largely destroyed by a boring sponge, (*P. maxima* Figure 5.44).

In all other specimens of radially broken surface of Prismatic Layer one, or more often, more than one of three structures was seen - the Intra-prismatic Organic Matrix, the Reteform Inter-prismatic Organic Matrix and/or the Linear Pattern Inter-prismatic Organic Matrix.

The Intra-prismatic Organic Matrix of a Major Prism is a series of parallel sheets in planes at right angles to the long axis of the Major Prism, perforated in three dimensions to present a netlike appearance from any aspect, and dividing the Major Prism into numerous compartments, (Figure 2.12.).

In each of these compartments is a moderately thick calcite tablet.

This material of which the Intra-prismatic Organic Matrix is made is very similar to, and may be the same as, the most commonly seen of the three different types of Inter-prismatic Organic Matrix - the Reteform Interprismatic Organic Matrix.

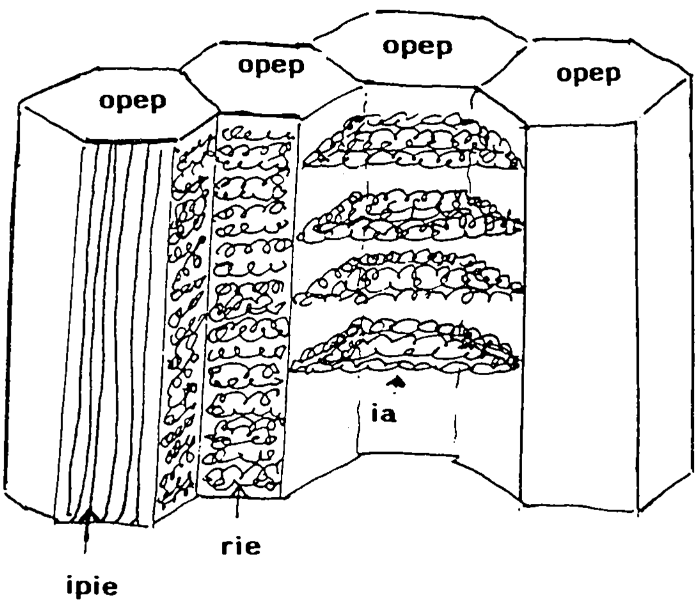

Figure 2.12. S.E.M., Sagittal view of radial broken surface of pearl shell Prismatic Layer. Ipie = Linear Pattern Inter-prismatic Organic Matrix; rie = Reteform Inter-prismatic Organic Matrix, ia = Intra-prismatic Organic Matrix; opep = Outer Prismatic End Plate of a Major Prism.

Most commonly seen on the walls of Growth Process Prisms and less commonly on the walls of Major Prisms is a sheet of Interprismatic Organic Matrix with a pattern of folds which run parallel to the long axes of the Prisms - the Linear Pattern Inter-prismatic Organic Matrix. (in *Pinctada maxima* Figure 5.39). It is believed that this structure lies between the Reteform Inter-prismatic Organic Matrix and the Transverse Parallel Side Walls seen under L.M. of decalcified pearl shell Prismatic Layer. The latter are common to adjacent Prisms. (Figures 5.97 - 5.99).

The Inner Prismatic End Plates which are commonly seen on L.M. of decalcified pearl shell Prismatic Layer are usually unclear on S.E.M. where it is difficult to distinguish mineral phase from Organic Matrix on the uncovered end of Major Prisms.

The medial surface of the distal part of the Growth Scales and the medial surface of all Growth Processes are covered with a relatively fine textured Inner Fibrous Sheath (in *Pinctada maxima*, Figures 5.34. c. and 5.40., b), lacking the small protruberances which are a feature of the Outer Fibrous Sheath.

Covering the distal surfaces, (most commonly the medial surface), of many Growth Scales is an apparently detrital material which, like the Outer Fibrous Sheath, bears small protruberances (Figure 5.92, a and b). This is thought to be the detrital remains of the Pleated Secretion of Groove F1F2.. (Figure 5.110, a and b). This detrital material appears to serve little or no structural function.

Only confusion is added to the picture by referring to any of the above structures as "Periostracum" or "Conchiolin" and for this reason neither of these confusing and abused terms will be used to describe any structure in this work.

2.3. EXTERNAL MANTLE AND MANTLE MARGIN NOMENCLATURE.

2.3.1. ANATOMICAL NOMENCLATURE.

Unless otherwise stated the description is of *Pinctada margaritifera*.

Inside the Valves the right and left lateral surfaces of a pearl oyster are covered by the tissues of the External Mantle and the Anterior, Ventral and Posterior periphery of the Mantle bear the Folds of the Mantle Margin.

2.3.1.1. Anatomical Nomenclature of the External Mantle.

Where the right and left Mantle Margins join at the antero-dorsal and postero-dorsal corners of the animal the junctions are referred to as the Anterior Mantle Symphysis and Posterior Mantle Symphysis respectively.

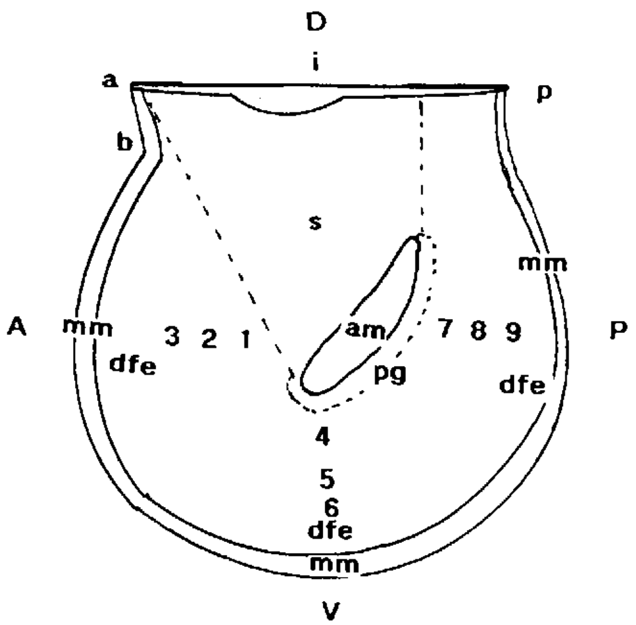

Figure 2.13. Anatomy of Left External Mantle and Mantle Margin of *Pinctada margaritifera*, lateral view. A = anterior; P = posterior; D = dorsal; V= ventral; a = Anterior Mantle Symphysis; p = Posterior Mantle Symphysis; i = Isthmus; s = Shoulder Region; am = Adductor Muscle; pg = Pallial Gland Region; dfe = Distal Folded Region; mm = Mantle Margin; 1 - 9 = Proximal, Middle and Distal, Anterior, Ventral and Posterior Pallial Regions respectively.

The raised ridge of tissue occupying the dorsal midline and joining the Anterior and Posterior Mantle Symphyses is the Isthmus.

For reasons of histological differentiation, the area bounded by the Isthmus dorsally, the dorso-anterior concavity of the Adductor Muscle ventrally, and the line joining the Anterior Mantle Symphysis to the most anterior point of the Adductor Muscle, and the perpendicular from the dorsal point of the Adductor Muscle to the Isthmus, together with the oppposing Inner Nacre of the Valve and the intervening space, is referred to as the Shoulder Region.

Viewed laterally the Anterior, Ventral and Posterior borders of the Adductor Muscle are surrounded by an area of Mantle which appears silvery to the naked eye. This is because of the strong sheet of subepithelial connective tissue which separates the surface epithelium of this region from the dense layer of secretory glands, the Pallial Gland, beneath it. This area and the opposing Inner Nacreous Layer and the intervening space is the Pallial Gland Region (Figure 2.13).

The Pallial Region is that part of the External Mantle epithelium and Subepithelium, the opposing Inner Nacreous Layer and the intervening space between the Pallial Gland Region proximally and the Distal Folded Region (q.v.) distally (Figure 2.13.). This is divided into nine region to accord with the nine divisions of the Pallial Mantle.

The Distal Folded Region refers to that area of the External Mantle and opposing Nacreous Layer and intervening space roughly lateral to the Circumpallial Nerve and characterized by more or less deep outfoldings of the Mantle in and about the region occupied by the Pallial Line in those Bivalves where the distal External Mantle is physically joined to the medial surface of the Valve.

2.3.1.2. Mantle Margin.

Distal to the Distal Folded Region are the structures and tissues of the Mantle Margin.

In the genus *Pinctada* there are three Marginal Mantle Folds while in the genera *Pteria*, *Isognomon* and *Malleus* there are four. However the structures and the resultant Pleated Secretion, (Figure 2.18), of the apical region of the Groove between the outer and middle Marginal Mantle Folds of the *Pictada* are very distinctive and all remarkably similar. They are also very similar to the structures and the secretion of the apical regions between the second from the outer and third from the outer Marginal Mantle Folds of all species of *Pteria*, *Isognomon* and *Malleus* studied, (Figures 5.147, 5.148, b, 5.149, c, 5.150, a and b, 5.153, c and d, 5.154,b). For these and other reasons more fully described later (Chapter 6.1.), the three Marginal Mantle Folds of the species of the genus *Pinctada* are termed, from without inwards, FoldF1., FoldF2., FoldF3., and the Marginal Mantle Folds of the species of *Pteria*, *Isognomon* and *Malleus* studied are, from lateral to medial, FoldF1., Ancillary FoldF1., FoldF2., and Fold F3.. The Folds are routinely referred to as F1.,F2.,F3., etc., and the words lateral and medial reduced to Lat and Med when used in conjunction with F1.,F2., etc. to denote a Region. Thus Middle LatF2. is read as the middle part of the lateral surface of the Marginal Mantle Fold second from the lateral surface and, depending on usage, may apply to surface secretions, surface epithelium, subepithelial connective tissues, subepithelial secretory glands, nerves, sinus, etc., (Figures 2.14 and 2.16 - 2, 20).

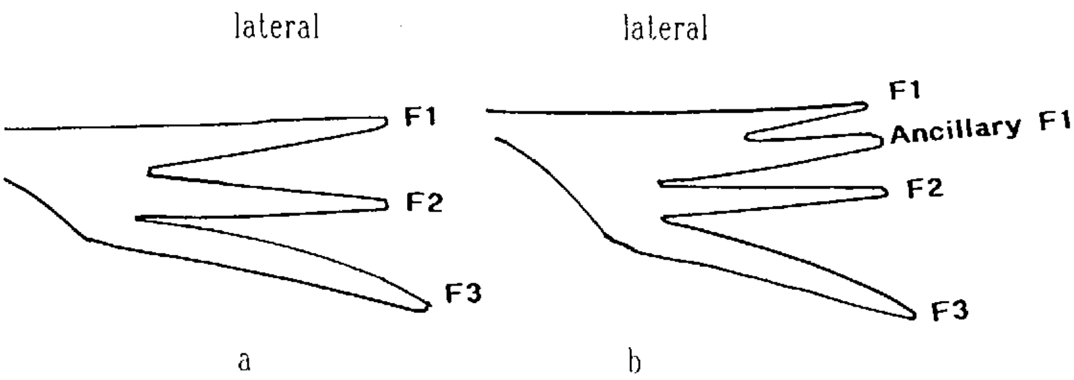

Figure 2.14. Radial Section of the Mantle Margins of a. *Pinctada* and b. *Pteria*.

The Marginal Mantle Folds are then further subdivided on anatomical grounds into LatF1., MedF1., (Lat Ancillary F1., Med Ancillary F1.) LatF2., MedF2., and LatF3., and further subdivided on histological grounds into tissues, (see below).

The perjorative terms "Shell Fold", "Sensory Fold" and "Muscular Fold" are considered both inaccurate and misleading and hence are not used in this work.

In the *Ostreoidea*, (Genera *Hyotissa*, *Ostrea* and *Crassostrea*), there are four Marginal Mantle Folds ("Results" Chapter 5), because of bifurcation of Fold F2.. In all other Bivalves studied there are between two and five Marginal Mantle Folds and their functions in shell formation and relationships to the three Marginal Mantle Folds of the *Pterioidea*, where known, will be described in the appropriate Chapters - ie. 5 and 6.

2.3.2. HISTOLOGICAL NOMENCLATURE OF THE EXTERNAL MANTLE AND MANTLE MARGIN.

Included under this heading are the names given to tissues and cellular structures, glands and secretions of the mantle and Mantle Margin.

2.3.2.1. The External Mantle - Tissues.

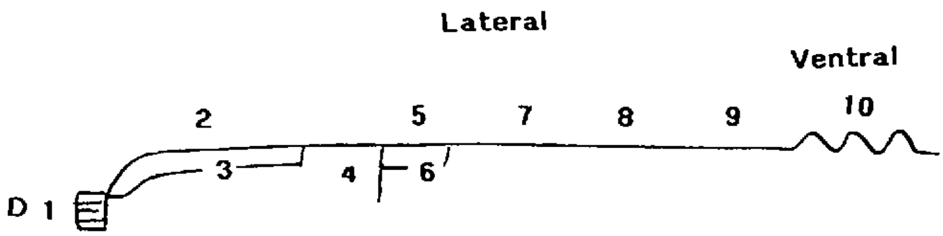

Figure 2.15. Tissues and Regions of the External Mantle of the *Pinctada*. 1 = Isthmusistic Epithelium; 2 = Shoulder Region; 3 = Shoulder Gland; 4 = Adductor Muscle; 5 = Pallial Gland Region; 6 = Pallial Gland; 7 = Proximal Pallial Region; 8 = Middle Pallial Region; 9 = Distal Pallial Region; 10 = Distal Folded Region.

The Isthmusistic Epithelium consists of elongate columnar epithelial cells which cover the dorsal surface of the Isthmus for its entire length and extend down its lateral surfaces paralleling the extent of the overlying Hinge enlargement, (Figure 5.100).

The Shoulder Epithelium is the surface epithelium lining the External Mantle in the Shoulder Region.

The Shoulder Gland is the densely glandular Subepithelium of the Shoulder Region.

The Pallial Gland Region Epithelium is the surface epithelium lining the External Mantle of this region and the Pallial Gland is the densely glandular Subepithelium.

On histological grounds the Pallial Region is divided into nine Regions- the Proximal, Middle and Distal, Anterior, Ventral and Posterior Pallial Regions and the related surface Epithelia and Subepithelia are named accordingly, (Figures 5.102, 5.116, and 5.121).

The Distal Folded Region is similarly covered by the Distal Folded Epithelium and the Distal Folded Region Subepithelium describes both the subepithelial secretory glands of this Region and the related system of sinus, muscles, nerves and connective tissue, (Figure 5.106).

2.3.2.2. The Mantle Margin - Tissues.

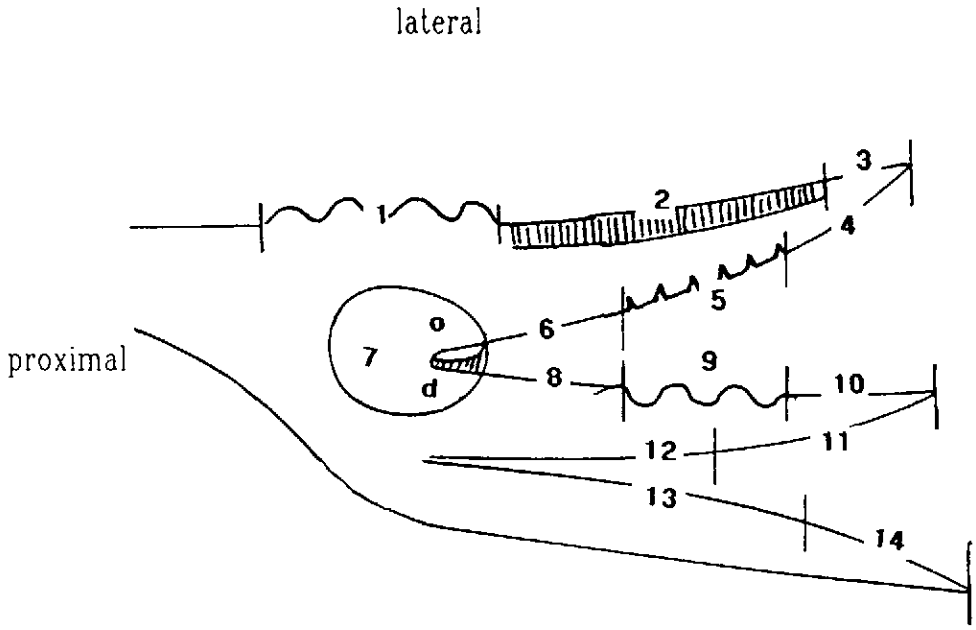

Figure 2.16. Sagittal view of Radial Section of Pinctada. Tissues of the Mantle Margin.
1 = Proximal LatF1.; 2 = Mantle Edge Gland; 3 = Terminal F1.; 4 = Distal MedF1.; 5 = Middle Med F1.; 6 = Proximal MedF1. 7 = Apical Region of Groove F1F2.; o = Omega Gland; d = Dactylocytes; 8 = Proximal LatF2.; 9 = Middle LatF2.; 10 = Distal Lat:F2; 11 = Distal MedF2.; 12 = Proximal MedF2.; 13 = Proximal LatF3.; 14 = Distal LatF3..

LatF1. of pearl oysters has three histological regions.

Proximally there is the Folded Region of LatF1.. Distal to this is the elongate columnar epithelium of the Mantle Edge Gland with a juxtapposed subepithelial sinus system. Distal again is the Terminal Epithelium of LatF1..

The medial surface of F1. of the species of the genus *Pinctada* has three distinct regions- the Distal, Middle and Proximal MedF1. Regions each with a distinctive epithelium, and subepithelium of fibrous connective tissue, secretory glands and associated system of sinus.

The Apical Groove F1F2. is histologically highly differentiated into the Omega Gland, the Unicellular Glands of the Omega Gland, Dactylocytes and the Black Granule Secretory Cells. Also included in this Region are the Circum-pallial Nerve and the Circum-pallial Sinus.

The lateral surface of the F2., (LatF2.) also has three distinct regions - Proximal, Middle and Distal LatF2., each of which has distinctive epithelial and subepithelial histology.

The medial surface of the F2. Fold (MedF2.) is divided into Distal and Proximal MedF2..

The lateral surface of the F3. Fold is similarly divided into the Proximal and Distal LatF3..

2.3.2.3. **External Mantle and Mantle margin** - sub-tissue features, cells and secretions.

Here cells, glands, and other histological features will be named and described sufficient for purposes of identification only. They and their tissue relationships, functions and/or possible functions will be described further in Chapters 5. and 6.

The Isthmus

The **Isthmusistic Epithelium** cells are greatly elongate columnar epithelium in all species of the Pterioidea and Arcoidea studied. A different epithelium underlies each different part of the Hinge in *Nucula superba* and these will be described in Chapter 5.

The Shoulder Region.

The tissues of the **Shoulder Region** are a low columnar surface epithelium, a subepithelial fibrous connective tissue, and beneath this, the cell bodies of a massive glandular structure - the **Shoulder Gland**. This is a massive agglomeration of the cell bodies of large unicellular glands which secrete through the surface epithelium. They are of two basic kinds - **Trabecular Turquoise Glands** and **Granular Cytoplasm Secretory Glands**.

Beneath the glandular tissue there is another layer of fibrous connective tissue which carries blood and nerve supply to the overlying epithelium and glands and the underlying musculature and internal organs.

The Pallial Gland Region.

The histology of the **Pallial Gland Region** is similar to that of the **Shoulder Region** with the following differences :

1. The fibrous connective tissue between the surface epithelium and the saccular bodies of the glandular cells is much denser, as is that between the bodies of the glands.

2. The cell bodies of the **Trabecular Turquoise Glands** form a more definite layer superficial to those of the other unicellular glands.

While the **Trabecular Turquoise Glands** appear to be the same in both loci there are differences in the staining of the other glands. It is not known whether this is a fixation artifact resultant from the different connective tissues.

The **Proximal Pallial Region**, **Middle Pallial Region** and **Distal Pallial Region**.

These three regions are all covered in the Pteriacea by a columnar epithelium with apical secretory microvilli (Figure 5.105).

All three Regions have **Trabecular Turquoise Glands** and a variety of **Granular Cytoplasm Secretory Glands** which secrete into the **Pallial Space**.

Whereas the density of **Trabecular Turquoise Glands** increases slightly from proximal to distal over the three Regions there is a considerable concomitant increase in the density of **Granular Cytoplasm Secretory Glands**, (Figures 5.102).

Further differences between the three regions will be given in Chapter 5.

The **Distal Folded Region**.

The surface epithelium and subepithelial surface secreting unicellular glands of this **Region** are similar to those of the **Distal Pallial Region** with the following differences;

1. The surface epithelium and subepithelium is usually thrown into conspicuous folds with a band of radially directed subepithelial sinus in each fold.

2. An elongate secretory gland with very small granules in its cytoplasm lies in the vicinity of the subepithelial sinus (Figure 5.106 and 5.55)

2.3.2.3.2. The Mantle Margin.

LatF1..

Proximal LatF1..

The surface epithelial cells are a more robust columnar epithelial cell than those of the Pallial Region and there is a further increase in the density of the subepithelial secretory glands compared with the Pallial Regions. The folding in this Region is lower than in the Distal Folded Region (Figure 5.103).

Middle LatF1. - the Mantle Edge Gland.

This is an elongate columnar epithelium which is ubiquitous throughout the Bivalvia in this locus (Figures 2.17 and 5.107). It is joined via a transitional epithelium to the Isthmusistic Epithelium just posterioir and just anterior to the Anterior Mantle Symphysis and Posterior Mantle Symphysis respectively.

Distal LatF1. - the Terminal Epithelium of LatF1.

This is a columnar epithelium which decreases in height distally. The Subepithelial glands beneath it almost all discharge through the Proximal MedF1. and will be described with that Region.

MedF1..

Distal MedF1..

The Surface epithelium is a cuboidal epithelium, with apical microvilli.

The array of subepithelial unicellular secretory glands of this region are unique to it and species specific in the Pterioidea. Glands similar to some of these locus-unique glands are found in species of other superfamilies. Full descriptions of the array found in each species examined will be given in Chapter 5.

Unique to this location in the Pterioidea, Pinnoidea, some Ostreoidea and the Arcoidea are the **Ovoid Blue Glands**. These are unique amongst the Unicellular secretory glands of the **Mantle** and **Mantle Margins** of the Bivalves studied in that they stain various shades of blue and purple with all other stains used and also stain a vivid green/turquoise with A.B./M.S.B.. They have a small, strongly staining nucleus which is invariably located at one pole of their ovoid shape. Under T.E.M. they have a characteristic line-stippled cytoplasm. (*Pinctada maxima,* Figures 5.59 and 5.60)

Also all but unique to this locus are the **Distal Diffuse Glands**. These are large secretory glands whose cell bodies areis invariably contiguous with the surrounding membrane of a parenchymal sinus. The staining reactions are the same in some species but not in others where the identity of the glands are established by their unique norphology and location. In *Pinctada margaritifera* and *P. maxima* they stain amber with Mallory's, pink with M.S.B., a brilliant claret red with Azan, khaki with A.B./M.S.B. and "liverish" purple/brown with Steedmans. No other glands seen in this study have this set of colour reactions to these stains.

Middle MedF1..

The array of subepithelial glands in this Region is both species specific and specific to the locus on the periphery and will be described in detail in Chapter 5.

The Surface Epithelium is a narrow ciliated columnar epithelium.

In all *Pinctada* studied, the subepithelial connective tissue is so arranged that this Region has a surface pattern of sharp vee-shaped infoldings separating short plateaux. In the subepithelium the transverse musculature lies in lacunae of dense fibrous connective tissue, which, with the surface pattern imparts a unique appearance to this Region in stained radial sections (Figure 5.106, b). There is no equivalent tissue to this in those species of the Pterioidea belonging to genera with an Ancillary F1. - *Pteria, Isognomon* and *Malleus.*

Proximal MedF1..

This Region has a robust columnar epithelium and again an array of subepithelial glands which are both species specific and specific to a location on the periphery and will be described in detail in Chapter 5.

Trabecular Turquoise Glands - External Mantle-F1. Type and F2.-LatF3. Type.

With the exceptions of the Mantle Edge Glands and Terminal LatF1. Regions where they are rare, Trabecular Turquoise Glands of apparently very similar if not the same staining affinities are found commonly in all the External Mantle and F1. Regions of the Pterioidea. A similar but slightly differently staining population of Trabecular Turquoise Glands are found in all Regions of F2. and LatF3. (Figure 5.154). (A third slightly different population of Trabecular Turquoise Glands occurs on MedF3. but these are not thought to be involved in shell formation (Figure 5.115).

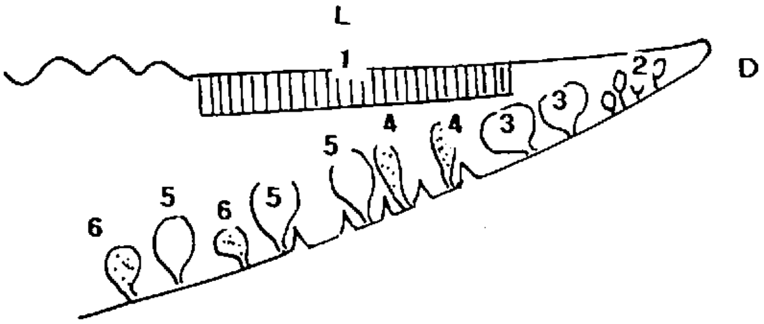

Figure 2.17. Some cells and tissues of F1.. 1 = Mantle Edge Gland; 2 = Ovoid Blue Glands; 3 = Distal Diffuse Glands; 4 = Granular Cytoplasm Secretory Glands of Middle MedF1.; 5 = External Mantle-F1. Type of Trabecular Turquoise Glands; 6 = Granular Cytoplasm Secretory Glands of Proximal MedF1..

Apical Groove F1F2..

The specialised histological features of this highly differentiated area are:
The Omega Gland
The Unicellular Glands of the Omega Gland
The Dactylocytes
The Black Granule Secretory Cells
The Circumpallial Sinus
The Circumpallial Nerve and its local branches.

The Omega Gland.

This is a ridge of epithelial tissue which occupies the lateral surface position of the Apex of Groove F1F2.. It Lies opposite the Dactylocytes which occupy the medial surface of the Apex of Groove F1F2.. Between the two is the Apical Channel from which issues the forming Pleated secretion of Groove F1F2..

The Omega Gland is composed of a Distal Part and a Proximal Part.

The Distal Part of the Omega Gland is a pseudo-stratified columnar epithelium which increases in height proximally, from the Proximal MedF1. epithelium. It is commonly separated from the Proximal Part of the Omega Gland by the bodies or secretory ducts of the Unicellular Glands of the Omega Gland, a group of glands consisting of Trabecular Turquoise Glands and sometimes Granular Cytoplasm Secretory Plands which discharge between the two parts of the Omega Gland (Figures 2.18 and 5.61).

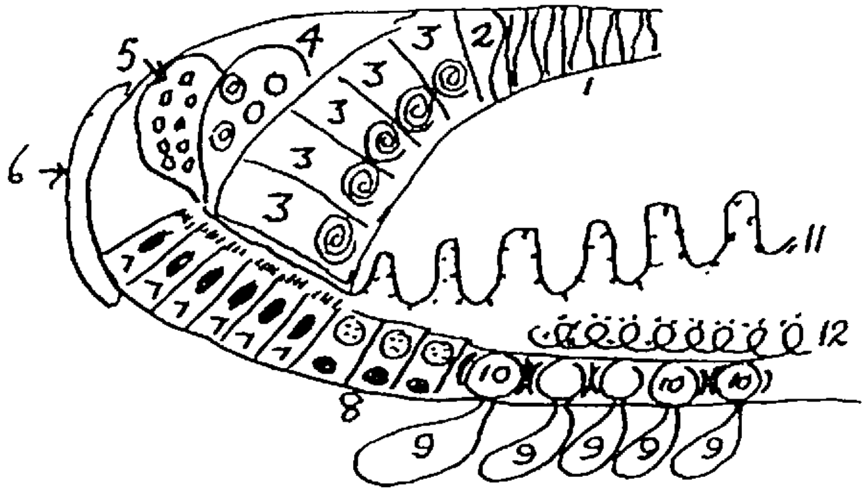

Figure 2.18. Apical Region of Groove F1F2.. 1 = Distal Part of Omega Gland; 2 = Unicellular Glands of the Omega Gland; 3 = Celtic Scroll Cells; 4 = Multivesiculate Cells; 5 = Fenestrated Cells; 6 = Sub-apical Fibrous Connective Tissue; 7 =. Dactylocytes; 8 = Black Granule Secretary Cells; 9 = Proximal Latf2. Sub-epithelial Secretory Cells; 10 = Receptacle Glands; 11 = Pleated Secretion of Groove F1F2.; 12 = Vesiculate Secretion of Groove F1F2..

The Proximal Part of the Omega Gland appears to be a two cells thick stratified epithelium. The outer layer of cells are the Celtic Scroll Cells so called from the morphology of their prominent array of cytoplasmic membranous structures seen with T.E.M. They secrete large vesicles into the proximal part of Groove F1F2. between Medf1. and the Pleated Secretion of Groove F1F2.. Deep to the Celtic Scroll Cells are two other types of secretory cells, the Multivesiculate Cells and the Fenestrated Cells which contribute vesicles and an amorphous secretion respectively to the proximal terminus of the Apical Channel where the Pleated Secretion of Groove F1F2. first commences to form.

The Dactylocytes are elongate columnar epithelial cells with very prominent central elongate ovoid nuclei. Their basment membrane merges with the Sub-apical Fibrous Connective Tissue and their apices are covered with very strong and equal lengthed microvilli whose ends touch the forming sheet of

Pleated Secretion of Groove F1F2.. Secretory granules are conveyed via the microvilli and contribute to the medial surface of the Pleated Secretion of Groove F1F2.

The Black Granule Secretory Cells are variable in morphology from species to species being elongate columnar cells in *Pinctada maxima*, (Figure 5.62, a) and squamous epithelium in *P. margaritifera*, (Figure 5.110, a). However in every species of the *Pinctada* studied they produced vesicles in their apical cytoplasm of electron dense particles which, when secreted, form the Black Granules of the medial surface of the Pleated Secretion of Groove F1F2. and of the lateral surface of the Vesiculate Secretion of Groove F1F2.. This latter is secreted by the secretory structures of Proximal Lateral F2. and lies in Groove F1F2. medial to the Pleated Secretion of Groove F1F2. (Figure 2.18).

LatF2..

Proximal LatF2..

This region is somewhat variable from one species of the *Pinctada* to another and the whole of LatF2. is sufficiently different in the other Genera of the *Pterioidea* as for this description to be inapplicable. The description of this Region in *Pinctada margaritifera* will be given here and the descriptions in the other species examined given in Chapter 5.

The surface epithelium of this Region in the *Pinctada* has a dense mat of apical microvilli but few cilia. It bears Receptacle Glands. These are formed by somewhat spherical invaginations in the epithelium. These are lined with epithelial cells which are crescent shaped in section from their Basement Membrane to their Apical membrane, and have crescent shaped central nuclei. They contain the granular secretion of a single subepithelial Granular Cytoplasm Secretory Gland. The subepithelium is host to species specific and peripheral locus specific arrays of seretory glands. These in some species in some loci can form a dense mass and in other species and at other loci are quite sparse.

Middle LatF2..

The surface epithelium of this Region is formed into a unique pattern of, in radial section, short flat plateaux separated by semicircular infoldings. (Figure 2.19). This structure is common to all species of the *Pinctada* examined.

In the subepithelium are Trabecular Turquoise Glands of the F2. - LatF3. type and Granular Cytoplasm Secretory Glands of several kinds including a heavy population of Light Blue Glands. These latter are unique to this locus. They stain only faint blue with all stains used. With T.E.M. the cytoplasmic granules appear to be similar in size and spherical.

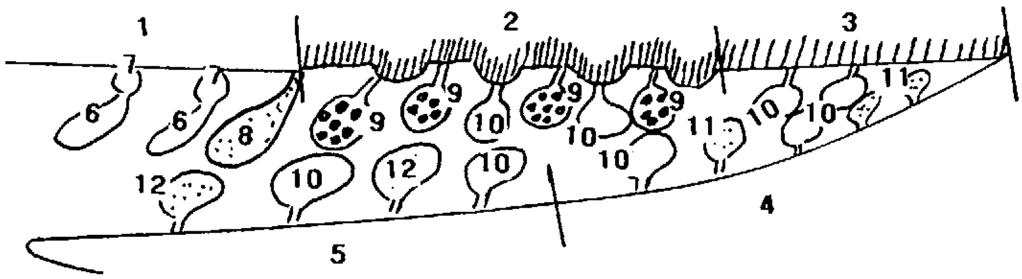

Figure 2.19. Tissues and Glands of F2. 1 = Proximal LatF2.; 2 = Middle LatF2.; 3 = Distal LatF2.; 4 = Distal MedF2.; 5 = Proximal MedF2.; 6 = Subepithelial Glands of Proximal LatF2.; 7 = Receptacle Glands; 8 = Granular Cytoplasm Secretory Glands of Middle LatF2.; 9 = Light Blue Glands; 10 = F2-LatF3 type of Trabecular Turquoise Glands; 11 = Granular Cytoplasm Secretory Glands of Distal MedF2.; 12 = Granular Cytoplasm Secretory Glands of Proximal Med F2..

Distal LatF2..

This is the Region from Middle LatF2. to terminal F2.

The surface epithelium of Distal LatF2. is a simple columnar epithelium with relatively few cilia and small basal nuclei.

The subepithelial secretory glands of this region consist of relatively few Granular Cytoplasm Secretory Glands and more abundant Trabecular Turquoise Glands of the F2 LatF3 type.

MedF2..

Distal MedF2..

The surface epithelium of this Region is a robust columnar epithelium with relatively large rounded basal nuclei and a densely pigmented apical cytoplasm. The pigment granules mostly stain brown with A.B./M.S.B..

The subepithelial secretory glands of Distal MedF2. consist of relatively few Granular Cytoplasm Secretory Glands and more abundant Trabecular Turquoise Glands of the F2. LatF3 type.

Proximal Med F2..

This Region has a surface epithelium of more elongate columnar cells than the Distal MedF2. Region and the densely packed apical pigment granules are about equally brown and amber staining with A.B./M.S.B..

The Proximal MedF2. subepithelial secretory glands are similar to those of Distal MedF2..

LatF3..

Proximal LatF3..

This Region occupies the greater part of LatF3. The epithelium covering the surface of this Region is relatively elongate columnar epithelium characterised by the apical pigment granules all staining amber with A.B./M.S.B.

The subepithelial secretory glands of Proximal LatF3. consist of some Granular cytoplasm Secretopry Glands and more abundant Trabecular Turquoise Glands of the F2. - LatF3. type.

Distal LatF3..

In this Region the surface epithelium is characterized by apical cytoplasmic pigment granules which all stain brown with A.B./M.S.B.

The subepithelial glands of Distal LatF3. are again Granular Cytoplasm Secretory Glands and Trabecular Turquoise glands of the F2. - LatF3. type.

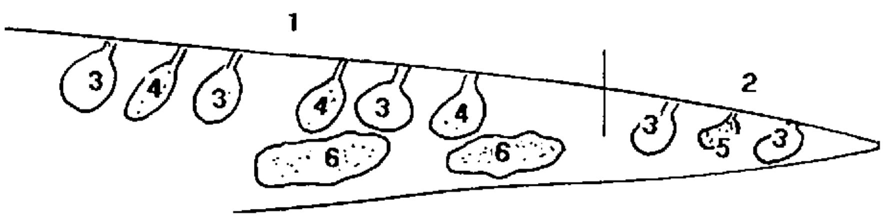

FIGURE 2.20. Tissue Regions and Unicellular Glands of LatF3.. 1 = Proximal LatF3.; 2 = Distal LatF3.; 3 = F2. - LatF3. type Trabecular Turquoise Glands; 4 = Granular Cytoplasm Secretory Glands Of Proximal LatF3.; 5 = Granular Cytoplasm Secretory Glands of Distal LatF3.; 6 = Microgranular Glands.

CHAPTER 3.

SUGGESTED ALTERATIONS TO CLASSIFICATION OF SOME PEARL OYSTERS FROM AUSTRALIAN WATERS.

INDEX.

3.1. INTRODUCTION.

As previously, common names used in the pearling industry and preliminary work done suggested that Hynd's (1955) classification of the Australian species of the Pinctada was sdeficient in that it failed to destinguish between several species with fairly similar gross shell features.

3.2. AUSTRALIAN SPECIES OF THE GENUS *PINCTADA*.

3.2.1. Hynd's Classification.

As in Chapter 1, Hynd (1955) reviewed the 31 recorded species of Australian pearl oysters and regrouped them into six species - *Pinctada margaritifera* Linnaeus, 1758, *P. maxima* (Jameson, 1901), *P. fucata* (Gould, 1850), *P. maculata* (Gould, 1850), *P. chemnitzi* (Philippi, 1849), and *P. albina* Lamarck, 1819. Of the latter he described two subspecies - *P. albina sugillata* (Reeve, 1857), and *P. albina carchariarum* (Jameson, 1901). This last is said to be confined to the coast from the north west of Western Australia to Port Darwin - *P. albina sugillata* from about there, around the north and east coasts of Australia to Southern New South Wales.

3.2.2 Species of Australian *Pinctada* used in this work.

3.2.2.1. Species described by Hynd.

The *P. maxima* used here were of both the "gold lip" and "silver lip" varieties of this species, and for them the author accepts the description in Hynd (1955). Similarly, Hynd's description of the "black-lip" pearl oyster *P. margaritifera*, of *P. fucata* (Figures 3.1.a. and 3.2.a. and Figures 5.126.-5.130.), and *P. chemnitzi* (Figure 3.3. f. and g. and Figure 5.139.) are agreed with and these names used in this work for the animals so described. The name *P. albina sugillata* is restricted in this work to the description given in Hynd but excluding all specimens which do not have a "delicate suffusion of yellow over all of the nacre". The histology of the Mantle Margin of *Pinctada albina sugillata* is given in Figure 5.141.

The description and the photographs of *P. maculata* given in Hynd (1955) do not allow this author to be certain whether this species is included in this work or not, but most likely it is not.

P. albina carchariarum is not included in this work.

Thus the animals used in this work where the classification of Hynd is agreed with are *Pinctada maxina*, *P.margaritifera*, *P.fucata*, *P.chemnitzi* and *P.albina sugillata*.

3.2.2.2. Species other than those described by Hynd.

There are however included here results from work on animals which appear to belong to ten species quite distinct from the five above about which this author agrees with Hynd's classification. There remains the possibility that one of these species is Hynd's *P. maculata* but this is uncertain. Seaman (pers comm.) says that it is definitely not the same as the animal called *P. maculata* in the Tuamoto Archipelago. It is not claimed that this increase in the number of species of the *Pinctada* in Australian waters from 6 to 15 (or 16) is exhaustive.

These species are called *Pinctada sp.1.* (Figure 3.1. b and 3.2. b and Figures 5.131., 5.132.), *Pinctada sp.2.*, (Figures 3.1. c and 3.2. c and Figures 5.133. - 5.137.), *Pinctada sp.3.* (Figure 3.3. a and c and Figures 5.138. a and b), *Pinctada sp.4.* (Figure 3.3. b and c and Figure 5.138. c), *Pinctada sp.5.* (Figure 3.3. d and e and Figure 5.140. a, b, c, d. and e.), *Pinctada sp.6.* (Figure 3.3. h and Figure 5.142. a), *Pinctada sp.7.* (Figure 3.3. i and Figure 5.142. b), *Pinctada sp.8.* (Figure 3.3. j and k and Figure 5.142. c), *Pinctada sp.9.* (Figure 5.142. d) and *Pinctada sp.10.* (Figure 5.142. e.).

FIGURE 3.1. VALUES OF *PINCTADA FUCATA, PINCTADA SP.1* AND *PINCTADA SP.2* - LATERAL SURFACES.

a. x approx 1.4 *Pinctada fucata* - Valves - lateral surfaces. The Growth Processes of *Pinctada fucata* are unique amongst the Australian *Pinctadae* seen, are spear-head shaped with the sharp point directed disto-laterally. Although the Growth Processes do occur on lines which radiate from the umbonal region this is not readily apparent.

b. x approx 1.4 *Pinctada sp.1* - Valves - lateral surfaces. The Growth Processes of *Pinctada sp.1* are unique amongst the Australian *Pinctadae* seen in that they may be greater than 10mm in length and their sides are about parallel for most of their length.

c. x aaprox 1.4 *Pinctada sp.2* - Valves - lateral surfaces. The Growth Processes of this species are again unique amongst those of the Australian *Pinctade* seen in that they are relatively very short and narrow and overlap each other in very discrete lines radiating from the umbonal region. Like the Growth Processes of *Pinctada margaritifera* and *Pinctada sp.5* they are bone white in colour.

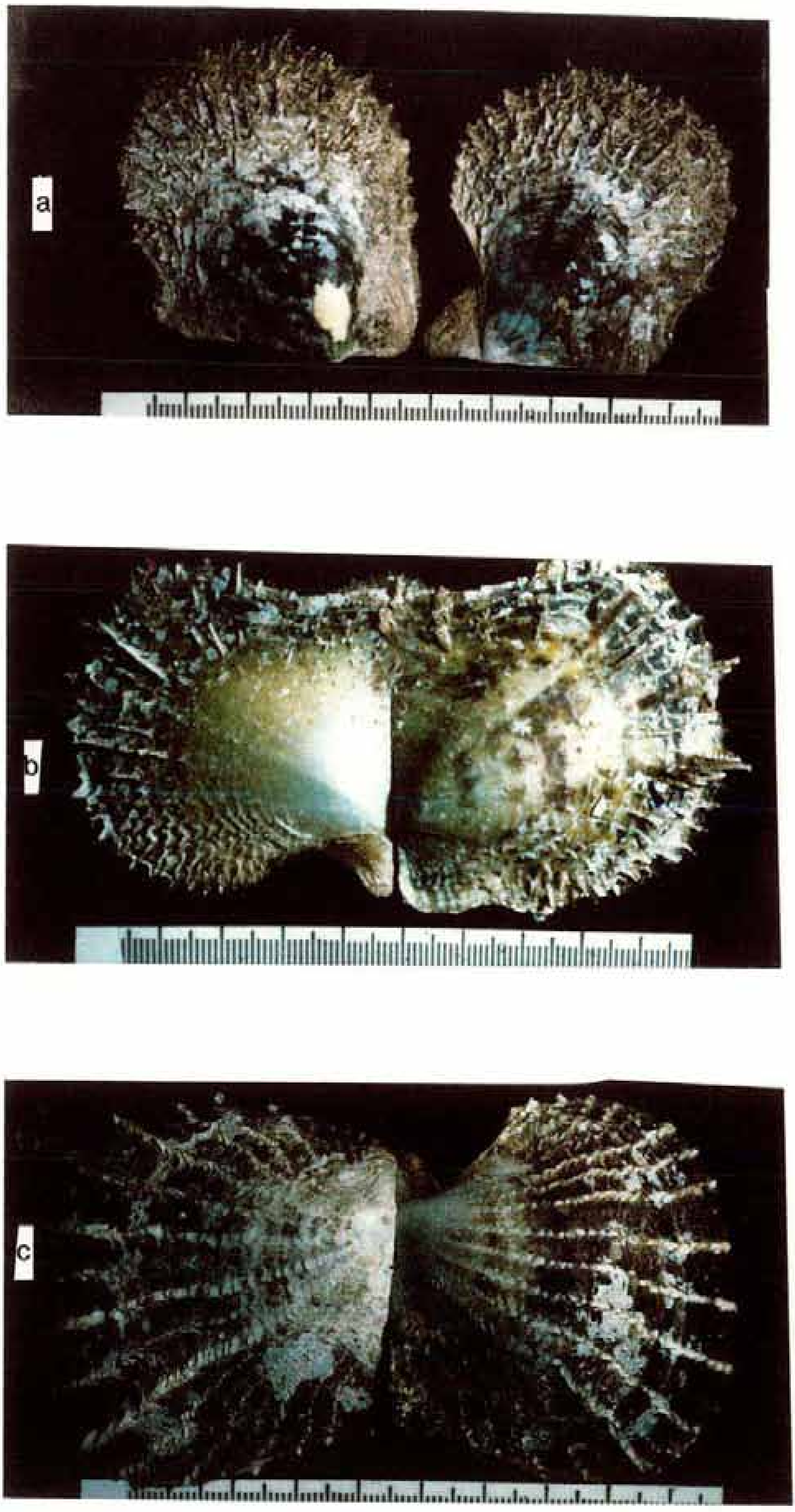

Figure
3.1

FIGURE 3.2. VALVES OF *PINCTADA FUCATA, PINCTADA SP.1 AND PINCTADA SP.2* - MEDIAL SURFACES.

a. x approx 1.4 *Pinctada fucata* - Valves - Medial Surfaces.
The area of the medial surfaces of the nacreous layers of the left valve of this species is far greater than that of the right valve and the lengths of the Nacre on the dorso-ventral axes are about 1.3 times those on the antero-posterior axes of both Valves.

b. x approx 1.4 *Pinctada sp.1* -Valves - Medial Surfaces.
The area covered by Nacre on the medial surface of the right valve is slightly greater than that on the left valve and the length of the dorso-ventral extent of the Nacre is slightly greater than the antero-posterior extent on either valve but neither to such a marked degree as in *P. fucata.*

c. x approx 1.4 *Pinctada sp. 2*- Valves - Medial Surfaces.
The area covered by Nacre on the medial surfaces of the two valves is almost the same and the length of Nacre on the antero-posterior axis is about 1.2 times that on the dorso-ventral axis. Further the location of the discrete lines of Growth Processes on the lateral surface of the Prismatic Layer is clearly indicated by narrow white lines crossing the medial surface of the otherwise dark coloured Prismatic Layer.

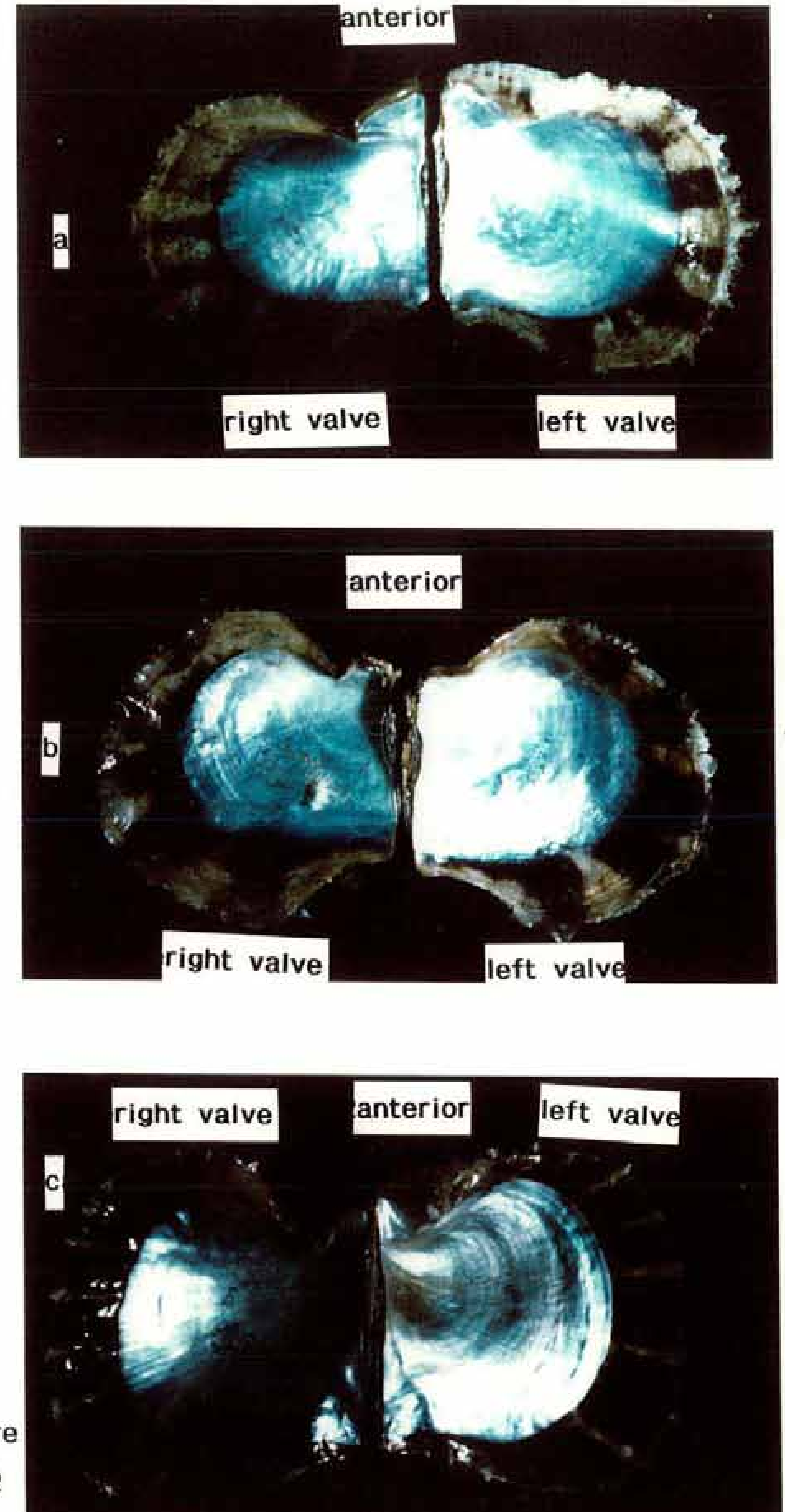
anterior
a
right valve
left valve
anterior
b
right valve
left valve
right valve
anterior
left valve
c

Figure
3.2

FIGURE 3.3. *PINCTADA SP.3, PINCTADA SP.4, PINCTADA SP.5, PINCTADA SP.6, PINCTADA SP.7* AND *PINCTADA SP.8.*

a. x 1.	*Pinctada sp.3,* valves, lateral surfaces.
b. x 1.	*Pinctada sp.4,* valves, lateral surfaces.
c. x 1.	*Pinctada sp.3* (above) and *Pinctada sp.4* (below), medial surfaces.
d. x 1.	*Pinctada sp.5,* valves, medial surfaces.
e. x 1.2	Pinctada sp.5, left valve, lateral surface.
f. x 1.1	*Pinctada chemnitzi* right and left valves, medial surfaces.
g. x 1.2	*Pinctada chemnitzi* left valve, lateral surface.
h. x 0.7	*Pinctada sp.6,* left valve, medial surface.
i. x 1.2	*Pinctada sp.7,* right and left valves, medial surfaces.
j. x 1.	*Pinctada sp.8,* left valve, medial surface.
k. x 1.2	*Pinctada sp.8,* left valve, lateral surface.

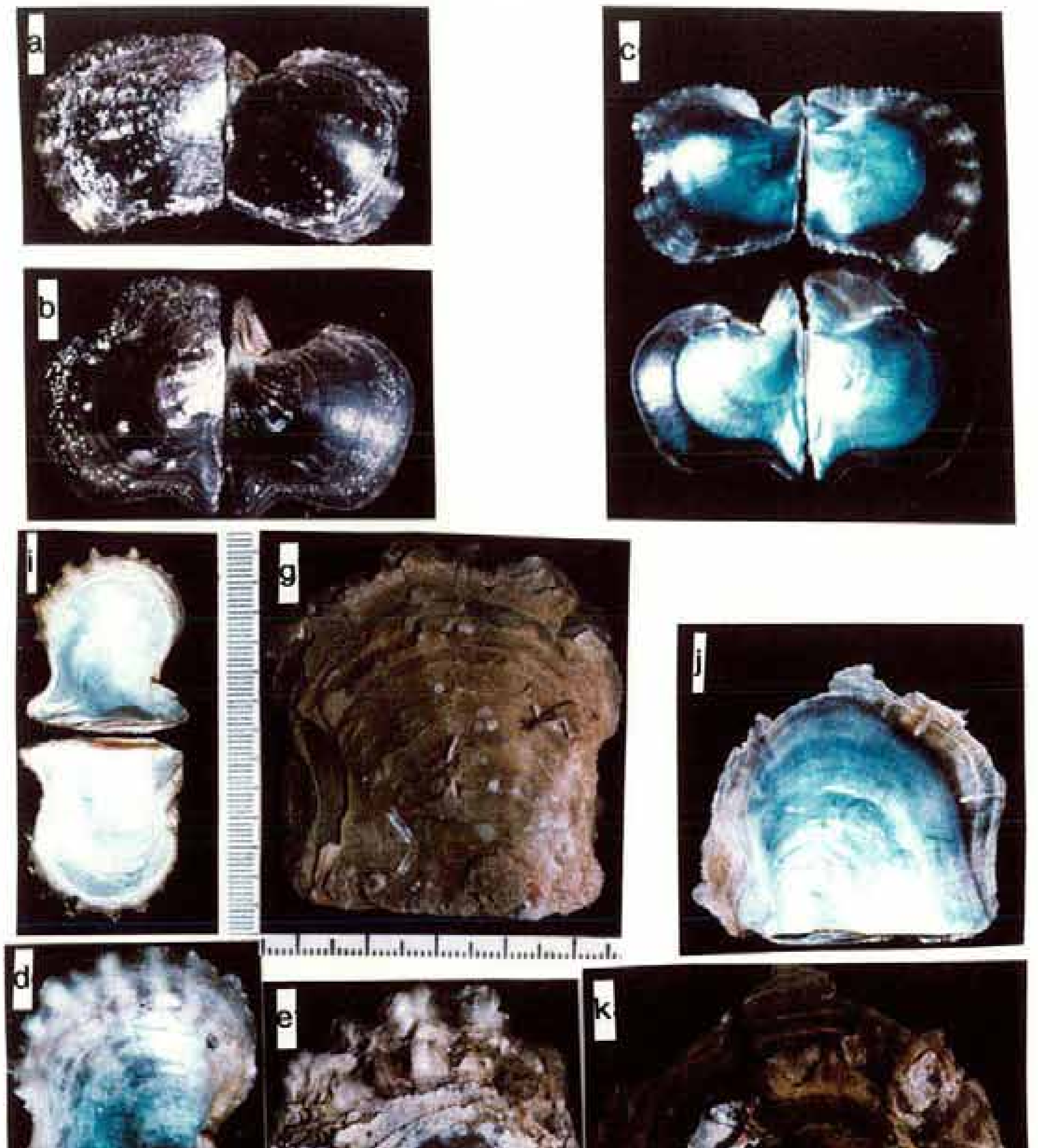

Figure 3.3

Resources are not available to check these species against the type specimens.

The extra species fall into three groups. The first two in size and opalescence of nacre are superficially akin to *Pinctada fucata* and thus will be compared and contrasted with that species. *Pinctada sp.3* and *Pinctada Sp.4* are quite similar and very different from any other species of *Pinctada* studied and thus will be described and differentiated from each other. The final five described here are part of a group of pearl oysters which to some extent superficially resemble *Pinctada albina sugillata* and therefore will be differentiated from that species and each other.

3.2.2.3. Description of additional species of the Genus *Pinctada*.

Pinctada sp.1. (Figure 3.1. b and 3.2. b and Figure 5.141.)

This species of *Pinctada* has been collected on several occasions from Fitzroy Island and Arlington Reef near Cairns and Quarantine Bay near Cooktown. Of the six species recognised by Hynd it is closest to *Pinctada fucata* but is distinguished from *P.fucata* by the following.

1. The valves are noticeably less convex.
2. It has less inequalities of nacreous areas between the right and left valves, (Figures 3.2. a and 3.2. b).
3. Its Growth Processes are relatively extremely elongate being commonly more than ten mm in length and of even width for most of that length. By comparison the Growth Processes of *P. fucata* are short and characteristically pointed distally. (Figures 3.1. a and 3.1. b).
4. The Mantle and Mantle Margin histologies are species specific and very different from those of *P. fucata* or from *Pinctada sp. 2* - the other species it somewhat resembles. (Figures 5.129. e and f, 5.132 and 5.134. b).

Pinctada sp. 2. (Figures 3.1.c. and 3.2.c. and Figures 5.133 - 5.137).

This species has been collected from Fitzroy Island to Cooktown. It is also superficially in size and opalescence of nacre more closely akin to *P.fucata* than to any of the other species listed by Hynd. (1955). and consequently in these respects not greatly unlike *Pinctada sp. 1.* However.

1. The area covered by nacre is about the same in the two valves. Figure 3.2. c. c.f. Figure 3.2. a and b).

2. The length of medial nacreous surface is markedly shortened dorso-ventrally whereas in *Pinctada fucata* and *Pinctada sp. 1* it is markedly shortened antero-posteriorly. (Figure 3.2. c. c.f. Figure 3.2. a and b).

3. Its Growth Processes are very different from any other species of the Genus seen. They are small. centrally light-coloured as in *P. margaritifera* and form narrow distinct light-coloured lines radiating from the Umbonal Region to the valve periphery . (Figure 3.1. c). Further the light-coloured lines of Growth Processes are. to an extent unique amongst species of *Pinctada* studied. clearly visible as light-coloured lines traversing the otherwise dark coloured medial surface of the Prismatic Layer beyond the Nacreo-prismatic Junction. (Figure 3.2. c).

4. The External Mantle and Mantle Margin histologies are species specific. (Figure 5. 134).

5. This species is more mobile than any other species of pearl oyster studied.

Pinctada sp. 3. (Figures 3.3.a. and c. and Figure 5.138 a and b). and
Pinctada Sp. 4. (Figures 3.3.b. and 3.3.c. and Figure 5.138. c).

These species have been collected from the Russell Islands to Torres Straits and variants. or similar pearl shells have been seen from the north of Western Australia. They are jointly distinguished from other pearl oysters in this study by their dark colours.

1. Small pearl oysters with dark Prismatic Layer and purple/green opalescent nacre.

2. The major difference between them on medial view is that the antero-dorsal corner of *Pinctada sp. 3* is much less pronounced than that of *Pinctada Sp. 4* and the postero-dorsal corners of the former are about normal to the hinge whereas those of the latter are sharply kinked posteriorly and join the hinge line at an acute angle. Further. whereas *Pinctada sp. 3* has nearly equal areas of nacre on each valve of a pair of valves the left valve of a pair of

Pinctada sp. 4 valves has a greater area of nacre than the right one.

3. The Growth Processes of *Pinctada Sp. 3* are very small, sharp pointed and form relatively few distinct lines on the Lateral Surface of the Valve. Those of Pinctada sp. 4 are inconspicuous and rounded.

4. The Histologies of the External Mantle and Mantle Margins of these pearl oysters are species specific, (Figure 5.138 a and b c.f. 5.138, c).

Pinctada sp. 5. (Figures 3.3.d. and e. and Figure 5.140.).

This species was collected from the Torres Straits.

1. It is chiefly characterised by the large Growth Processes' porcelain like appearance.

2. Medially, the nacre is thin, silvery and translucent.

3. The histology of the External Mantle and Mantle Margin is species specific (Figure 5.140).

Pinctada sp. 6. (Figures 3.3., h, and 5.142, a.).

This species has been collected from Townsville to the Torres Straits.

1. Medially the Nacre is opaque and silver with no trace of the yellow suffusion of the Nacre of *Pictada albina sugillata.*

2. The Byssus lies in a deep groove in the Byssal Notch.

3. Growth Processes are moderate and the Prismatic Layer distinguished by discrete relatively evenly spaced broad bands of dark and light colour.

4. The Histology of the Mantle and Mantle Margin are species specific, (Figure 5.142, a).

Pinctada sp. 7. (Figure 3.3. i and 5.142, b).

This pearl oyster has been frequently collected from Balgal Beach fringing reef and from Kissing Point in Townsville. It is distinguished from *P.albina sugillata* by:

1. The Nacreous Layers on the medial surfaces of the Valves reach nearly to

the Valve periphery.

2. The Nacreous surfaces of the Valves, especially of the Right Valve, are about 1.5 times greater in their dorso-ventral dimension than in their Antero-posterior one, and about evenly split by the right bisector of the Hinge.

3. The Byssal Notch is an obtuse angle and relatively distant from the Hinge.

4. The Growth Processes are relatively large and usually only seen on the Ventral and Postero-ventral periphery.

5. The histology of the Mantle and Mantle Margin are species specific, (Figure 5. 142, b).

Pinctada sp. 8. (Figures 3.3. j and k, and 5.142, c).

This species has been collected frequently from Balgal Beach fringing reef. While its Mantle Margin histology is similar in some respects to that of P. albina sugillata, the staining affinities of the glands of LatF2. are markedly different, (Figure 5.142, c, c.f. Figure 5.141, a, b, c and d), the subepithelial glands of MedF2. and LatF3. are far more abundant, (Figure 5.142 c, c.f. Figure 5.141, a, b, c and d), and the nacre has a bright silver lustre.

Pinctada sp.9. (Figure 5.142, d).

This species has been collected from Balgal Beach fringing reef. It is distinguished from all other species of Pinctada used in this work by the unique tubular habit of the Granular Cytoplasm Secretory Glands of lateral F2, nearly all of which stain deep red with Azan. The nacre has a silver lustre.

Pinctada sp. 10. (Figure 5.142, e).

This species was collected from Balgal Beach fringing reef. It is distinguished from all other species of pearl oysters in this study by the tubular Granular Cytoplasm Secretory Glands of Proximal MedF1. staining purple with A.B./M.S.B., (Figure 5.142, e).

CHAPTER 4

MATERIALS AND METHODS

4.1 SOURCES OF ANIMALS.

Velesunio ambiguus was obtained from a fresh water section of the Ross River above Aplin's weir, Townsville.

The marine bivalves used other than the pearl oysters were all obtained from mangrove swamps, coastal mud flats, fringing reefs or trawled from shallow seas between Cape Cleveland and Balgal Beach - ie.. from the shore of the Pacific Ocean from near Townsville to about fifty kilometres north. Figure 4.1. gives the location from which each species was obtained, and Figure 4.3. locates the place names in Figure 4.1. on a map.

The pearl oysters used were obtained from numerous locations between Townsville and the Torres Straits. The locations from which the various species of pearl oysters were obtained are shown in Figure 4.2. and these locations are shown on the map, Figure 4.3..

Source	Non-pearl oyster bivalve species
Pallarenda	*Nucula superba, Nucula sp., Trisidos tortuosa, Phylloda foliacea, Tellina sp., Tapes sp., Solen vagina, S. grandis, Mactra abbreviata.*
Balgal Beach	*Trichomya hirsuta, Lithophaga teres, Botulopa silicula infra, Pinna bicolor, Spondylus lamarcki, Anadara antiquata, A.pilula, Arca aladdin, Barbatium amygdalumtostum, Mesocibota luana, Gafrarium divaricatum, G. tumidum, Gafrarium sp. Placamen calophyllum, Cardita variegata, Mactra dissimilis, Gastrochaena cuneiformis.*
Trawled east of Magnetic Island	*Hyotissa hyotis, Ostrea sp., Placuna placenta, Amusium pleuronectes,* Melaxinaea labyrintha, Dosinia juvenilis, Circe *trigona, Globivenus embrithes.*
White Lady Bay	*Saccostrea echinata, S. cuccullata.*
Magnetic Island	*Geloina coaxans*

FIGURE 4.1. Locations from which the non-pearl oyster bivalves used in this work were obtained

Pearl oyster species	Source
Pinctada maxima.	Fitzroy Island, Arlington Reef, North East of Cooktown, Friday Passage and "Old Ground" Off Badu Island, Torres Straits.
P. margaritifera.	Magnetic Island, Fitzroy Island, Arlington Reef, Quarantine Bay, North East of Cooktown, Marulag, Torres Straits.
P. fucata.	Fitzroy Island, Arlington Reef and Friday Passage, Torres Straits
Pinctada sp.1.	Fitzroy Island, Arlington Reef, Quarantine Bay.
Pinctada sp.2	Fitzroy Island, Quarantine Bay.
Pinctada sp. 3.,	Russell Is. Fitzroy Island, Arlington Reef, Schnapper Island, Friday Passage.
Pinctada sp. 4..	Russell Is., Arlington Reef, Friday Passage.
P. chemnitzi	Kissing point (Townsville), Balgal Beach, Friday Passage.
Pinctada sp.5.	Friday Passage
P. albina sugillata.	Kissing Point, Magnetic Island, Balgal Beach, Arlington Reef, Quarantine Bay, Friday Passage.
Pinctada sp.6.	Kissing Point, Balgal Beach, Friday Passage.
Pinctada sp.7.	Kissing Point, Balgal Beach.
Pinctada sp.8.	Balgal Beach fringing reef.
Pinctada sp.9.	Balgal Beach fringing reef
Pinctada sp. 10.	Balgal Beach fringing reef.
Pteria penguin.	Magnetic Island, Fitzroy Island and Arlington Reef.
Pteria avicula.	Magnetic Island and Arlington Reef.
Isognomon isognomon	Magnetic Island and Balgal Beach.
Isognomon ephippium.	Estuary of Rollingstone Creek.
Malleus alba.	Palleranda

FIGURE 4.2. Locations from which the pearl oysters used were obtained.

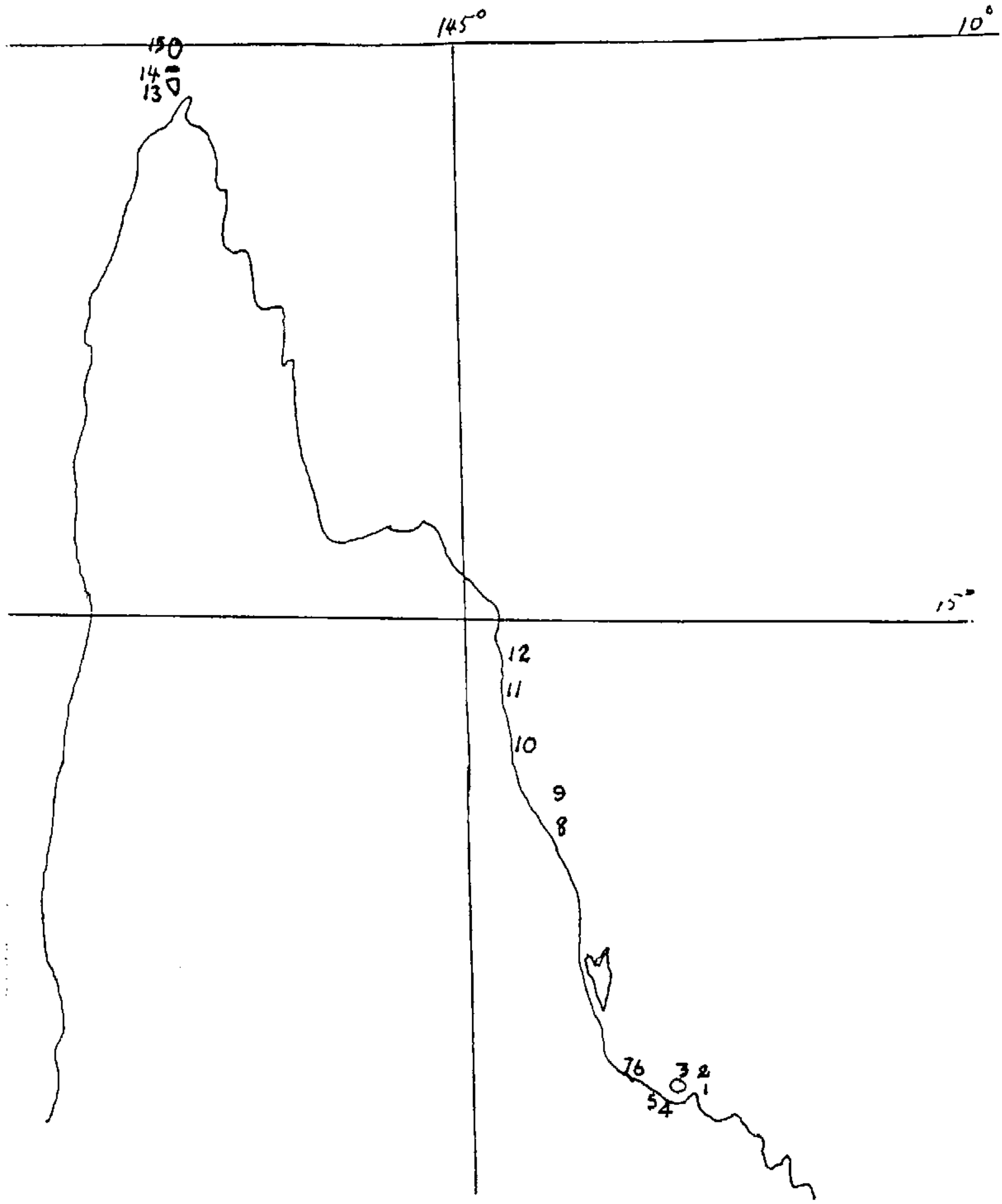

FIGURE 4.3. North Queensland from south of Townsville to the Torres Straits. 1 = Cape Cleveland; 2 = Magnetic Island; 3 = White Lady Bay; 4 = Kissing Point; 5 = Pallarenda; 6 = Balgal Beach; 7 = Rollingstone Creek; 8 = Fitzroy Island; 9 = Arlington Reef; 10 = Schnapper Island; 11 = Quarantine Bay; 12 = north-east of Cooktown; 13 = Marulag; 14 = Friday Passage; 15 = Badu.

4.2. LIGHT MICROSCOPY.

Narcosis, Fixation, Embedding, Sectioning and Staining.

Note. Several different fixatives for L.M. were employed in the preliminary work. However, as explained in 1.12, the most useful method tried for simultaneous fixation of the soft tissues of the Mantle and Mantle Margin and fixation of the Shell Organic Matrices concurrently with decalcification of the inorganic phase of the Shell Layers to achieve a preparation which could be sectioned so as to display geometrical physical and histochemical relationships of tissues and shell parts was that described below. Since this is a comparative study, the methodology of narcosis, fixation embedding, sectioning and staining was rigidly adhered to even where only soft tissues were involved, and even where the stains were designed to be used with a specific fixative (e.g. Steedman's triacid stain, see below).

4.2.1. Narcosis and Fixation.

All specimens of bivalves for L.M. were narcotised by adding 7.8 mg/100ml magnesium chloride to sea water in which the animals were immersed until their adductor muscles became flaccid. If decalcified valves were not required attached to the soft parts, the animals were then removed from their shells and fixed in marine Bouins - a saturated solution of picric acid in 85% by volume sea water, 10% by volume formalin and 5% acetic acid - approximately 10 volumes of fixative to 1 of tissue. After 24 hours the specimens were rinsed with 70% ethanol until the rinsings were only slightly cloudy and then stored in 70% ethanol for the minimum possible time before processing and embedding.

If decalcified valves were required for sectioning *in situ* with the whole animal, following magnesium chloride narcosis as above, the entire animal in its shell was immersed in 10 volumes of marine Bouins fixature. The rate of bubble production from the acidic fixative was noted and as bubble production decreased, 2% acetic acid was added drop-wise so that the rate of bubble production remained about constant at this somewhat reduced level over the first 24 hours. The rate of addition of the acid solution was adjusted to suit each specimen. After 24 hours, when it was considered that the soft tissues would be fixed to the extent that weak acid would have little effect on them, the addition of 2% acetic acid was speeded up until decalcification was complete. This was determined by inserting a metal probe in what had been the thickest part of the shell after bubble production had ceased. The acid and Bouins fixative was then rinsed away with 70% ethanol until very little colour remained in the rinsings. Again the specimens were stored in 70% ethanol for the minimal possible time before processing and embedding.

4.2.2. Embedding, Sectioning and Staining.

The tissue blocks or whole specimens were processed on a Shandon Duplex Processor, dehydrated through an ascending ethanol series, cleared in toluene, and infiltrated in paraffin wax (Paraplast, mp 56 C).

The tissue blocks were sectioned at 6 μm.

Whole animals, tissue blocks and shell Organic Matrices were serially sectioned to the extent necessary to reveal the three dimensional structure and relationships of the subject of study..

The stains used were:

1. Mayer's haemalum and Young's eosin-erythrosin (H. and E.).
2. Mallory - Heidenhain (Mallory's).
3. Heidenhain's azan (Azan).
4. M.S.B. technique (M.S.B.).
5. Alcian blue/M.S.B. technique (A.B./M.S.B.).
6. Steedman's triple stain (Steedman's).

The first two of these were as described by Winsor, (1984).

Heidenhain's azan technique was a modification of Gabe (1976). The time in azocarmine stain was decreased to thirty minutes as sufficiently brilliant colour was achieved with less damage to the tissues than when left in this stain for 45 minutes or 1 hour.

The M.S.B. technique was the martius yellow, brilliant crystal scarlet, methyl blue technique of Dury and Wallington (1980).

A.B./M.S.B. was the same technique as M.S.B. above except that the slides were stained for five minutes in alcian blue and then rinsed in distilled water before the phosphotungstic acid step in the Dury and Wallington (1980) M.S.B. technique. This was to stain the acid mucopolysaccharide secretory glands which were refractory to staining with the other stains. The staining with alcian blue so enhanced the action of the other dyes in this technique as to render the celestine blue step unnecessary, the nuclei now staining pink-red.

Steedman's Stain is a one step triacid stain (Steedman, 1970). Although this was designed to be used with a p-toluene sulphonic acid - formaldehyde fixative it was found to function quite satisfactorily as an aid in distinguishing different glands, tissues and secretions in bivalve material fixed in marine Bouin's. It was thus considered that whatever gains may have been achieved by using two fixatives on separate blocks of tissue were more than offset by the added information gained from viewing serial sections with this stain used sequentially with the other stains.

The six stains listed above were used serially to maximise the recognition firstly, of morphologically and chemically different structures in shells, and secondly of the differentiation into different tissues and glands and their secretions in the Mantles and Mantle Margins of pearl oysters and other bivalves.

4.3. TRANSMISSION ELECTRON MICROSCOPY.

Selection of Tissues, Fixation, Embedding, Sectioning, Staining.

4.3.1.Selection of tissues.

The aim of T.E.M. was to more accurately characterise the glands and secretions, and hence hopefully the functions of the pearl oyster tissues identified with L.M. as likely to be involved in Shell Layer formation. To this end tissue blocks were prepared from the Isthmi, Shoulder Regions, Pallial Gland Regions, Proximal, Middle and Distal Pallial Regions, the Distal Folded Regions and the tissues of the Mantle Margins of *Pinctada maxima*, *P. margaritifera*, *P. fucata*, *Pinctada sp. 1*, *Pinctada sp. 2*, *Pinctada sp. 3*, *Pinctada sp. 4*, *Pinctada sp. 5*, *P.albina sugillata*, *Pteria penguin* and *Isognomon ephippium*.

4.3.2. Fixation Embedding, Sectioning and Staining.

4.3.2.1. Fixation and embedding.

The fixation method is that used routinely in this laboratory for molluscan mantle tissue, and, in a study contemporaneous with this work, was found to be optimul of several fixatives tried for fixation for T.E.M. of *Pinctada* mantle (pers. comm. B. Aquilina).

The animals were removed from their shells into 2.5% glutaraldehyde in 0.1M cacodylate buffer in filtered sea water at 24C. The required tissues were dissected in the fixative as soon as possible into strips less than 1mm wide, and left in the fixative for 1h.

The strips of tissue were then washed twice in 0.1M cacodylate buffer, pH 7.2, in filtered sea water for ten minutes.

They were then post-fixed in 1% osmium tetroxide in 0.1M cacodylate buffer, pH 7.2, in filtered sea water for 1h at 24 C.

The tissues were again washed in cacodylate buffer for ten minutes.

Tissues were then dehydrated through an anascending ethanol series - 50%, 60%, 70%, 80%, 85%, 90%, 95%, 100% - for 2-5 minutes each, then two more changes in absolute ethanol for ten to twenty minutes each.

The tissues were then placed in equal volumes of ethanol and Spurr's resin and agitated on a rotator for three hours (Spurr, A.R. 1969).

A volume of Spurr's resin equal to that of the solution of Spurr's resin in alcohol was then added and returned to the rotator for a further three hours.

The 75% solution of Spurr's resin in ethanol was then removed and the tissues left in 100% Spurr"s resin on the rotator overnight.

The used Spurr's was then removed and the tissues left in new Spurr's resin for another three hours, and then embedded in moulds in pure Spurr's resin.

The resin blocks were then cured for 16 h at 70 C.

4.3.2.2. Sectioning and staining.

Sections of 60-100nm were cut with glass or diamond knives using an LKB ultratome. The sections were then mounted on copper grids and stained for 8 minutes in saturated uranyl acetate in 50% ethanol followed by 1 minute in Reynold's lead citrate.

The transmission electron microscope used was a Jeol JEM- 2000FX.

4.4. SCANNING ELECTRON MICROSCOPY.

Specimens for S.E.M. were usually hard parts of shells in which case they were washed with distilled water, dehyrated with absolute ethanol, dried, mounted and sputter-coated with gold.

Where tissue was left attached To the shell periphery for S.E.M. examination of the tissue-shell relationships in *Nucula sp.* and *Velesunio ambiguus* the specimens were critical point dried before gold coating.

One specimen of *Pinclada margaritifera* shell Prismatic Layer was lightly acid etched by placing in 2% acetic acid for a few minutes.

The S.E.M used was a Siemens ETEC Autoscan.

CHAPTER 5
RESULTS

5.1. UNIONOIDEA

5.1.1. *VELESUNIO AMBIGUUS*

5.1.1.1. VALVES.

These consist of a trilaminate outer non-calcareous Shell Layer (f in Figures 5.2. a and b. and 5.3. b and c). outside three calcareous Shell Layers - an outer aragonite Prismatic layer. (P in Figures 5.1. e and 5.2. b). outside an Outer Nacreous Layer (Figure 5.1. b and d. N in Figure 5.1. e. and onl in Figure 5.2. b) and an Inner Nacreous Layer (Figure 5.1. a and c).

The Inner Nacreous Layer Nacre Sheets are about 1.4μm thick (Figure 5.1. c). The Outer Nacreous Layer Nacre Sheets are about 0.3μm thick (Figure 5.1. d).

The Partly-bound and Free Nacre Tiles of the Inner Nacreous Layer are truncated diamond shaped (Figure 5.1. a). Those of the Outer Nacreous Layer are diamond shaped (Figure 5.1. b).

The Inner and Outer Nacreous Layers of this species should be compared with and contrasted against those of *Pinctada maxima* (Figs. 5.12 - 5.30). and those of the other pearl oysters illustrated.

FIGURE 5.1. *Velesunio ambiguus.* - Calcarious Shell Layers.

a. S.E.M. x 1500 Medial view Inner Nacreous Layer.

b. S.E.M. x 1500 Medial view Outer Nacreous Layer.

c. S.E.M. x 1500 Sagittal view Inner Nacreous Layer.

d. S.E.M. x 3800 Sagittal view Outer Nacreous Layer.

e. S.E.M x 950 Radial broken surface of aragonite Prismatic Layer and Outer Nacreous Layer.

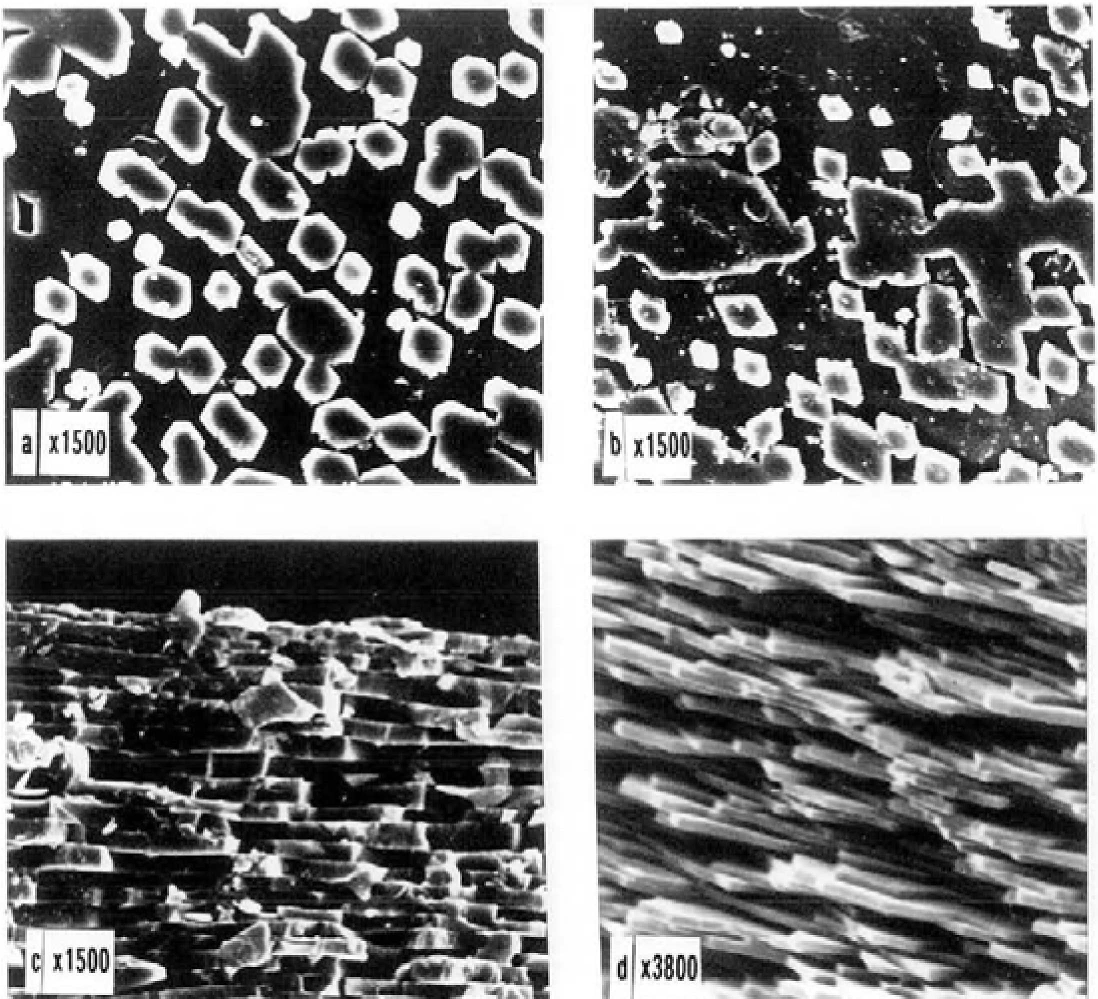

Figure 5.1.

5.1.1.2. Outer Fibrous Layers, Aragonite Prismatic Layer and Outer Nacreous Layer.

The Trilaminate Outer Fibrous Layer of the Valve of *Velesumio ambiguus* recurves around the distal extremity of Fold F1. and is thrown into outfoldings on the lateral surface of the Valves, (f in Figures 5.2, a and b and 5.3, b and c). In Figure 5.2 L is lateral and M medial. From the medial part of the outfolding, by some process which remains obscure, the medial lamina of the trilaminate Outer Fibrous Shell Layer curves proximally and then medially and then recurves to form a bilaminate sigmoid structure, (S in Figure 5.2, a and b).

The Aragonite Prismatic Layer, (P in Figure 5.2 b), occurs on the medial surface of the medial lamina of the Outer Fibrous Shell Layer and on both the medial and lateral surfaces of the sigmoid part of the medial lamina. It is thus lateral to, and at the proximal end of the above sigmoid structure intrudes into, the Outer Nacreous Layer, (onl in Figure 5.2 b).

The similarity of the Prismatic Layer of this species (Fig. 5.1, c and 5.2, a and b), to the Radial Layer of a cultured pearl should be noted, (Fig. 5.42, a, c and d). Both of these should be contrasted with the calcitic Prismatic Layers of the species of the *Pinctada*, (e.g. *P. maxima*, Figs. 5.30 - 5.40, etc).

FIGURE 5.2 *Velesunio ambiguus* - Outer Nacreous Layer, Aragonite Prismatic Layer and Outer Fibrous Shell Layer.

a. S.E.M. x 390

b. S.E.M. x 770

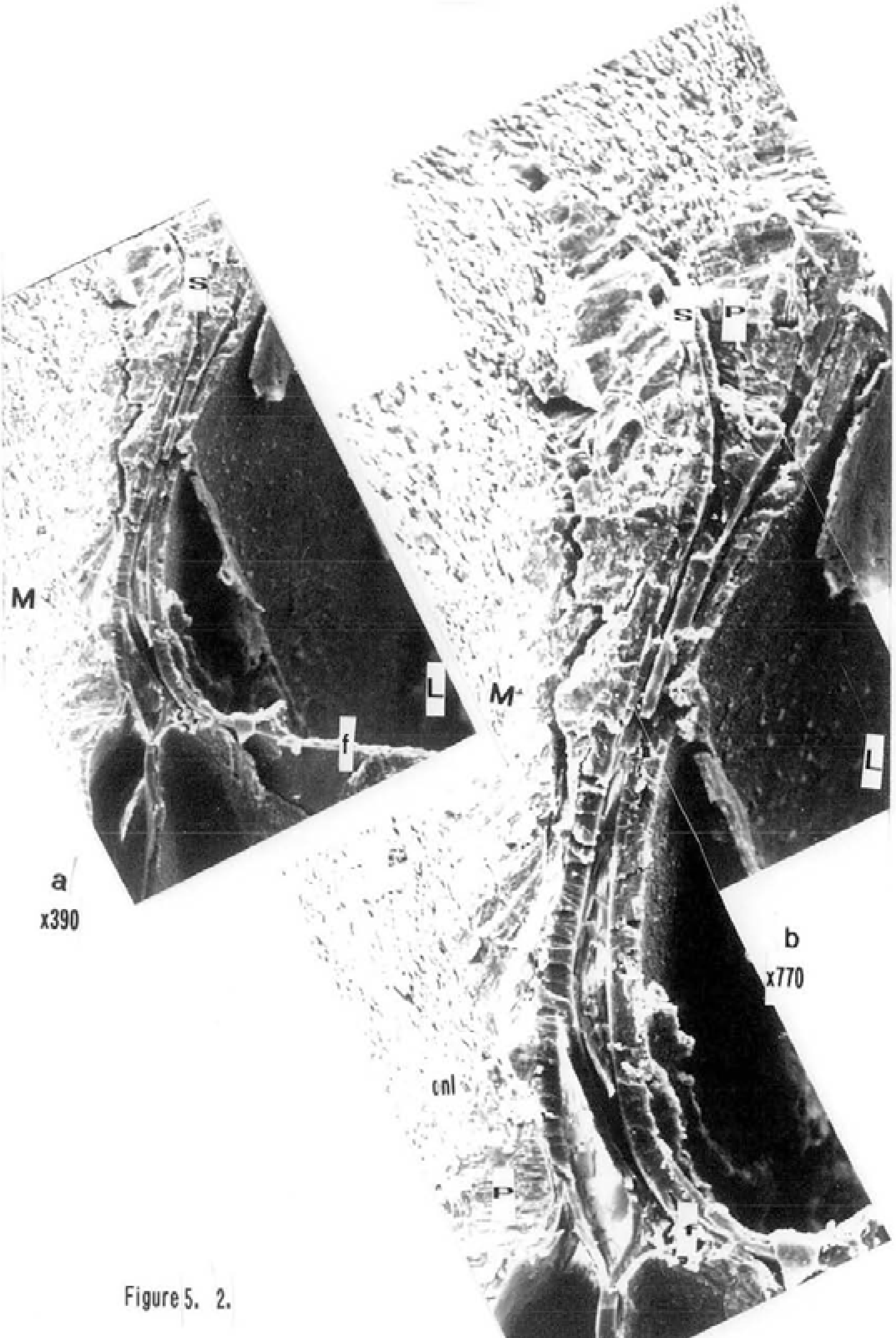

Figure 5. 2.

5.1.1.3. External Mantle, Mantle Margin and Outer Fibrous Shell Layer.

The Inner Nacreous Layer forms the lateral surface of the Pallial Space which is bounded medially by the Pallial Epithelium, (P.S. and P respectively in Figure 5.3 a). The Pallial epithelium is a simple squamous epithelium with apical nuclei. In the parenchyma of the Mantle are spherical cells with granular cytoplasm which appear to secrete into the sinus beneath the surface epithelia (c in Figure 5.3, b, c and e).

The outer lamina of the trilaminate Outer Fibrous Layer is produced by the proximal part (p) of the glandular ridge (g) of elongate columnar cells on the proximal part of the MedF1., (p and g in Figure 5.3, b, e and f). There may also be material contributed from Proximal LatF2., (F2 in Figure 5.3, e and f).

The middle lamina of the Outer Fibrous Shell Layer is produced largely by the main part of the glandular ridge (g in Figure 5.3, b, e and f), with perhaps a contribution from Proximal MedF1. (F1. in Figure 5.3 e and f).

The Inner lamina of the Trilaminate Outer Shell Layer is necessairily contributed by MedF1. distal to the tissues which produce the middle lamina as the three laminae appear fully formed by the recurvature of this Shell Layer around distal F1., (r in Figure 5.3 b).

The Extrapallial Space (eps in Figure 5.3 b, c and d) is bordered proximally by the Pallial Line Junction, (PL in Figure 5.3 d), distally by the recurvature of the Outer non-calcareous Shell Layer (r in Figure 5.3 b), medially by LatF1. and laterally by the growing surfaces of the Outer Nacreous Layer and Prismatic Layer, and, distal to these, the medial lamina of the Outer non-calcareous Shell Layer.

The Mantle Edge Gland (meg in Figure 5.3, b, c and d), lines about the proximal half of LatF1. - the medial surface of the Extra Pallial Space.

The origin, nature and staining affinities of the trilaminate Outer Shell Layer of this species, (Fig. 5.3, b,c,d,e and f) should be compared with the trilaminate Outer Shell Layer of *Nucula superba*, (Fig.5.4, a and c), that of the Mytilids, (Fig. 5.6, a,c and d; 5.7, a,b and c; 5.8, a, b and c), the decalcified Prismatic Layer Shell Organic Matrices of the *Pinctada* (e.g. *P. maxima*, Fig. 5.40), and that of all other Martius Yellow positive Shell Organic Matrices throughout the following taxa.

FIGURE 5.3 *Velesunio ambiguus* - External Mantle and Mantle Margin.

a. L.M. x 310 H & E. Pallial epithelium.

b. L.M. x 77 M.S.B., Mantle Margin.

c. L.M. x 310 H & E. Mantle Edge Gland

d. L.M. x 310 Mallory's. Mantle Edge Gland.

e. L.M. x 310 Mallory's. Apical Groove F1F2..

f. L.M. x 310 Azan. Apical Groove F1F2..

a
x310

b
x77

c
x310

d
x310

e
x310

f
x310

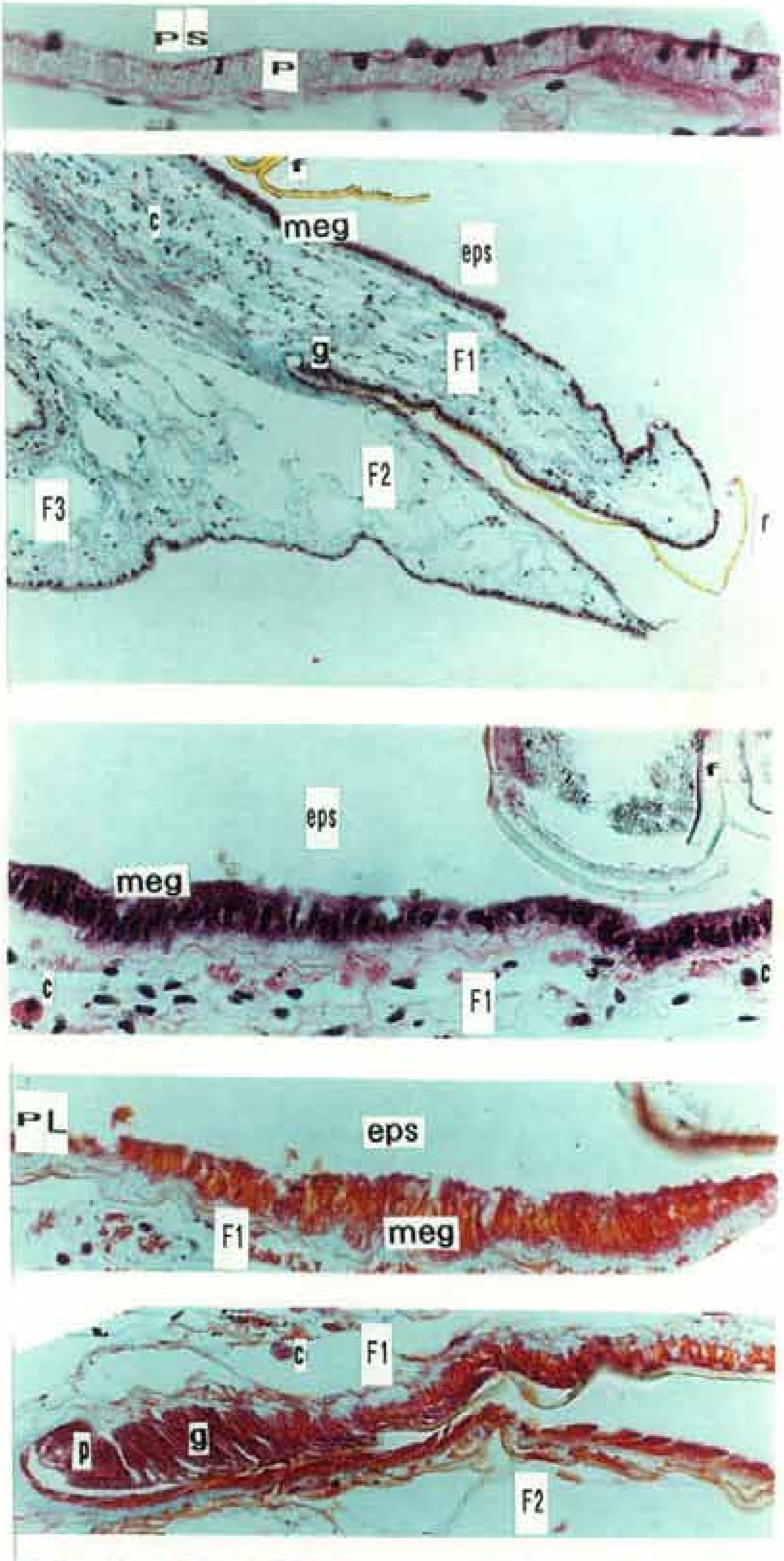

Figure 5. 3.

5.2. NUCULOIDEA.

5.2.1. *Nucula superba, Nucula sp.*

The Outer Shell Layer of *Nucula superba,* (cp in Figure 5.4. a), and *Nucula sp.,* (cp in Figure 5.4., d and e), consists of a thin outer lamina, (ol in Figure 5.4. a, d and e) outside a thicker part. In decalcified valves of *N. superba* this latter appears striate, (s in Figure 5.4. a), and as curved elongate prisms with S.E.M. in a radial broken surface of *Nucula sp.* (s in Figure 5.4. d), with the convexity of the curves directed disto- laterally. In Figure 5.4., D is distal, L, lateral and M, medial. In decalcified valves of *Nucula superba* there is a medial lamina (ml in Figure 5.4. a) which is not discernable in *Nucula sp.* with S.E.M.

The entire Outer Shell Layer is produced in the large Marginal Mantle Groove which is recurved. (To maintain consistency with all other bivalves studied the parts of the recurved Mantle Margin are named as if not recurved and then written in inverted commas - thus "lateral" will in fact be medial to "medial" for the parts of the Mantle Margin).

The middle Shell Layer is an Outer Nacreous Layer. This originates in a notch (n in Figure 5.4. a) on the "lateral" surface of the Mantle Margin which is thought to be a reduced "Groove F1F2.". If this is correct then the large Mantle Margin folds are Fold "F2." and Fold "F3." and are named accordingly in Figure 5.4., a and c.

The Nacre Sheets of the Outer Nacreous Layer (onl in Figure 5.4. d and e), are concave proximo-laterally so that the elongate prisms of the Prismatic Layer join them at about right antles (j in Figure 5.4 d). The Nacre Sheets of the Outer Nacreous Layer are much thinner than those of the Inner Nacreous Layer (onl and inl respectively in Figure 5.4 e). In Figure 5.4 e from lateral to medial (L to M) is the Composite Prismatic Layer, Outer Nacreous Layer, Myostracal prisms and Inner Nacreous Layer (CPL, onl, MP and inl respectively in Figure 5.4 e).

The Medial Shell Layer is the Inner Nacreous Layer (inl in Figure 5.4 a), which is produced by the Pallial Mantle. It is continuous with the Lateral Denticles (ld in Figures 5.4., b and f). The broken surface of the lateral denticles in 5.4., f shows that these Nacre Tiles have curved surfaces roughly parallel to the outer curved surface of the Lateral Denticle.

The ventral part of the Hinge, (vp in Figure 5.4 b) is adjacent to a specialised epithelium. The concave surfaces of the paired lateral parts of the Hinge (lp in Figure 5.4 b) are adjacent to a very different specialised epithelium with elongate columnar cells (ec in Figure 5.4 b). The epithelium lining the Lateral Denticles, (eld in Figure 5.4 b) appears indistinguishable from that which lines the Pallial Space (ps in Figure 5.4 a).

The Dorsal Part of the Hinge (dp in Figure 5.4 b) is continuous with and has the same staining affinities for all stains used as the Medial Lamina (ml in Figure 5.4 a), of the Trilaminate Outer Shell Layer.

Going from before backwards, (or behind forwards), along the dorsal margin of this animal, from where the right and left recurved Mantle Margins are separate, and each has the forming Organic Matrices of the respective right and left Outer Shell Layers lodged in their Grooves "F2F3", (as in Figure 5.4 a) to where the right and left mantles are fused beneath the dorsal part of the hinge (near Figure 5.4 b) the right and left "F3"s are lost at the same locations as the outer laminae of the Trilaminate Outer Shell Layers are lost; and proceeding further, the middle laminae of the Trilaminate Outer Shell Layers are lost at the same locations where the epithelia which in Figure 5.4 a only cover Distal "MedF2." (dm2 in Figure 5.4 a) come to cover the entire surfaces of the now opposed "MedF2."s, (dm2 in Figure 5.4, c and b). Concomitantly with the loss of the Proximal "MedF2." epithelia, the subepithelial glands of Proximal "MedF2." are lost.

Nucula superba demonstrates four morphologically distinct examples of apparently homogenous Shell Layer or Hinge being generated by four different specialised secretory epithelia. Where the Shell Layer Organic Matrix is more complicated, e.g. the middle lamina of the trilaminate Outer Shell Layer, both a specialised epithelium and subepithelial secretory glands are involved in its production.

FIGURE 5.4. *Nucula superba* and *Nucula sp.* - Mantle, Mantle Margin and Shell Layers.

a. L.M. x 460 Mallorys. Mantle Margin.

b. L.M. x 150 Mallorys. Hinge.

c. L.M. x 770 A.B./M.S.B., Fusing Mantle Margins Anterior to Posterior Mantle Symphysis.

d. S.E.M. x 770 Composite Prismatic Layer and Outer Nacreous Layer.

e. S.E.M. x 1500 Radial Broken Surface.

f. S.E.M. x 380 Broken Lateral Denticles.

Figure 5.4

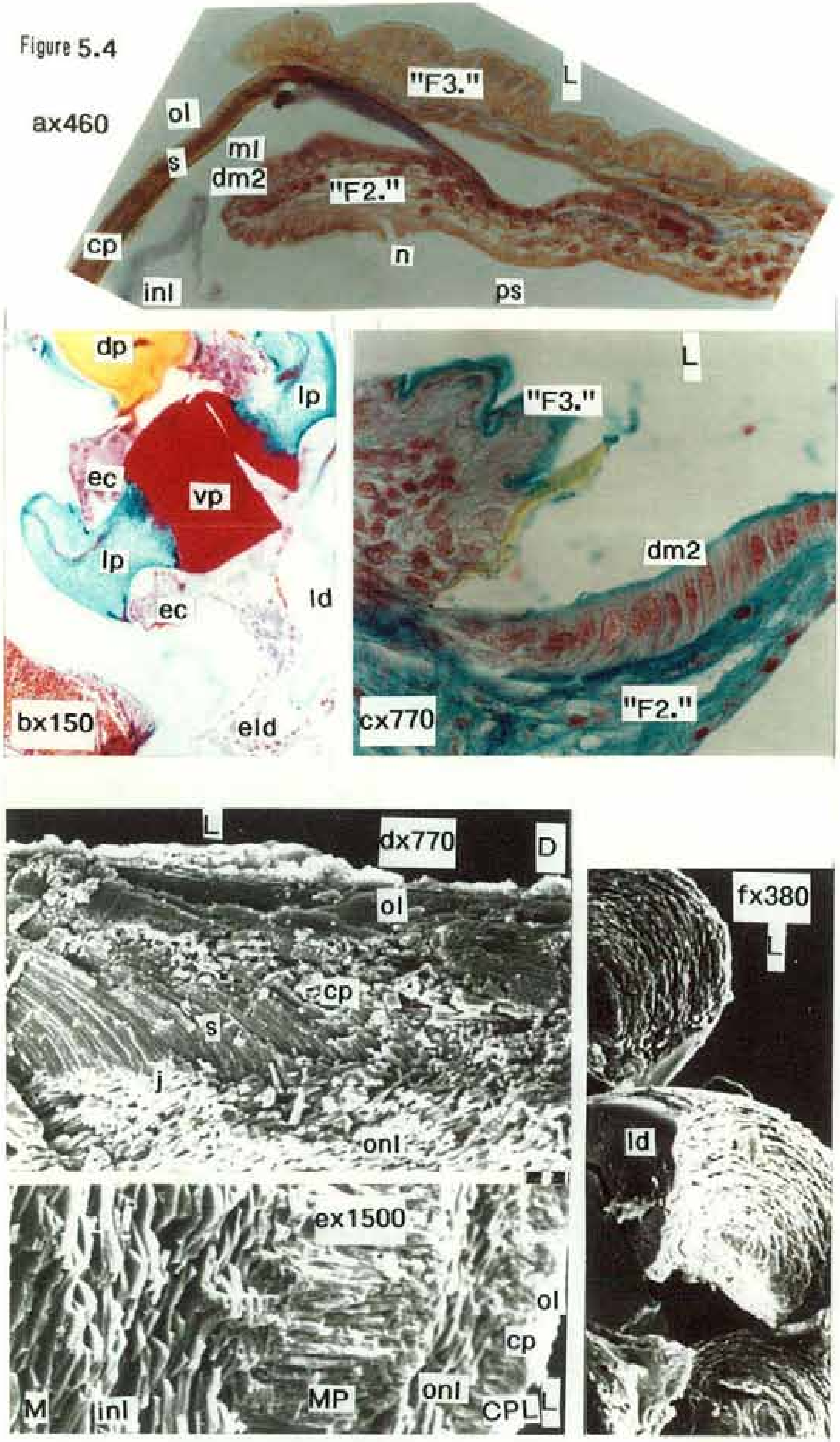
ax460
ol
s
ml
dm2
"F3."
L
"F2."
cp
n
inl
ps
dp
lp
ec
vp
lp
ec
ld
bx150
eld
L
"F3."
dm2
"F2."
cx770
L
dx770
D
ol
cp
s
j
onl
ex1500
ol
cp
M
inl
MP
onl
CPL
L
fx380
L
ld

5.3. MYTILOIDEA.

5.3.1. *Trichomya hirsuta.*

5.3.1.1. Mantle Margin.

The External Mantle is joined to the medial surface of the valve at the Pallial Line, proximal to P in Figure 5.5, thus enclosing a Pallial Space.

The trilaminate outer Shell Layer originates in the Apical Channel of Groove F1F2., (c in Figure 5.5. b). There is thus an Extra-pallial Space which is enclosed between the recurved forming Outer Shell Layer and the Pallial Line Junction, (e in Figure 5.5. a and b).

The Mantle Margin consists of three folds F1., F2., F3., (1, 2 and 3 respectively in Figure 5.5. a and b).

All Folds, but especially F1. and F3. have a parenchyma of spongiform tissue with the sinovial walls lined with cells with granular cytoplasm.

The epithelium lining the medial surface of the Extra-pallial Space gradually lengthens distally (D in Figure 5.5.) to the elongate columnar cells of the Mantle Edge Gland on LatF1. (meg in Figure 5.5.)

Between the elongate columnar epithelium lining the lateral surface of the Apical Channel and the Terminal Epithelium (c and t respectively in Figure 5.5. b) the MedF1. bears a columnar epithelium which elongates going distally but in other respects the cells appear uniform. (m in Figure 5.5. b). The nuclei are in the basal half of the cell and the apical cytoplasm stains strongly with H and E..

The surface epithelia of LatF2. are differentiated into Proximal, Middle and Distal LatF2. (pl2, ml2 and dl2 in Figure 5.5. b), of which Middle LatF2. is an elongate columnar epithelium with relatively very small basal nuclei and a deeply staining apical cytoplasm.

There is a deep notch between Proximal LatF2. and Middle LatF2., (n in Figure 5.5. b).

FIGURE 5.5. *Trichomya hirsuta.* Mantle Margin.

a. L.M. x 39 H and E.

b. L.M. x 190 H and E.

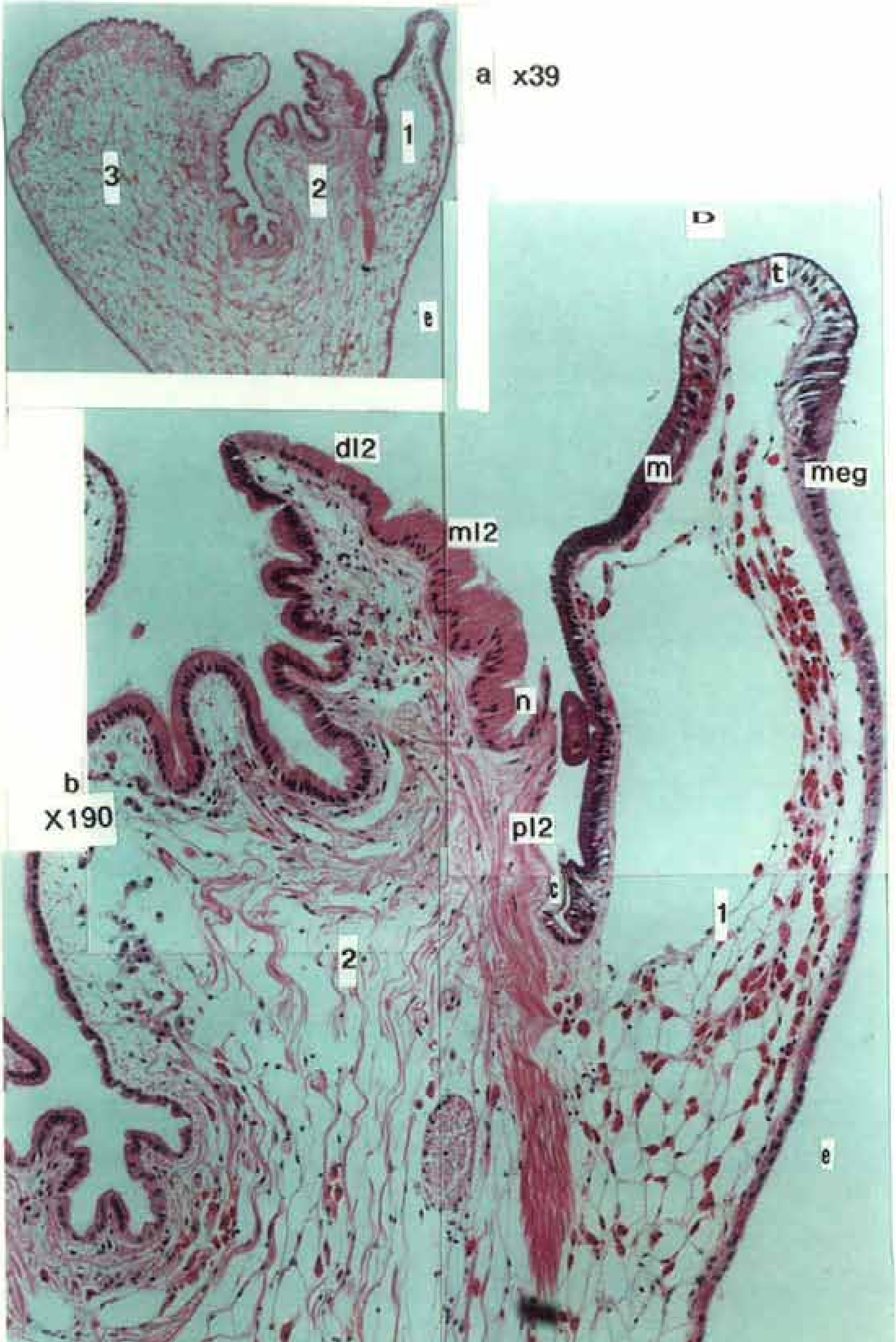

Figure 5.5

5.3.1.2. Tissues of Folds F1. and F2. and their secretions.

The trilaminate outer Shell Layer appears to commence in the Apical Channel of Groove F1F2., (c in Figure 5.6. a). The thick middle lamina, (o in Figure 5.6. a, c and d) lies opposite the epithelium lining MedF1. (m in Figure 5.6. a, b and c) and reflects the colour of its apical granules (gold with M.S.B. Figure 5.6. a, red with Azan Figure 5.6. c).

The secretory structures of Middle LatF2. (ml2 in Figure 5.6. b and d) and the Granular Cytoplasm Secretory Glands of Distal LatF2. (G at dl2 in Figure 5.6. d) if they are involved in Shell Layer production are geometrically limited to either augmentation of the outer lamina of the outer non-calcareous Shell Layer or production of the external "hairs" from which the specific name derives.

The Outer Shell Layer of this species is the Martius Yellow positive layer secreted by Groove F1F2. The differentiation of the tissues of LatF2., MedF2. and LatF3. into specific tissue Regions may be related to the formation of the elongate "hairs" on the outer surface of the shell. This should be contrasted againt the simplicity of structure of F2. and F3 in *Velesunio ambiguus*; and the highly differentiated tissue Regions of F2. and LatF3. in the *Pinctada*

FIGURE 5.6. *Trichomya hirsuta* - Tissues of F1. and F2. and their secretions.

a. L.M. x 460 M.S.B., Secretion of outer and middle lamina of outer Shell Layer.

b. L.M. x 460 M.S.B., Histology of Middle MedF1. and Middle LatF2..

c. L.M. x 150 Azan. Apical Groove F1F2..

d. L.M. x 310 Azan. Middle LatF2., Distal. LatF2..

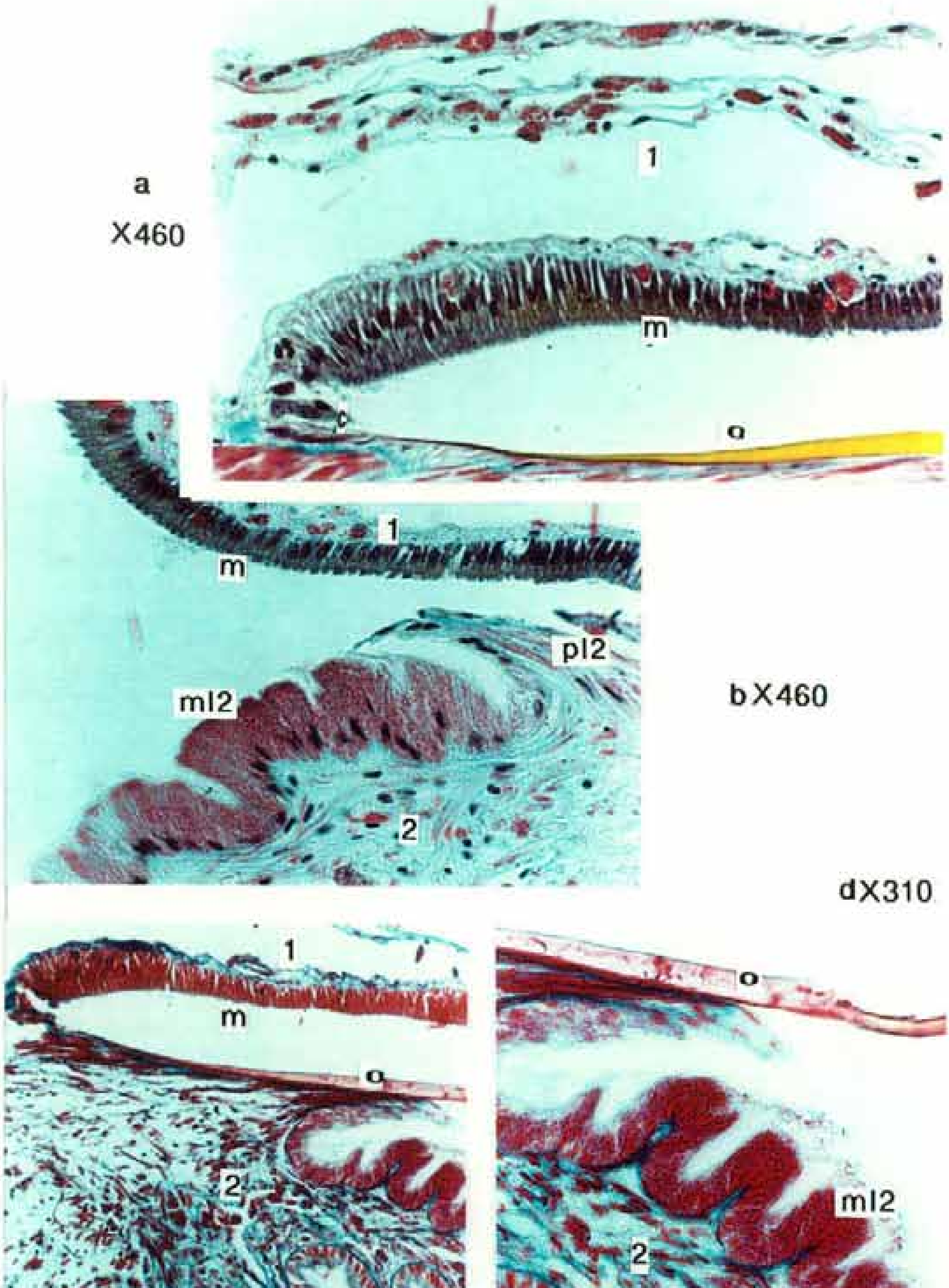

Figure 5.6

5.3.2. *Lithophaga teres.*

5.3.2.1. Decalcified Shell Layers.

The Valve of *Lithophaga teres* consists of a trilaminate outer Shell Layer (osl in Figure 5.7, a, b and c), an Outer Nacreous Layer and an Inner Nacreous Layer, (onl and inl respectively in Figure 5.7, a, b and c). In radial section the fibres of the Outer Nacreous Layer Organic Matrix are directed parallel to the outer Shell Layer and those of the Inner Nacreous Layer are normal to these.

The dissimilarity of the two Nacreous Layers in this species should be contrasted with the morphological similarity of the Nacreous Layers in other species illustrated, e.g. *Velesunio ambiguus, Nucula superba* and the pearl oysters. Again, differentiation of the Mantle Margin tissues medial to Groove F1F2. is related to functions other than shell Layer formation - in this case probably the production of an acidic secretion for dissolution of calcified structures and the neutralisation of that secretion.

FIGURE 5.7. *Lithophaga teres* - Decalcified Shell Layers.

a. L.M. x 77 Mallory's. Decalcified outer, middle and inner Shell Layers.

b. L.M. x 310. Mallory's. As for a above at higher magnification.

c. L.M. x 770. Azan. Decalcified outer and middle Shell Layers.

a

x 77

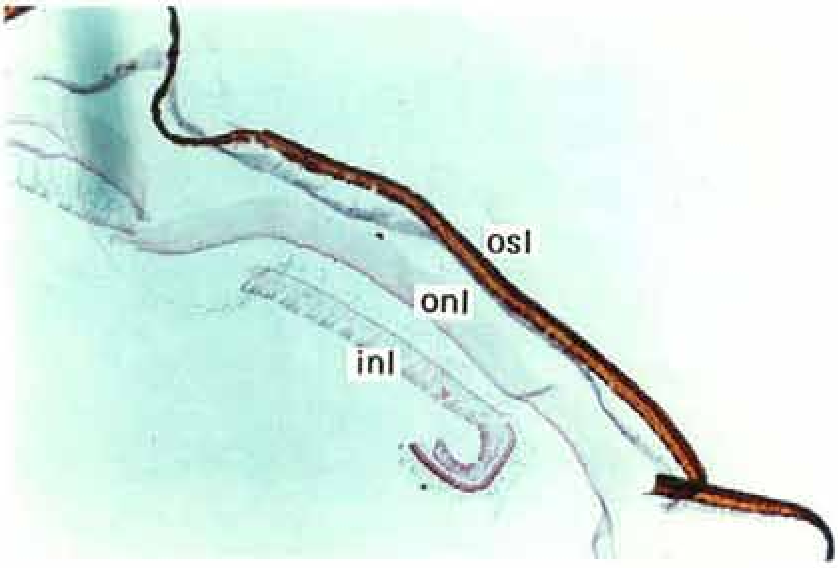

b

x 310

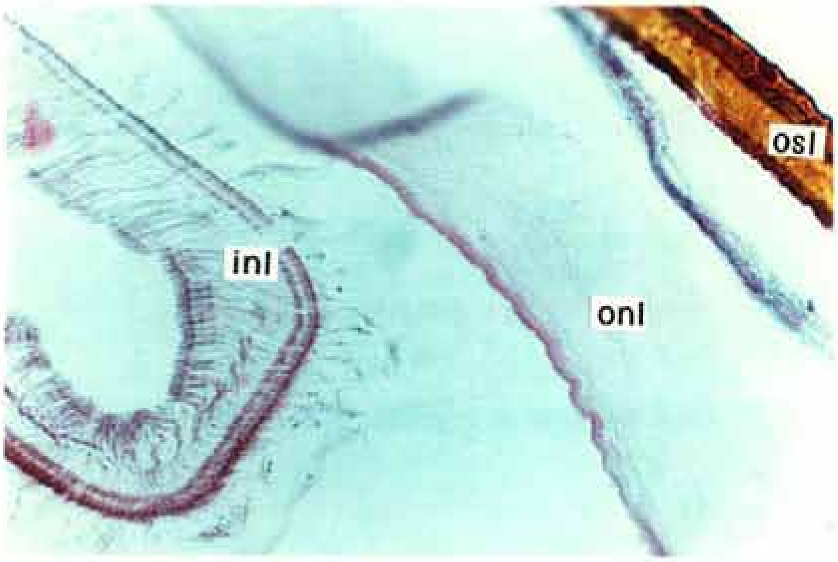

c x 770

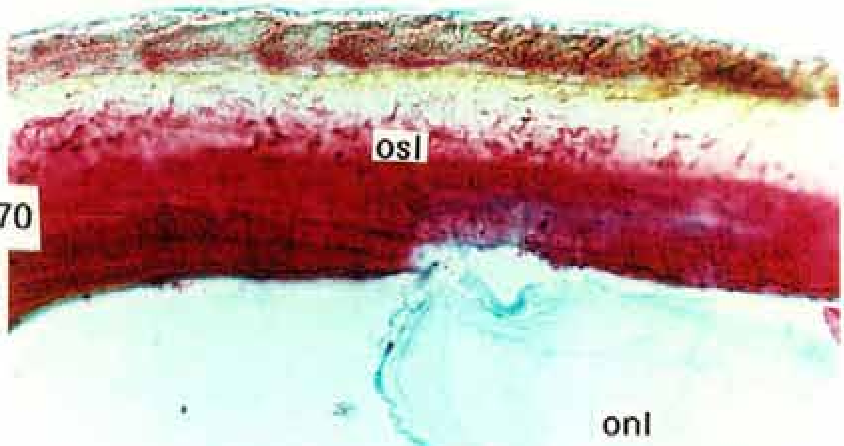

Figure

5.7

5.3.2.2. *Lithophaga teres* - Mantle Margin.

The Mantle Margin has three Marginal Mantle Folds. F1. (F1 in Figure 5.8, a, b and c), has a large internal sinus. F2. has two very distinctive basophilic glandular structures, one opening on the lateral surface near the Fold terminus (lg in Figure 5.8, a and c) and the other opening on the medial surface (mg in Figure 5.8, a and c) into Groove F2F3.. Fold F3 has a large acidophillic gland.

LatF1. proximally has a cuboidal epithelium. Distally the epithelial cells elongate to the columnar cells of the Mantle Edge Gland (meg in Figure 5.8 b). A distinct notch separates this from the Terminal epithelium (t in Figure 5.8. b).

Medial F1. (mf1. in Figure 5.8. b) bears a columnar epithelium opposite which, in Groove F1F2., the middle lamina (m in Figure 5.8, b and c) of the trilaminate outer Shell Layer develops to its full width.

The lateral lamina of the outer Shell Layer (l in Figure 5.8 c) is produced in an indentation (a in Figure 5.8 b) on LatF2. - histologically akin to the Apical Channel of *Trichomya hirsuta* (c in Figure 5.5. b).

The External Mantle is joined to the medial surface of the valve at the Pallial Line. There is thus an enclosed Pallial Space. The Inner Nacreous Layer (inl in Figure 5.7. a and b) is coextensive with the External Pallial epithelium and forms the lateral surface of the Pallial Space.

The growing surface of the Outer Nacreous Layer (onl in Figure 5.8. a and c), is enclosed in the Extra-pallial Space (eps in Figure 5.8. c).

FIGURE 5.8. *Lithophaga teres* - Mantle Margin.

a. L.M. x 77 Mallory's.Mantle Margin Folds F1., F2. and F3..

b. L.M. x 310 Mallory's. F1. and LatF2. and secretion of the lateral and middle lamina of outer Shell Layer

c. L.M. x 77 Mallory's. F1. and F2.. Outer Shell Layer and Outer Nacreous Layer.

a X77

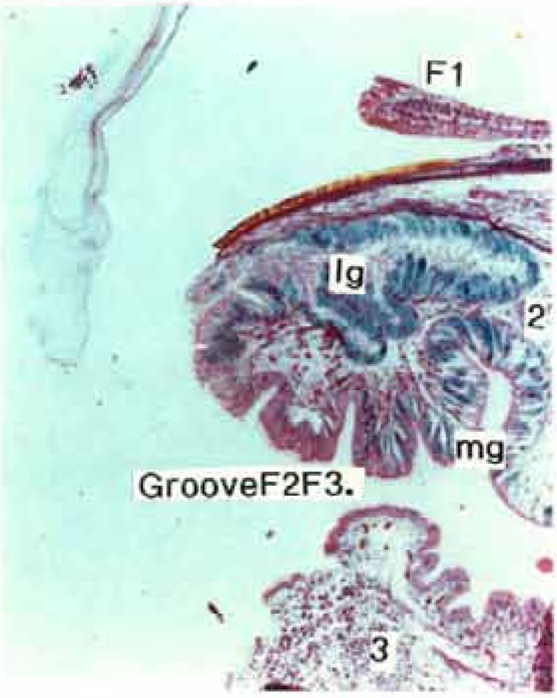

bX310

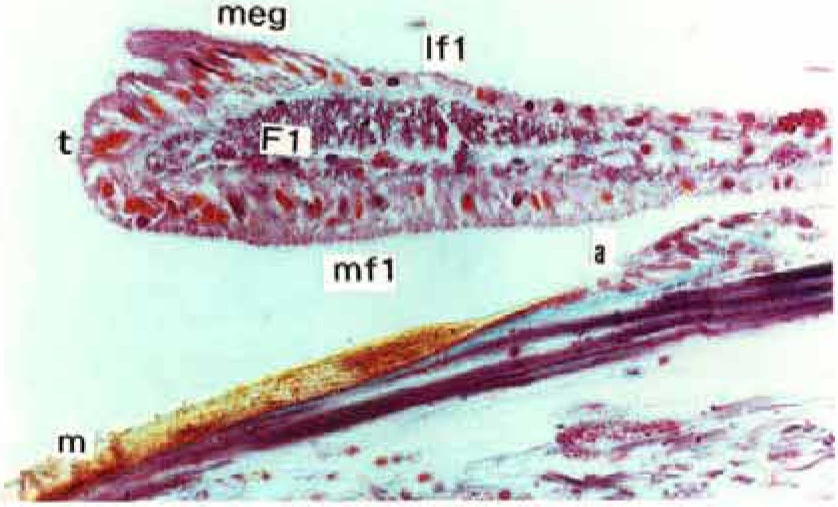

c X77

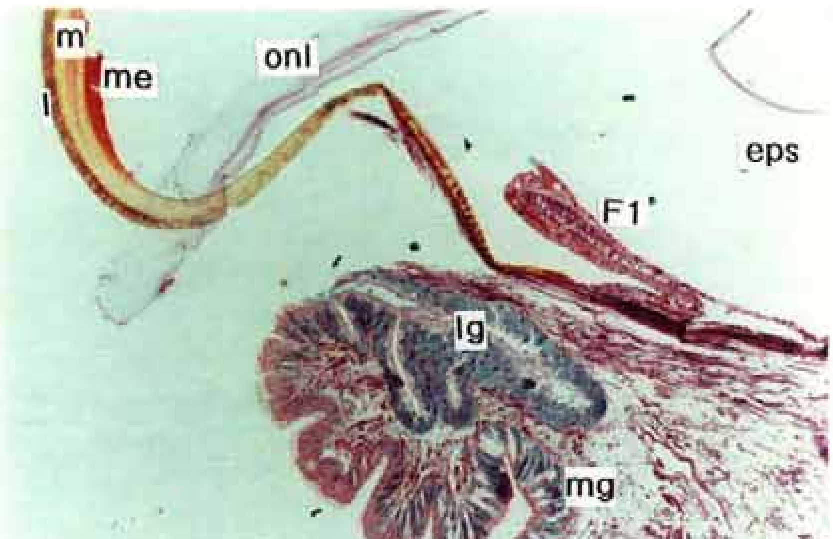

Figure

5.8

5.4.PINNOIDEA.

5.4.1. *Pinna bicolor.*

5.4.1.1. Mantle Margin.

The Mantle Margin of *Pinna bicolor* has three Folds F1., F2., and F3., (1, 2 and 3 in Figure 5.9, a, b and c).

LatF1. has a Mantle Edge Gland, (meg in Figure 5.9, b and d), of columnar epithelium with subepithelial Trabecular Turquoise Glands (tt, Figure 5.9. d).

The Ventral Mantle Margin is remote from the restricted area of Nacre on the Proximal part of the Valve and has a MedF1. distal to the Omega Gland (o in Figure 5.9. a, b and c), apparently devoid of Trabecular Turquoise Glands or any other kind of Unicellular secretory gland, (mfl in Figure 5.9, a and c).

The Omega Gland (o in Figure 5.9, a, b and c) is on proximal MedF1. and forms an apical channel with the opposing surface of LatF2. from which a Pleated Secretion of Groove F1F2. issues (P in Figure 5.9, a, b and c).

The Circum-pallial Nerve (n in Figure 5.9. a and b) lies immediately beneath the Omega Gland in close proximity to the Circum-pallial sinus (s in Figure 5.9. a and b).

The subepithelium of LatF2., MedF2. and LatF3. (l2, m2 and l3 in Figure 5.9, b and c) all bear populations of Trabecular Turquoise Glands.

There is a mass of secreted material (se in Figure 5.9, c) in Groove F2F3.

The Mantle Margin of this species, where distant from the part of the shell which has nacreous layers has a structurally simple MedF1.. This should be compared with differentiation of the tissues of MedF1. of the *Pinctada.*

FIGURE 5.9. *Pinna bicolor* - External Mantle and Mantle Margin.

a. L.M. x 150 Azan. Distal External Mantle and Mantle Margin.

b. L.M. x 120 A.B./M.S.B. As for a above.

c. L.M. x 120 A.B./M.S.B. As for a and b above.

d. L.M. x 1200 A.B./M.S.B. LatF1..

a
X150

b
X120

c
X120

d
X1200

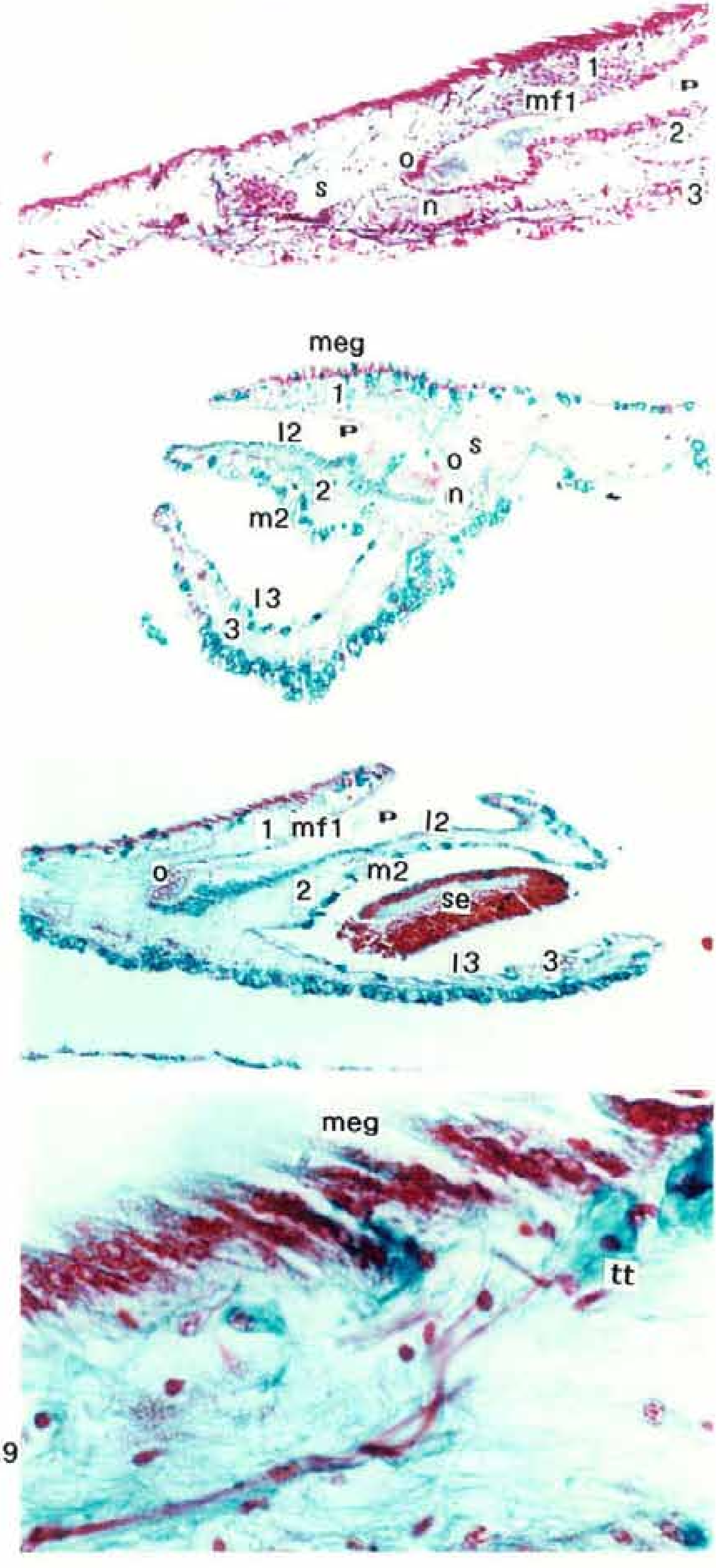

Figure 5.9

5.5. PTERIOIDEA.

5.5.1. *PINCTADA MAXIMA.*

5.5.1.1. Valves.

The valves of the young adult *Pinctada maxima* (figure 5.10., scale bars in mm) have about equal dorso-ventral (Figure 5.10. D - V) and antero-posterior axes. (Figure 5.10. A - P).

The linear extents of the Nacre (Figure 5.10. N) on both axes are slightly greater on the Left Valve (Figure 5.10. a) than the Right Valve (Figure 5.10. b), and therefore conversely the medial linear extent of the Prismatic Layer (Figure 5.10. PL) is greater on the Right Valve than the Left Valve.

Growth Processes (Figure 5.10 G.P) partially obscure the right end of the scale in Figure 5.10. b., and are near the Ventral periphery on the lateral surface of the Right Valve (Figure 5.10. c).

The Hinge (Figure 5.10. a and b. H) has narrow Anterior and Posterior parts and the middle about third and fourth sevenths are enlarged ventrally. The Byssal Notch (BN in Figure 5.10.) occupies the dorsal part of the anterior border.

The Adductor Muscle Scar (ams) is slightly concave Antero-dorsally and situated just Postero-ventrally to the geometric centre of the medial surface of the Nacre.

FIGURE 5.10. *Pinctada maxima*.- Valves.

a. Medial View Left Valve.

b. Medial View Right Valve.

c. Lateral view Right Valve.

a

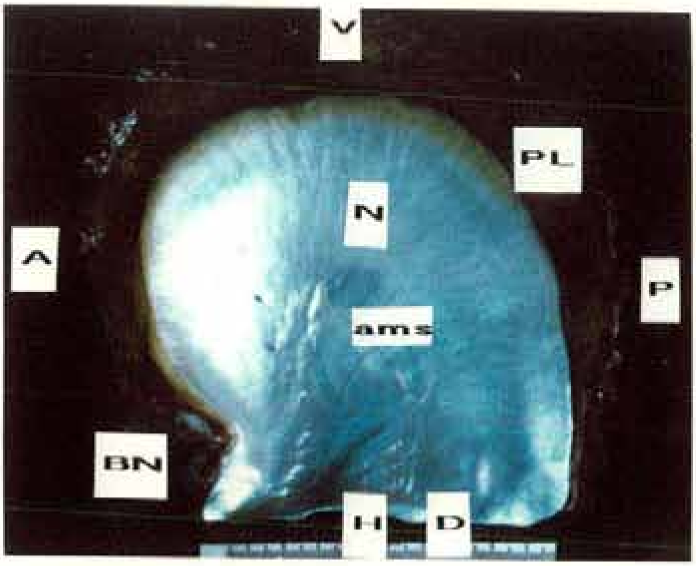

b

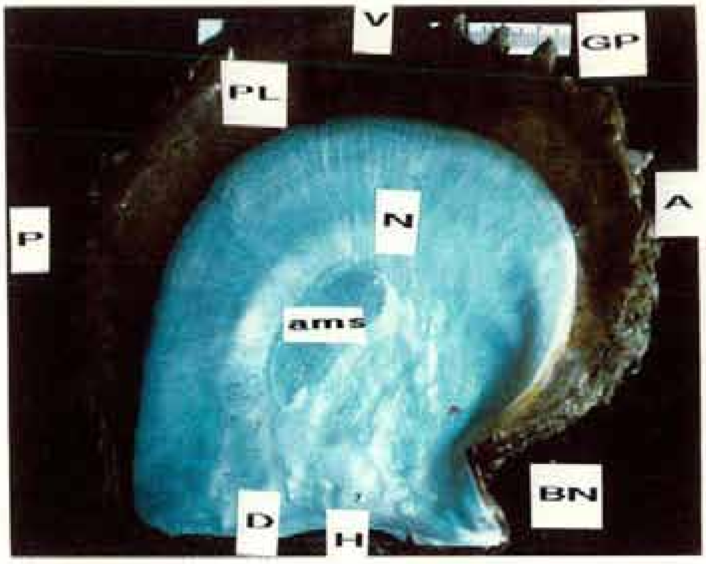

c

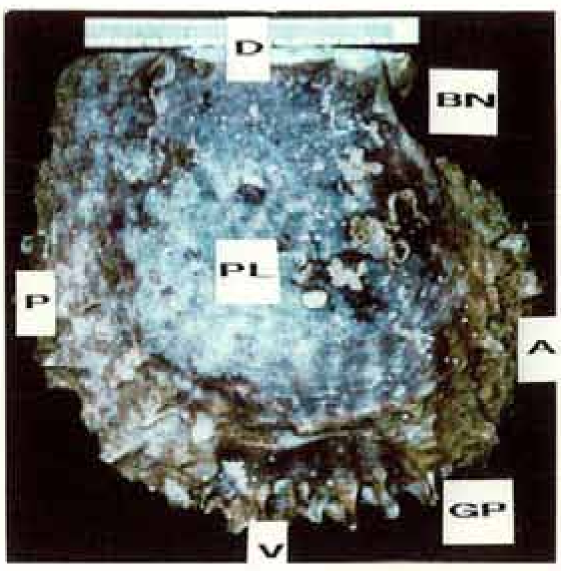

Figure 5.10

5.5.1.2. Hinge.

The enlarged middle part of the Hinge, (Figure 5.11, H) is composed of parallel fibrils of about 0.1μm diameter, (Figure 5.11 b and c). These fibrils lie in planes about normal to the hinge line and hence to the plane of symmetry. The plane of breakage shown in Figure 5.11 of half the Hinge (H) and the adjacent Nacre (N) is such a plane.

In Figure 5.11. a. L is lateral and M medial. The Hinge Fibrils have artefactually pulled away from their abutment at right angles with the Nacre (N in Figure 5.11. a).

From this abutment the fibrils run first medially and then curve ventrally to where they join, (j in Figure 5.11. a), the fibrils of the other half of the Hinge in the midline, at about fifty degrees, (Figure 5.11. a).

The fibres of the Hinge protein rubber appear to display periodicity (Figure 5.11. c).

FiIGURE 5.11. *Pinctada maxima* - Hinge and adjacent Nacre.

a. S.E.M. x 65 Relationships of a Dorso-ventrally broken face of half the Hinge and the adjacent Nacre.

b. S.E.M. x 6700 Higher magnification at about H in Figure 2a.

c. S.E.M. x 27000 Higher magnification at about H in Figure 2b.

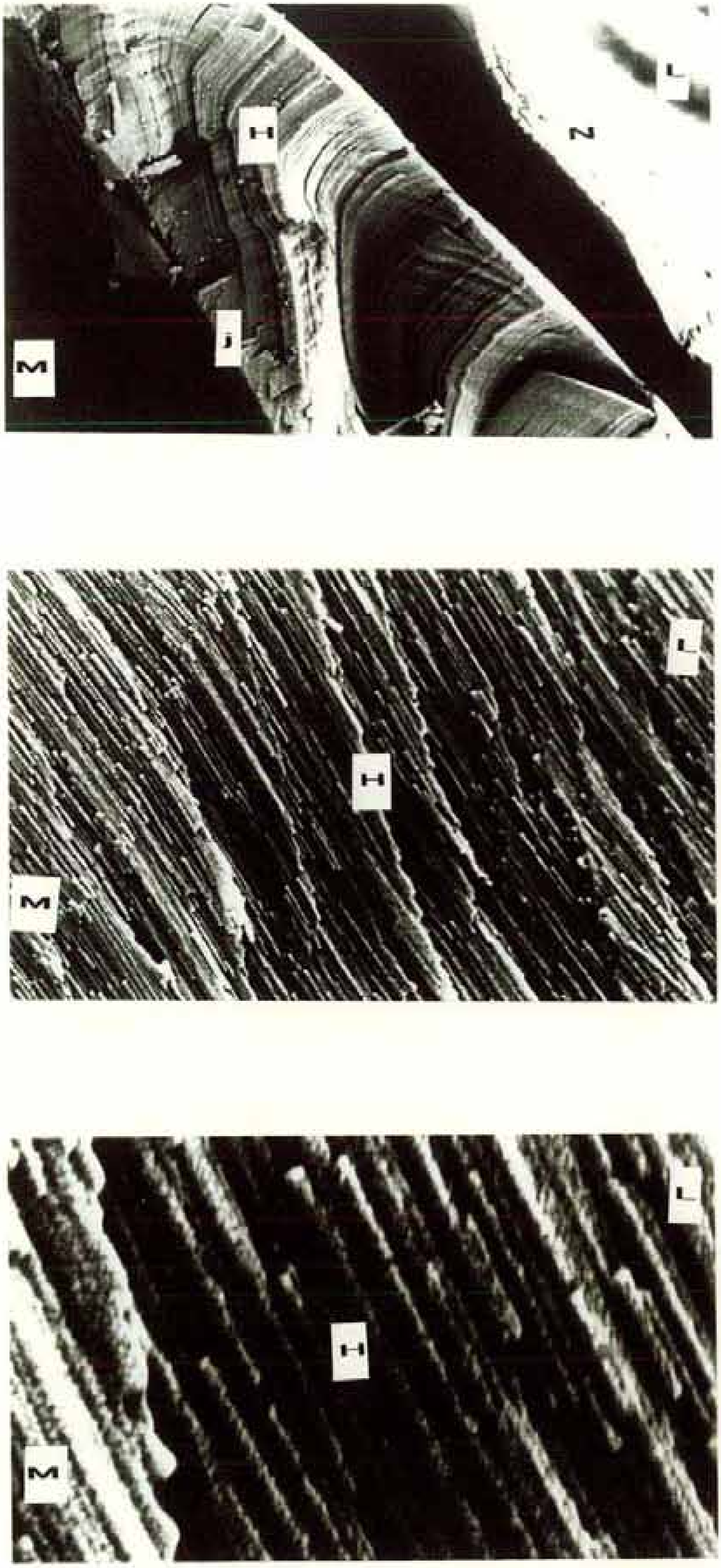

a

x 65

b

x6700

c

x27000

Figure 5.11

5.5.1.3. S.E.M. of Nacreous Layers.

5.5.1.3.1. Selection of specimens for L.M. and S.E.M. Study of the Medial Surface of the Nacreous Layers.

The External Mantle of members of the *Pinctada* is divided on histological grounds into the Shoulder Region, Pallial Gland Region and nine Pallial Regions - the Proximal Middle and Distal, Anterior Ventral and Posterior Pallial Regions. (Figures 5.52, 5.102, 5.116 and 5.121).

These alterations in External Mantle histology are broadly reflected in alterations in the patterns of edges of Nacre Sheets in these Regions. Further, there are alterations in these patterns between the medial surfaces of the Inner Nacreous Layer and the adjacent Outer Nacreous Layer.

To investigate these differences in this species, and also shell micro-morphology at the adjacent Nacreo-prismatic Junctions, samples from the positions 1 - 16 in Figure 5.12. were photographed using L.M. and then cut from the Valve for S.E.M. These positions are:

1, Shoulder Region near Hinge, 2, Shoulder Region near Adductor Muscle; 3, Ventral Pallial Gland Region; 4, Posterior Pallial Gland Region; 5, 6 and 7, Proximal Middle and Distal Ventral Pallial Regions; 8, Ventral Outer Nacreous Layer and Nacreo-prismatic Junction; 9, 10 and 11, Proximal, Middle and Distal Posterior Pallial Regions; 12, Posterior Outer Nacreous Layer and Nacreo-prismatic Junction; 13, 14 and 15, Proximal Middle and Distal Anterior Pallial Regions; 16, Anterior Outer Nacreous Layer and Nacreo-prismatic Junction.

The overall similarity in the patterns of edges of Nacre Sheets in the different specified Regions of the shells of pearl oysters and the several other features common to all pearl oyster nacreous Layers are illustrated in Figs. 5.12- 5.28, (*Pinclada maxima*); 5.84 - 5.90, (*P. margaritifera*); and other pearl oysters at 5.126; 5.131, a-c; 5.133, a - c; 5.143; and 5.151.

FIGURE 5.12. *Pinctada maxima* - location of samples for S.E.M. of Nacre. Tracing of Right Valve of *Pinctada maxima* from Figure 1, actual size showing positions used for L.M. and S.E.M. of Medial surface of Nacreous Layers. A Anterior, V Ventral, PL Prismatic Layer, N Nacre.

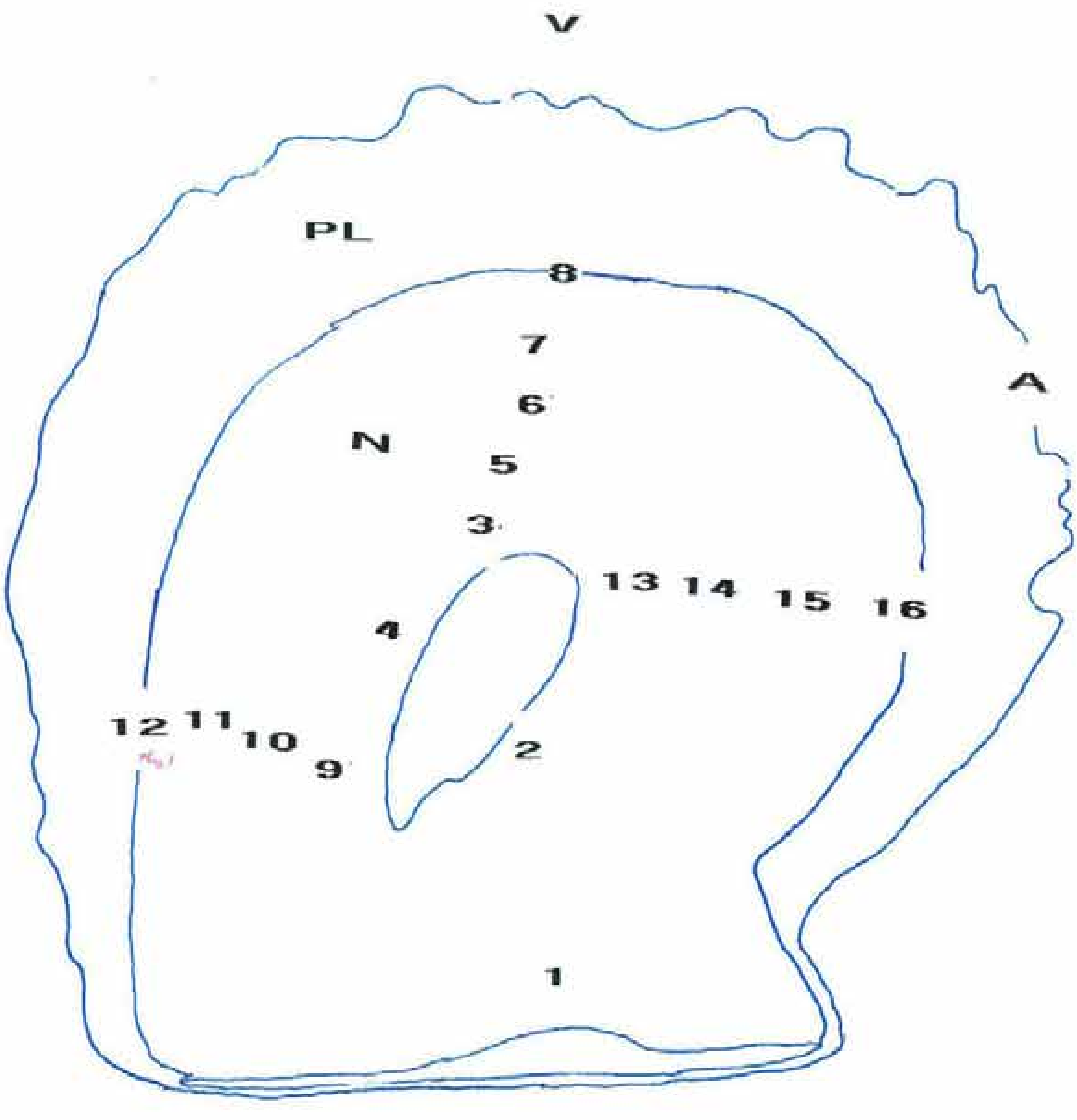

Figure 5.12

5.5.1.3.2. Medial Inner Nacreous Layer, Shoulder Region near Hinge.

The medial surface of the Inner Nacreous Layer near the Hinge is characterized by concentric circular and spiral patterns of Edges of Nacre Sheets. These are joined by variously curvilinear, and fairly straight parallel line patterns (Figure 5.13. a and b).

The average distances between the Edges of the Nacre Sheets range from 80 μm between a and b to 65 μm between a and c and 40 μm between d and e on Figure 5.13. b.

The individual Free, Partly-bound and Bound Nacre Tiles (f, pb and b in Figure 5.13. d) throughout this Region tend to extended hexagonal shapes with three pairs of parallel sides with two pairs equal in length and the other pair longer.

In some areas (Figure 5.13. d) the Nacre Tiles have a raised central area. Throughout the Region the Partly-bound and Free Nacre Tiles cover about half of the distance between edges of Nacre Sheets (e, e in Figure 5.13. c) and the Free Nacre Tiles are smaller with distance from the Edges of the Nacre Sheets. The long axes of the Bound and Partly-bound Nacre Tiles are about 11 μm (Figure 5.13. d).

Figure 5.13. *Pinctada maxima* - Medial Surface, Inner Nacreous Layer - Shoulder Region near Hinge, Position 1 in Figure 5.12.

a. L.M. x 40. Some of the variety of patterns of edges of Nacre Sheets found in this region.

b. S.E.M. x 77. A spiral pattern of edges of Nacre Sheets.

c. S.E.M. x 770. Near s on Figure 4b at higher magnification.

d. S.E.M. x 1500. Near s on Figure 4c at higher magnification.

a

x40

b

x77

c

x770

d

x1500

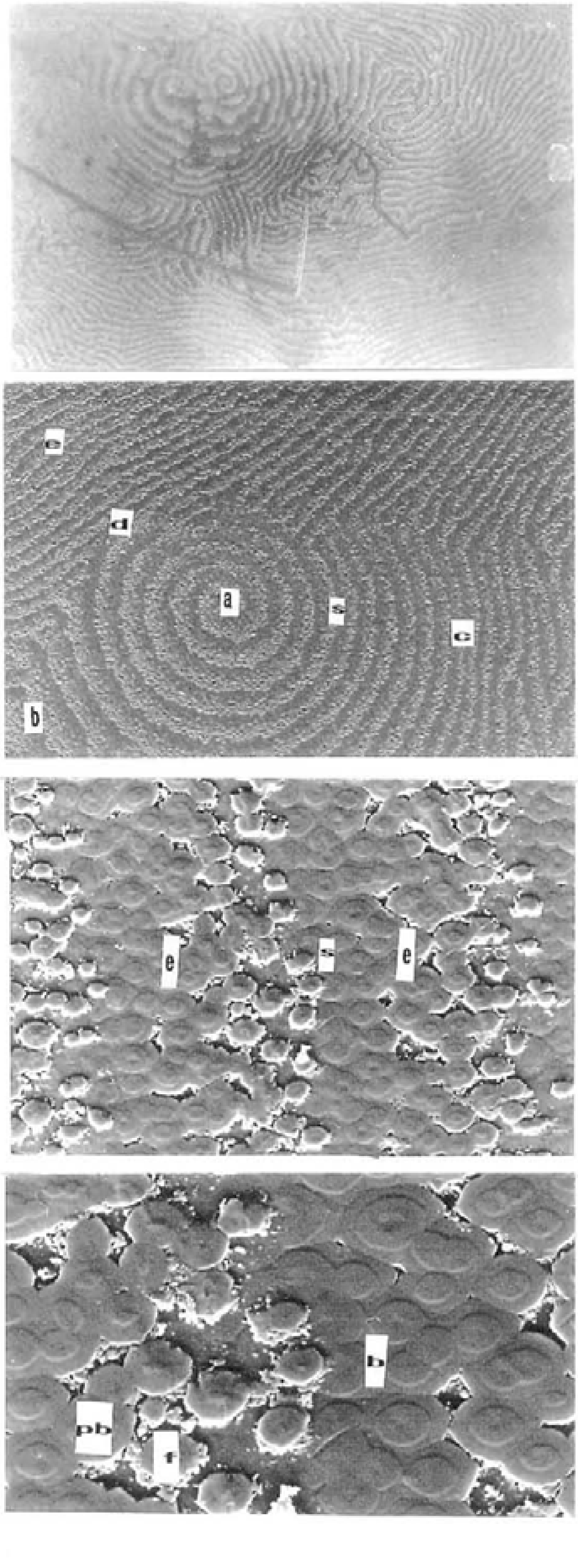

Figure 5.13

5.5.1.3.3. Medial View, Inner Nacreous Layer - Shoulder Region near Adductor Muscle.

Up to a few mm distant from the edge of the Adductor Muscle Scar (ams Figure 5.14 b) the patterns of Edges of Nacre Sheets here, as in 5.5.1.3.2., are commonly concentric circles, less commonly spirals, with intervening curvilinear patterns, (Figure 5.14. a). This mixture of patterns both near the Hinge and here is associated with numerous anastomoses, (Figure 5.13. a and b and 5.14. e). The partly-bound and free Nacre Tiles extend from the edge of each Nacre Sheet about half way across the distance between successive Nacre Sheets (Figure 5.14. e and c), which in the patterns shown in Figure 5.14. e range from about 100µm to about half that. Where the edge of a Nacre Sheet tightly recurves on itself (r and x in Figure 5.14. e) the intervening Partly-bound and free Nacre Tiles may occupy the entire space between the recurved edge of the Nacre Sheet (e, e in Figure 5.14. f and g).

Adjacent to the Adductor Muscle Scar the patterns change to narrowly spaced parallel patterns (Figure 5.14. b) with much smaller Bound and Partly-bound Nacre Tiles, (about 7 µm in Figure 5.14. c and d), than in the patterns in (Figure 5.14. f and g) where they are about 10 µm in their longest axes.

FIGURE 5.14. *Pinctada maxima* - Inner Nacreous Layer, Medial Surface - Shoulder Region near Adductor Muscle Postion 2 in Figure 5.12.

a. L.M. x 28 Some of the variety of patterns of edges of Nacre Sheets found in this region.

b. S.E.M. x 77 Pattern of narrowly spaced parallel linear edges of Nacre Sheets adjacent to Adductor Muscle Scar (ams).

c. S.E.M. x 770 Higher magnification, centre near u Figure 5b.

d. S.E.M. x 1500 Higher magnification, centre near z in Figure 5c.

e. S.E.M. x 77 Pattern of anastomosing edges of Nacre Sheets (above r) and recurving edges of Nacre Sheets (at and below r and at x).

f. S.E.M. x 770 Higher magnification centre about r in Figure 5 e.

g. S.E.M. x 1500 Higher magnification, centre about y in Figure 5f.

Figure 5.14

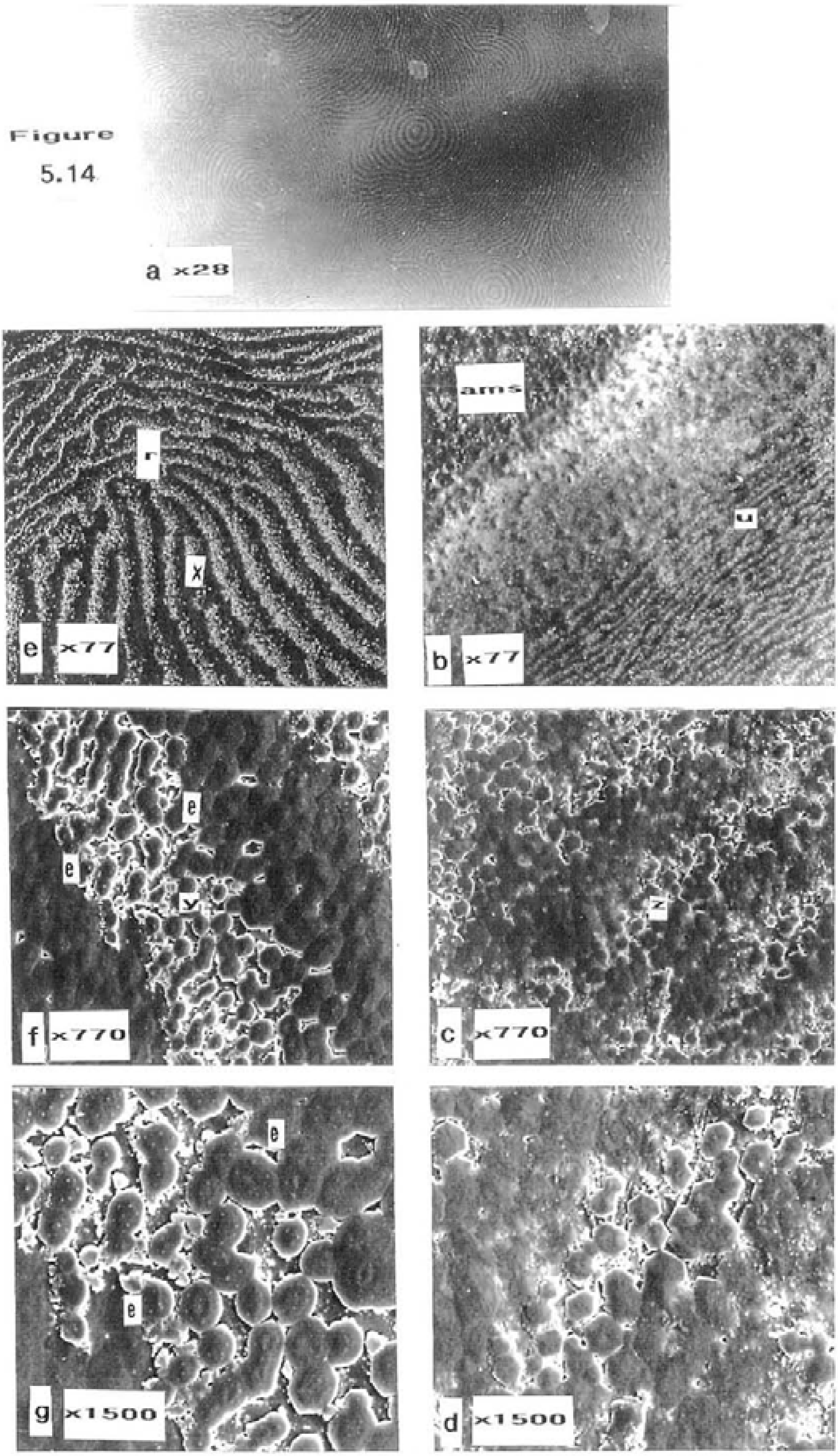

5.5.1.3.4. Medial Surface Inner Nacreous Layer - Ventral Pallial Gland Region.

Here the Patterns are largely made by tightly curved, anastomosing and recurved edges of Nacre Sheets (h, i and k respectively, Figure 5.15 b).

Where there are tightly curved edges of Nacre Sheets (near h in Figure 5.15b) the distance between them is about 100 µm but where the edges of the Nacre Sheets approach parallel linearity (left of i, Figure 5.15. b) it is about 50 µm.

Where the edges of the Nacre Sheets display a regularly spaced pattern either of curves (h in Figure 5.15. b) or near straight parallel lines (left of i in Figure 5.15. b), the partly-bound and free Nacre Tiles cover about half the distance between the edges of the Nacre Sheets (Figure 5.15. a and b). Where there is anastomoses or tight recurving this arrangement does not hold (Figure 5.15. c and d).

The partly-bound and bound Nacre Tiles, some of which display a pattern on their medial surface, (Figure 5.15. d), are here up to about 10 µm in their longest axes.

FIGURE 5.15. *Pinctada maxima* - Medial Surface Inner Nacreous Layer, Ventral Pallial Gland Region - Position 3 in Figure 5.12.

a. L.M. x 28 Kinds of Patterns seen in this Region

b. S.E.M. x 77 As for a at higher magnification.

c. S.E.M. x 770 Higher magnification centre about y in Figure 5.15. b.

d. S.E.M. x 1500 Higher magnification, centre about z in Figure 5.15. c.

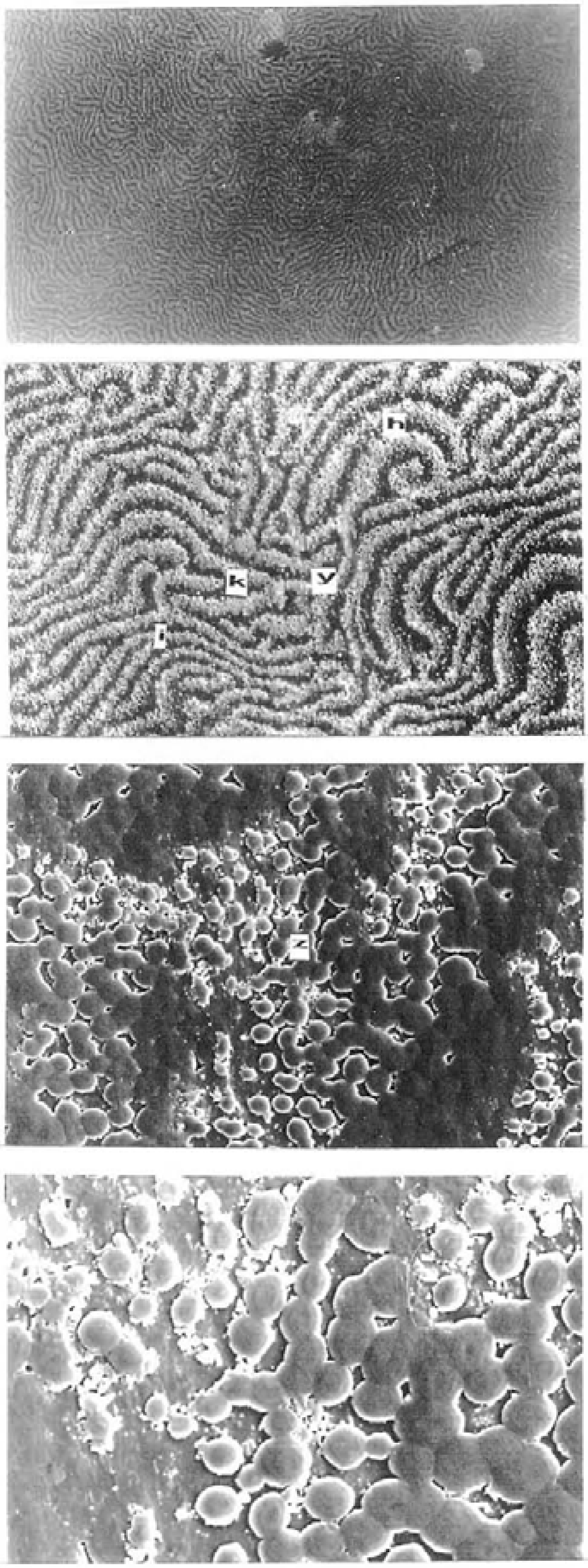

a
x28

b
x77

c
x770

d
x1500

Figure 5.15

5.5.1.3.5. Medial Surface, Inner Nacreous Layer - Posterior Pallial Gland Region.

Here patterns of tightly curved, anastomosing and recurved Edges of Nacre Sheets are joined by less tightly curved parallel, near linear patterns, (Figure 5.16. a). The strongly curved patterns are most commonly concave proximally and convex distally, (in Figure 5.16., a and b, p and d respectively).

The partly-bound and free Nacre Tiles cover about half the distance between the bound edges of successive Nacre Sheets whether strongly curved and widely separated as at b in Figure 5.16. b, or approaching parallel linearity and narrowly separated as near a in Figure 5.16. b.

Where two successive Nacre Sheets anastomose by the Nacre Sheet edge of the more lateral (L Figure 5.16. c) recurving sharply to join the edge of the more medial, (M Figure 5.16. c), the geometric relationships of the bound and free Nacre Tiles of the two Nacre Sheets is shown in Figure 5.16. c and d. This geometrical relationship is distinguished from the recurving of the edge of the same Nacre Sheet seen in Figure 5.14. e f and g.

The medial geometric shapes and the orientation of their axes are commonly maintained throughout the full width of the spread of Free Nacre Tiles between two successive Nacre Sheets despite the progressive decrease in size away from the edge of the Nacre Sheet, (Figure 5.16. d), and often over a larger area, (Figure 5.16. c).

FIGURE 5.16. *Pinctada maxima* - Inner Nacreous Layer Medial Surface - Posterior Pallial Gland Region. Postion 4, Figure 5.12.

a. L.M. x 28 Patterns of edges of Nacre Sheets in this Region.

b. S.E.M. x 77 As for a above at higher magnification.

c. S.E.M. x 770 a in Figure 5.16. b is near a in Figure 5.16. c.

d. S.E.M. x 1500 Higher magnification, same centre as Figure 5.16. c.

a

x28

b

x77

c

x770

d

x1500

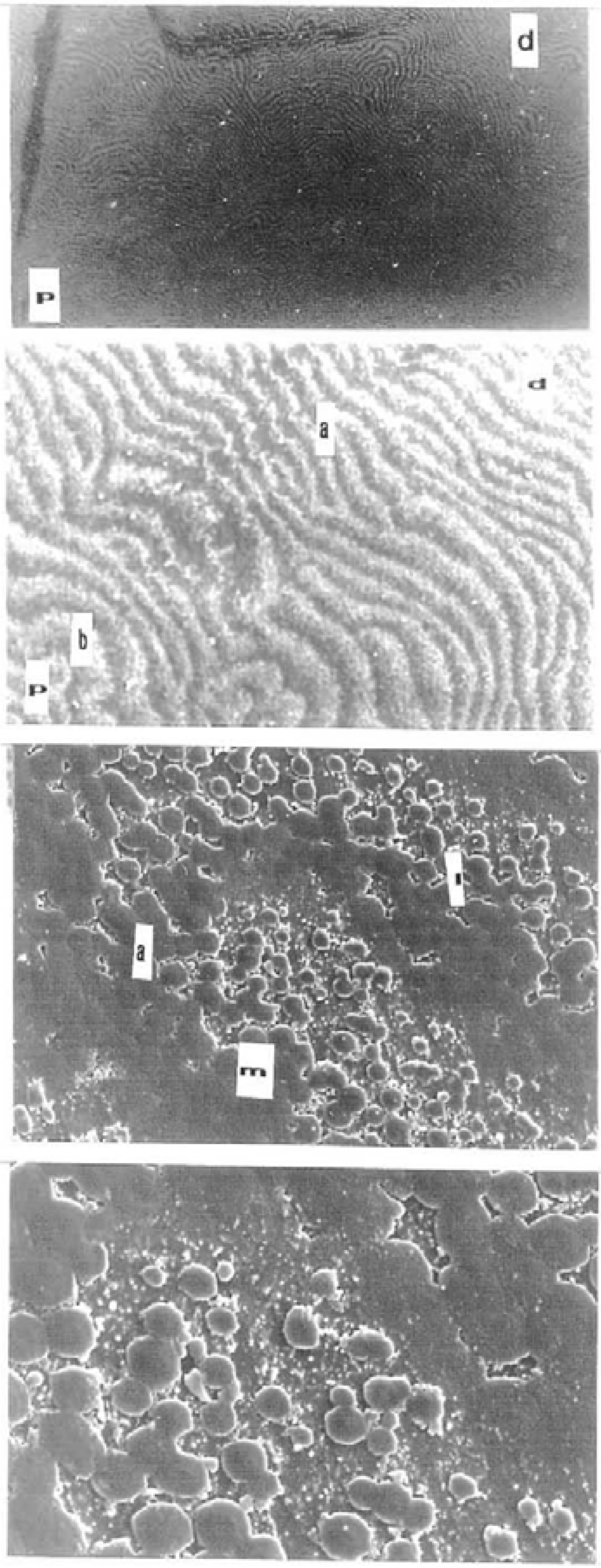

Figure5.16

5.5.1.3.6. Medial Surface, Inner Nacreous Layer - Proximal Ventral Pallial Region.

In Figure 5.17, a and b, p is proximal and d distal.

Although there are still some anastomoses and small spiral structures and discontinuous edges to Nacre Sheets, overall the pattern here is more even than in Figures 5.13. - 5.16.

In Figure 5.17, a and b, the average distance between edges of Nacre Sheets is about 60 μm (Figure 5.17. a, b and c). The free and partly-bound Nacre Tiles extend over about half the distance between the edges to the Nacre Sheets (Figure 5.17. c). The Bound and Partly-bound Nacre Tiles have long axes up to about 8-9 μm in length (Figure 5.17. d).

A similar anastomosis to that in Figure 5.16. c is shown in Figure 5.17. c. Again the Free and Partly bound Nacre Tiles have locally sililar medial shapes and similar orientation of their axes, (Figure 5.17. c and d).

FIGURE 5.17. *Pinctada maxima* - Inner Nacreous Layer, Medial Surface - Proximal Ventral Pallial Region. Position 5 in Figure 5.12.

a. L.M. x 28 Patterns of edges of Nacre Sheets in this Region.

b. S.E.M. x 77 As for a above at higher magnification.

c. S.E.M. x 770 Anastomosis of a Nacre Sheet with the next more lateral Nacre Sheet.

d. S.E.M. x 1500 Same centre as c above.

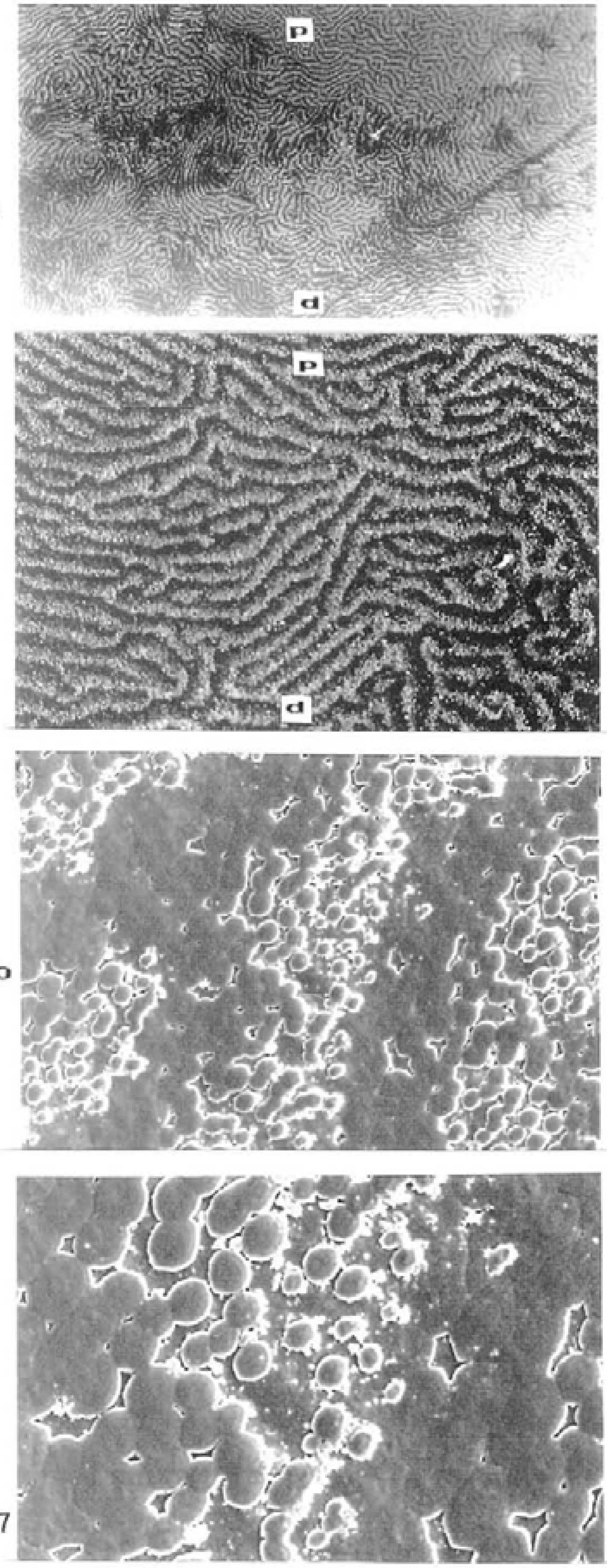

a
x28

b
x77

c
x770

d
x1500

Figure 5.17

5.5.1.3.7. Medial Surface Inner Nacreous Layer – Middle Ventral Pallial Region.

Here there are relatively large areas with patterns of edges of Nacre Sheets which are composed of relatively straight lines evenly and closely spaced – about 30 – 50 µm apart. (Figure 5.18. a. and at i in Figure 5.18. b). Other areas have more strongly curved and anastomosing patterns of edges of Nacre Sheets which may be up to 70 µm apart (Figure 5.18. b. k). The bands of Partly-bound and Free Nacre Tiles extend over about half the distance between the edges of successive Nacre Sheets irrespective of type of pattern (Figure 5.18. b. c and d). and the length of the long axes of the bound and partly-bound Nacre Tiles is about 8.0 µm (Figure 5.18. d).

The free and Partly Bound Nacre Tiles are nearly all extended hexagons in medial view and the geometric axes of their medial surfaces are commonly aligned at similar angles to the direction of the edges of the adjacent Nacre Sheets. (Figure 5.18. c and d).

FIGURE 5.18. *Pinctada maxima* – Inner Nacreous Layer. Medial Surface – Middle Ventral Pallial Region. Position 6 in Figure 5.12.

a. L.M. x 28 Largely parallel linear patterns of this Region.

b. S.E.M. x 77 Junction of largely parallel linear patterns and an area of strongly curved anastomosing patterns.

c. S.E.M. x 770 Narrowly spaced parallel linear patterns near i in b above.

d. S.E.M. x 1500. Same centre as c above.

a

x28

b

x77

c

x770

d

x1500

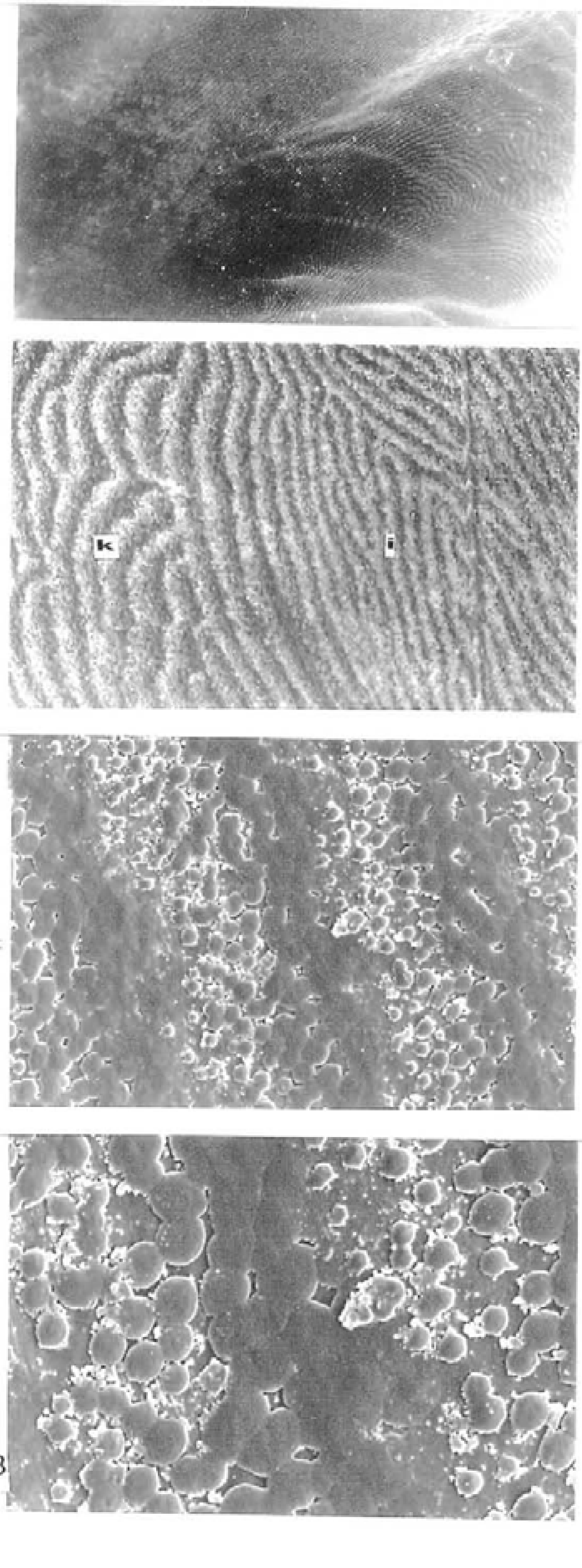

Figure 5.18

5.5.1.3.8. Medial Surface of Inner Nacreous Layer - Distal Ventral Pallial Region.

In Figure 5.19, p is proximal abd d is distal

There are relatively large areas where the patterns of edges of Nacre Sheets are relatively closely spaced parallel straight lines about 30-50 μm apart (Figure 5.19. a, b and c, l). Interspersed are areas of complex patterns of curved, anastomosing and discontinuous edges to Nacre Sheets (Figure 5.19. a, b and e) where the interval between successive Nacre Sheets may be up to 70 μm. The Partly-bound and Free Nacre Tiles extend over about half the distance between Nacre Sheets irrespective of their pattern (Figure 5.19. b, c and e). The Bound and Partly-bound Nacre Tiles are about 6-7μm in their longest axes in the linear patterns (Figure 5.19. d). The morphology of the centre of a spiral pattern to Edges of Nacre Sheets is shown in Figure 5.19. f and g.

FIGURE 5.19. *Pinctada maxima* - Medial Surface Inner Nacreous Layer - Distal Ventral Pallial Region. Position 7, Figure 12.

a. L.M. x 28

b and e. S.E.M. x 77 Strongly curved, linear parallel and complex patterns of edges of Nacre Sheets.

c. S.E.M. x 770 Right of i in Figure 5.19. b.

d. S.E.M. x 15000 Higher magnification, same centre as c above.

e. S.E.M. x 770 Centre of small spiral structure below and left of c in e above.

f. S.E.M. x 1500 Higher magnification of structures near centre of Figure 5.19, f, above.

Figure 5.19

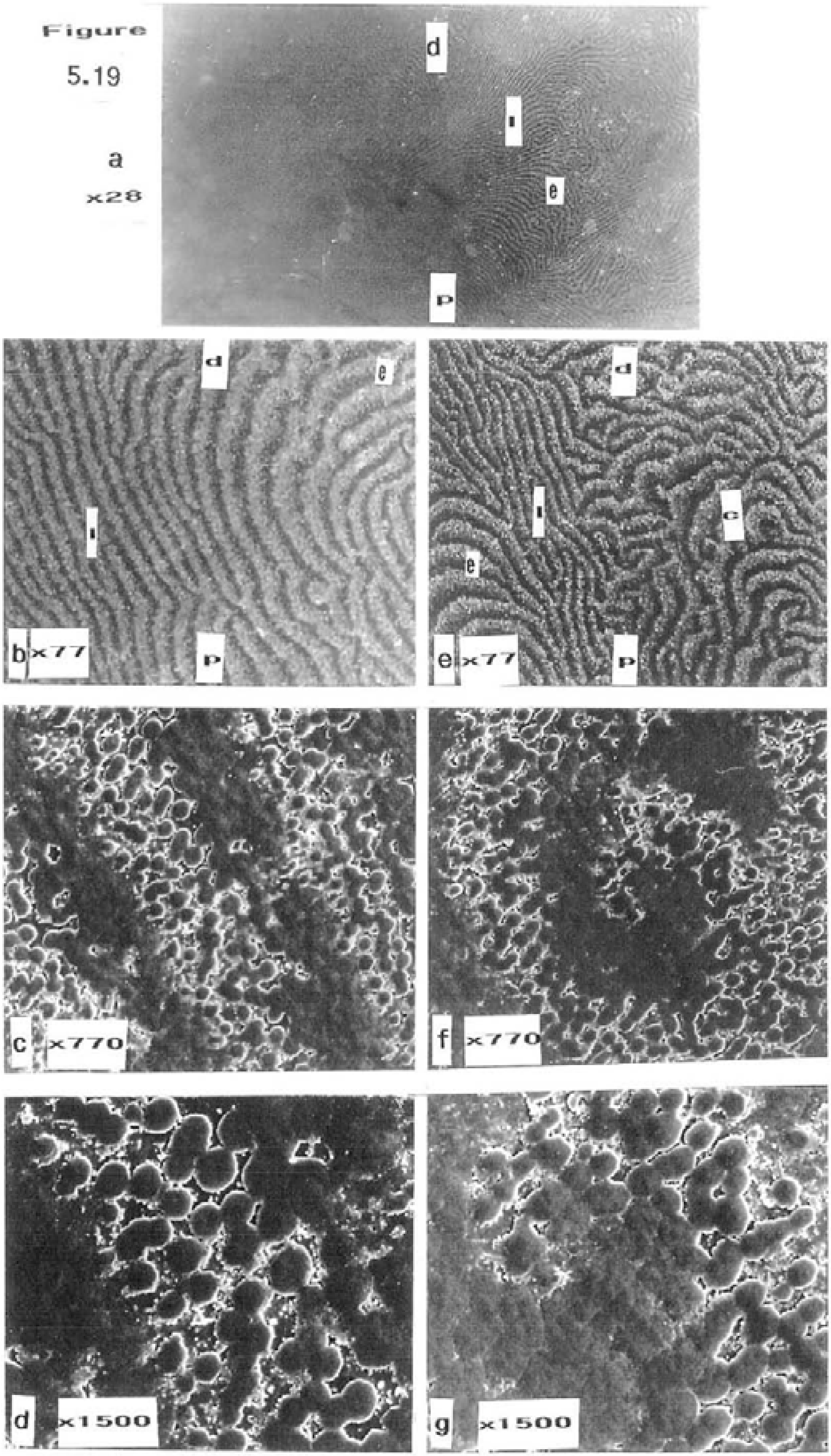

5.5.1.3.9. Medial View, Ventral Outer Nacreous Layer and Ventral Nacreo-prismatic Junction.

In Figures 5.20. a and b N = Outer Nacreous Layer and PL is the medial surface of the Prismatic Layer. The patterns of edges of Nacre Sheets near the Ventral Nacreo-prismatic Junction (i in Figure 5.20. a and b) are markedly more linear, continuous, and more closely spaced than in any of the regions shown in Figure 5.13. - 5..19. The distance between successive edges of Nacre Sheets remains close to 20 μm for about 5 mm proximal to the Nacreo-prismatic Junction (Figure 5.20. a, b, c and top of d), where it rises to about 35 μm. (bottom of Figure 5.20. d). The Partly-bound and Free Nacre Tiles extend for about half the distance between successive Nacre Sheets (Figure 5.19. e, f and g). The length of the long axes of the bound and partly-bound Nacre Tiles is about 3 μm at the Nacreo-prismatic Junction rising to about 5.0 μm, 3 mm (Figure 5.20. f), and 5 mm (Figure 5.20. g), proximal to it. Figure 5.20, e, f and g are higher magnification of the ventral areas of Figure 5.20, b, c and d.

Lines of Partly Bound and Free Nacre Tiles lie in the grooves around the medial ends of the prims just distal to the peripheral Nacreo-prismatic Junction, Figure 5.20, a and b).

FIGURE 5.20. *Pinctada maxima* - Medial Surface. Ventral Outer Nacreous Layer and Ventral Nacreo-prismatic Junction. Position 8 Figure 5.12.

a. L.M. x 28

b. S.E.M. x 77 Ventral Nacreo-prismatic Junction.

c. S.E.M. x 77 Outer Nacreous Layer centre about 3 mm proximal to Ventral Nacreo-prismatic Junction.

d. S.E.M. x 77 Nacreous Layer, Centre about 5 mm proximal to Ventral Nacreo-prismatic Junction.

e. S.E.M. x 1500 Higher magnification same centre as Figure 5.20. b.

f. S.E.M. x 1500 Higher magnification same centre as Figure 5.20. c.

g. S.E.M. x 1500 Higher magnification same centre as Figure 5.20. d.

Figure 5.20

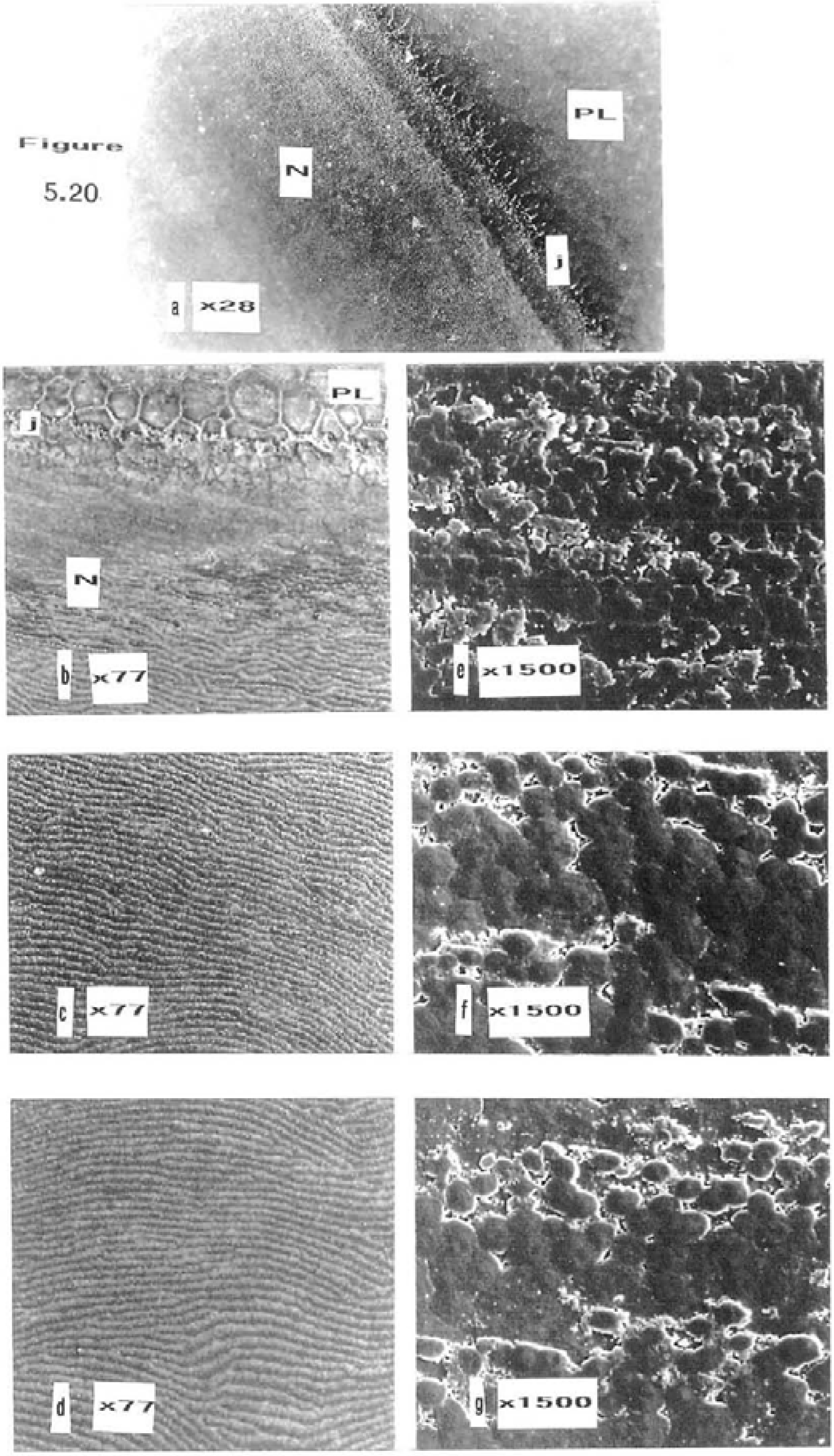

5.5.1.3.10. Medial Surface Inner Nacreous Layer - Proximal Posterior Pallial Region.

This Region has wavy and relatively strongly curved patterns of edges of Nacre Sheets with some anastomoses, (Figure 5.21. a and b).

The distance between successive edges of Nacre Sheets decreses from an average of about 65 μm in the tightly curved pattern to about 45 μm where there are parallel linear patterns, (Figure 5.21. b). The Partly-bound and Free Nacre Tiles extend for about half the distance between successive Nacre Sheets, and the size of the Free Nacre Tiles decreases with distances from the edges of the Nacre Sheets (Figure 5.21. c). The average length of the long axes of the bound and partly-bound Nacre Tiles is about 10 μm (Figure 5.21. d).

The geometric shapes of the medial surfaces of the free and Partly bound Nacre Tiles are elongate hexagons, and their geometric axes are aligned at the same angle to the direction of the adjacent edge of a nacre Sheet in any location (Figure 5.21, c and d).

FIGURE 5.21. *Pinctada maxima* - Medial Surface, Inner Nacreous Layer - Proximal Posterior Pallial Region. Position 9, Figure 5.12.

a. L.M. x 28 Patterns of edges of Nacre Sheets in this Region.

b. S.E.M. x 77 As for a above at higher magnification.

c. S.E.M. x 770 Higher magnification, same centre as b above.

d. S.E.M. x 1500 Higher magnification same centre as c above.

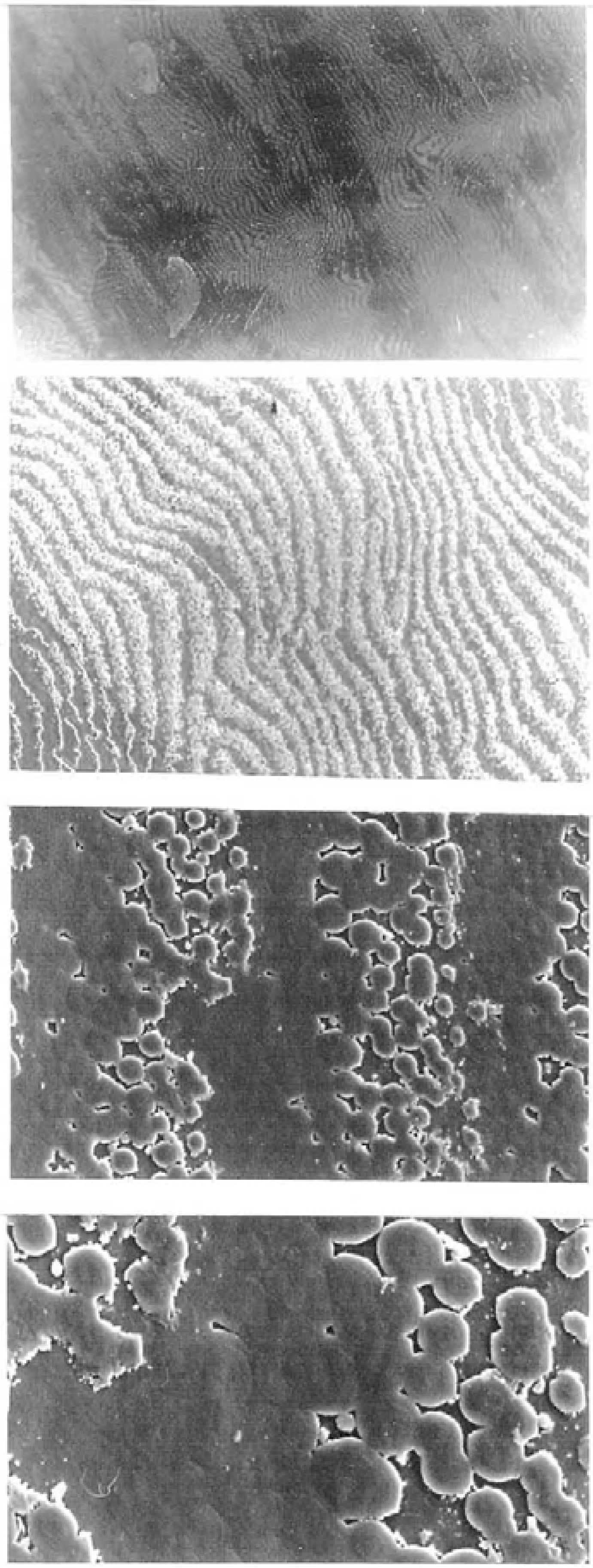

a

x28

b

x77

c

x770

d

x1500

Figure5.21

5.5.1.3.11 Medial Surface of Inner Nacreous Layer -
Middle Posterior Pallial Region.

Here areas of parallel linear pattern Nacre Sheet edges (Figure 5.22. a and b) are interspersed with lesser areas with strongly curved relatively small concentric circular and spiral patterns with numerous anastomoses (Figure 5.22. a and e). The distance between the edges of Nacre Sheets in the former is about 45 µm and that in the latter about 60 µm.

The partly-bound and free Nacre Tiles extend over about half the distance between the successive edges of Nacre Sheets in all patterns (Figure 5.22. a, b c and d).

Figure 5.22. e shows the junction between the two types of patterns found in this Region - parallel linear pattern and the more strongly curved patterns (i and k respectively).

Figure 5.22. f and g show free Nacre Tiles in the angle between two anastomosing Nacre Sheets. The bound and partly bound Nacre Tiles in d and g are about 8um in their longest axes. Some of the free Nacre Tiles have a raised central area on the lateral surface (Figure 5.22. d and g). Figure 5.22. d and c are enlargements of structures in b, and f and g are enlargements of structures in e.

FIGURE 5.22. *Pinctada maxima* - Medial Surface Inner Nacreous Layer Middle Posterior Pallial Region. Postion 10, Figure 12.

a. L.M. x 28

b. S.E.M. x 77

c. S.E.M. x 770 Higher magnification, same centre as b.

d. S.E.M. x 1500 Higher magnification, same centre as c.

e. S.E.M. x77

f. S.E.M. x 770 Higher magnification same centre as e.

g. S.E.M. x 1500 Higher magnification same centre as f.

Figure 5.22

a

×28

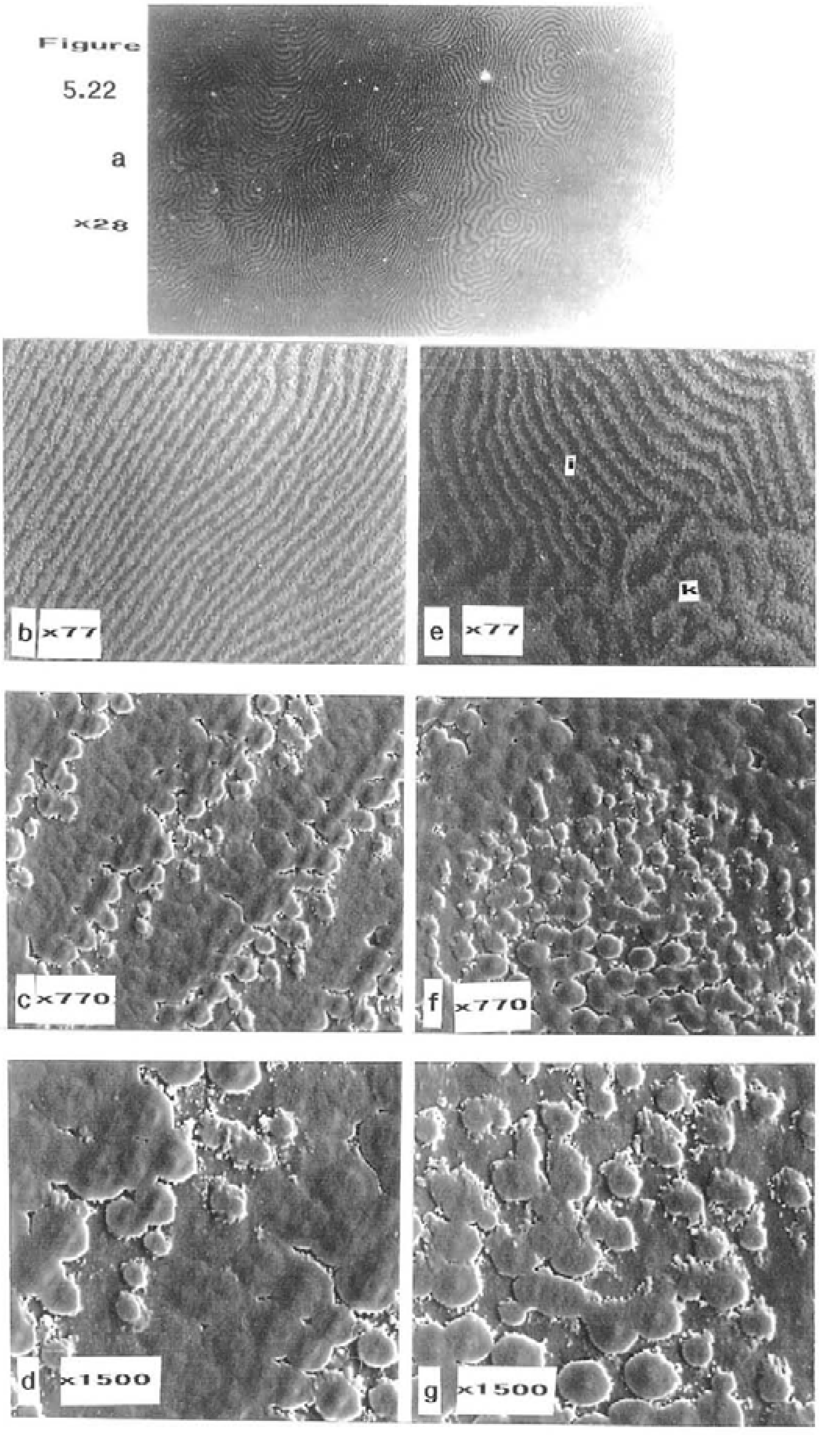

5.5.1.3.12. Medial Surface Inner Nacreous Layer - Distal Posterior Pallial Region.

In Figure 5.23, P is proximal and D, distal.

The pattern of Edges of Nacre Sheets seen throughout this region is of relatively slightly curved parallel lines with few anastomoses and relatively closely (about 35μm) and evenly spaced edges of successive Nacre Sheets, Figure 5.23. a. b and c. The Partly-bound and Free Nacre Tiles extend over about half the distance between successive Nacre Sheets (Figure 5.23. b and c).

The long axes of the Partly-bound and Bound Nacre Tiles which tend to elongate hexagons viewed laterally are about 8 μm (Figure 5.23. d).

There appears to be a central depression on the lateral surface of many partly-bound and free Nacre Tiles (Figure 5.23. d).

FIGURE 5.23. *Pinctada maxima* - Medial Surface Inner Nacreous Layer - Distal Posterior Pallial Region. Position 11 Figure 12.

a. L.M. x 28

b. S.E.M. x 77

c. S.E.M. x 770 Higher magnification at same centre as b.

d. S.E.M. x 1500 Higher magnfication at same centre as c.

a

x28

b

x77

c

x770

d

x1500

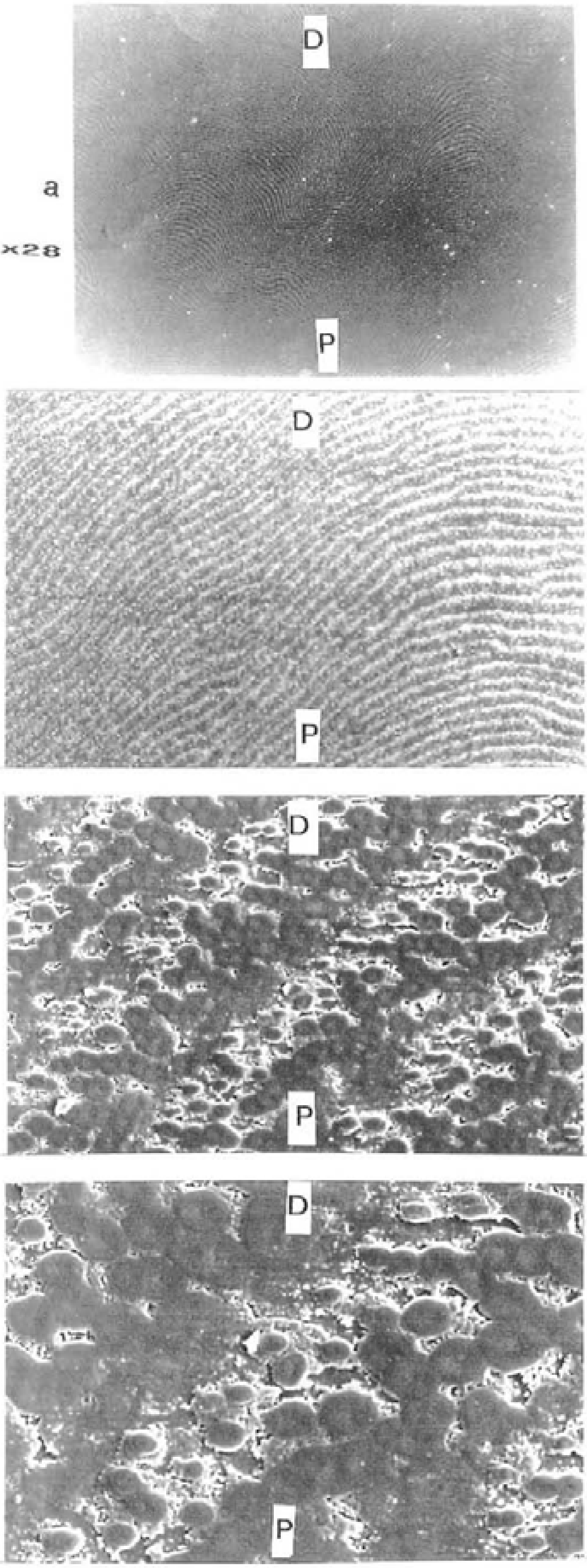

Figure 5.23

5.5.1.3.13. Medial Surface of Posterior Outer Nacreous Layer and Nacreo-Prismatic Junction.

Prismatic Layer and Nacre are indicated in Figure 5.24. a and b by PL and N respectively. In Figure 5.24., c and e, d indicates distal and p proximal.

The patterns of edges of Nacre Sheets in this Region are of fairly regularly spaced wavy lines but with numerous anastomoses. The average distance between Edges of Nacre Sheets increases from about 20μm near the Nacreo-Prismatic Junction to about 35μm 3mm proximal to it (Figure 5.24. b and e).

Figure 5.24., c and d, and f and g are enlargements of Figure 5.24. b and Figure 5.24. e respectively.

The Partly-bound and Free Nacre Tiles occur on the proximal half of the distance between the Edges of successive Nacre Sheets.

The length of the long axes on the lateral surface of the Nacre Tile (which are slightly elongate hexagons) increases from about 5μm near the Nacreo-prismatic Junction (Figure 5.24. d) to about 9μm 3mm proximal to it (Figure 5.24. g).

FIGURE 5.24. *Pinctada maxima* - Medial Surface Outer Nacreous Layer and Nacreo-prismatic Junction - (Posterior). Position 12 Figure 12.

a. L.M. x 28
b. S.E.M. x 77
c. S.E.M. x 770
d. S.E.M. x 1500
e. S.E.M. x 77
f. S.E.M. x 770
g. S.E.M. x 1500

Figure 5.24

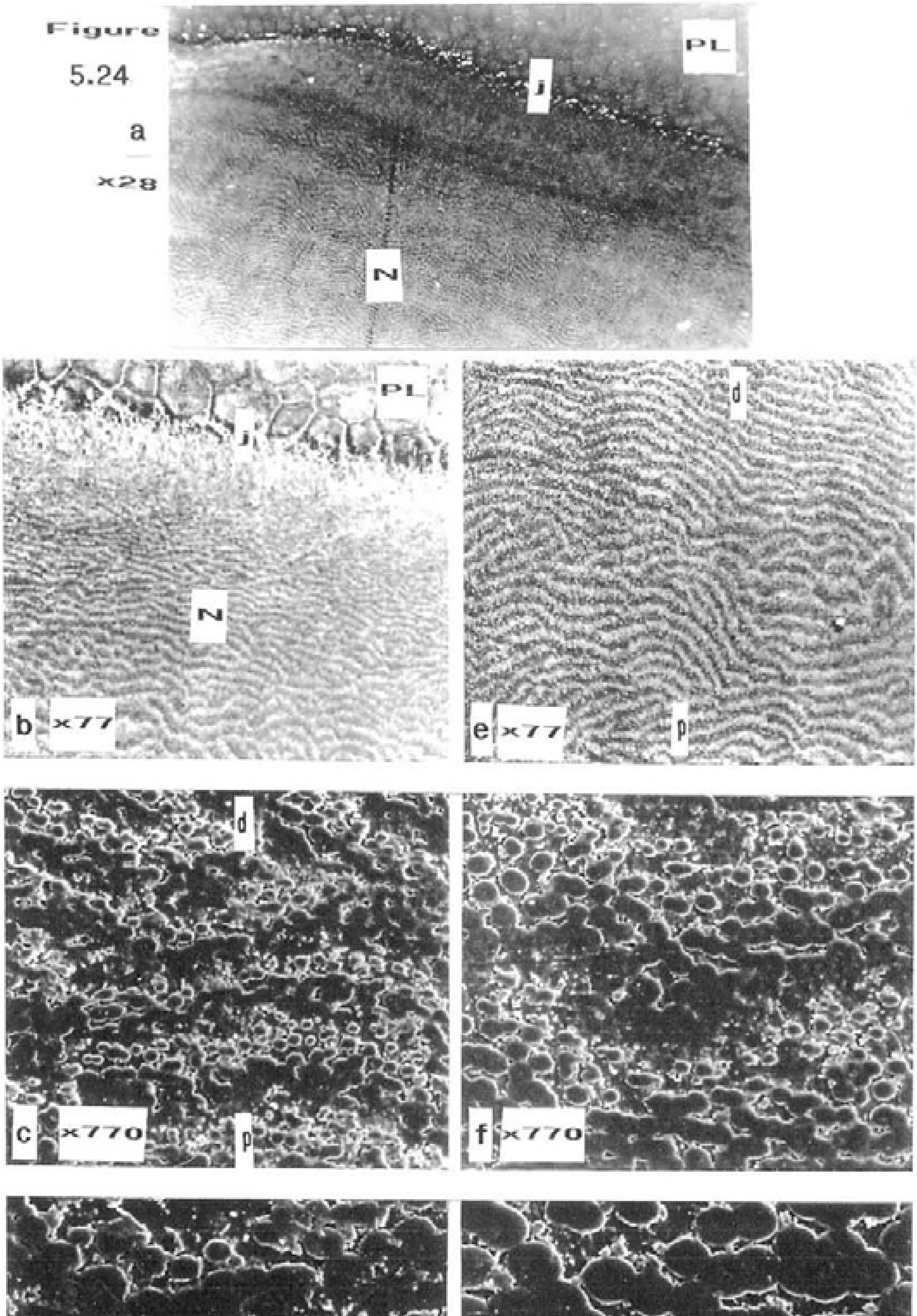

5.5.1.3.14. Medial Surface of Inner Nacreous Layer – Proximal Anterior Pallial Region.

This displays an irregular pattern of tightly curved, short spiral, anastomosing and discontinuous edges of Nacre Sheets (Figure 5.25. a and b). The average distance between edges of successive Nacre Sheets is about 65μm.

The micromorphology of the central origin of a spiral Nacre Sheet pattern and an anastomosis between a Nacre Sheet and the one more lateral to it are essentially similar. In Figure 5.25. c the free Nacre Tiles at about f lie on the medial surface of the more lateral part of the Nacre Sheet which has edges e and after recurving, e. The Partly-bound and Free Nacre Tiles extending from the edge of the Nacre Sheet e, e, are pb and f in Figure 5.25. c and d.

The Partly-bound and Free Nacre Tiles occupy about the proximal half between the edges of successive Nacre Sheets (Figure 5.25. b).

The individual Partly-bound and Bound Nacre Tiles have an almost ovoid appearance with a long axis averaging 10μm. If, as on most Regions of the medial surface of the valve of *P.maxima* the aragonite is in the shape of an extended hexagon, the angles are very indistinct (Figure 5.25. d).

FIGURE 5.25. *Pinctada maxima* – Medial Surface, Inner Nacreous Layer – Proximal Anterior Pallial Region. Position 13 Figure 12.

a. L.M. x 28

b. S.E.M. x 77

c. S.E.M. x 770

d. S.E.M. x 1500

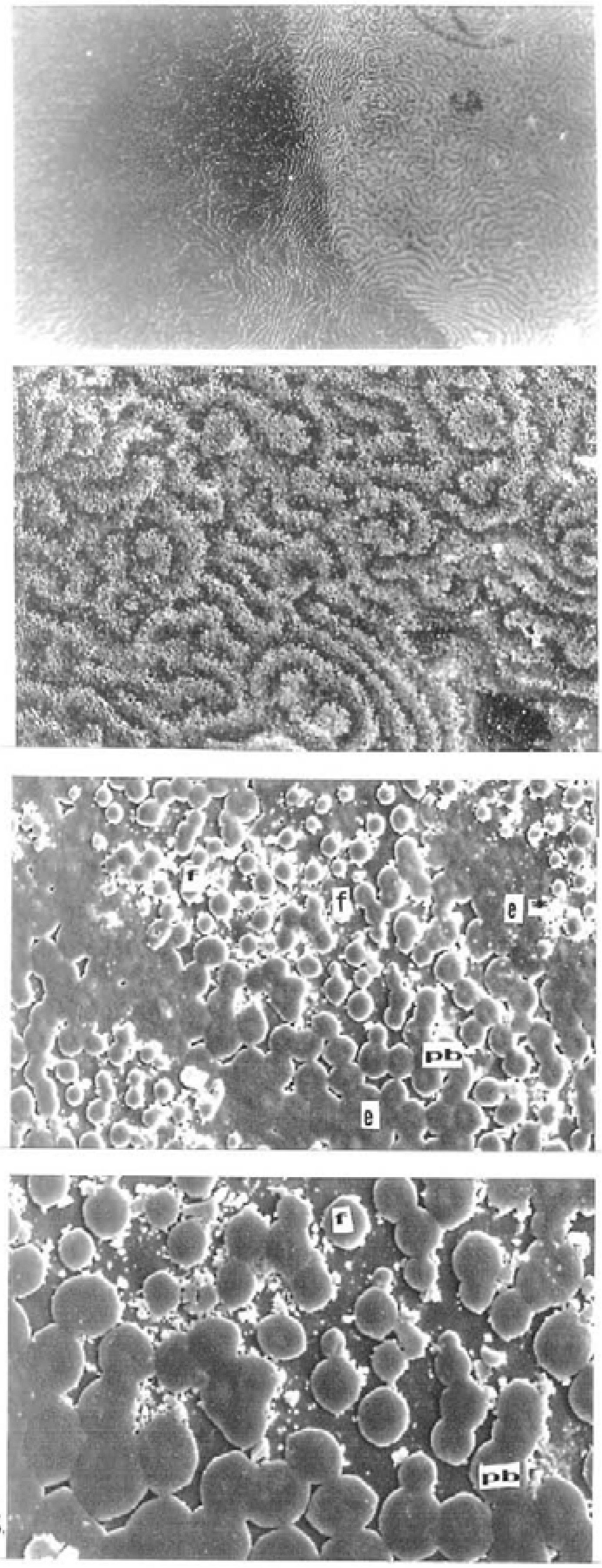

a
×28

b
×77

c
×770

d
×1500

Figure5.25.

5.5.1.3.15 Medial Surface of Inner Nacreous Layer -
Middle Anterior Pallial Region.

The patterns of Nacre Sheet Edges here are relatively strongly curved, short spiral or anastomosing, but the lengths of relatively straight segments are noticeably greater in Figure 5.26. a and b than in Figure 5.25. a and b.

The Partly-bound and Free Nacre Tiles (Figure 5.26. pb and f respectively) cover about the proximal half of the distance between edges of successive Nacre Sheets which here averages 90 μm (Figure 5.26. c).

The Bound and Partly-bound Nacre Tiles are about 10 μm in their longest axes and have the appearance of rounded extended hexagons, (Figure 5.26. d).

FIGURE 5.26. *Pinclada maxima* -Medial Surface of Inner Nacreous Layer -

Middle Anterior Pallial Region. Position 14. Figure 12.

a. L.M. x 28

b. S.E.M. x 77

c. S.E.M. x 770 Higher magnification, same centre as b.

d. S.E.M. x 1500 Higher magnification, same centre as c.

a

x28

b

x77

c

x770

d

x1500

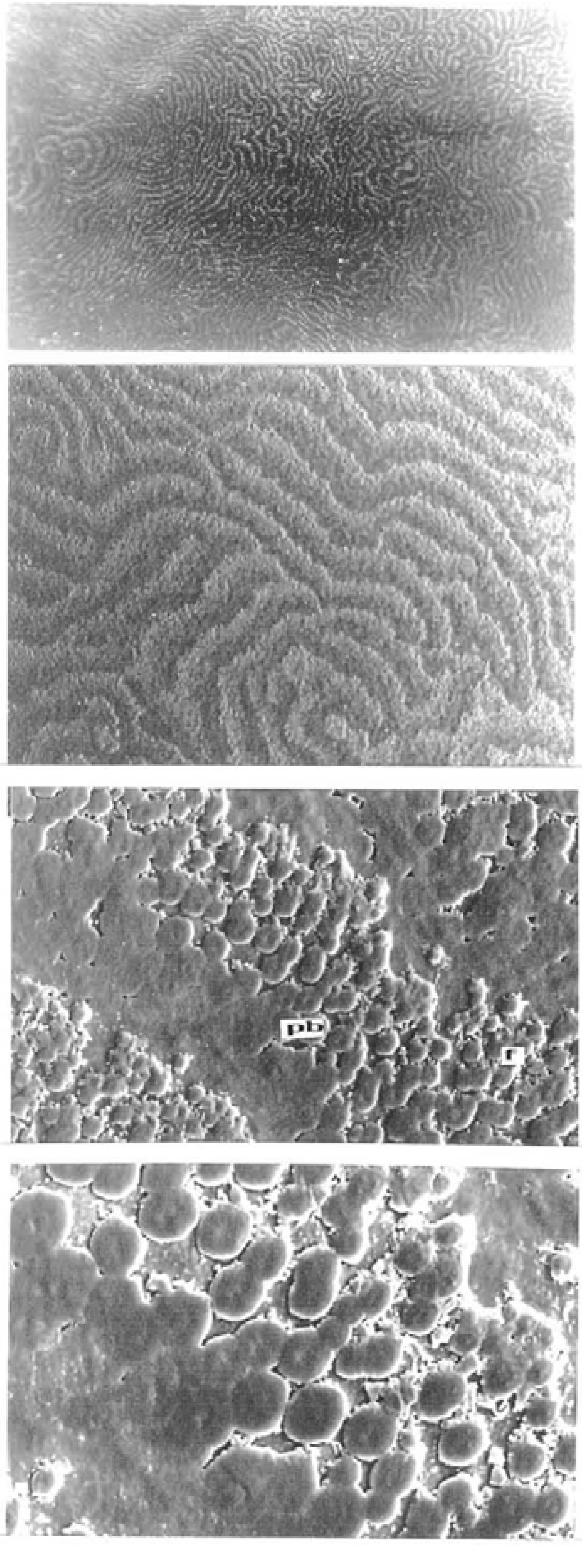

Figure5.26

5.5.1.3.16 Medial Surface of Inner Nacreous Layer – Distal Anterior Pallial Nacre.

Here the patterns of Nacre Sheet Edges are a mixture of relatively tightly curved curvilinear structures and bent parallel lines with occasional spiral structures and numerous anastomoses (Figure 5.27. a and b). The distance between successive Nacre Sheets increases with the tightness of curvature ranging from about 35 μm to about 120 μm (Figure 5.27. a and b).

The Edges of the Nacre Sheets are less distinct than in any other Region of the medial surface and there are also more relatively very small free Nacre Tiles. Perhaps because of both of these features the Partly-bound and Free Nacre Tiles extend over somewhat more than half the distance between successive Nacre Sheet Edges. (Figure 5.27. b and c).

The Bound and Partly-bound Nacre Tiles appear to be extended hexagons with indistinct angles and have long axes of about 10 μm. (Figure 5.27. d).

FIGURE 5.27. *Pinctada maxima* – Medial Surface Inner Nacreous Layer, Distal Anterior Pallial Region. Position 15, Figure 12.

a. L.M. x 28.

b. S.E.M. x 77

c. S.E.M. x 770 Higher magnification, same centre as b.

d. S.E.M. x 1500 Higher magnification same centre as c.

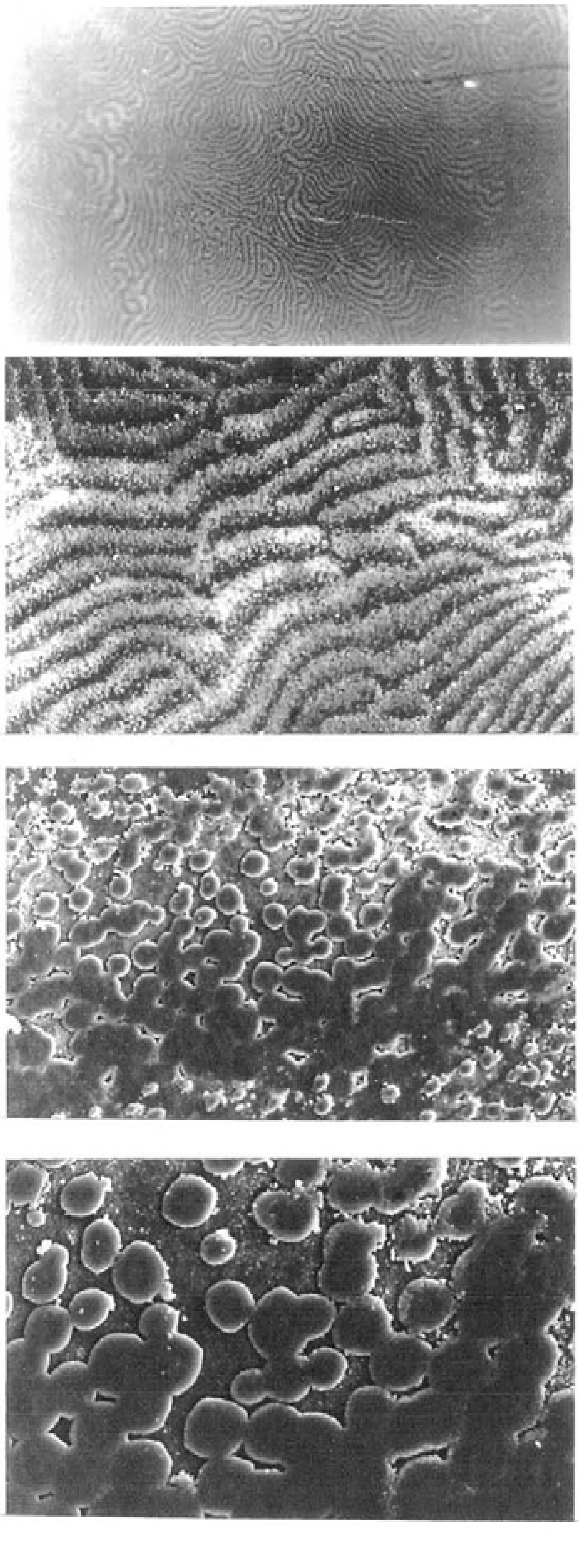

a
x28

b
x77

c
x770

d

Figure5.27

5.5.1.3.17. Medial Surface. Anterior Outer Nacreous Layer and Nacreo-prismatic Junction.

The Outer Nacreous Layer (Figure 5.28. a, N) meets the medial surface of the Prismatic Layer (Figure 5.28. a, PL) at the Anterior peripheral Nacreo-prismatic Junction (Figure 5.28. a, j). For about 1mm proximal to this Junction, the patterns of the edges of the Nacre Sheets are largely of closely spaced parallel lines with few anastomoses, the direction of the parallel lines being about normal to the Nacreo-prismatic Junction (Figure 5.28. a and b, l). In between these areas of parallel lines are areas with patterns of tightly curved and anastomosing edges to Nacre Sheets (Figure 5.28. b and e).

The distance between successive edges of Nacre Sheets in the parallel linear pattern ranges from 25 µm to 35 µm (Figure 5.28. b). That in the tightly curved pattern near e in Figure 5.28. b ranges up to 65 µm.

Proximal to these two patterns there are parallel linear patterns with the edges to the Nacre Sheets about parallel to the peripheral Nacreo-prismatic Junction (Figure 5.28. a, p).

Where the parallel linear pattern joins the tightly curved pattern in Figure 19 b near b, there are numerous anastomoses of the parallel linear edges to Nacre Sheets (Figure 5.28. c). Partly-bound Nacre Tiles (Figure 5.28. c, pb) extend for an abnormally long distance from the edges of the Nacre Sheets in the area near the anastomoses so that the major part of the medial surface is here covered with them (Figure 5.28. c and d). The Bound and Partly-bound Nacre Tiles are about 7 µm in their longest axes (Figure 5.28. d).

FIGURE 5.28. *Pinctada maxima* - Anterior Outer Nacreous Layer and Nacreo-prismatic Junction. Position 16 Figure 12.

a. L.M. x 28

b. S.E.M. x 77

c. S.E.M. x 770 Higher mag., centre near b of Figure 5.28. b.

d. S.E.M. x 1500 Higher magnification - same centre as c.

a
x28

b
x77

c
x770

d
x1500

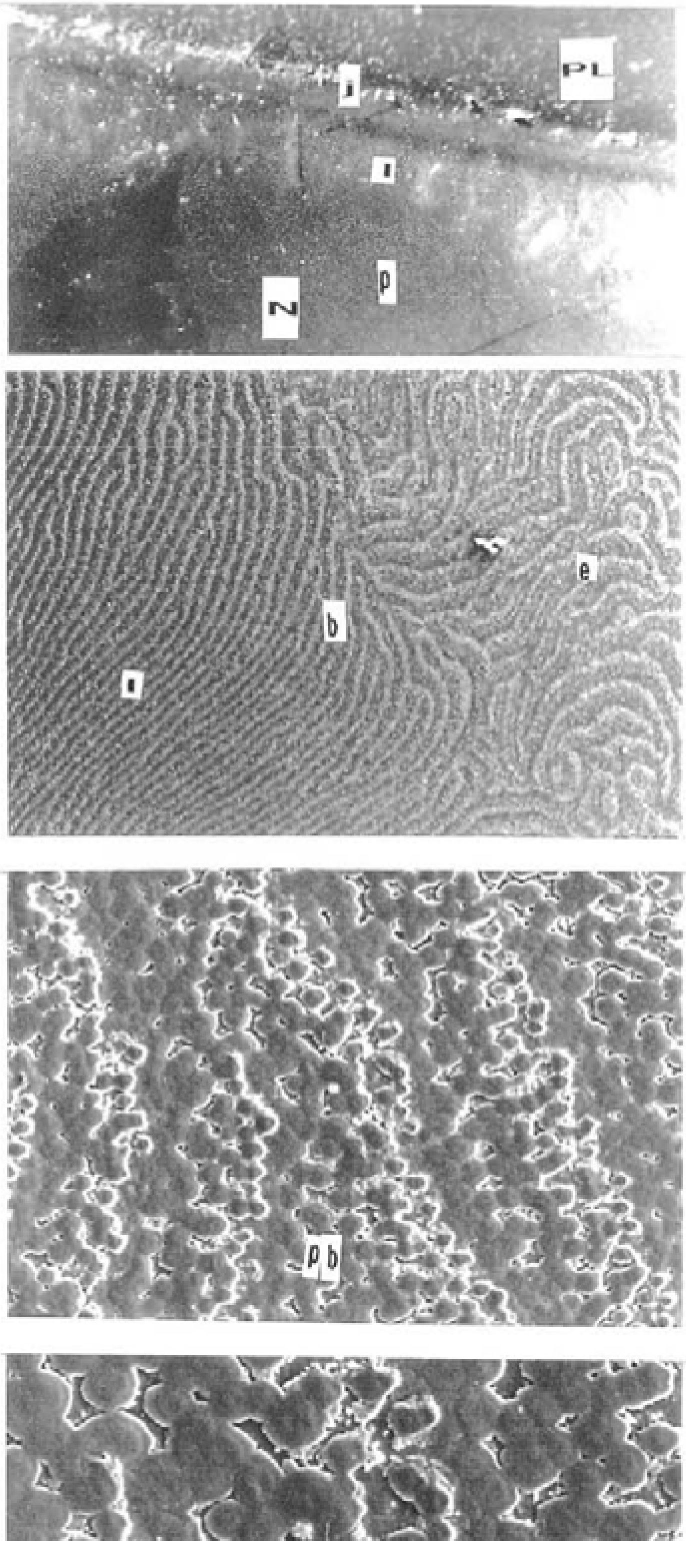

Figure5.28

5.5.1.3.18. Inner Nacreous Layer, Shoulder Region near Hinge - Radial Broken Surface.

Viewed medially, the Nacre Tiles here appear to be about 7 µm across. They are irregular polygons which tend towards regular hexagons (Figure 5.29. a). The marked thickening of the Inner Nacreous Layer in adult specimens near the middle of the Hinge compared with the Inner Nacreous Layer near the Postero-dorsal part of the Valve is reflected in the thickness of the Nacre Tiles - up to 1.0 µm for the former (Figure 5.29. b) compared with about 0.3 µm for the latter (Figure 5.29. c). The individual Nacre Tiles here show marked variations in thickness and the lateral and medial surfaces are often curved planes (Figure 5.29. b, cp).

The radial broken surface of Nacreous Layers viewed sagittally commonly shows Nacre Stairs. These are generated by Nacre Tiles in successively more lateral Nacre Sheets being displaced, (e.g. distally), approximately equal amounts relative to the Nacre Tiles medial to them. Nacre Stairs which extend through ten or more Nacre Sheets are not uncommon. ns in Figure 5.29. d, is a Nacre Tile in such a Nacre Stair. In this case the Nacre Tiles forming the Nacre Stair appear to be hooked over each more medial participant in the formation of the Nacre Stair.

FIGURE 5.29. *Pinctada maxima* - Inner Nacreous Layer, Shoulder Region Near Hinge - Radial Broken Surface.

a. S.E.M. x 6000 Medial View.

b. S.E.M. x 6300 Sagittal View near Hinge enlargement.

c. S.E.M. x 6000 Sagittal View near Postero-Dorsal part of Shell.

d. S.E.M. x 1000 As for b. - Nacre Stairs.

a

×6000

b

×6300

c

×6000

d

×6000

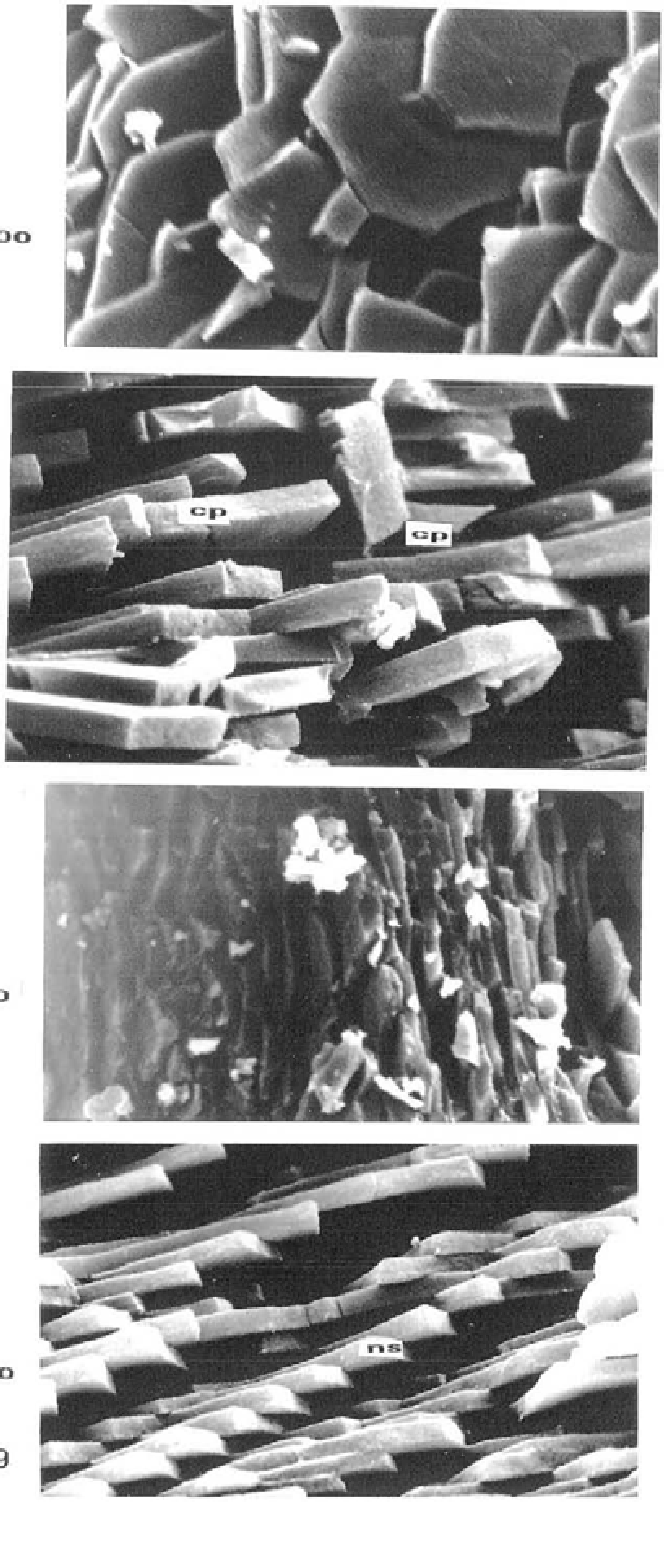

Figure5.29

5.5.1.3.19. Ventral Outer Nacreous Layer, Nacreo-prismatic Junction. Radial Broken Surface.

The Outer Nacreous Layer (Figure 5.30. a and b, N) in the sagittal view of a radial broken surface tapers off quite steeply to the peripheral Nacreo-prismatic Junction - at about 5° in figure 5.30. a. The individual Nacre Tiles are about 0.5µm thick but variable in thickness (Figure 5.30. d) and may have curved medial and lateral surfaces (Figure 5.30. c, cp).

In this species the proximal end of a Growth Scale (Figure 5.30. b GS) is commonly seen between the External Nacre (Figure 5.30. b N) and the Major Prisms of the previous Growth Scale (Figure 5.30. b, PL) from which it is usually demarcated by Outer Prismatic End Plates, (OPEP in Figure 5.30 b).

Various features of the Prismatic Layer of this species are shown (Figs. 5.30 - 5.40), for comparison with that of *Velesunio ambiguus*, (Figs. 5.1, e; 5.2, a and b), and *Nucula superba* (Fig. 5.4, a and c), the Outer Shell Layer of the Mytilids, (Fig. 5.6, a, c and d; 5.7, a - c; 5.8, a - c) with the aragonite radial Layer of a cultured pearl, (Fig. 5.42, a, c and d), and either in addition to or comparison with features of the Prismatic Layer of *Pinctada margaritifera*, (Figs 5.92 - 5.97, 5.98 a, b and c; 5.99). *P.fucata* (Figs %.127; 5.128), *Pinctada sp. 1* (Fig 5.131 c - i), *Pinctada sp. 2*, (Fig. 5.133, d-g) and *Pteria penguin* (Figs. 5.144; 5.145), *Isognomon ephippium*, (Fig. 5.152), and the origin and location of all the Martius Yellow positive shell parts in the remaining taxa.

FIGURE 5.30. *Pinctada maxima* - Radial Broken Surface - Outer Nacreous layer Near Ventral Peripheral Nacreo-prismatic Junction.

a. S.E.M. x 25 Radial Broken Surface of Prismatic Layer (PL) lateral to Outer Nacreous Layer N.

b. S.E.M. x 1600 As for "a" above.

c. S.E.M. x 6300 Radial broken surface of Outer Nacreous Layer just beneath Nacreo-prismatic Junction.

d. S.E.M. x 6300 Radial broken surface Outer Nacreous Layer medial to c above.

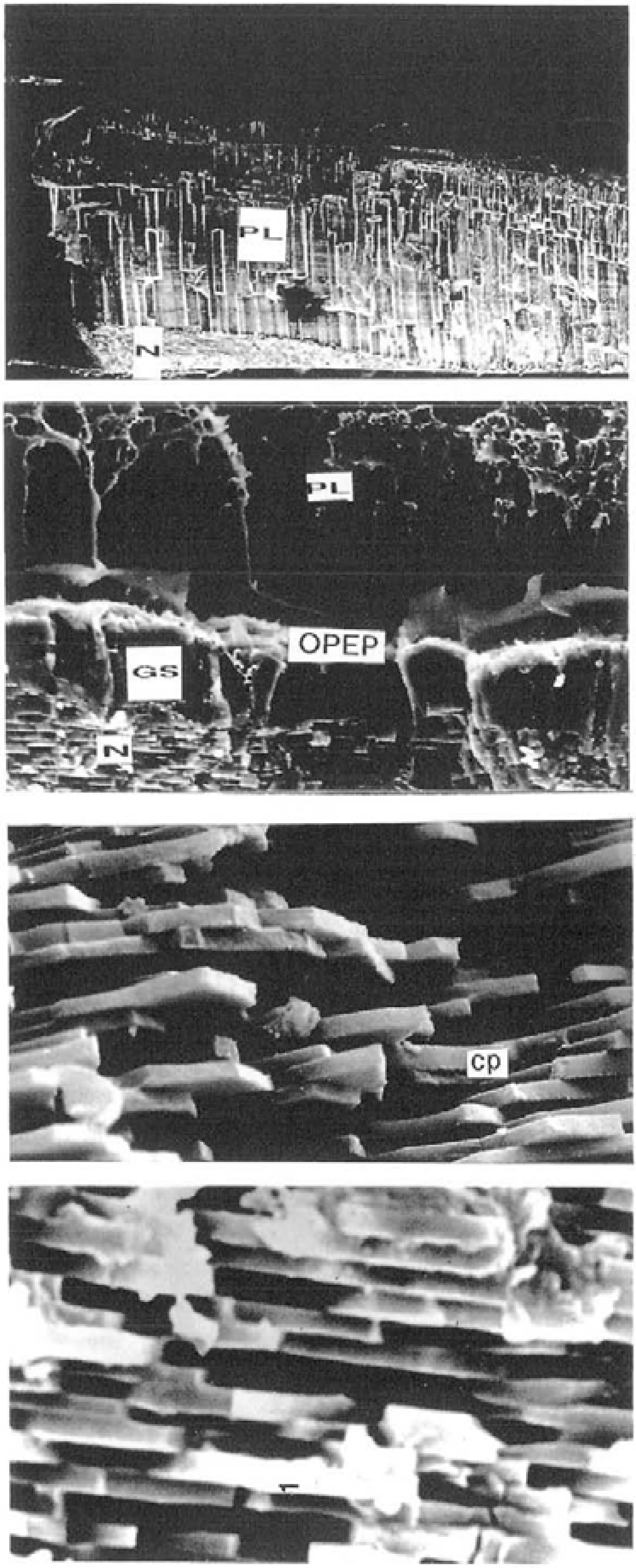

a
x25

b
x1600

c
x6300

d
x6300

Figure5.30

5.5.1.4.1. Medial Surface Prismatic Layer distal to Nacreo-prismatic Junction.

The medial ends of the Major Prisms of the Prismatic Layer are irregularly polygonal and the sides may be quite strongly curved (Figure 5.31. a, c and d, c). Proximally, close to the Nacreo-prismatic Junction the adjacent prisms are closely applied to each other (Figure 5.31. b) compared with more distally (Figure 5.31. d).

Distally, there is an increase in the relative numbers of small prisms (Figure 5.31. c, sp).

The proximal part of the medial surface of Growth Scales (i.e. the surface just distal to the peripheral Nacreo-prismatic Junction) is not covered medially by the Inner Fibrous Sheath. Thus here the medial surface of the prisms is bare as in Figure 5.31.

FIGURE 5.31. *Pinctada maxima* - Medial surface of Prismatic Layer beyond

Ventral Nacreo-prismatic Junction.

a. S.E.M. x 400 Medial surface of Prismatic Layer adjacent to Ventral Nacreo-prismatic Junction.

b. S.E.M. x 3200 Higher magnification of a above.

c. S.E.M. x 200 Distal to a above.

d. S.E.M. x 3200 Higher magnification of c above.

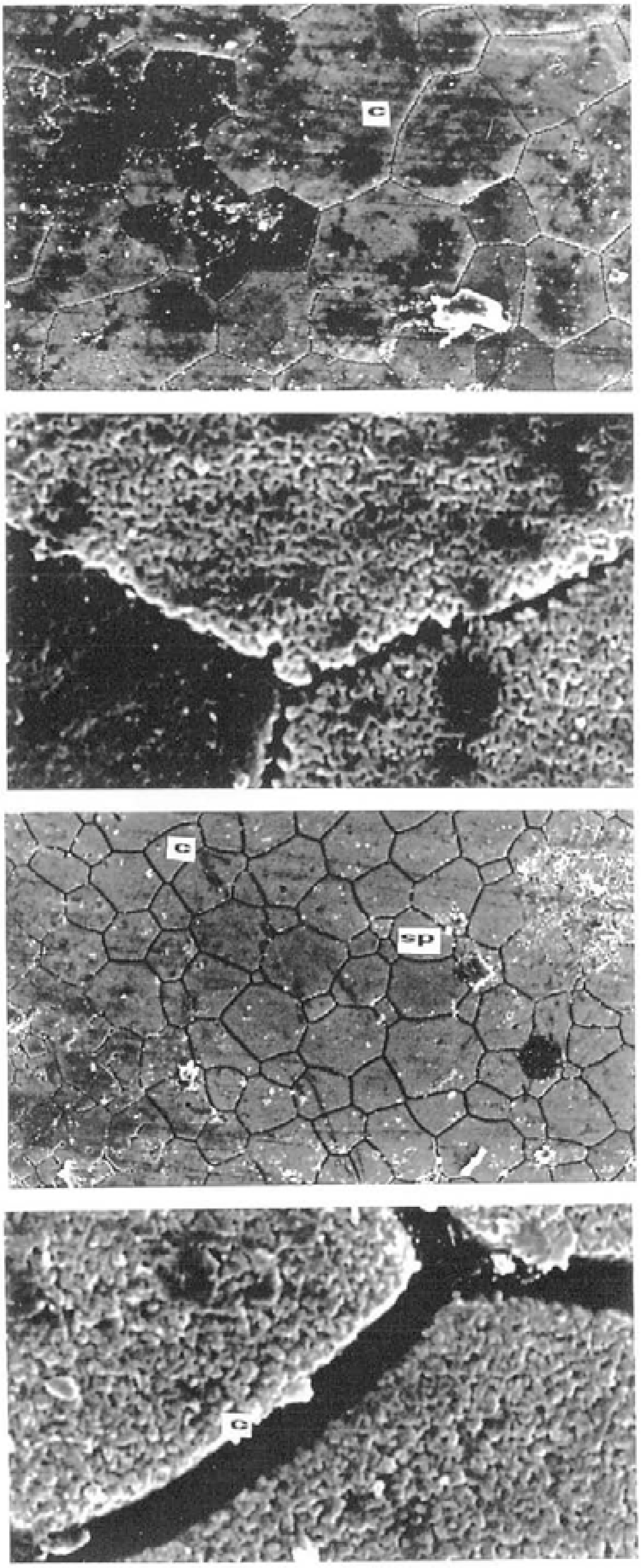

a

×400

b

×3200

c

× 200

d

×3200

Figure 5.31

5.5.1.4.2. Medial Surface of Prismatic Layer.

The proximal part of the medial surface of the Prismatic Layer is invariably not covered with an Inner Fibrous Sheath (Figure 5.31. a - d, Figure 5.32. a-c) but the distal part of the medial surface of both the Major Prisms (Figure 5.32. d and e) and the Growth Processes (Figure 5.34. c), is. Figure 5.32. b and c are higher magnifications of the Junction of the three prisms to the left and below a in Figure 5.32. a. The structure on the medial surface of the prism on the left in Figure 5.32. b and c shows lines parallel to side s and that on the prism to the right bottom to side p.

FIGURE 5.32. *Pinctada maxima* - Proximal and Distal Medial Surface of Growth Scale.

a. S.E.M. x 400 Medial Surface Proximal part Prismatic Layer Growth Scale.

b. S.E.M. x 3200 Higher magnification of a.

c. S.E.M. x 6300 Higher magnification of b.

d. S.E.M. x 3200 Medial surface Distal part of Growth Scale.

e. S.E.M. x 6300 Higher magnification of d showing Inner Fibrous Sheath.

a

x400

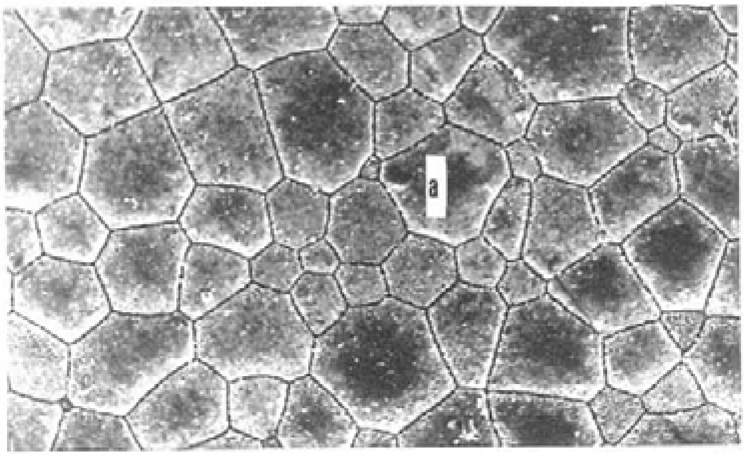

b

x3200

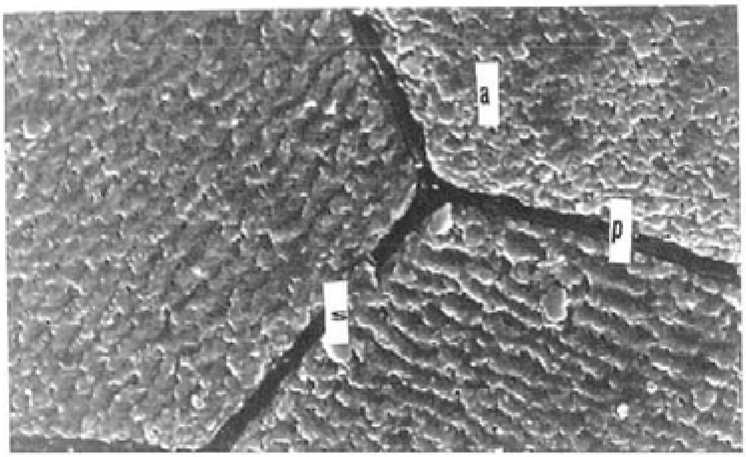

c

x6300

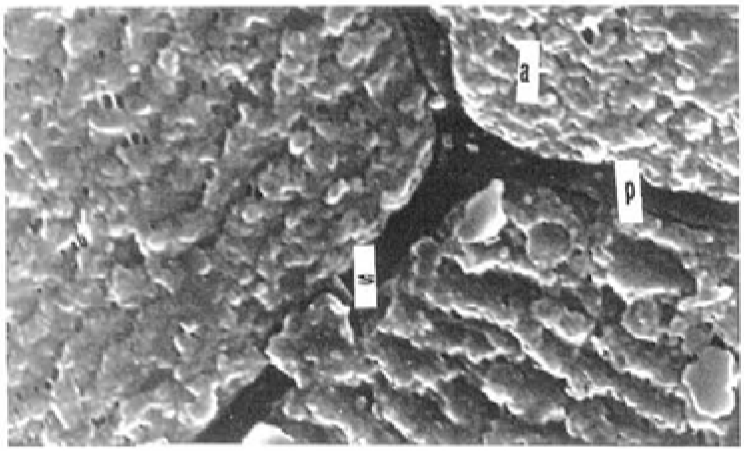

Figure 5.32

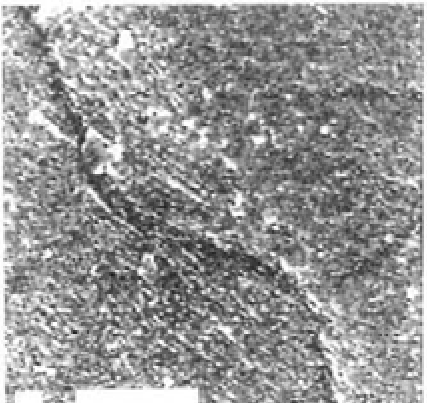

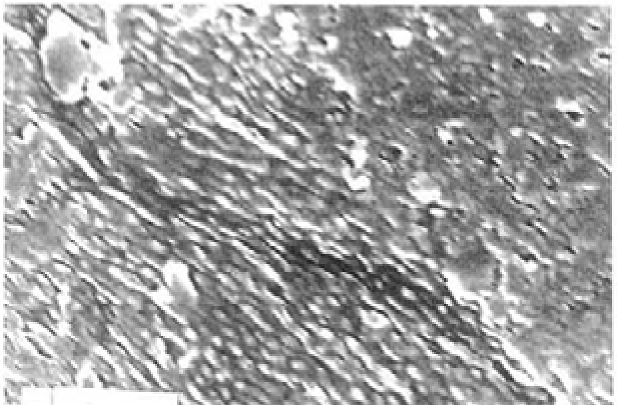

5.5.1.4.3. Lateral Surface Prismatic Layer - Outer Fibrous Sheath

The Outer Fibrous Sheath covers the entire exposed outer surface of the Major Prisms (Figure 5.33. a, b, c and d). The lay of the fibres is related to the position of the underlying prisms, being denser over the Interprismatic Organic Matrices and less dense over the centre of the lateral ends of the prisms (Figure 5.33. b left of "a").

Anastomoses between fibres are often rounded and in any area the roundnesses tend to be in the same direction (near ds in Figure 5.33. c and d).

The Outer Fibrous Sheath is far coarser than the Inner Fibrous Sheath (Figure 5.32. d) and bears small protruberances (Figure 5.33. d near p).

FIGURE 5.33. *Pinctada maxima* - Lateral Surface of Prismatic Layer - Outer Fibrous Sheath.

a. S.E.M. x 780 Lateral view of Outer Fibrous Sheath (OFS) and radial broken surface of Prismatic Layer (PL).

b. S.E.M. x 780 Lateral View Outer Fibrous Sheath.

c. S.E.M. x 3200 Higher magnification of b.

d. S.E.M. x 6300 Higher magnification of c.

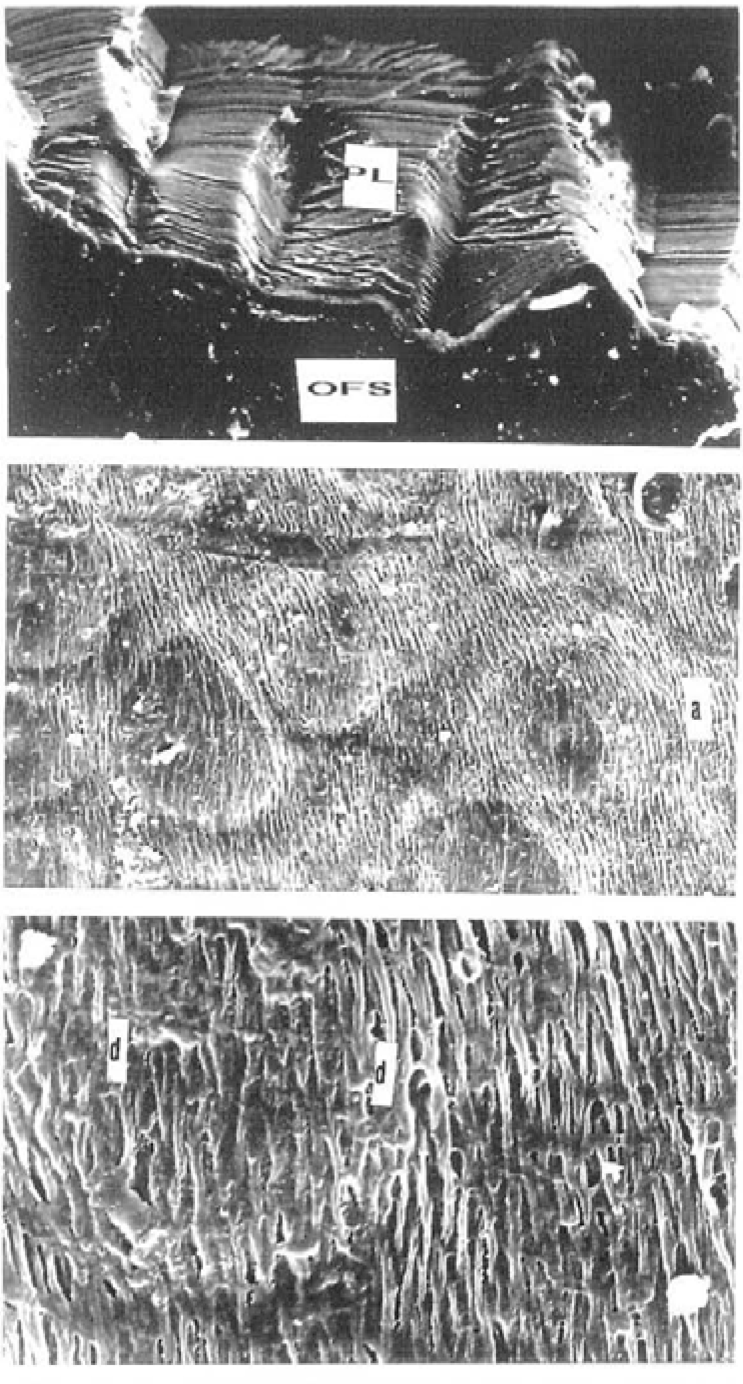

a

x780

b

x780

c

x3200

d

x6300

Figure 5.33

5.5.1.4.4. Medial Surface of Growth Process.

The medial surface of the Growth Processes is covered with an Inner Fibrous Sheath which appears in Figure 5.34. b and c to be identical with that of the distal Medial surface of the Major Prisms. (Figure 5.32. d and e).

Where it is eroded the irregular shape and structure of the Inner Prismatic End Plates is shown (Figure 5.34. a).

FIGURE 5.34. *Pinctada maxima* Medial Surface of Growth Process.

a. S.E.M. x 780 Denuded medial surface of Growth Process.

b. S.E.M. x 1600 Partly destroyed Inner Fibrous Sheath medial surface of Growth Process.

c. S.E.M. x 3200 Inner Fibrous Sheath medial surface of Growth Process.

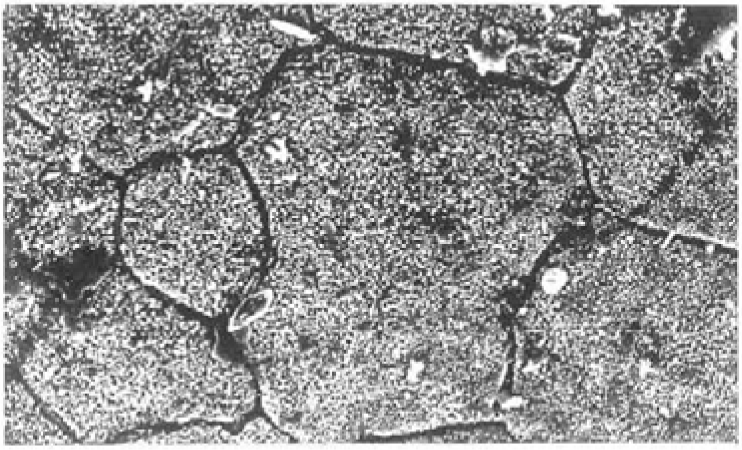

a

x780

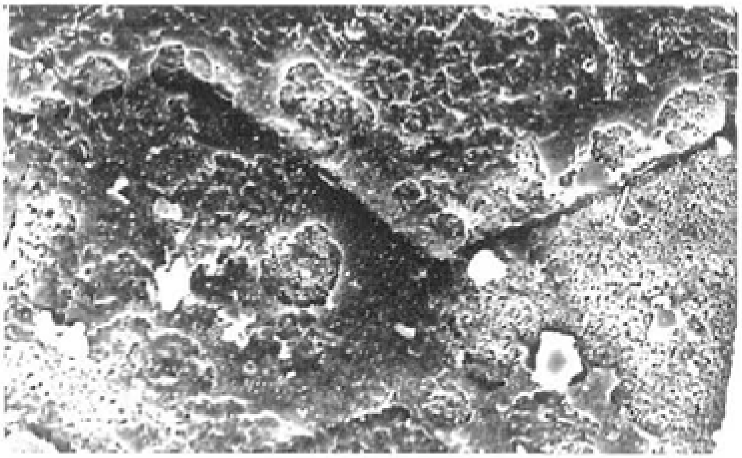

b

x1600

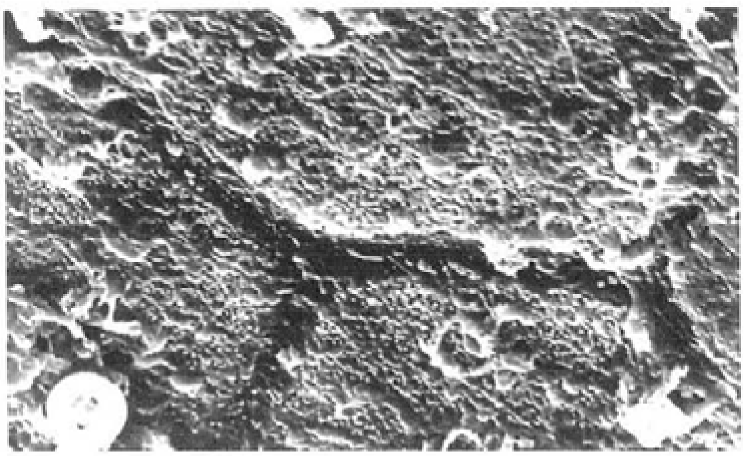

c

x3200

Figure 5.34

5.5.1.4.5. Lateral Surface of Growth Process.

The Outer Fibrous Sheath covers the lateral surface of the Growth Processes except where eroded (Figure 5.35. a OFS). Where the Outer Fibrous Sheath is eroded the underlying Outer Prismatic End Plates are seen (Figure 5.35. a, OPEP). In this species they have a central depression and a fine concentric circular pattern.

Where a medio-laterally thin Growth Scale has broken away, (Figure 5.35. b and c) the lateral surface of the underlying Growth Scale also has an Outer Fibrous Sheath (Figure 5.35. c OFS).

FIGURE 5.35. *Pinctada maxima* - Lateral Surface of Growth Process - Outer Fibrous Sheath - Outer Prismatic End Plates.

a. S.E.M. x 780 Lateral surface of Growth Process.

b. S.E.M. x 780 Broken Lateral Surface of Growth Process.

c. S.E.M. x 3200 As for b at higher magnification.

a

x780

b

x780

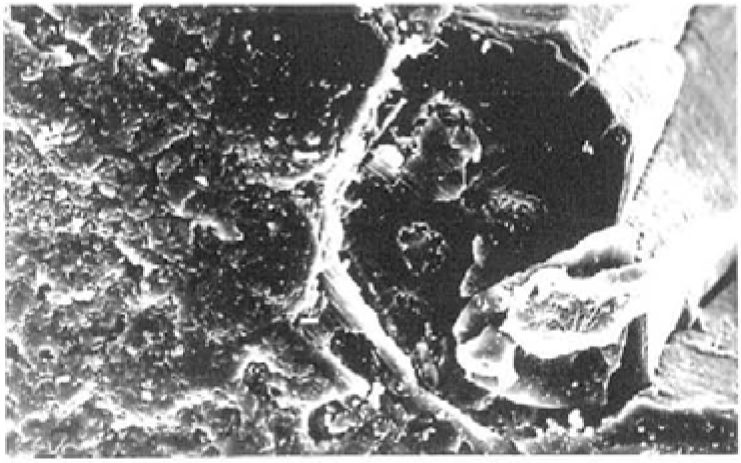

c

x3200

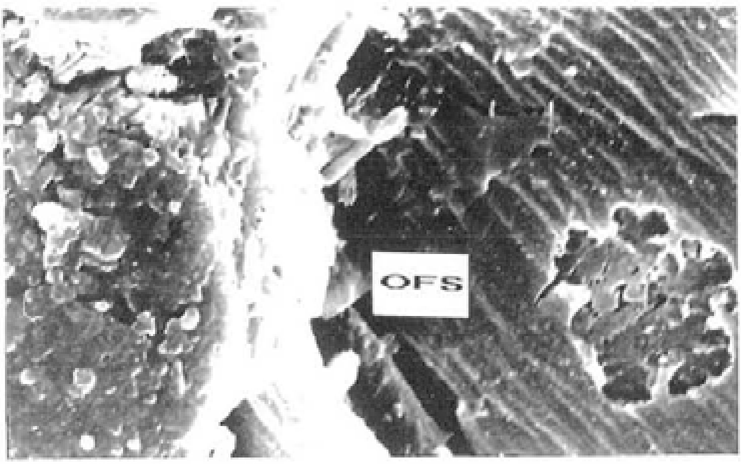

Figure 5.35

5.5.1.4.6. Radial Broken Surface Major Prisms - Reteform Interprismatic Organic Matrix.

This is the most commonly seen material lining the radial broken surface of the Prismatic Layer. A transverse layering of the material is usually obvious (Figure 5.36. a). In places it has a much finer structure than usual (Figure 5.36. b). It is uncertain whether the material on the left of Figure 5.36. b is another manifestation of the same material.

FIGURE 5.36. *Pinctada maxima* - Sagittal View Radial Broken Surface Major Prisms - Reteform Interprismatic Organic Matrix.

a. S.E.M. x 1600 Radial broken face of Major Prisms.

b. S.E.M. x 6300 As for a.

Different structured Interprismatic Organic Matrix.

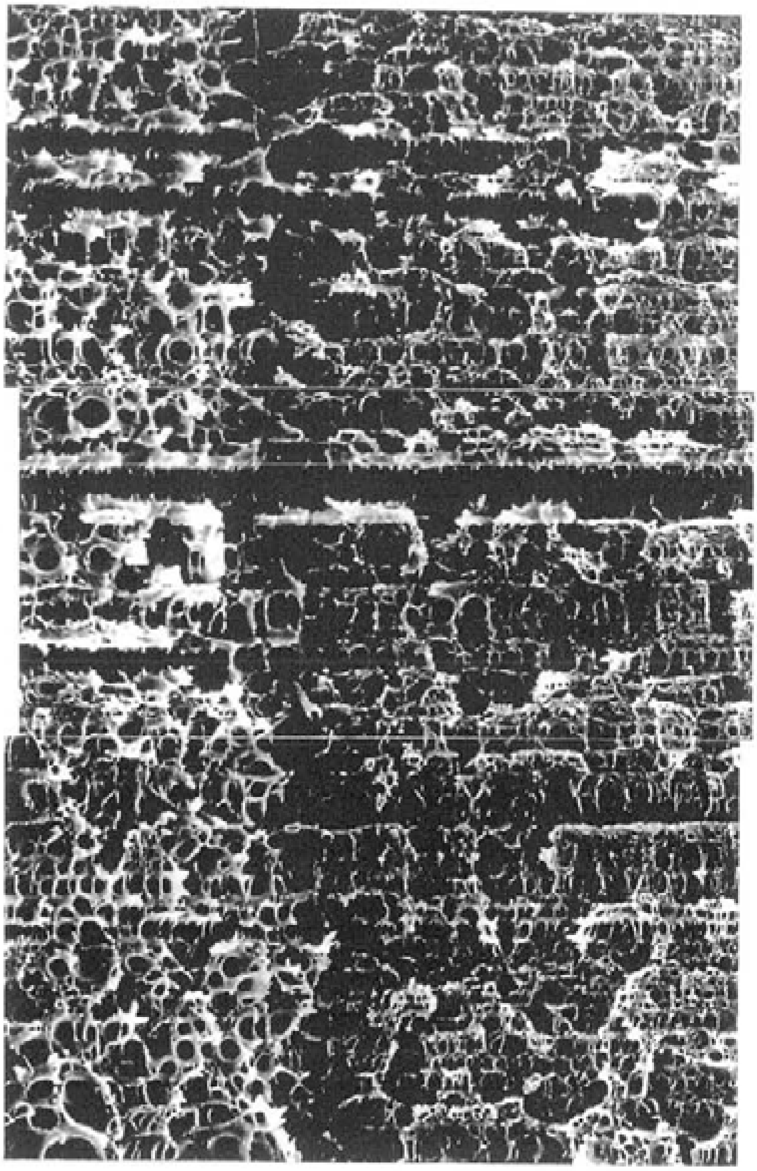

a

x1600

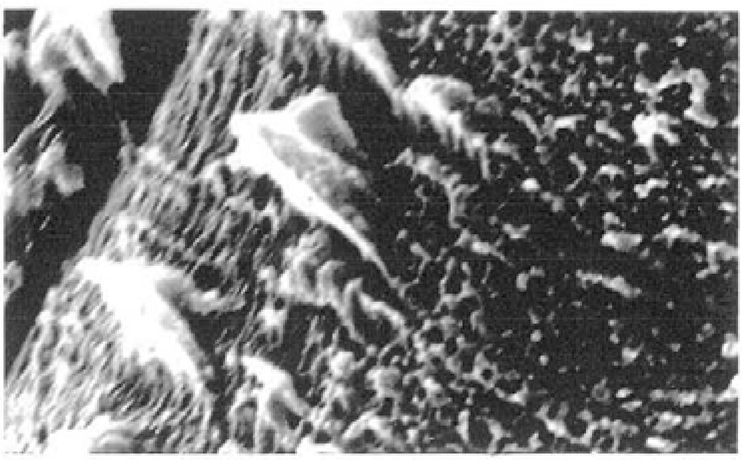

b

x6300

Figure 5.36

5.5.1.4.7. Calcite Tablets.

Unusually, a Major Prism breaks longitudinally showing broken calcite tablets (Figure 5.37. a, b and c). The broken tablets in Figure 5.37. b are about 40 μm across and between 3-7 μm in thickness.

Lens shaped spaces can (l), be seen in Figure 5.37. b where the Intraprismatic Organic Matrix has pulled out on fracturing.

FIGURE 5.37. *Pinctada maxima* - Sagittal View Prismatic Layer Radial Broken Surface - Calcite Tablets.

a. S.E.M. x 780 Radial broken surface Major Prism - broken Calcite Tablets.

b. S.E.M. x 1600 As for a above at higher magnification.

c. S.E.M. x 1600 As for b above.

a
x780

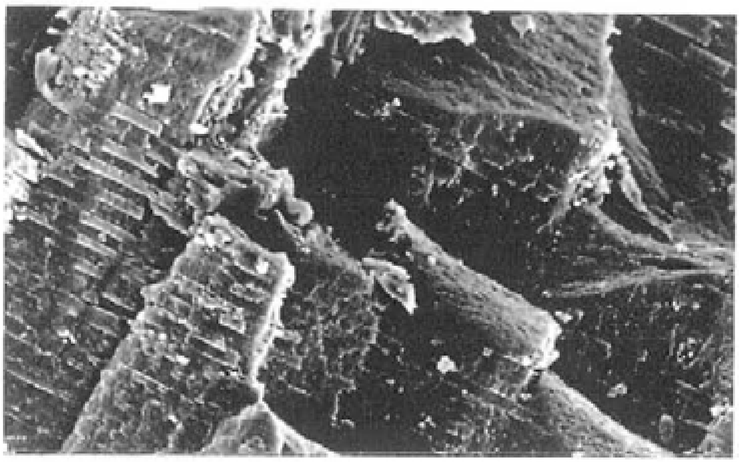

b
x1600

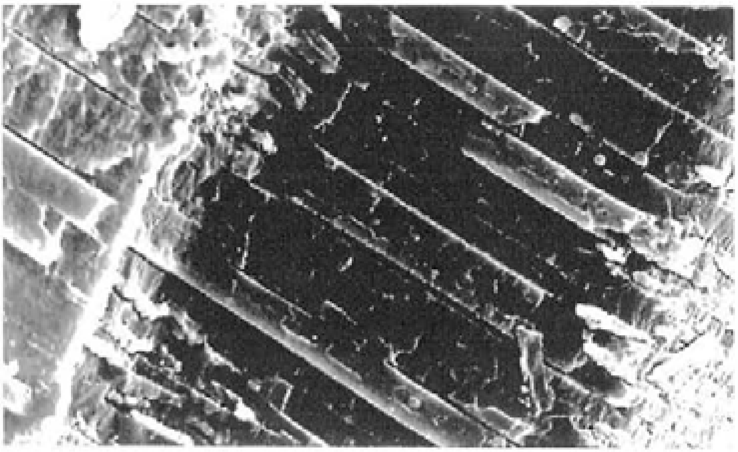

c
x 1600

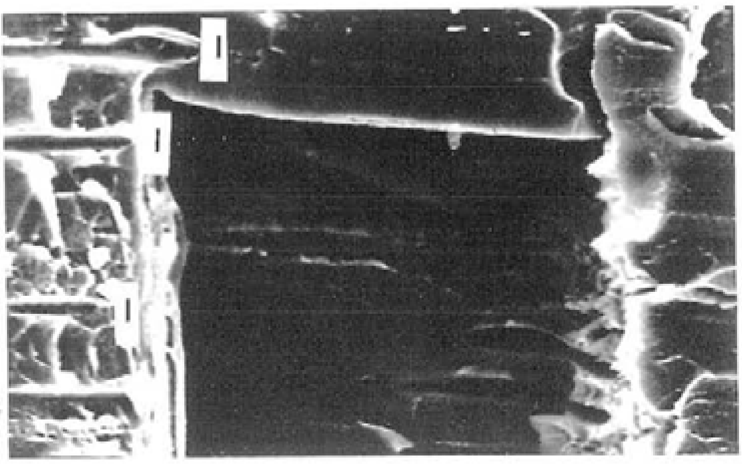

Figure 5.37

5.5.1.4.8. Radial Broken Surface Major Prisms - Aberrant Forms.

Major Prisms of *P.maxima* while irregular in cross-sectional shape, usually tend towards constancy in their transverse dimensions throughout their length, and the greater part of the volume of the prismatic layer is composed of prisms of between 1200 μm^2 and 2000 μm^2 cross-sectional area (Figures 5.31., 5.32., 5.33., 5.34., 5.35. and 5.37.). Where the lateral end of the prisms in one specimen had cross-sectional areas between 240 μm^2 and 450 μm^2 (a in Figure 5.38., a) the centre to centre dimensions were of the same order of magnitude as for normal sized prisms and the former prisms increased rapidly in size medially so that for the greater part of their length their cross-sectional area was normal (Figure 5.38., b).

Prisms with abnormally small cross sectioal areas on an otherwise normal lateral surface of a Growth Scale commonly taper to a point where they terminate within the Growth Scale, (p, p in Figure 5.38, b).

Outer Prismatic End Plates are usually slightly convex, (OPEP in Figure 5.38, b). Where there appears to be a juxtapposition of Growth Scales divided by neither an Inner Fibrous Sheath nor an Outer Fibrous Sheath the lateral surface of the Major Prisms of the more medial Growth Scale may be concave, (e in Figure 5.38, c).

Interprismatic Organic Matrix appears to project upwards in the grooves separating the lateral surfaces of the Prisms (i in Figure 5.38, d) and in places appears torn, (t in Figure 5.38, c and d).

FIGURE 5.38. *Pinctada maxima* - Sagittal View ofRadial Broken Surface of Prismatic Layer - Aberrant Forms.

a. S.E.M. x 780 Aberrantly decreased lateral ends of Prisms.

b. S.E.M. x 400 Apposition of surfaces of two Growth Scales.

c. S.E.M. x 1600 As for b above.

d. S.E.M. x 3200 Outer surface of a Growth Scale.

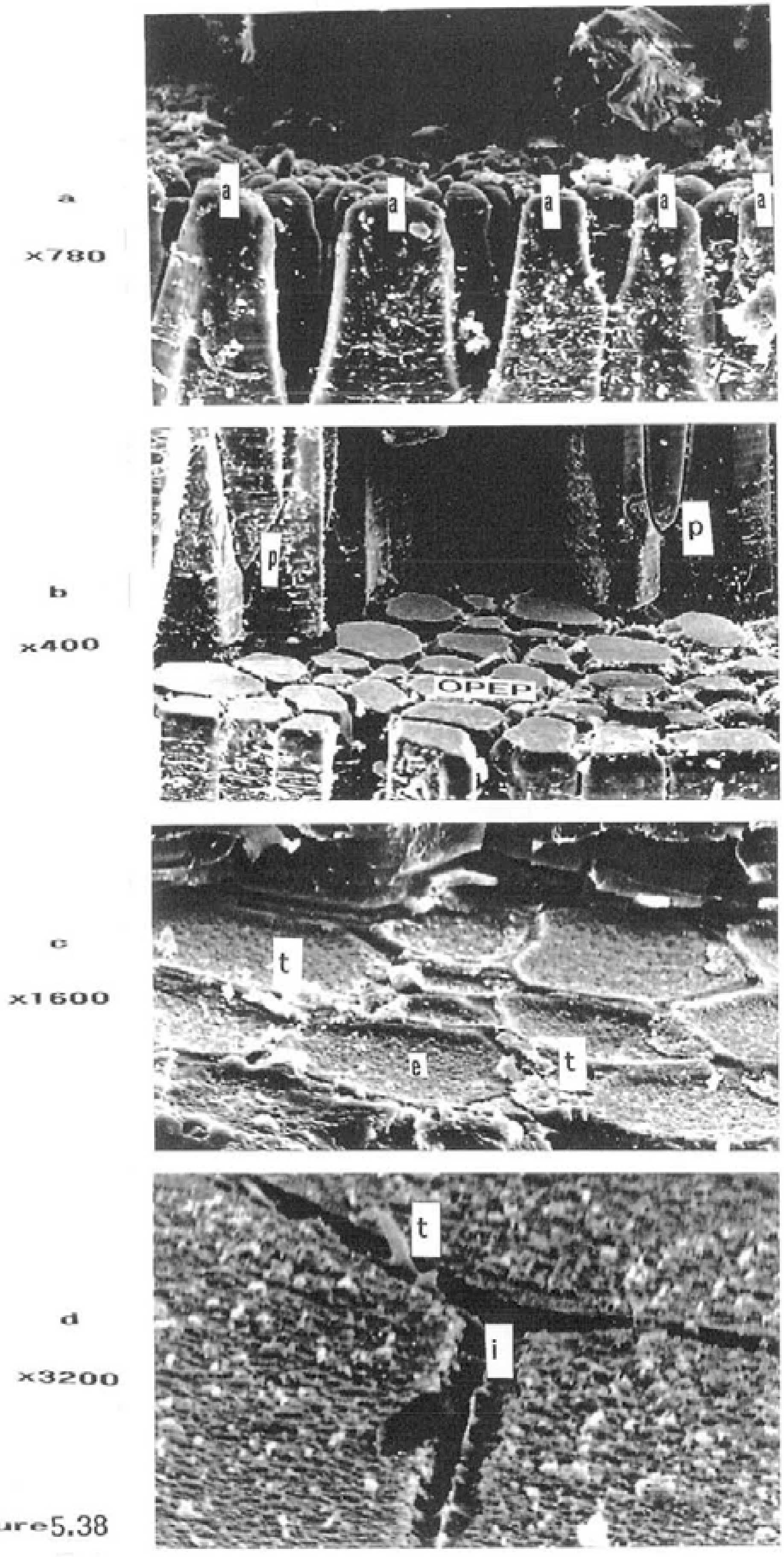

Figure5.38

5.1.4.9. Sagittal View Radial Broken Surface of Prismatic Layers.

Growth Processes - Linear Pattern Interprismatic Organic Matrix.

Linear Pattern Interprismatic Organic Matrix is often seen on the radial broken surface beween Growth Process prisms (Figure 5.39. a, b and c, ip), and, less frequently, Major Prisms.

On the other parts of the same radial broken surfaces Reteform Inter-prismatic Organic Matrix occurs. (Figure 5.39. b and c, ri).

Outer Fibrous Sheath covers the lateral surface of the Growth Process. (ofs in Figure 5.39. c).

FIGURE 5.39. *Pinctada maxima* - Sagittal View of Radial Broken Surface of Prismatic Layer Growth Process. Linear Pattern Interprismatic Organic Matrix.

a. S.E.M. x 860 Near the Proximal Origins of three Growth Processes.

b. S.E.M. x 860 Interprismatic Organic Matrices near the proximal origin of a Growth Process.

c. S.E.M. x 3200 Reteform and Linear Pattern Interprismatic Organic Matrices.

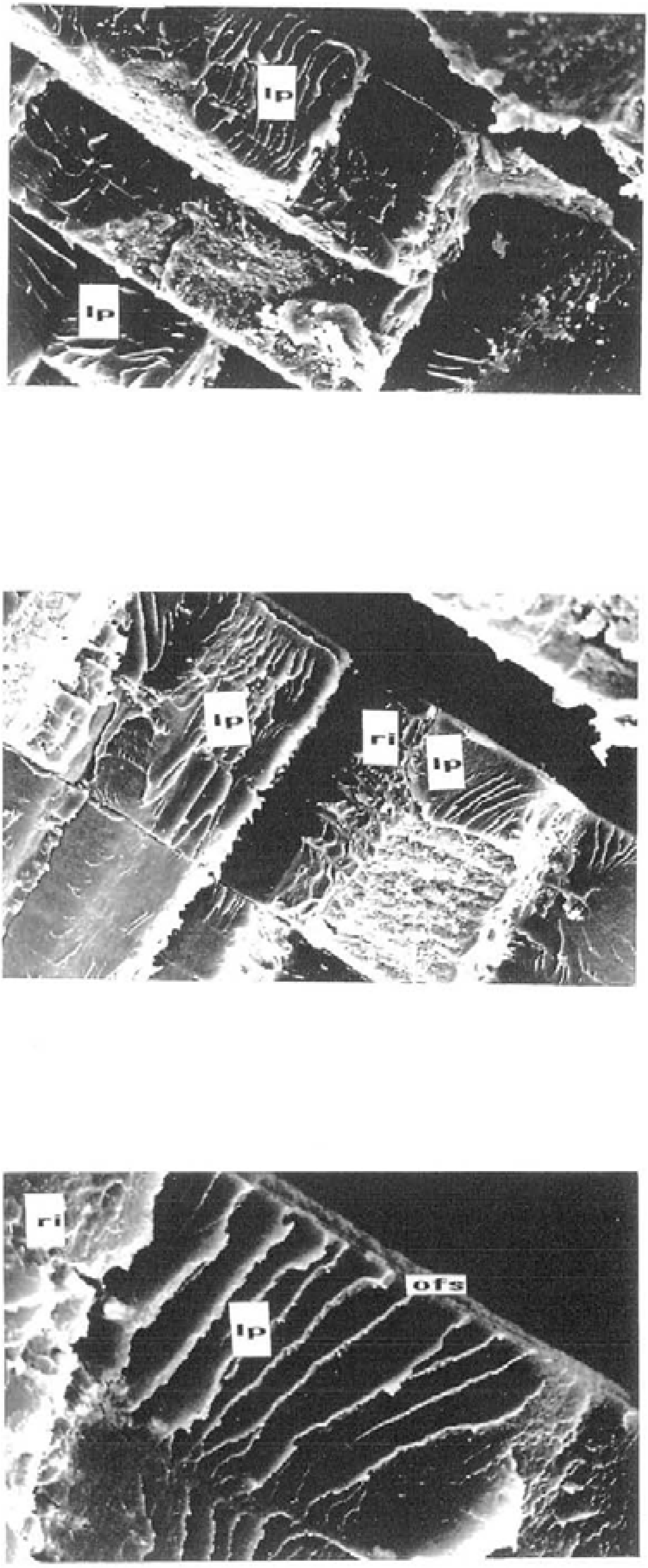

a
x860

b
x860

c
x3200

Figure 5.39

5.5.1.5. L.M. Prismatic and Nacreous Layers. Decalcified Shell.

The Nacreous Layers in radial section of decalcified Valve appear as anastomosing and splitting bands of fibrous material (Figure 5.40 a N).

The Proximal end of Growth Scales (Figure 5.40. a. GS) start as narrow bands of Prismatic Layer material between bands of Outer Nacreous Layer.

Distal to the Nacreo-prismatic Junction the medial surfaces of the Prismatic Layer and Growth Processes are covered with the Inner Fibrous Sheath (Figure 5.40. b. ifs). This stains puce with A.B./MS.B.

In sagittal view of radial section the Transverse Parallel Side Wall Organic Matrices usually stain yellow gold with M.S.B. or A.B./M.S.B. (p in Figure 5.40. a, b, c, d and e) but in places (often in bands) may stain differently (f in Figure 5.40. c and e). The non-yellow/gold staining Transverse parallel material appears to be partly destroyed by acid decalcification (f, f in Figure 5.40. c).

Remnants of Intraprismatic Organic matrix are seen in Figure 5.40. e (i, i). They stain turquoise with A.B./M.S.B.

Outer Prismatic End Plates (OPEP) and Inner Lateral Structure (ILS) occur in the lateral part of Major Prisms (Figure 5.40. e).

FIGURE 5.40. *Pinctada maxima.* L.M. Decalcified Shell.

a. M.S.B. x 310 Radial Section near peripheral Nacreo-prismatic Junction.

b. M.S.B. x 1200 Prismatic Layer Inner Fibrous Sheaths.

c. M.S.B. x 1200 Sagittal View Prismatic Layer Radial Section.

d. M.S.B. x 1200 Transverse Parallel Side Wall Organic Matrix.

e. M.S.B. x 310 Sligtly slanting near sagittal section through junction of two Growth Scales.

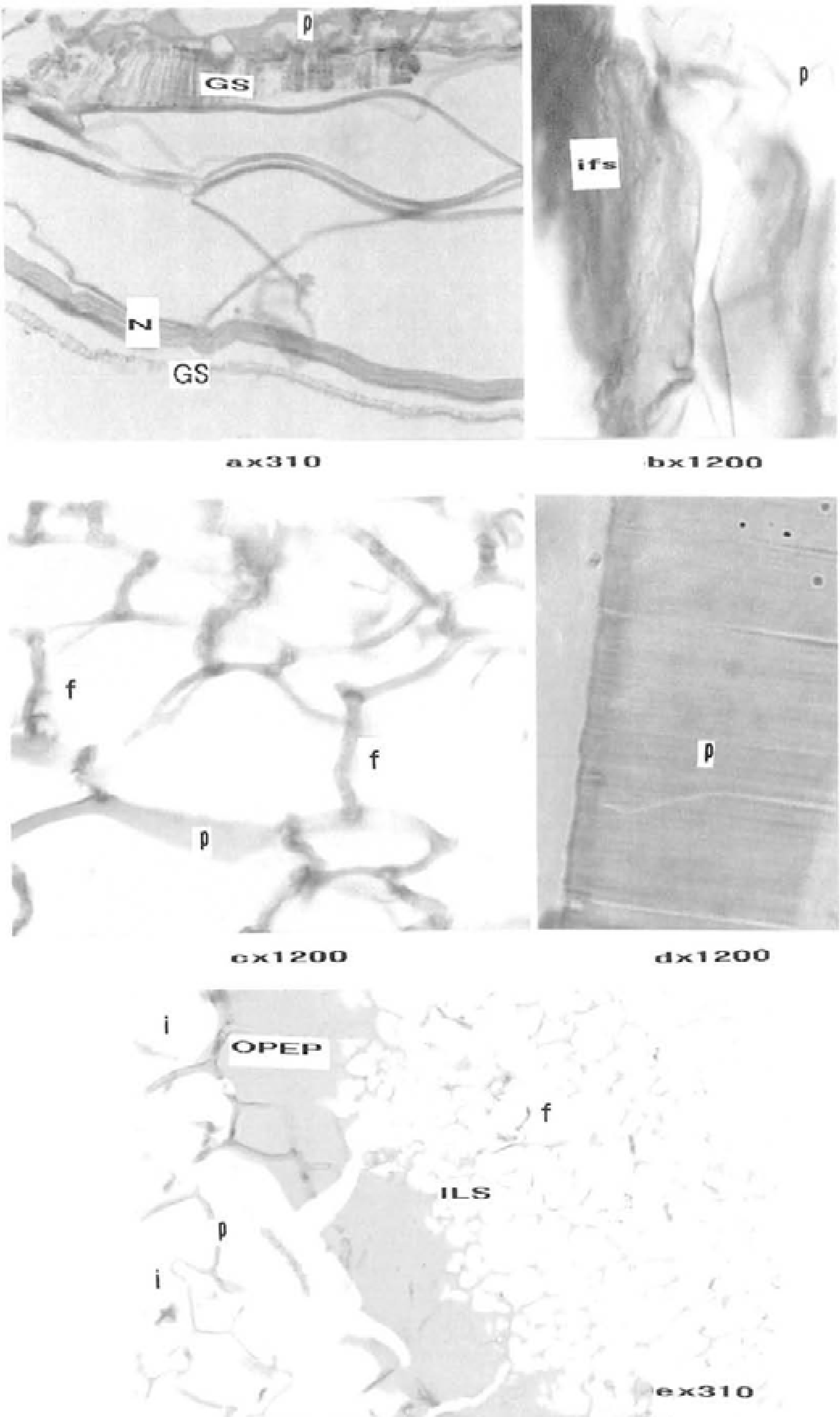
p
GS
N
GS
ax310
ifs
p
bx1200
f
f
p
cx1200
p
dx1200
i
OPEP
f
ILS
p
i
ex310

Figure 5.40

5.5.1.6. Cultured Pearl.

The broken radial surface of a cultured pearl, outside the nucleus, has three types of layer. Opposed to the nucleus is a thin, apparently non-calcareous fibrous layer (f in Figure 5.41. a, b, and d and in Figure 5.42. b).

Outside this is a calcareous layer with radial lines which resembles the simple aragonite prismatic layer of *Velesumio ambiguus* - Radial Layer, (r in Figure 5.41. a, b, c and d and in Figure 5.42. a, c and d).

Outside this is the nacreous layer (n in Figure 5.41. a, b, c and e, and in Figure 5.42. a and d).

FIGURE 5.41. *Pinctad maxima* - Radial Broken Surface of Cultured Pearl.

a. S.E.M. x 40 Fibrous Layer, Radial Layer and Nacre.

b. S.E.M. x 400 Fibrous Layer Radial Layer and Nacre.

c. S.E.M. x 780 Radial Layer and Nacre.

d. S.E.M. x 3200 Fibrous Layer and Radial Layer.

e. S.E.M. x 3200 Nacreous Layer.

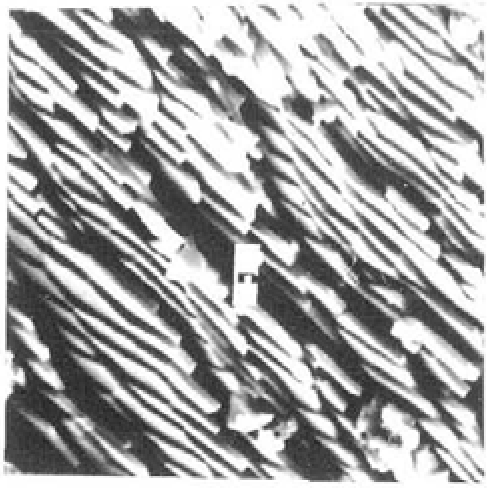

e

x3200

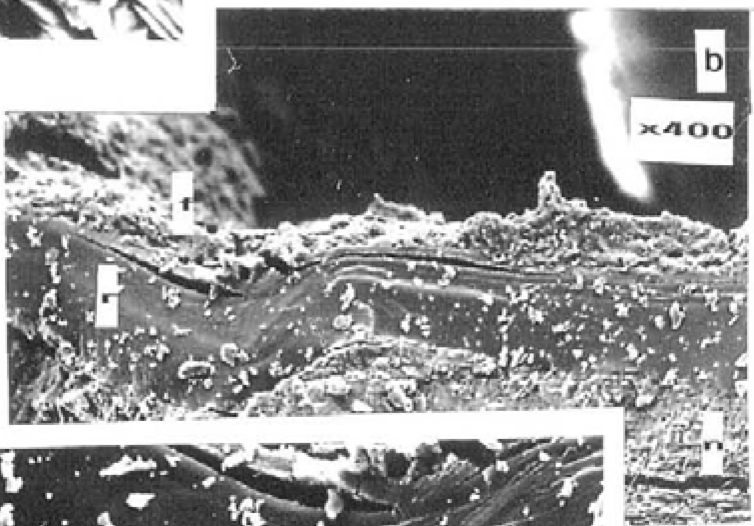

Figure

5.41

c

x780

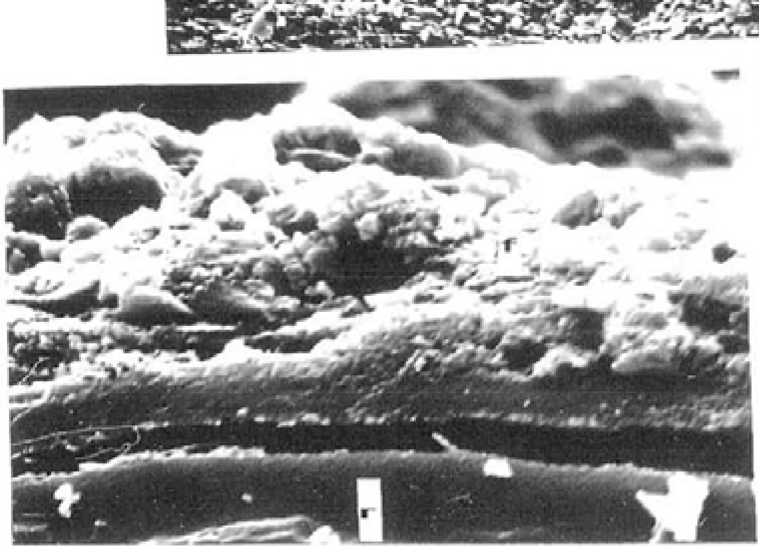

d

x3200

5.5.1.6. Cultured Pearl (Continued).

The fibrous layer opposed to the nucleus has a structure of very short fibres (2 μm x 0.3 μm) lying parallel in rows, (Figure 5.42. b, f). The fibres lie at about 60° to the direction of the rows (Figure 5.42. b).

Near the nucleus the Radial layer alternates with thin bands of Nacreous Layer (r and n in Figure 5.42. a).

The aragonite radial Layer is shown at higher magnification in Figure 5.42. c).

The Nacre Tiles of the Nacreous Layer are about o.6 μm thick. (at n in Figure 5.42. d).

FIGURE 5.42. *Pinctada maxima* - Fibrous Layer, Radial Layer and Nacreous Layer of Cultured Pearl.

a. S.E.M. x 770 Alternating Radial Layers and Nacreous Layers in radial broken surface.

b. S.E.M. x 6300 Inner surface of Fibrous Layer.

c. S.E.M. x 3200 Radial Layer Radial Broken Surface.

d. S.E.M. x 3200 Junction of Radial Layer and Nacreous Layer - Radial Broken Surface.

a
x770

b
x6300

c
x3200

d
x3200

Figure 5.42

5.5.1.6. Cultured Pearl (Continued).

The Nacreous Layer of cultured pearl is essentially similar to the Inner Nacreous Layer of a *Pinctada maxima* Valve. Away from the Radial Layer, the Nacre Tiles are about 0.4 µm thick and about 4.5 µm across (Figure 5.43. a and c). What appears to be a layer of thickened Nacre Sheet Nacreous Organic Matrix is labelled nom in Figure 5.43. a.

The Inter Nacre Tile Organic Matrices in some places lie in the one plane over several Nacre Sheets (om - om in Figure 5.43. b).

Centrally placed on a number of Nacre Tiles are depressions on their lateral surface (d in Figure 5.43. b and c).

FIGURE 5.43. *Pinctada maxima* - Radial Broken Face of Cultured Pearl. Nacre Tiles and Nacreous Organic Matrices.

a. T.E.M. x 3200 Nacre Tiles in Nacre Sheets

b. T.E.M. x 6300 Planar lines of Inter-nacre Tile Organic Matrices.

c. T.E.M. x 6300 Surface depressions on the medial surfaces of Nacre Tiles.

a
×3200

b
×6300

c
×6300

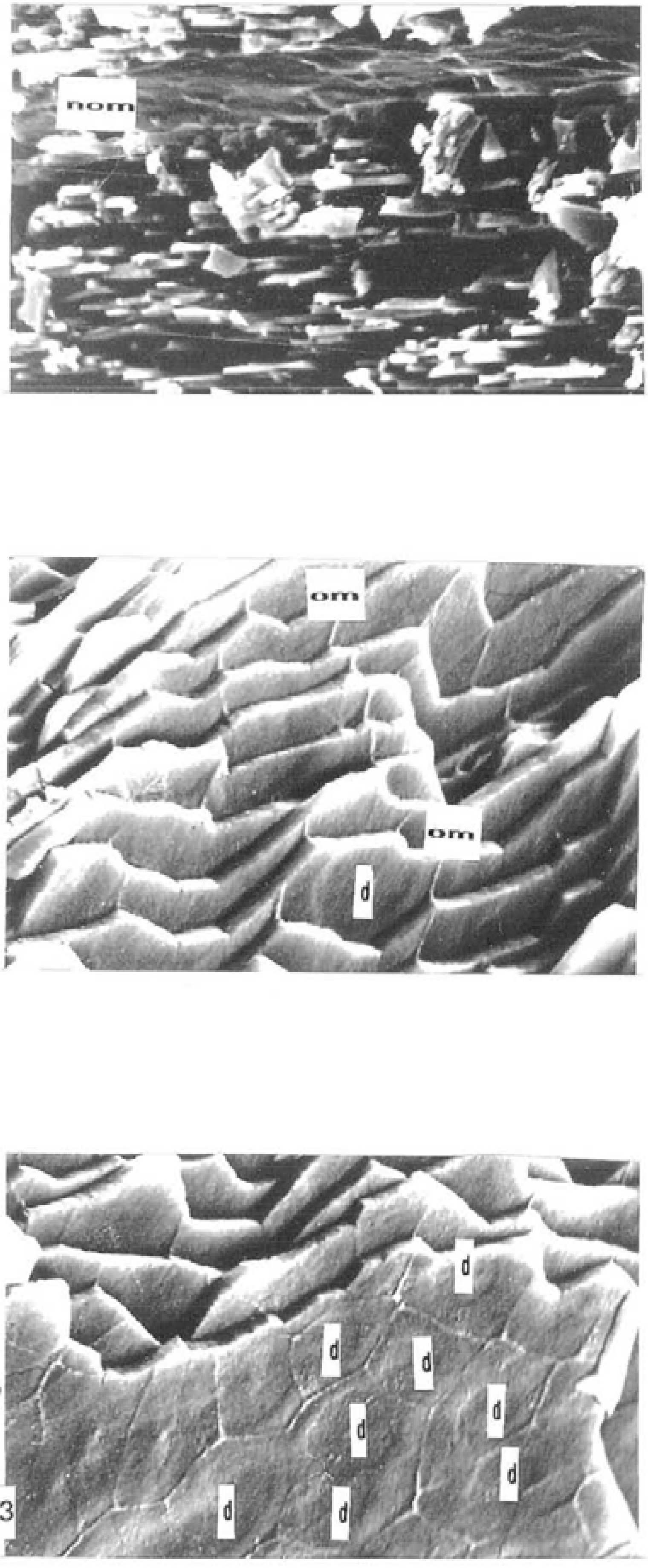

Figure 5.43

5.5.1.7. Shell Damage from Boring Sponge.

Cavernous damage from boring sponges is common in the Nacreous Layers of pearl shells (cd in Figure 5.44. a and e), and uncommon in their Prismatic Layer (c in Figure 5.44. a). In Prismatic Layer the damage is more usually confined to a single Major Prism (p in Figure 5.44. c) or a group of adjacent Major Prisms (p in Figure 5.44. a and c). The Prismatic Layer adjacent to invaded regions may be unaffected (PL in Figure 5.44. b and c). In Valves where the Prismatic Layer is still largely intact and structurally little affected the underlying Nacreous Layers are often largely destroyed (Figure 5.44. e).

Destruction of the calcite tablets (c in Figure 5.44. d), of a Major Prism often leaves the intervening Intra-prismatic Organic Matrices more easily seen than in a radial broken face of Prismatic Layer (i in Figure 5.44. d). Where a Nacreous Layer is being destroyed it appears that destruction proceeds from the periphery of each Nacre Tile (Figure 5.44. f). Where destruction of the Inner Nacreous Layer reaches the medial surface of the Nacre the destruction commonly involves destruction in a lace-like pattern (at N in Figure 5.44. g) around the centre of destruction.

FIGURE 5.44. *Pinctada maxima* - Destruction of Shell Layer of *P.maxima* by a Boring Sponge.

a. S.E.M. x 160 Radial Broken surface of Prismatic Layer PN and Nacreous Layer N.

b. S.E.M. x 92 Invasion of a single Major Prism.

c. S.E.M. x 370 Boring Sponge in Prismatic Layer.

d. S.E.M. x 5800 Prismatic Layer Calcite Tablets separated by Intraprismatic Organic Matrix.

e. S.E.M. x 91 Cavernous Destruction of Nacre.

f. S.E.M. x 2900 Remnant Extended hexagons of Nacre Tiles

g. S.E.M. x 740 Damage to medial Nacreous Surface.

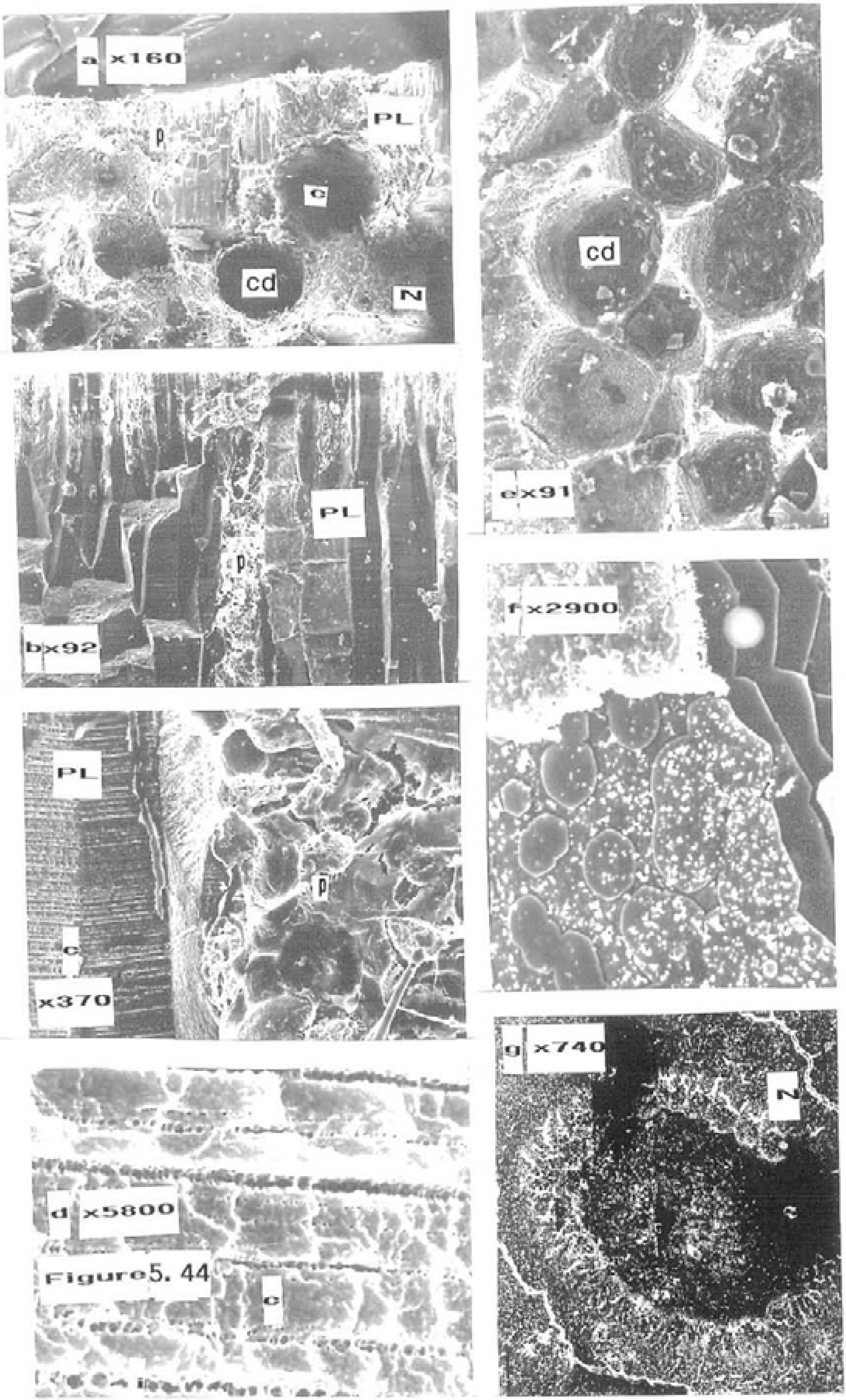
a x160
PL
p
c
cd
N
cd
e x91
b x92
PL
p
f x2900
PL
p
c
x370
g x740
N
c
d x5800
c

Figure5. 44

5.5.1.8. Tissues and Glands of External Mantle.

5.5.1.8.1.

The External Mantle is divided on histological grounds into the Shoulder Region, which opposes the Shoulder Region of the Valve; the Pallial Gland Region (PGR between asterisks in Figure 5.45. a); Proximal Pallial Region, (PPR beneath the asterisk in Figure 5.45. a); the Middle Pallial Region, (MPR, Figure 5.45. b); the Distal Pallial Region (DPR, in Figure 5.45. c), and the Distal Folded Region (DFR, between the asterisks in Figure 5.45. d).

For orientation, the Folds of the Mantle Margin (5.1.9) are also shown on Figure 5.45., where l is lateral, m is medial, F1. is Mantle Margin Fold F1., F2. is Mantle Margin Fold F2. and F3. is Mantle Margin Fold F3..

FIGURE 5.45. *Pinctada maxima* - Histological Regions of the External Mantle

and the Mantle Margin Folds from Pallial Gland to LatF3..

a. L.M. x 38 Radial Section of Pallial Gland Region and Proximal Pallial Region.

b. L.M. x 38 Middle Pallial Region.

c. L.M. x 38 Distal Pallial Region.

d. L.M. x 38 Distal Pallial Region.

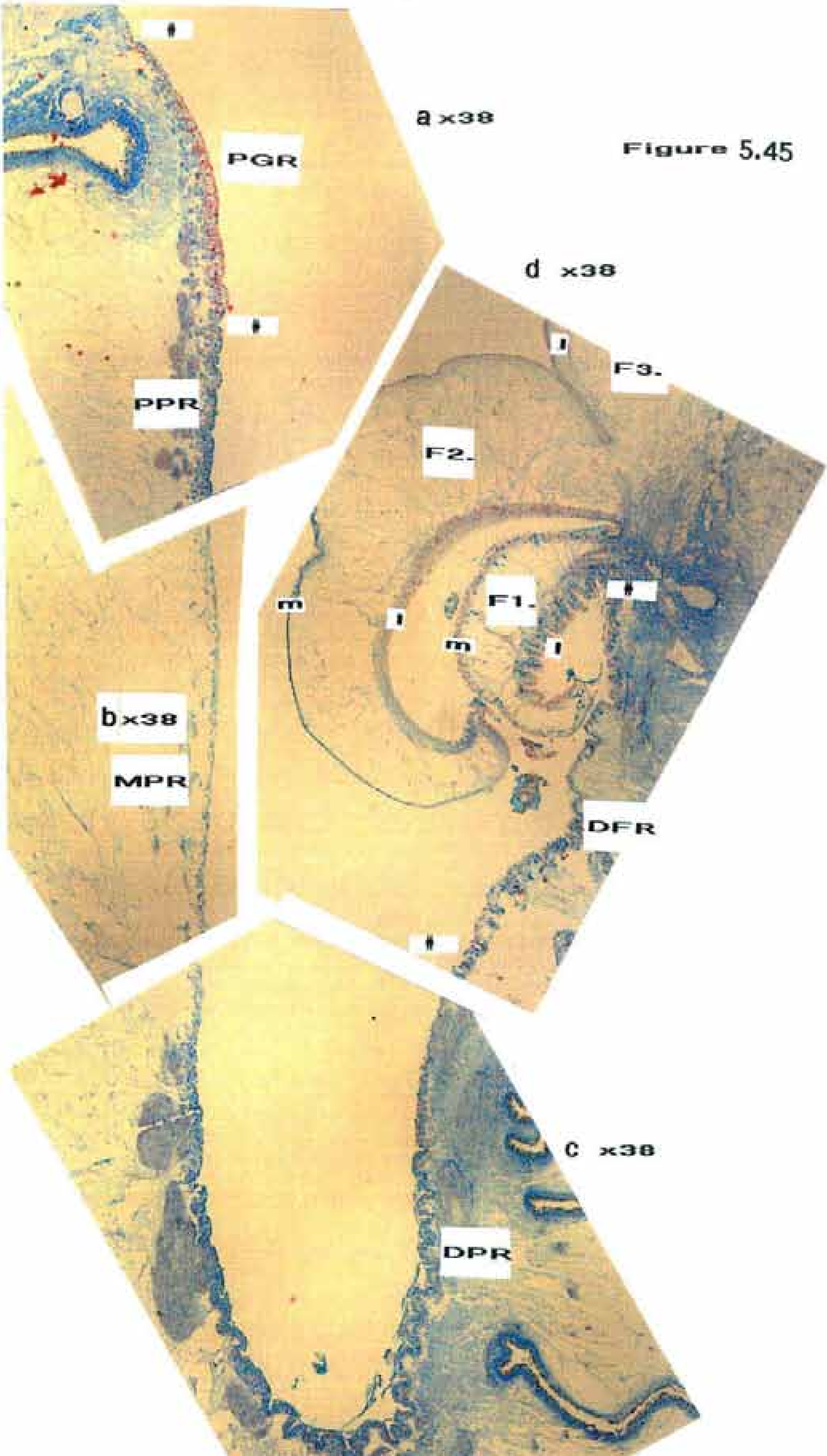

Figure 5.45

5.5.1.8.2. The Isthmusistic Epithelium.

The Isthmusistic epithelium is an extremely elongate columnar epithelium with very elongate subcentral Nuclei (Figure 5.46. nu. with prominent nucleoli (Figure 5.46. ni). There are areas of densely packed endoplasmic reticulum (Figure 5.46. er), visicles (Figure 5.46. v) and elongate mitochondria (Figure 5.46. mit) in the sub-apical and the central cytoplasm. The apical cytoplasm bears small electron dense granules (Figure 5.46. edg) and numerous rounded mitochondria (Figure 5.46. mi).

The tissues of the various specified Regions of the External mantle and Mantle Margin of this species are illustrated, (Figs 5.45 - 5.81) to match the previously given illustrations of the same Regions of the valve, (Figs. 5.12 - 5.40). Species specificity of the histologies of the External Mantle and Mantle Margin of the *Pinctada* is illustrated by contrasting the above with the equally detailed illustrations of the same specified Regions of the Mantle and Mantle Margin of *Pinctada margaritifera*, (Figs. 5.45 - 5.81), and with illustrations of the External Mantle and Mantle Margin in other species of *Pinctada*, (Figs. 5.129; 5.130; 5.134; 5.136; 5.138; 5.139, 5.140, 5.141; and5.142). Rigid species specificity of the histologies of the Mantle Margin tissues is illustrated in different specimens of *P.albina sugillata* in Fig. 5.141. The illustrations of the tissues of the various Regions of the External mantle and mantle margin of the *Pinctada* should be contrasted with those of the same regions of the *Pteria*, *Isognomon* and *Malleus* and also those of the same Regions of the *Ostreoidea*, *Limopsoidea* and *Arcoidea*.

FIGURE 5.46. *Pinctada maxima* Isthmusistic Epithelium.

a. T.E.M. x 3500 Isthmusistic Epithelial Cells from Basement Membrane to Apical Membrane.

b. T.E.M. x 18000 Apical cytoplasm.

c. T.E.M. x 18000 Part of Nucleus and central cytoplasm.

d. T.E.M. x 18000 Organelles of the sub-apical cytoplasm.

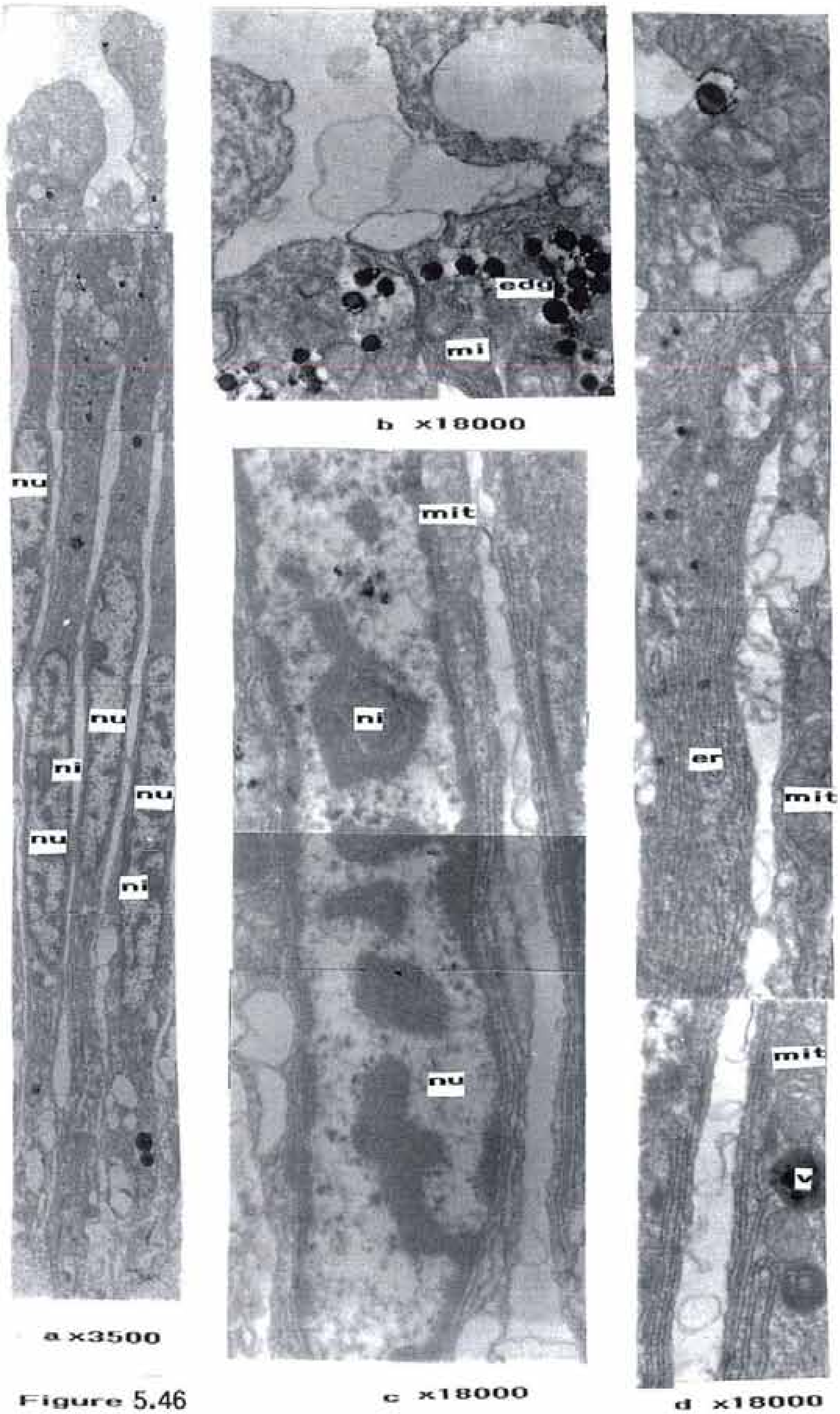
nu
nu
ni
nu
nu
ni
a x3500
edg
mi
b x18000
mit
ni
nu
c x18000
er
mit
mit
v
d x18000

Figure 5.46

5.5.1.8.3. Shoulder Region.

Secretory material organised into membranes is commonly seen between the Shoulder Region surface epithelium and the adjacent medial surface of the Inner Nacreous Layer (Figure 5.47. a). The Shoulder Region surface eptihelium is underlain by a massive glandular structure - the Shoulder Gland. This glandular structure is up to about 500 μm thick latero-medially. (In Figure 5.47. l is lateral, m, medial and l of c. is medial to m of b., l of d. is medial to m of c.). All the underlying unicellular glands discharge through tubules into the space lateral to the Shoulder epithelium.

The unicellular secretory glands consist of Spherular Cytoplasm Turquoise Glands (Figure 5.47. b T), Trabecular Turquoise Glands (Figure 5.47. b and c TT) and several varieties of Granular Cytoplasm Secretory Glands (gc in Figure 5.47. b, c and d). The cell bodies of the latter tend to be situated deep to those of the Turquoise Glands (Figure 5.47. b, c and d).

Nerves infiltrate the entire glandular structure. There are three distinct kinds of neurosecretory granule: large spherical granules as at n in Figure 5.47. c; small spherical granules as at n in Figures 5.47. d and e; and ovoid shaped granules as at N in Figures 5.47. d and e.

FIGURE 5.47. *Pinctada maxima* - Glands and Secretion of the Shoulder Gland.

a. T.E.M. x 18000 Membranous Secretion.

b. T.E.M. x 1800 Superficial one third (aprox.) of Shoulder Gland.

c. T.E.M. x 1800 Middle one third (aprox.) of Shoulder Gland.

d. T.E.M. x 1800 Deep one third (aprox) of Shoulder Gland.

e. T.E.M. x 7000 Neural structures of the Shoulder Gland.

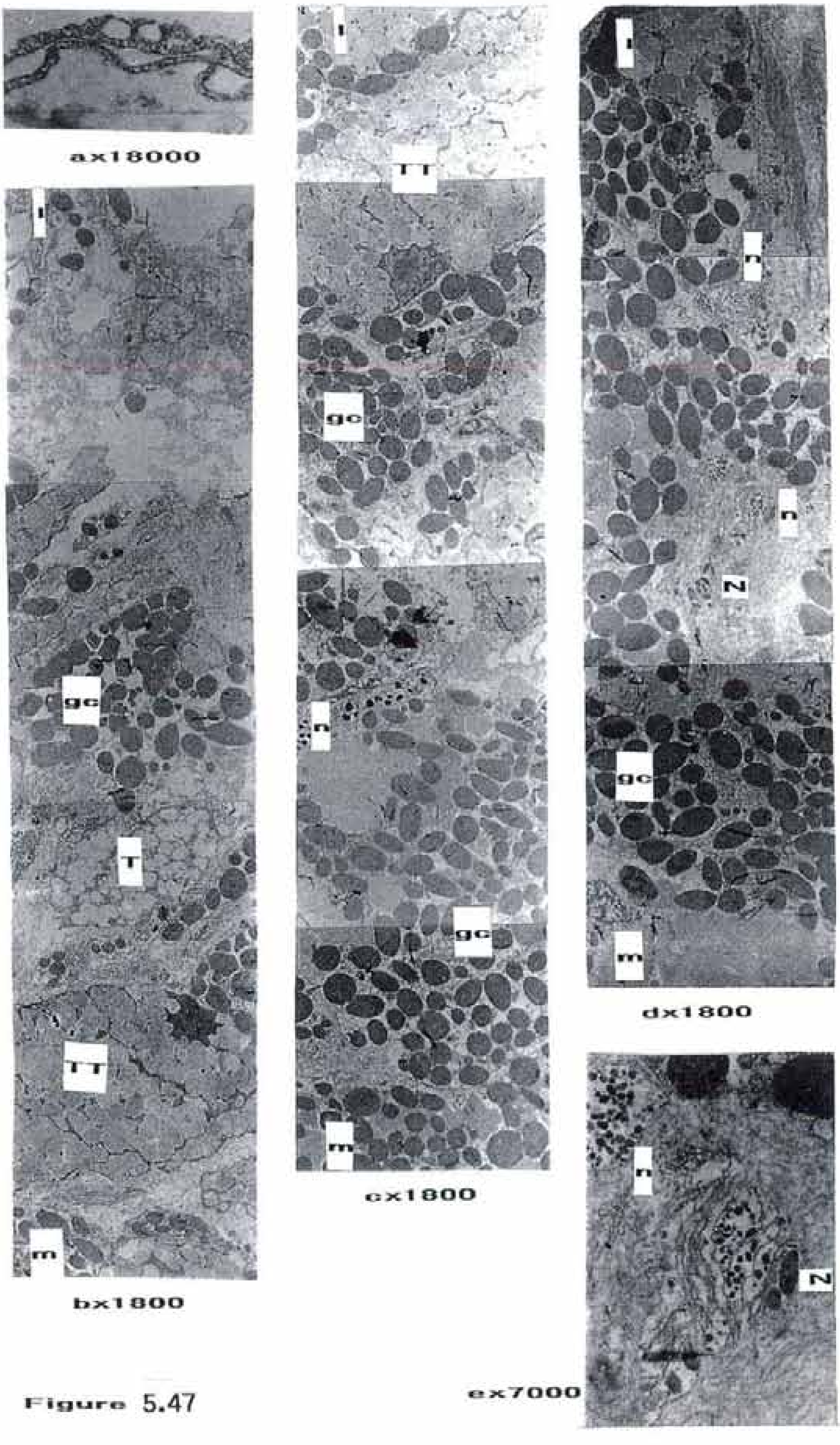
I
ax18000
I
gc
T
TT
m
bx1800
I
TT
gc
n
gc
m
cx1800
I
n
n
N
gc
m
dx1800
n
N
ex7000

Figure 5.47

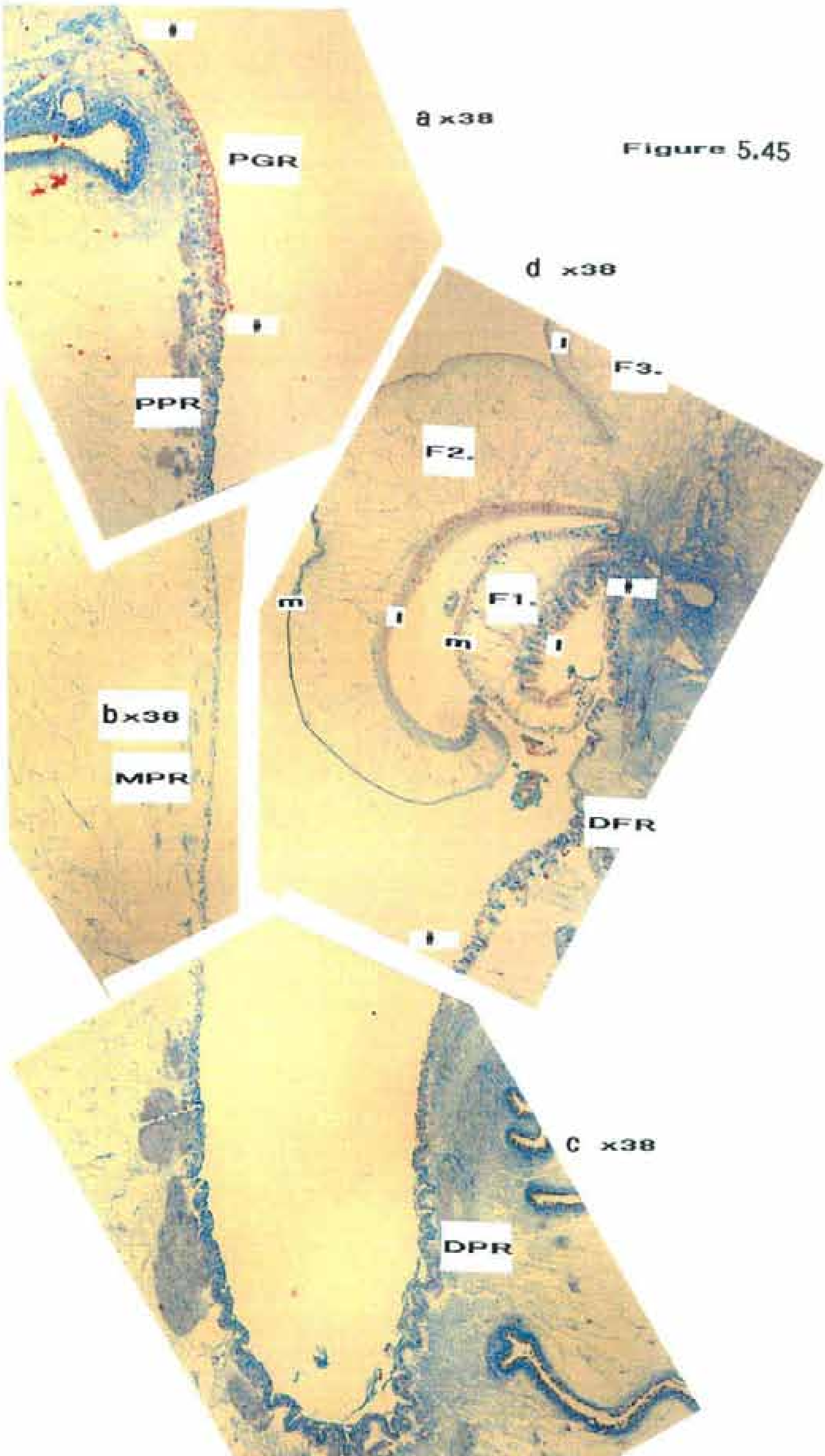

Figure 5.45

5.5.1.8.2. The Isthmusistic Epithelium.

The Isthmusistic epithelium is an extremely elongate columnar epithelium with very elongate subcentral Nuclei (Figure 5.46. nu. with prominent nucleoli (Figure 5.46. ni). There are areas of densely packed endoplasmic reticulum (Figure 5.46. er), visicles (Figure 5.46. v) and elongate mitochondria (Figure 5.46. mit) in the sub-apical and the central cytoplasm. The apical cytoplasm bears small electron dense granules (Figure 5.46. edg) and numerous rounded mitochondria (Figure 5.46. mi).

The tissues of the various specified Regions of the External mantle and Mantle Margin of this species are illustrated, (Figs 5.45 - 5.81) to match the previously given illustrations of the same Regions of the valve, (Figs. 5.12 - 5.40). Species specificity of the histologies of the External Mantle and Mantle Margin of the *Pinctada* is illustrated by contrasting the above with the equally detailed illustrations of the same specified Regions of the Mantle and Mantle Margin of *Pinctada margaritifera*, (Figs. 5.45 - 5.81), and with illustrations of the External Mantle and Mantle Margin in other species of *Pinctada*, (Figs. 5.129; 5.130; 5.134; 5.136; 5.138; 5.139. 5.140. 5.141; and5.142). Rigid species specificity of the histologies of the Mantle Margin tissues is illustrated in different specimens of *P.albina sugillata* in Fig. 5.141. The illustrations of the tissues of the various Regions of the External mantle and mantle margin of the *Pinctada* should be contrasted with those of the same regions of the *Pteria*, *Isognomon* and *Malleus* and also those of the same Regions of the *Ostreoidea*, *Limopsoidea* and *Arcoidea*.

FIGURE 5.46. *Pinctada maxima* Isthmusistic Epithelium.

a. T.E.M. x 3500 Isthmusistic Epithelial Cells from Basement Membrane to Apical Membrane.

b. T.E.M. x 18000 Apical cytoplasm.

c. T.E.M. x 18000 Part of Nucleus and central cytoplasm.

d. T.E.M. x 18000 Organelles of the sub-apical cytoplasm.

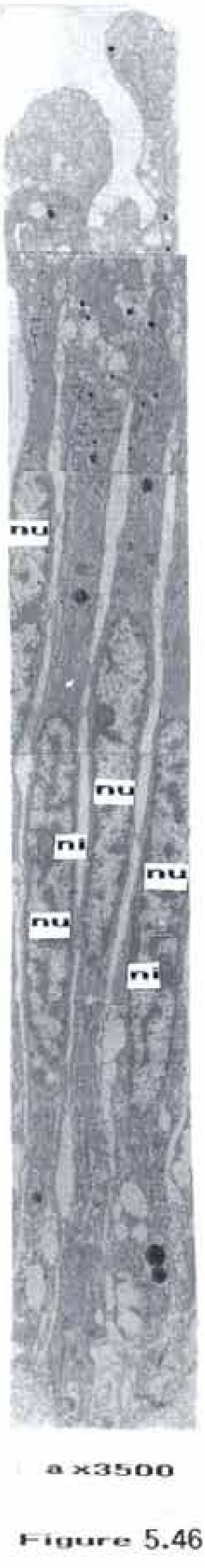

a x3500

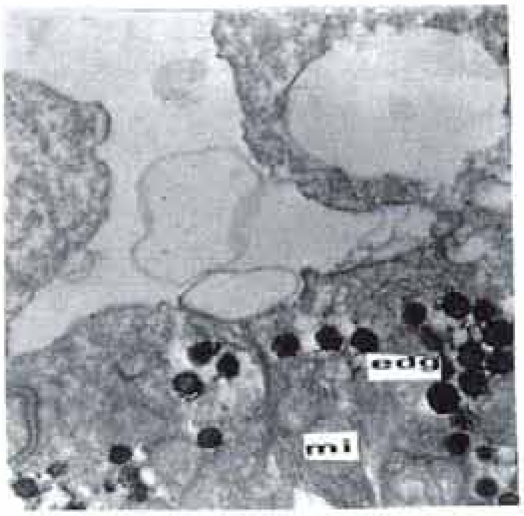

b x18000

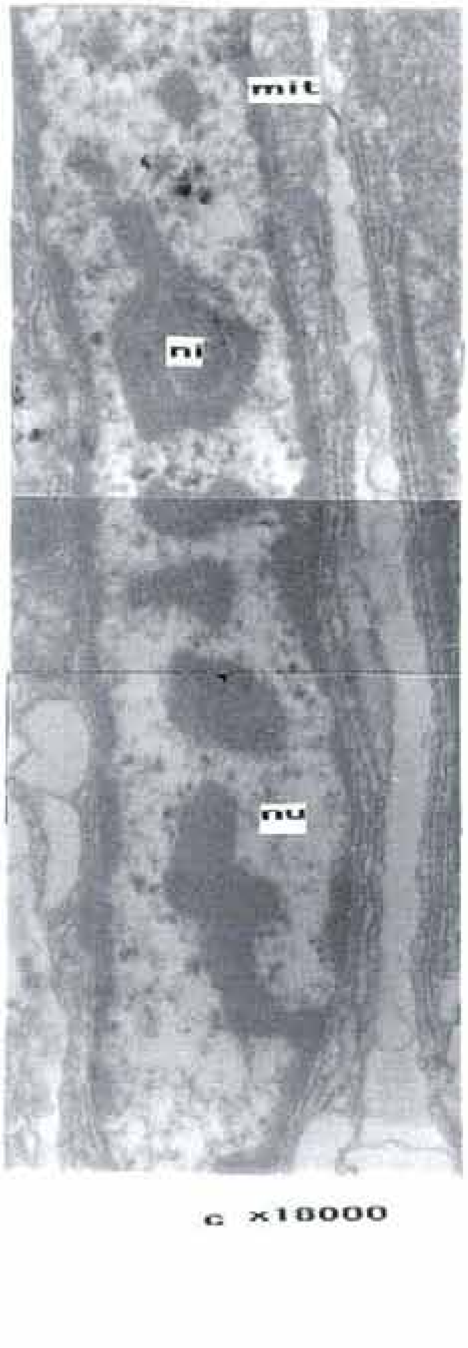

c x18000

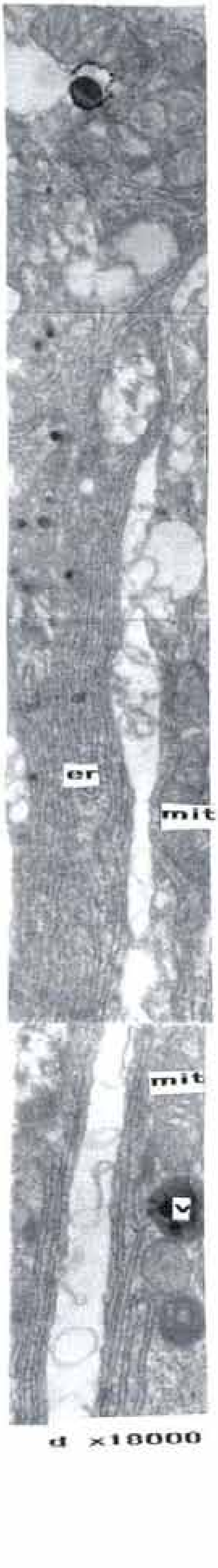

d x18000

Figure 5.46

5.5.1.8.3. Shoulder Region.

Secretory material organised into membranes is commonly seen between the Shoulder Region surface epithelium and the adjacent medial surface of the Inner Nacreous Layer (Figure 5.47. a). The Shoulder Region surface eptihelium is underlain by a massive glandular structure – the Shoulder Gland. This glandular structure is up to about 500 μm thick latero-medially. (In Figure 5.47. l is lateral, m, medial and l of c. is medial to m of b., l of d. is medial to m of c.). All the underlying unicellular glands discharge through tubules into the space lateral to the Shoulder epithelium.

The unicellular secretory glands consist of Spherular Cytoplasm Turquoise Glands (Figure 5.47. b T), Trabecular Turquoise Glands (Figure 5.47. b and c TT) and several varieties of Granular Cytoplasm Secretory Glands (gc in Figure 5.47. b, c and d). The cell bodies of the latter tend to be situated deep to those of the Turquoise Glands (Figure 5.47. b, c and d).

Nerves infiltrate the entire glandular structure. There are three distinct kinds of neurosecretory granule: large spherical granules as at n in Figure 5.47. c; small spherical granules as at n in Figures 5.47. d and e; and ovoid shaped granules as at N in Figures 5.47. d and e.

FIGURE 5.47. *Pinctada maxima* – Glands and Secretion of the Shoulder Gland.

a. T.E.M. x 18000 Membranous Secretion.

b. T.E.M. x 1800 Superficial one third (aprox.) of Shoulder Gland.

c. T.E.M. x 1800 Middle one third (aprox.) of Shoulder Gland.

d. T.E.M. x 1800 Deep one third (aprox) of Shoulder Gland.

e. T.E.M. x 7000 Neural structures of the Shoulder Gland.

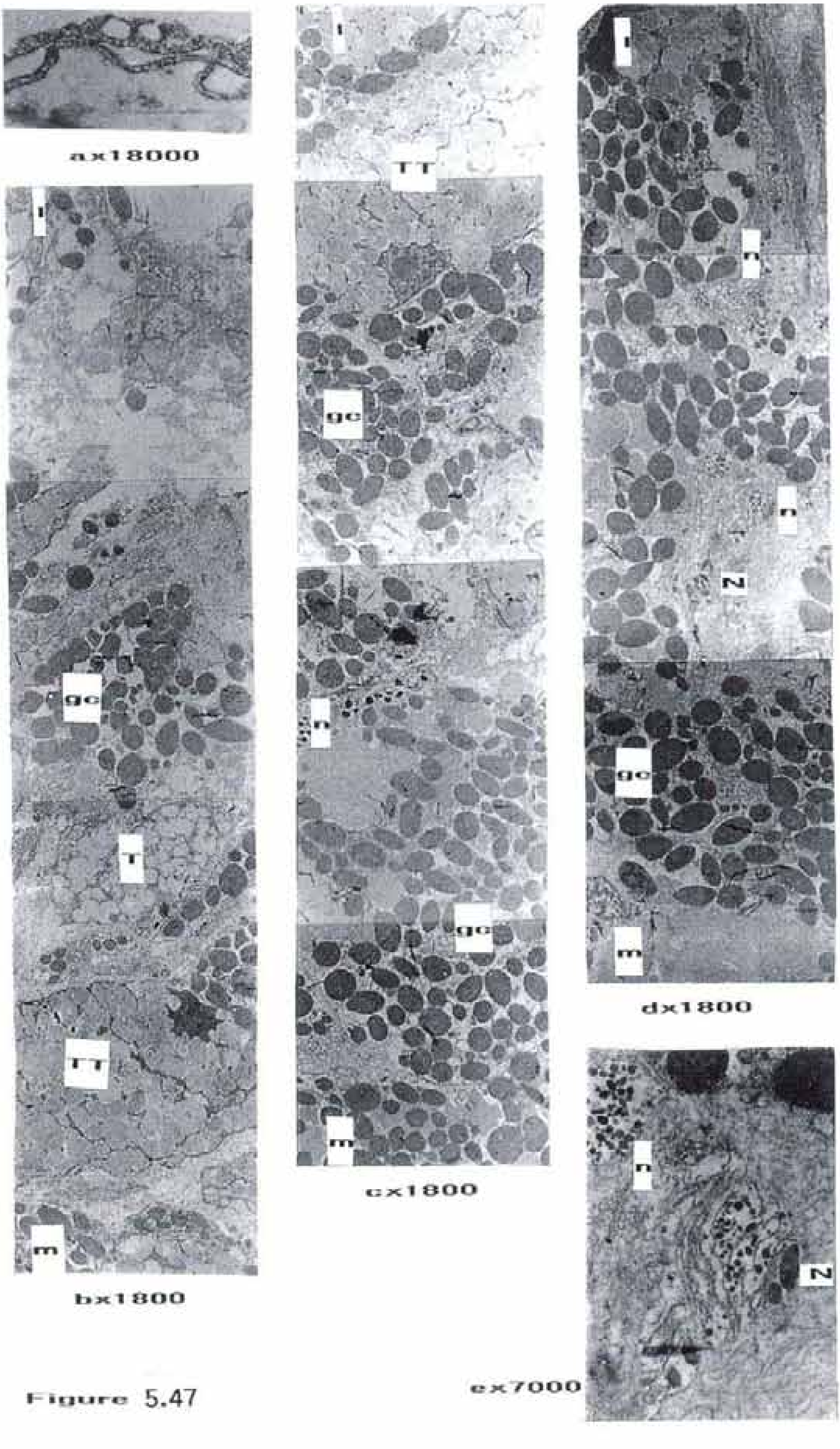

l
ax18000
l
gc
T
TT
m
bx1800
l
TT
gc
n
gc
m
cx1800
l
n
n
N
gc
m
dx1800
n
N
ex7000

Figure 5.47

5.5.1.8.4. Shoulder Region - Acute Inanition.

With inanition for a period of two weeks the morphology of the Shoulder gland alters drastically in that it contracts from about 500 µm in depth to about 100 µm in depth. There are far fewer Trabecular Turquoise Glands and the Granular Cytoplasm Secretory Glands markedly decrease in size both by decrease in size of the granules but more noticeably by a great decrease in the intergranular cytoplasm (Figure 5.48. a c.f. Figure 5.47. b, c and d).

Secreted material from the Shoulder Gland of the starved animal consists largely of disintergrating granules and vesicles from the apical microvilli of the surface epithelium.

FIGURE 5.48. *Pinctada maxima* Shoulder Epithelium and Shoulder Gland in Acute Starvation.

a. T.E.M. x 1800. Shoulder Gland in acute inanition.

b. T.E.M. x 7000. Secretions of Shoulder Gland in inanition.

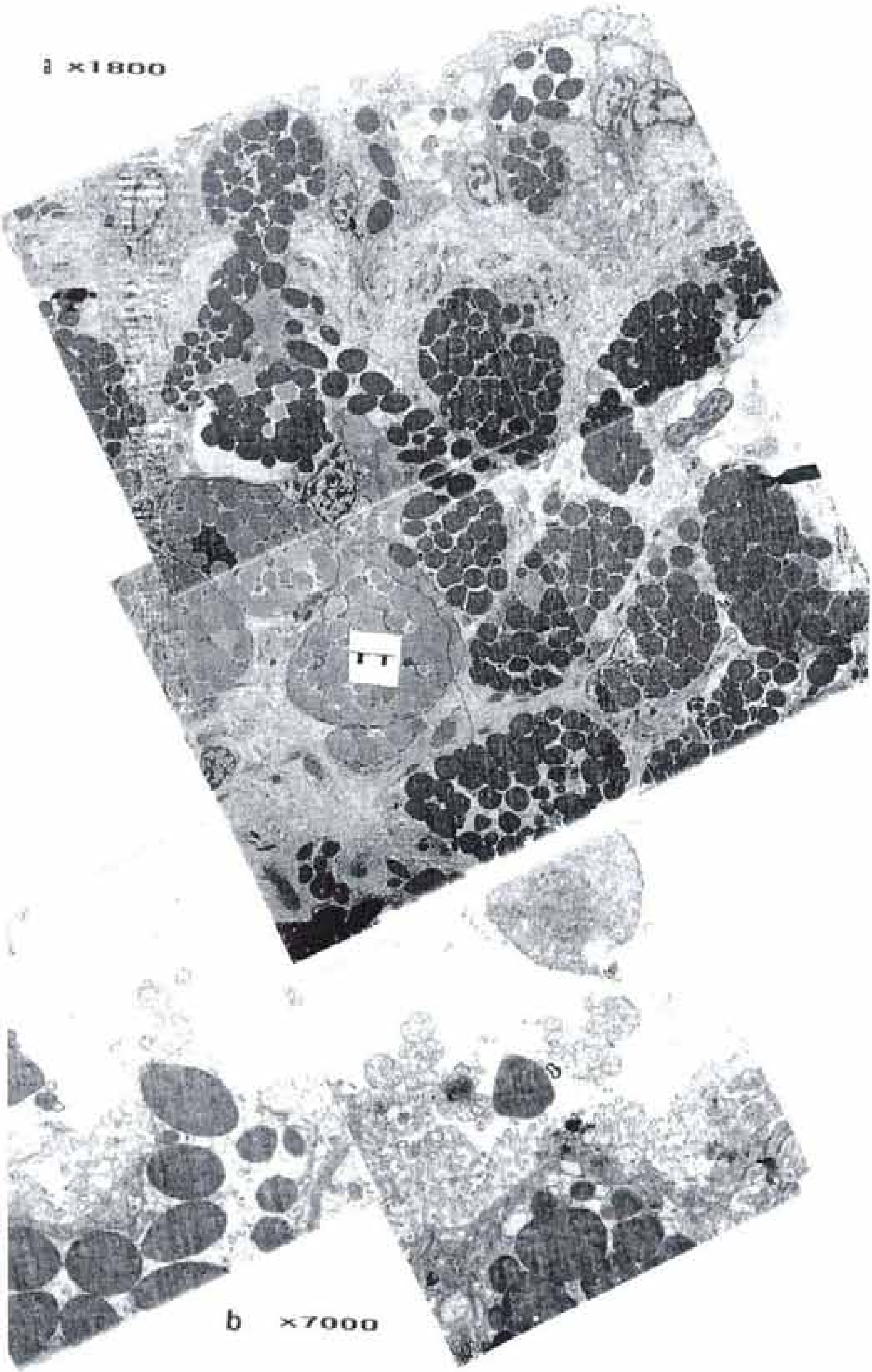

Figure 5.48

5.5.1.8.5. L.M. Pallial Gland.

The Pallial Gland in this species is about 100 µm in thickness. The unicellular glands are Trabecular Turquoise Glands (TT in Figure 5.49. b and c) and several types of Granular Cytoplasm Secretory Glands (1, 2 and 3 in Figure 5.49. a).

A dense fibrous connective tissue separates the bodies of the secretory glands from the surface epithelium and from each other. (c in Figure 5.49. b and c).

FIGURE 5.49. *Pinctada maxima* Pallial Gland.

a. L.M. x Mallorys

b. L.M. x A.B./M.S.B.

c. L.M. x A.B./M.S.B.

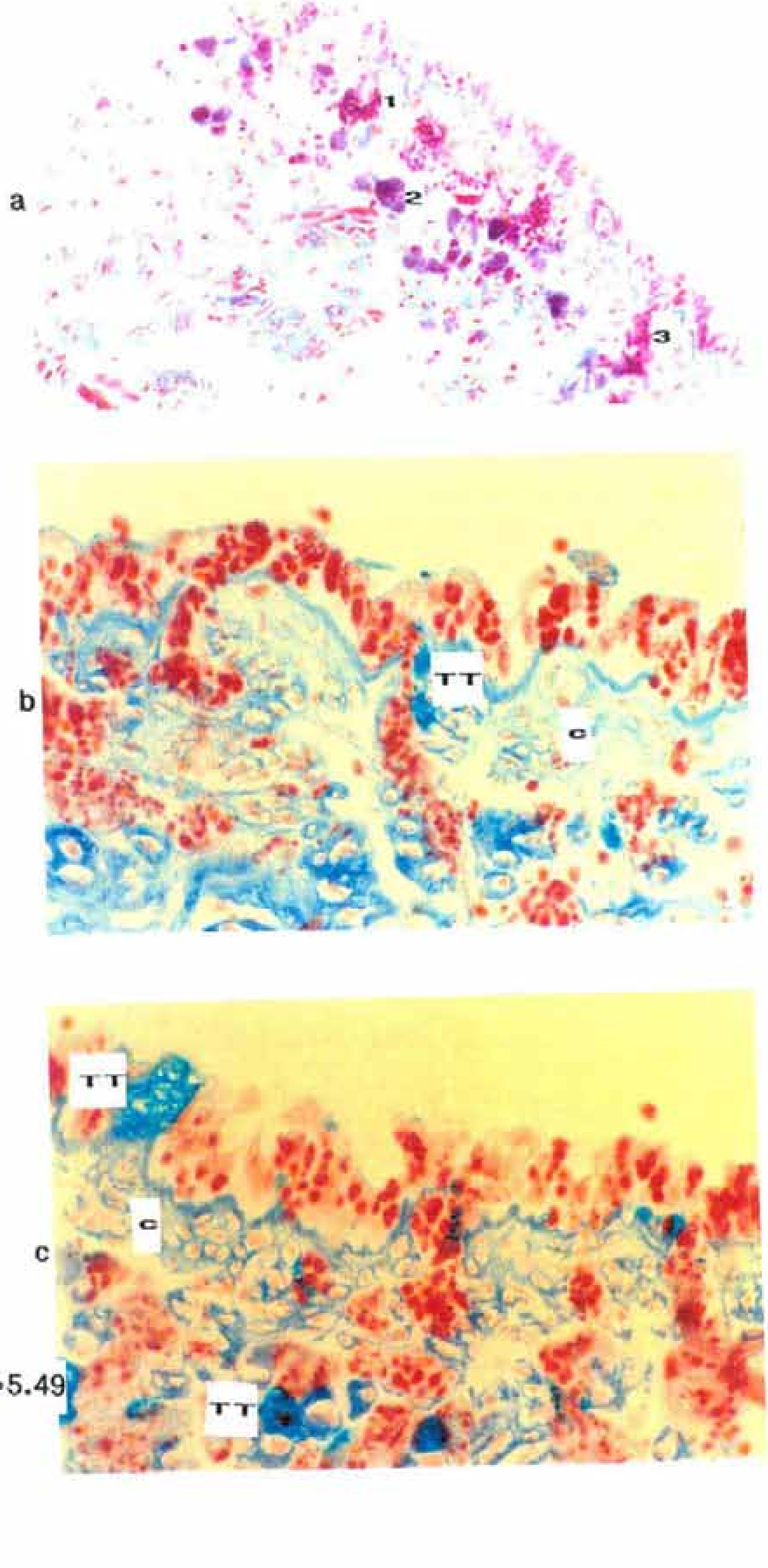

Figure5.49

5.5.1.8.6. T.E.M. Pallial Gland.

The cytoplasm of at least some Trabecular Turquoise Glands of the Pallial Gland is striate especially in that part of the gland near the epithelial surface (TT in Figure 5.50. a and c). Deeper in the Pallial Gland the cytoplasm is the more frequently seen fairly featureless light grey between trabeculi (TTa in Figure 5.50. a).

Nerves with fine spherical neurosecretory granules are commonly seen adjacent to Trabecular Turquoise Glands (n in Figure 5.50. c).

The surface epithelium has microvilli with pronounced terminal vesicles (SV in Figure 5.50. b) which bud off as secreted vesicles (V in Figure 5.50. b).

FIGURE 5.50. *Pinctada maxima* Pallial Gland.

a. T.E.M. x 1800 Glands of the Pallial Gland.

b. T.E.M. x 18000 Secreted Vesicles from Terminal microvilli.

c. T.E.M. x 7000 Neural supply to a Turqoise Gland.

a x1800

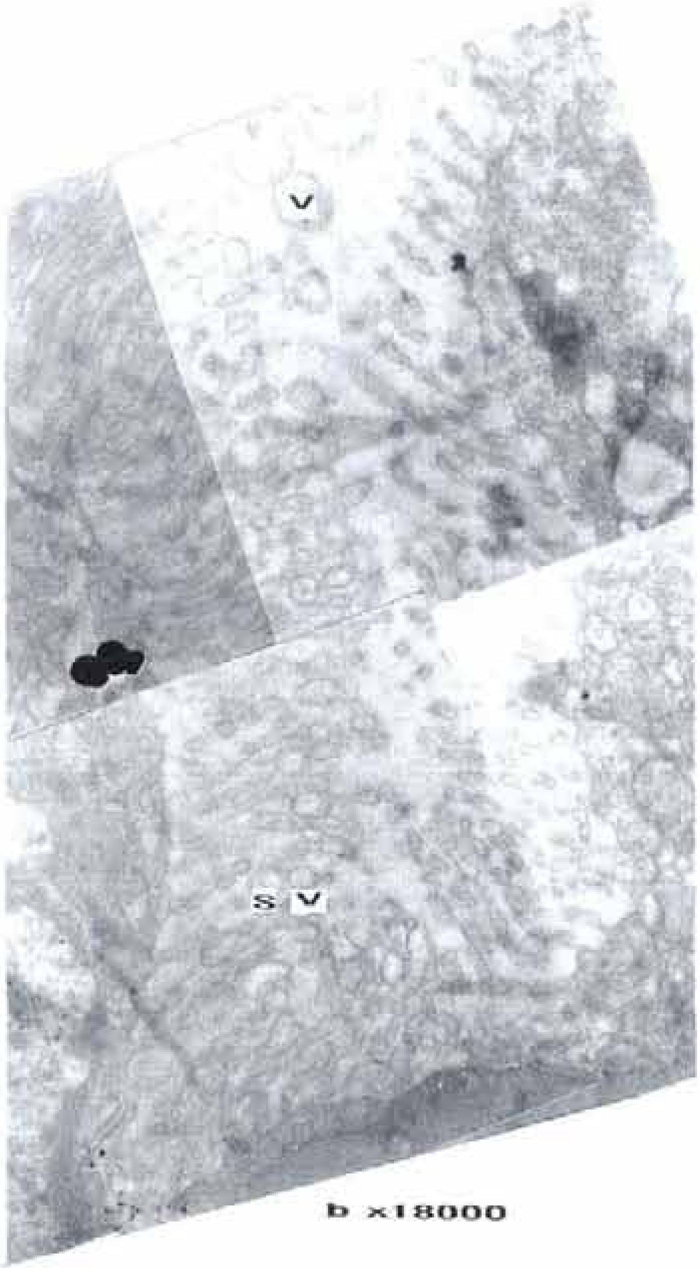

b x18000

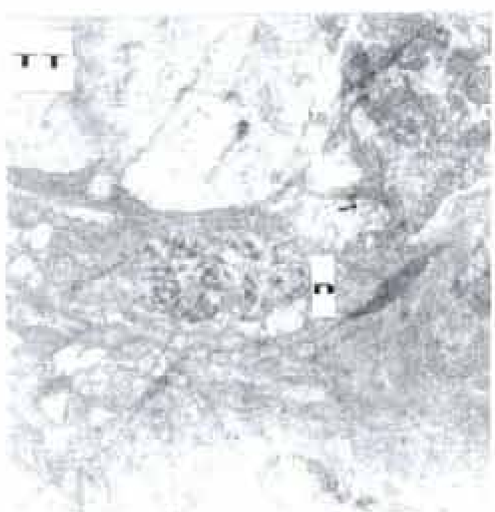

c x7000

Figure 5.50

5.5.1.8.7. T.E.M. T.S. Nerve Trunk Pallial Region.

Relatively large nerves run in the fibrous connective tissue between the secretory structures of the External Mantle and the underlying musculature. Relatively large neurosecretory granules are concentrated in places near the periphery of the nerve trunk and in nerve branches (G in Figure 5.51.). There are concentration of very small neurosecretory granules in nerve fibres within the nerve trunk (ng in Figure 5.51.).

The nerve trunk is surrounded by a sheath (S in Figure 5.51.) with specialised sheath cells with flattened nuclei (Figure 5.51. c) lying against its outer surface.

FIGURE 5.51. *Pinctada maxima* Nerve Trunk in Pallial Gland.
T.E.M. x 6000

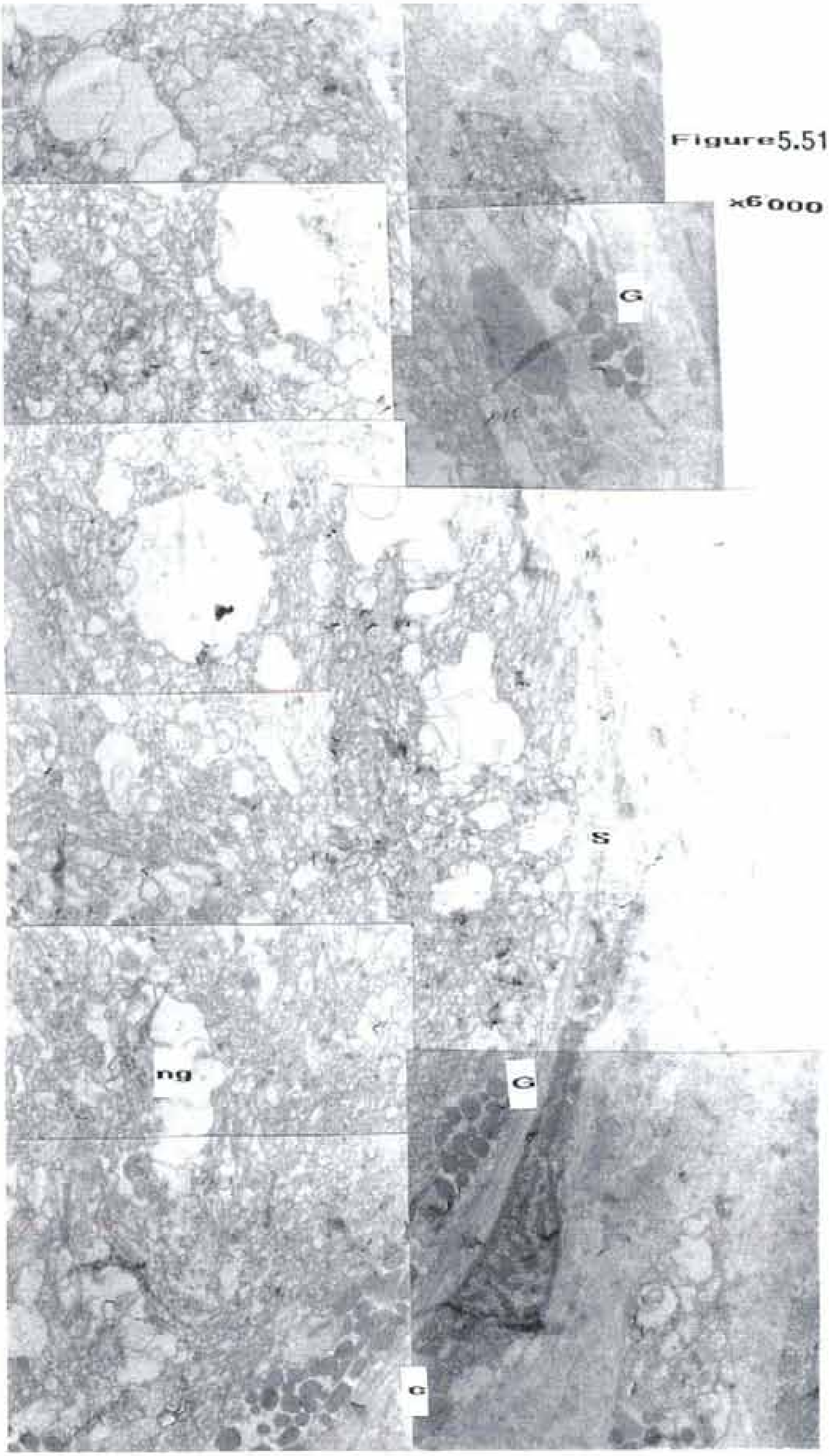

Figure 5.51

x6000

5.5.1.8.8. L.M. Proximal, Middle and Distal Ventral Pallial Regions.

The Proximal Pallial Region has a columnar epithelium. This is commonly disrupted by ovoid shapes of the intraepithelial part of Turquoise Glands. Since these appear considerably more commonly than subepithelial Trabecular Turquoise Glands it seem likely that many of them are wholly intraepithelial. Trabecular Turquoise Glands do not stain with Mallorys and hence appear as open spaces with whispy trabeculae (TT in Figure 5.52. a). Granular Cytoplasm Secretory Glands are rare.

Middle Pallial epithelium is like the Proximal Pallial Epithelium but there is a small increase in numbers of both Trabecular Turquoise Glands and Granular Cytoplasm Secretory Glands (G in Figure 5.52. b). Again for the reasons given above it appears that these are two populations of Trabecular Turquoise Gland one of which is wholly intraepithelial (TT in Figure 5.52. b). The Distal Pallial Epithelium has a stronger and deeper fibrous connective tissue than the other Pallial Regions (Figure 5.52. c). There is a further increase in secretory glands especially Trabecular Turquoise Glands of both intraepithelial and subepithelial types to the extent that they largely obscure the structure of the Pallial epithelium (Figure 5.52. c TT).

At its distal part the Distal Pallial Region fibrous connective tissue becomes shallower and the density of Trabecular Turquoise Glands decreases (Figure 5.52. d). Secretion from the Turquoise Glands form sheets of secretory material which entrap secreted granules from the other secretory glands (s in Figure 5.52. d).

FIGURE 5.52. *Pinctada maxima* Proximal Middle and Distal Ventral Pallial Regions.

a. L.M. x 460 Mallorys Proximal Pallial Region.

b. L.M. x 770 A.B./M.S.B. Middle Pallial Region.

c. L.M. x 770 A.B./M.S.B. Distal Pallial Region.

d. L.M. x 770 A.B./M.S.B. Distal part of Distal Pallial Region.

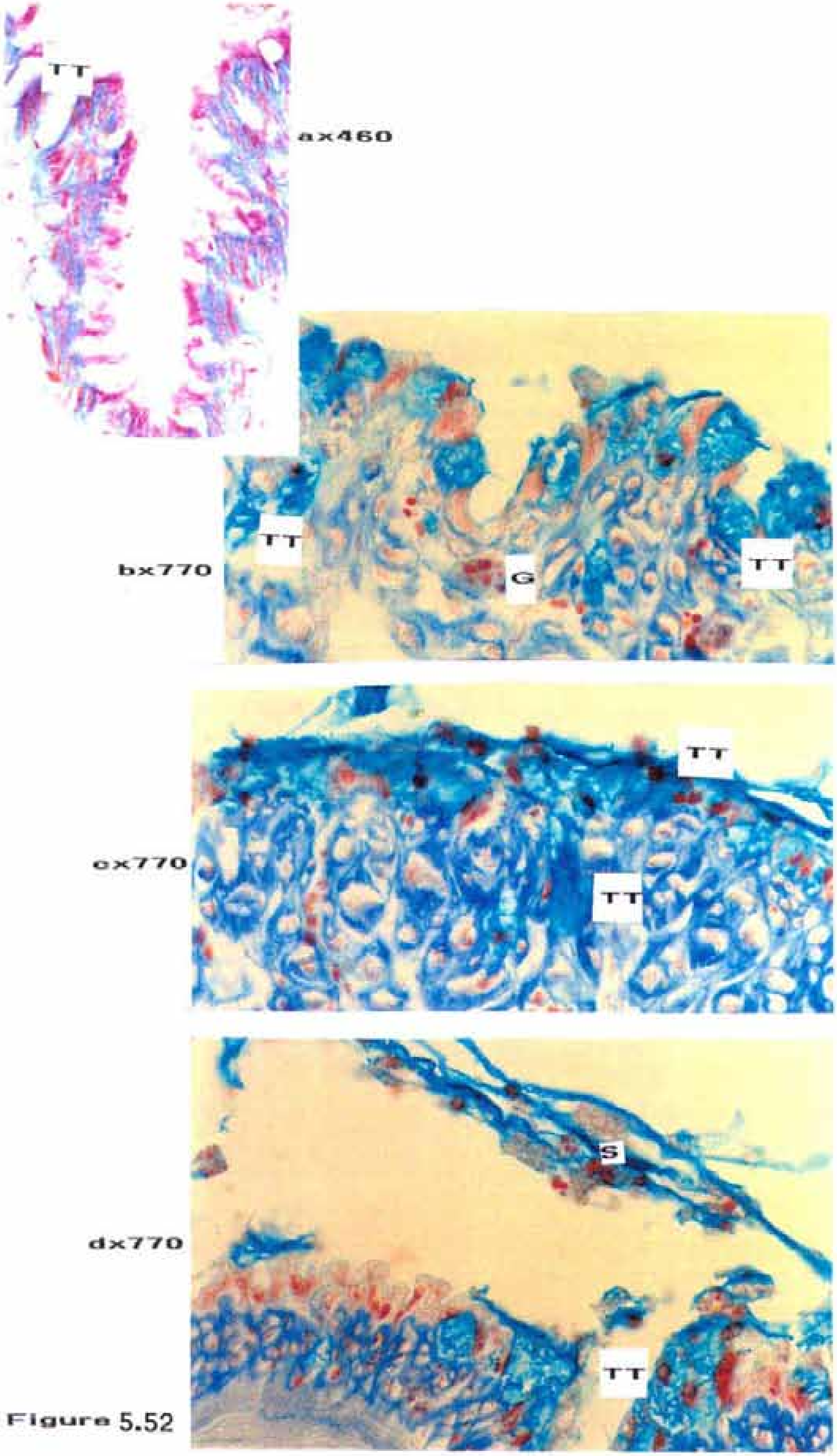

Figure 5.52

5.5.1.8.9. Middle Ventral Pallial Region.

With T.E.M. the striate nature of the cytoplasm of an intraepithelial Trabecular Turquoise Gland is shown (Figure 5.53. TT). The nucleus of the Turquoise Gland is moulded to the positions of the cytoplasmic trabeculae (Figure 5.53. n). Adjoining the Trabecular Turquoise Gland is the nucleus of a surface columnar epithelial cell (Figure 5.53. nu).

Fine and coarse neurosecretory granules occur in nerves supplying the secretory tissues (ng in Figure 5.53.).

FIGURE 5.53. *Pinctada maxima* Middle Ventral Pallial Region.
T.E.M. x 8500. Secretory Glands and their nerve supply.

Figure 5.53

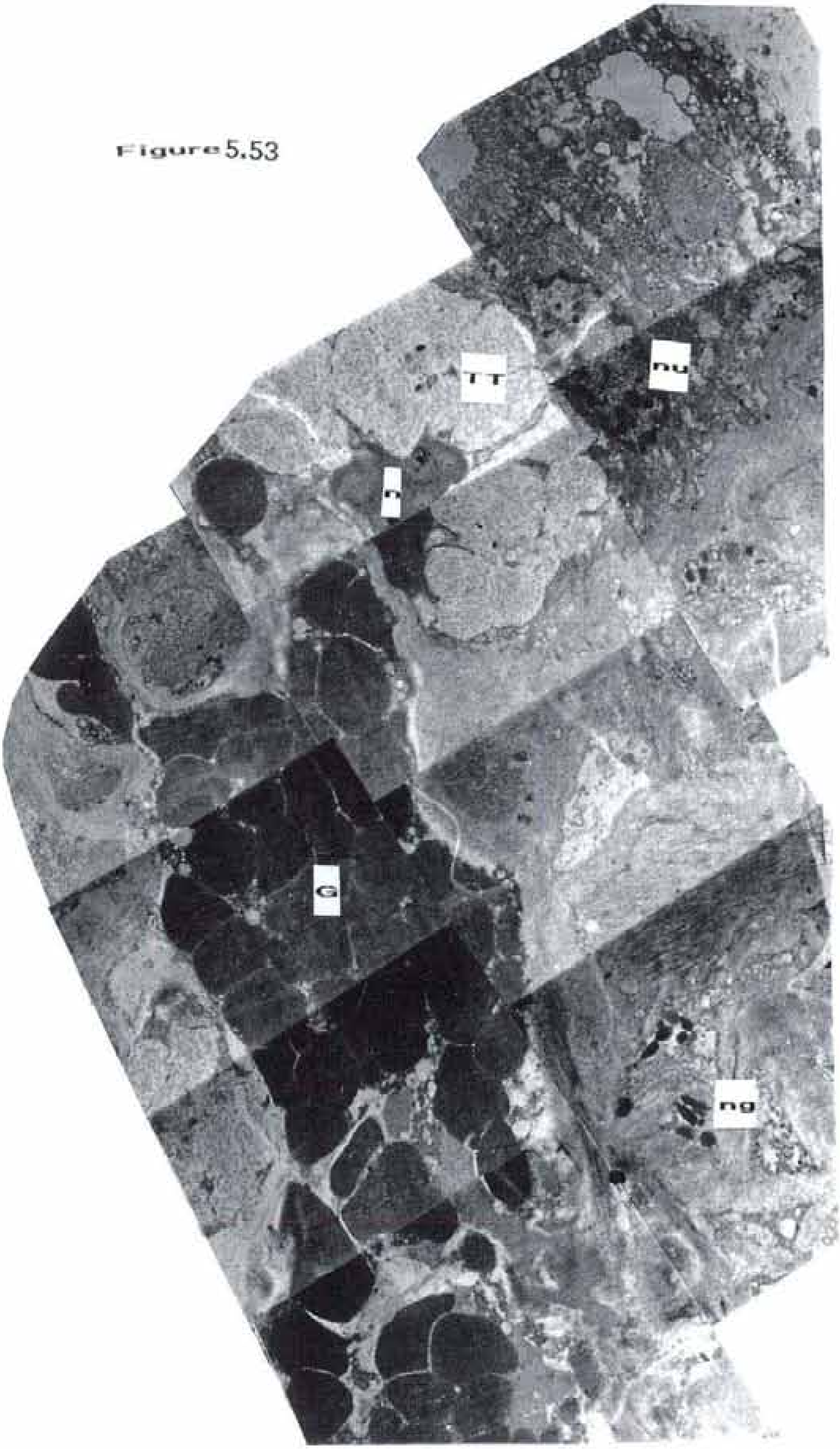

5.5.1.8.10. Distal Folded Region.

A surface eptiehlium of columnar cells with secretory apical microvilli covers the Distal Folded Region. Here the dense subepithelial fibrous connective tissue is much reduced relative to the Pallial Regions (f in Figure 5.54. b). There is also a reduction of intraeptiehlial Trabecular Turquoise Glands but an increase in Granular Cytoplasm Secretory Glands (TT and G respectively in Figure 5.54. a and b). There is a complex of subepithelial sinus (S in Figure 5.54. b).

FIGURE 5.54. *Pinclada maxima* Distal Folded Region.

a. L.M. x 770 A.B./M.S.B. Epithelium and Subepithelium Glands.

b. L.M. x 770 A.B./M.S.B. Epithelium and Subepithelium Glands and Sinus.

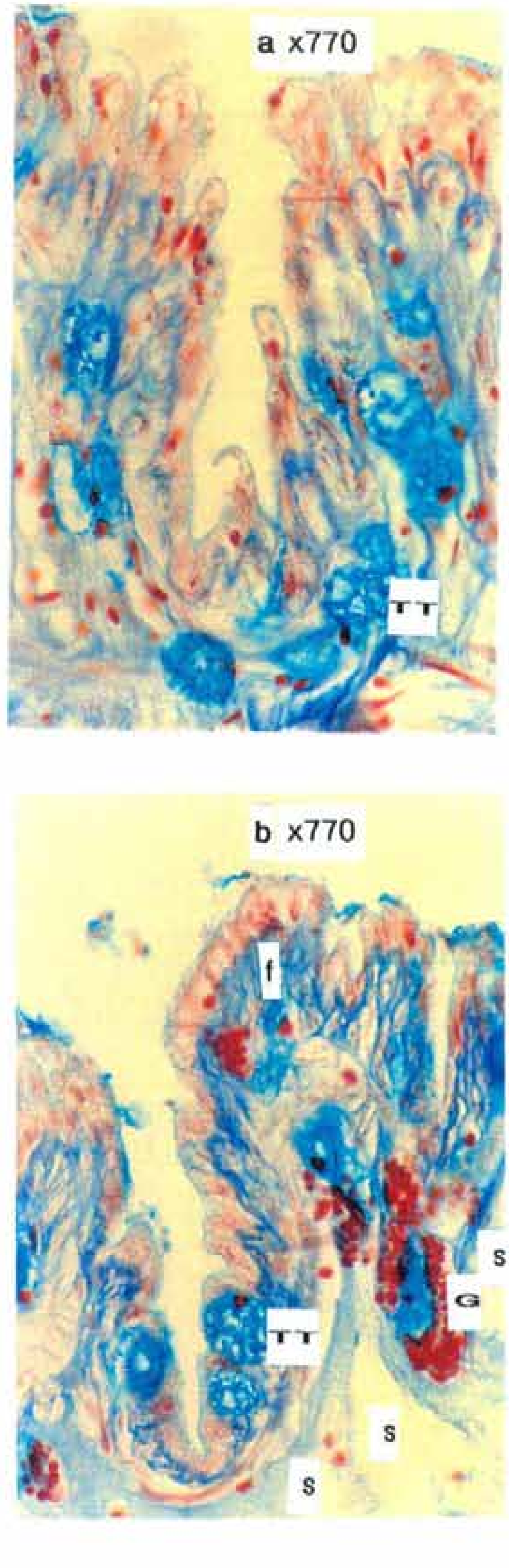

Figure5.54

5.5.1.8.11. Distal Folded Region.

The pronounced foldings of this Region are lined externally by elongate apical microvilli, (e in Figure 5.55. a and d).

As well as Trabecular Turquoise Glands and a variety of large granuled Granular Cytoplasm Secretory Glands (TT and G in Figure 5.55. a, b and c) characteristic of this area is a species of secretory gland with evenly sized small spherical granules (S in Figure 5.55. a, b and c).

These latter occur both in the subepithelium and intraepithelially (S in Figure 5.55. a).

The subapical cytoplasm of the surface epithelium displays numerous vesicles, membranous structures and mitochondria, (V, f and m in Figure 5.55. d).

FIGURE 5.55. *Pinctada maxima* Secretory Structures of Distal Folded Epithelium.

a. T.E.M. x 1800 Secretory Structures of surface infolding.

b. T.E.M. x 1800 Unicellular Secretory Glands.

c. T.E.M. x 1800 As for b. above.

d. T.E.M. x 7000 Ultrastructure of surface epithelial cells.

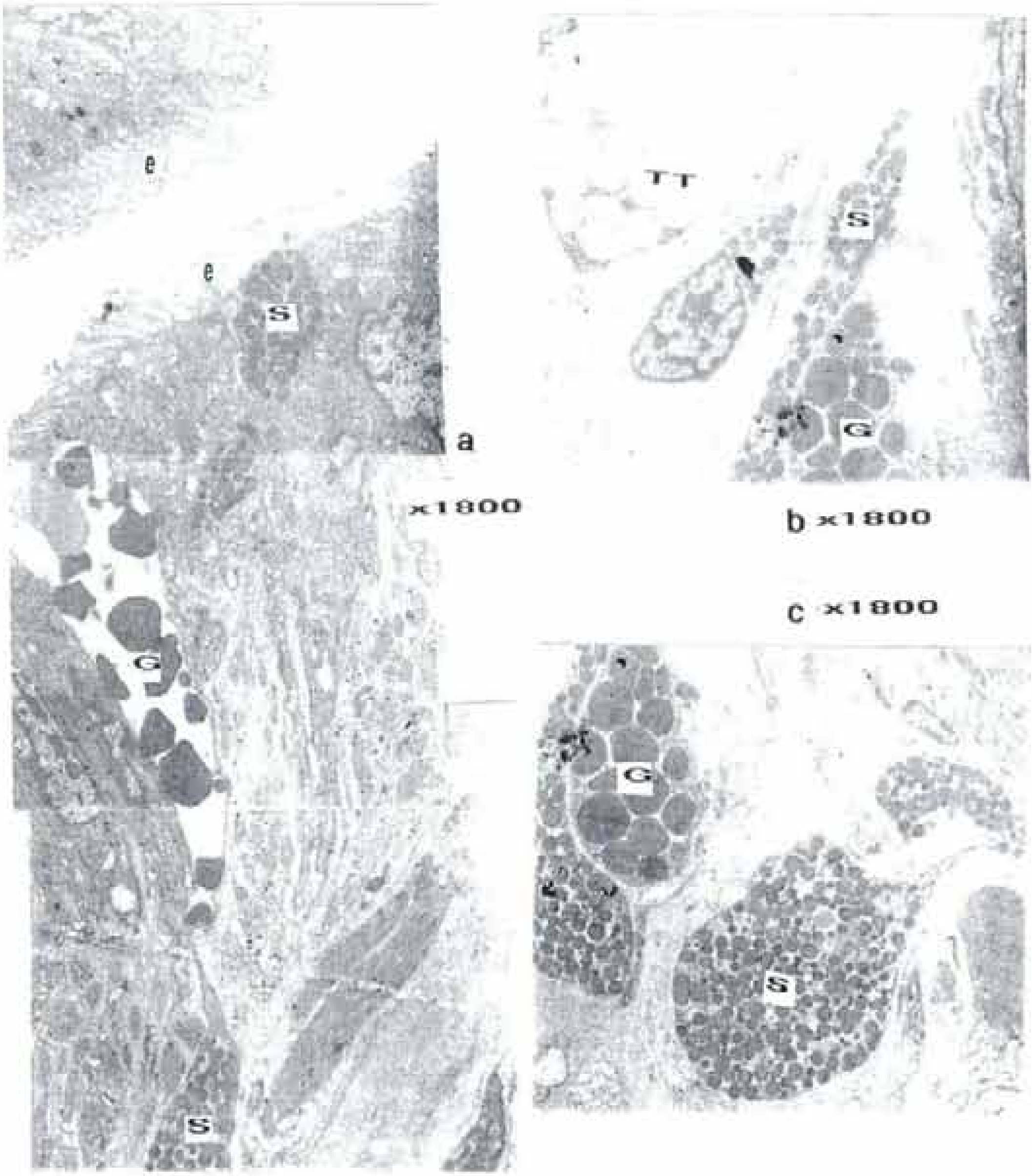

Figure 5.55

d ×7000

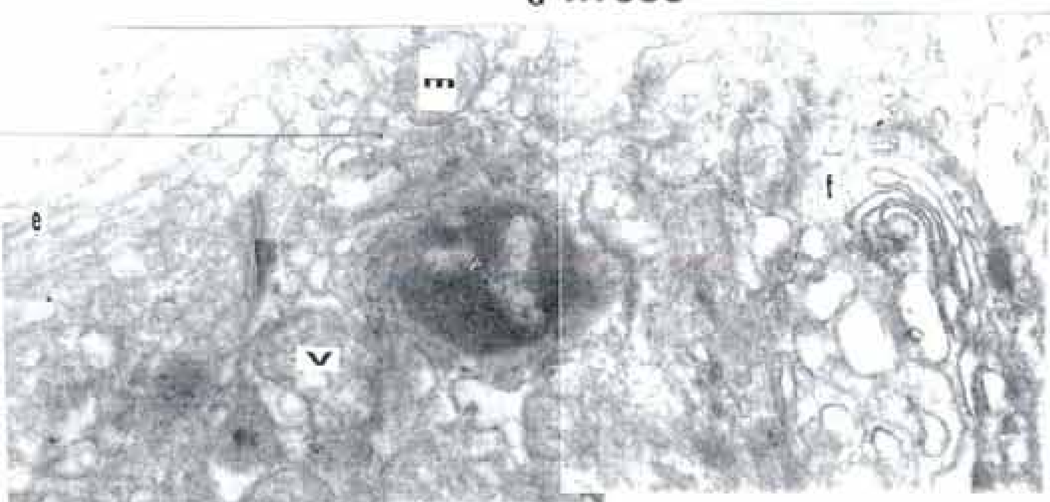

5.5.1.8.12. Glands and Secreted Material Distal Folded Region.

Secreted from the Distal Folded Region are bodies which appear striate in section, are often adjacent in the tissue with Trabecular Turquoise Glands, and usually display electron dense granules (b in Figure 5.56. a, b, c, e and f).

They are of the same order of magnitude as the intra-trabecular segments of the cytoplasm of the Turquoise Glands (Figure 5.56. a and e), which in this location are also striate (Figure 5.56. b and d).

They sometimes have associated mitochondria which also occur on the trabeculae of Trabecular Turquoise Glands (m in Figure 5.56. c).

They appear to unravel following secretion. (Figure 5.56. f).

FIGURE 5.56. *Pinctada maxima* Striate Secretory Bodies of Distal Folded Region.

a. T.E.M. x 3500 Striate bodies adjoining Trabecular Turquoise Glands.

b. T.E.M. x 18000 Higher magnification of striate body in a.

c. T.E.M. x 18000 Mitochondria associated with striate body in a.

d. T.E.M. x 18000 Striate cytoplasm of Trabecular Turqoise Gland and nucleus of epithelial cell - Higher magnification of a.

e. T.E.M. x 3500 Trabecular Turqoise Gland and striate bodies.

f. T.E.M. x 18000 Unravelling secreted striiate bodies.

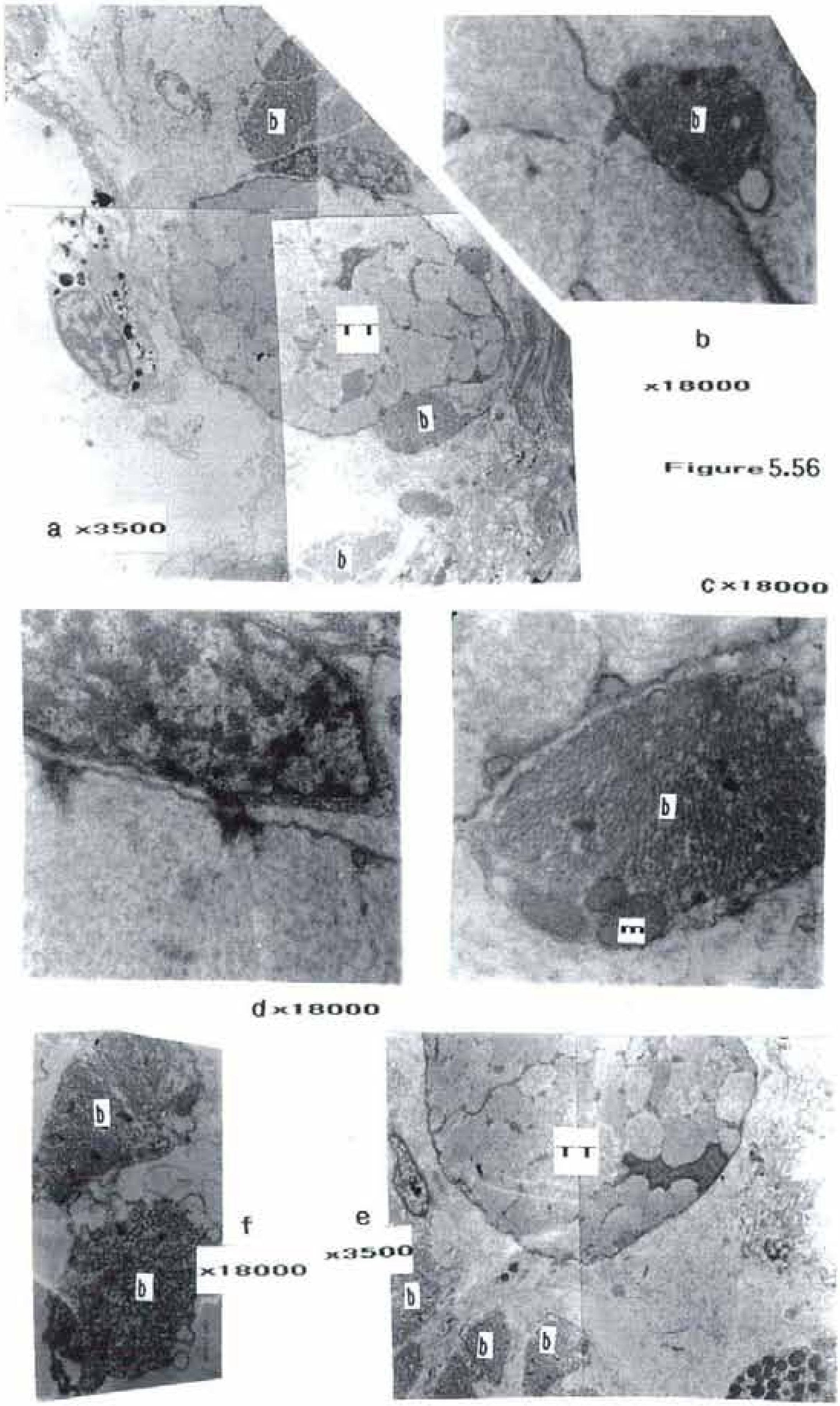

Figure 5.56

5.1.9. L.M. and T.E.M. of Mantle Margin.

5.1.9.1. LatF1..

The secretion produced by Proximal LatF1. consists of a fine vesiculate secretion from swollen ends of apical microvilli, and the products of the unicellular glands including cytoplasmic granules (V and G respectively in Figure 5.57. a).

The Trabecular Turquoise Glands and the species of unicellular secretory gland with small spherical cytoplasmic granules seen in the Distal Folded Epithelium persist in the Proximal LatF1. (TT and S in Figure 5.57. b).

The Mantle Edge Gland (Middle LatF1.) consists of elongate columnar epithelial cells, is almost devoid of unicellular secretory Glands and generates a secretion consisting almost exclusively of vesicles from the swollen ends of surface epithelial apical microvilli (V in Figure 5.57. c and d).

The Terminal F1. epithelium (i.e., Distal LatF1.) is an unremarkable columnar epithelium (T in Figure 5.57. e). A few of the small Trabecular Turquoise Glands (TT in Figure 5.57. e) discharge through it, but most of the Ovoid Blue Glands (obg in Figure 5.57. e) and the other unicellular glands of Terminal F1. discharge through Distal MedF1..

FIGURE 5.57. *Pinctada maxima* LatF1..

a. T.E.M. x 3500 Proximal LatF1.

b. T.E.M. x 3500 Proximal Middle LatF1.

c. T.E.M. x 1800 Mantle Edge Gland (Middle LatF1.)

d. L.M. x 770 Mantle Edge Glands (Middle LatF1.)

e. L.M. x 770 Terminal F1. (Distal LatF1.).

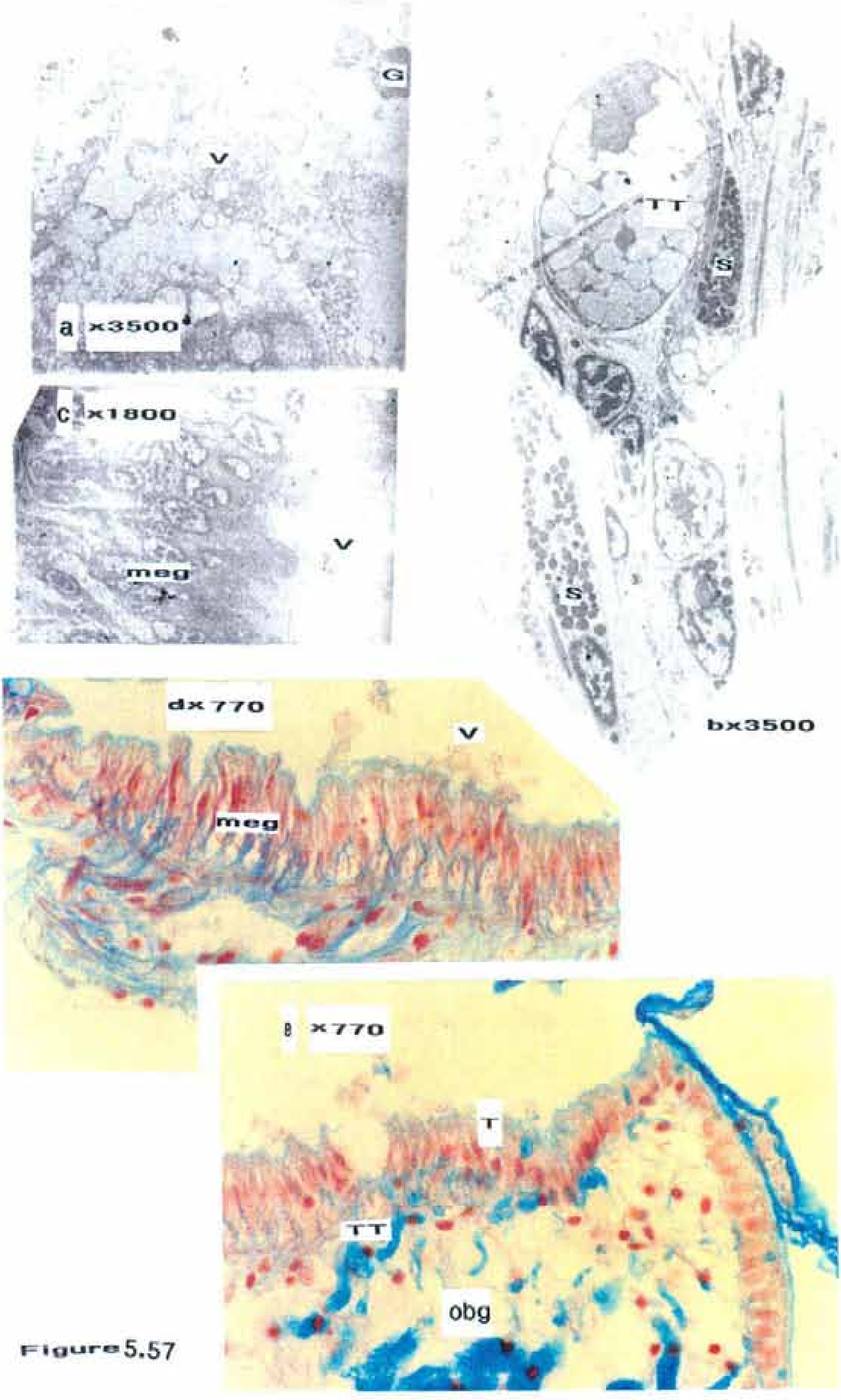

Figure 5.57

5.5.1.9.2. Terminal LatFl. and Ovoid Blue Glands.

The Terminal Epithelium of Distal LatFl. (T in Figure 5.58. a and b) bears apical microvilli. Very small Trabecular Turquoise Glands lie intraepithelially or just beneath the Basement Membrane and secrete laterally (TT in Figure 5.58. b).

Ovoid Blue Glands and Granular Cytoplasm Secretory Glands lie in the Terminal Fl. parenchyma and secrete through Distal MedFl. (obg and G respectively in Figure 5.58. a and b).

FIGURE 5.58. *Pinctada maxima* Terminal LatFl. and Ovoid Blue Glands.
a. T.E.M. x 1800 Terminal Epithelium and Ovoid Blue Glands and other

unicellular secretory glands of Terminal Fl..

b. T.E.M. x 1800 As for a. above.

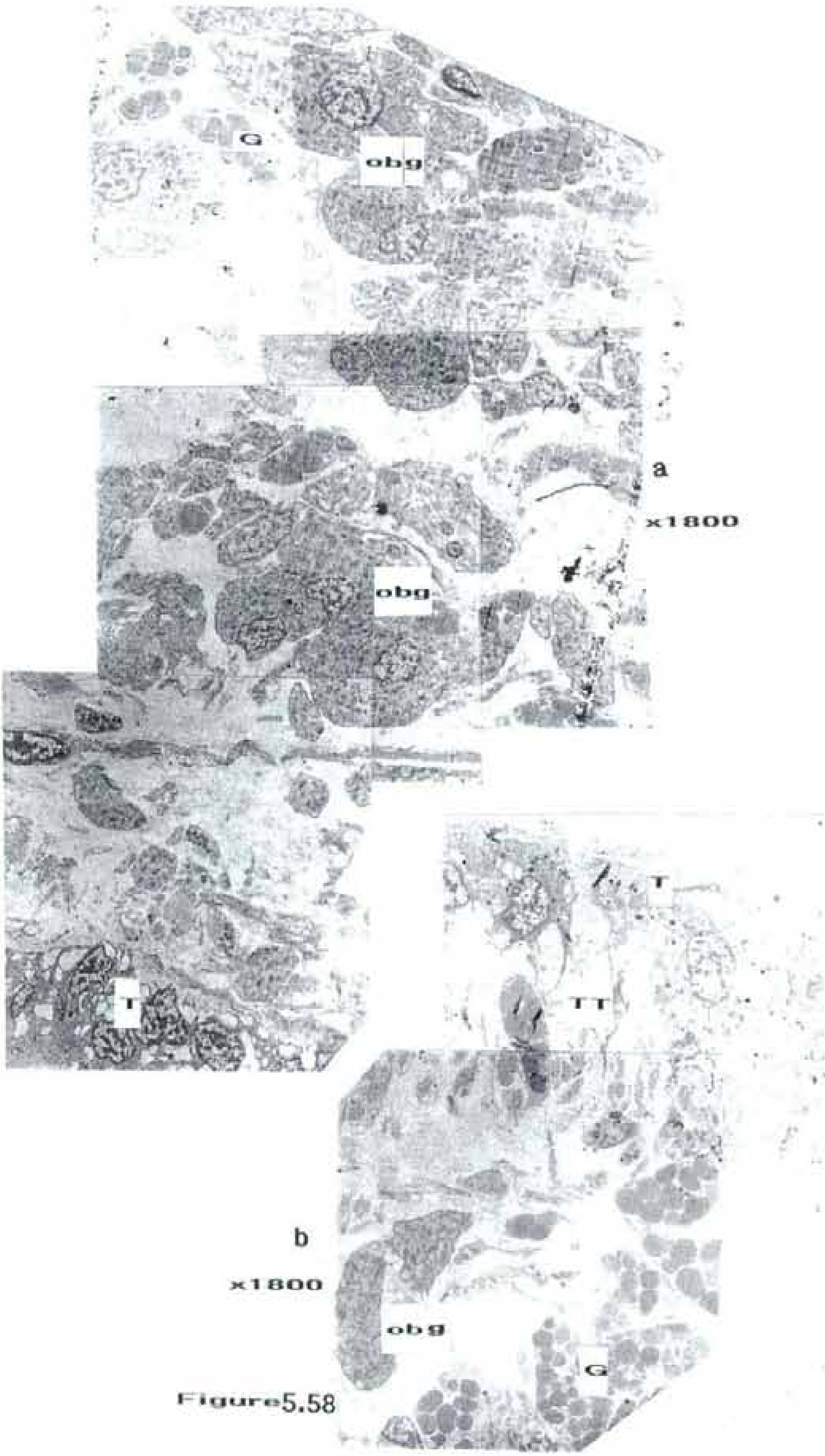

Figure5.58

5.5.1.9.3. Distal Middle and Proximal MedF1..

Distal MedF1. (Figure 5.59. a and b) has a low columnar surface epithelium with a relatively insignificant subepithelial connective tissue.

The population of unicellular glands in the parenchyma varies from place to place around the periphery. However there are two species of glands nearly unique to this location and nearly ubiquitously present in all radial sections studied. They are the Ovoid Blue Glands (obg in Figure 5.59. a) and the Distal Diffuse Glands (DD in Figure 5.59. b). Both discharge via fine tubular structures through the Distal MedF1. epithelium. The Distal Diffuse Glands in this species stain amber with Mallorys, khaki with M.S.B., claret red with Azan, gold khaki with A.B./M.S.B. (Figure 5.59. b) and liverish grey with Steedmans.

The Middle MedF1. bears a columnar epithelium which is characteristically formed into short plateaux divided by narrow vee shaped infoldings (I in Figure 5.59. c). There is a dense subepithelial fibrous connective tissue in which the circular muscle fibres (cm in Figure 5.59. c) lie in lacunae (L in Figure 5.59. c). The subepithelium bears Trabecular Turquoise Glands and Granular Cytoplasm Secretory Glands which vary with the position on the periphery (TT and G respectively in Figure 5.59. c).

The Proximal MedF1. has a strong columnar epithelium (e in Figure 5.59. d), a less conspicuous subepithelial connective tissue and the circular musculature which is shallow to a stronger radial musculature, (cm and rm respectively cf Figure 5.59. d), is separated from the Basement Membrane of the surface epithelium by diffuse fibrous connective tissue (Figure 5.59. d). There is an increase in number and size of Trabecular Turquoise Glands compared with the rest of MedF1. (TT in Figure 5.59.).

A secretion which stains turquoise with A.B./M.S.B. (S in Figure 5.59. d) is codntributed to by the secretory structures of MedF1. and lies between the surface epithelium and the Pleated Secretion of Groove F1F2. (e and P respectively in Figure 5.59. d).

FIGURE 5.59. *Pinctada maxima* MedFl..

a. L.M. x 770 Distal MedFl. near Terminal Fl..

b. L.M. x 770 Distal MedFl. proximal to a.

c. L.M. x 770 Middle MedFl..

d. L.M. x 770 Proximal MedFl..

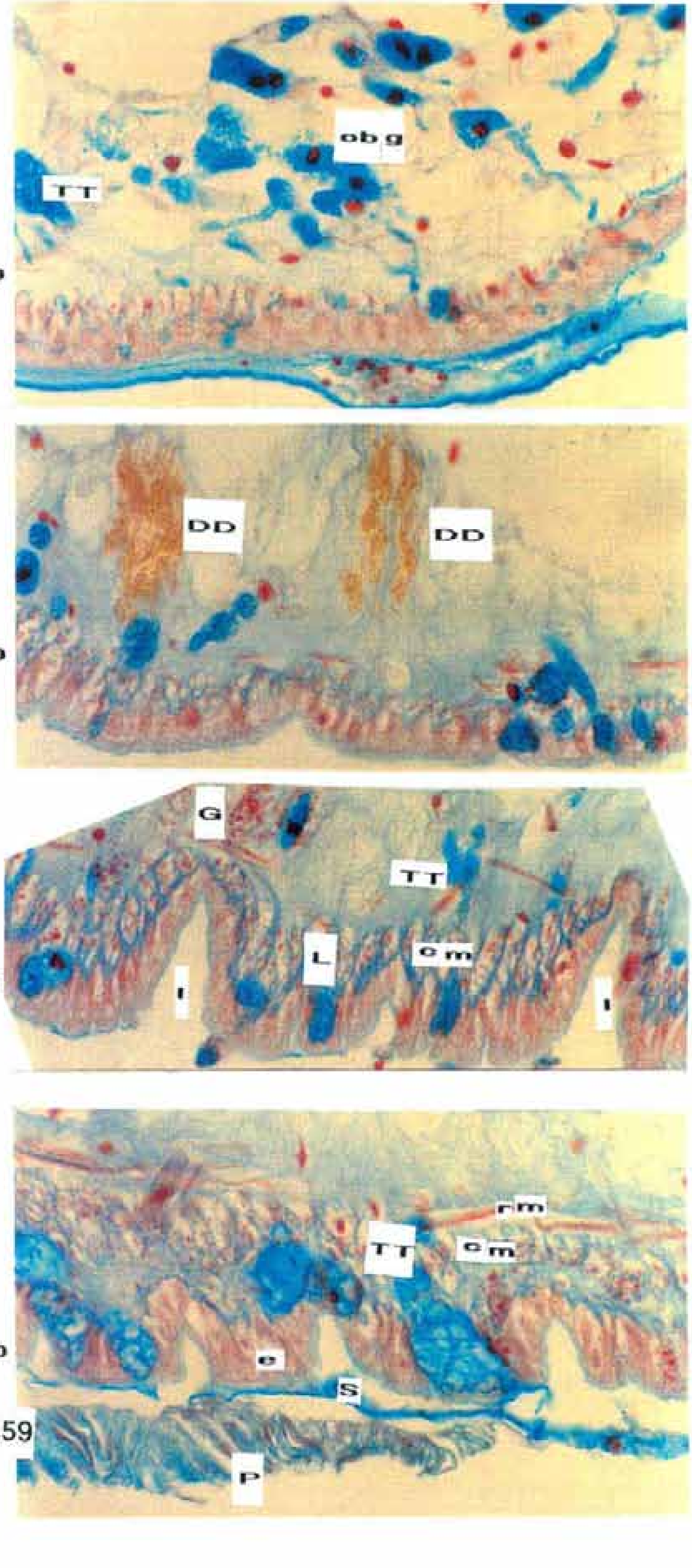

a

× 770

b

× 770

c

× 770

d

× 770

Figure5.59

5.5.1.9.4 Distal Middle and Proximal MedF1..

T.E.M. shows that the entire surface epithelium of MedF1. Proximal, Middle and Distal, (Figure 5.60. a, b and c respectively), bears apical microvilli.

Ovoid Blue Glands secrete into Distal and Middle MedF1. (Figure 5.60. a and b respectively). They are rare in the latter location.

The apical cytoplasm of the surface epithelium is highly vesiculate (a in Figure 5.60. a, b and c).

Granular Cytoplasm Secretory Glands and more common proximally Trabecular Turquoise Glands lie in the subepithelium and secrete into Groove F1F2. (Figure 5.60. a, b and c).

FIGURE 5.60. *Pinctada maxima* Distal Middle and Proximal MedF1..

a. T.E.M. x 1800 Ovoid Blue Glands and other unicellular glands of Distal MedF1..

b. T.E.M. x 1800 Ovoid Blue Glands and other unicellular glands of Middle MedF1..

c. T.E.M. x 1800 Epithelium and Trabecular Turquoise Glands of Proximal MedF1..

a ×1800

Figure 5.60

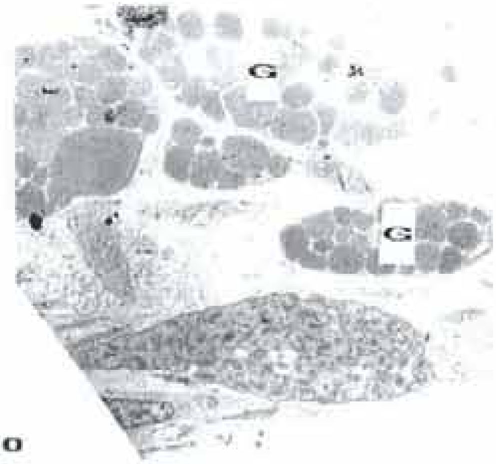

b ×1800

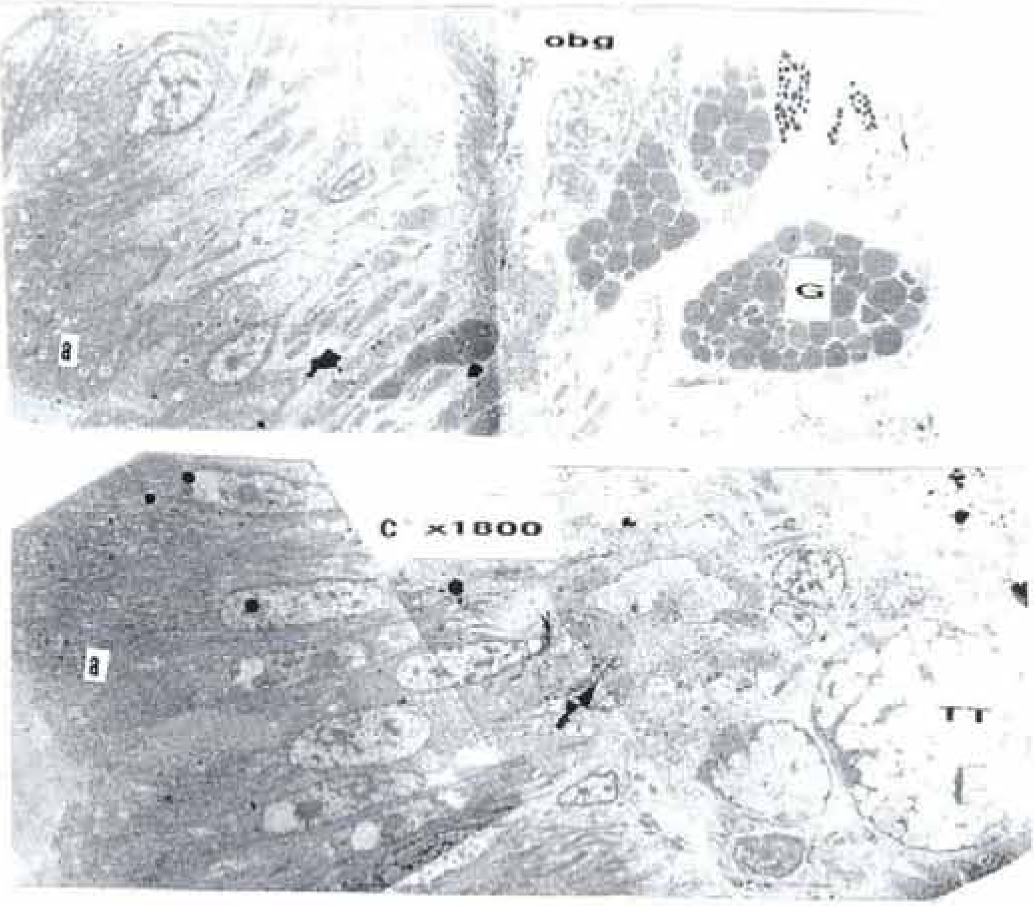

c ×1800

5.5.1.9.5. Apical Groove F1F2.

Figure 5.61. illustrates many of the histological features of this Region. Proximal to the Proximal MedF1. (PMF1. in Figure 5.61.) the Omega Gland (O in Figure 5.61.) occupies the lateral surface of the apex. The distal part of the Omega Gland (d in Figure 5.61.) encloses unicellular secretory glands usually including large Trabecular Turquoise Glands (TT in Figure 5.61.). The proximal part of the Omega Gland appears to be a truly stratified epithelium. The outer surface is composed of Celtic Scroll Cells (c in Figure 5.61.). Deep to these are the Multivesiculate Cells (mv in Figure 5.61.). From the Apical Channel (A in Figure 5.61.) issues the Pleated Secretion of Groove F1F2., (P in Figure 5.61.).

The Omega Gland Cells are opposed across the Apical Channel by the Dactylocytes (D in Figure 5.61.). These are elongate specialised columnar cells and have elongate centrally placed nuclei. They stain pink with A.B./M.S.B. Medial to them, and also elongate columnar cells in this species, are the Black Granule Secretory Cells (b in Figure 5.61.). These have rounded basal nuclei and stain greenish with A.B./M.S.B. Distal to these are the epithelium and subepithelial glands of Proximal LatF2. (PLF2. in Figure 5.61.).

The epithelial structures of Apical Groove F1F2. are underlain by the strong dense Subapical Connective Tissue (sct in Figure 5.61.). A branch of the Circum-pallial Nerve, (n in Figure 5.61.), runs beneath the musculature which underlies the Subapical Connective Tissue .

FIGURE 5.61. *Pinctada maxima* Apical Groove F1F2..
L.M. x 770 A.B./M.S.B.. Epithelia, secretory structures, fibrous tissues and nerves.

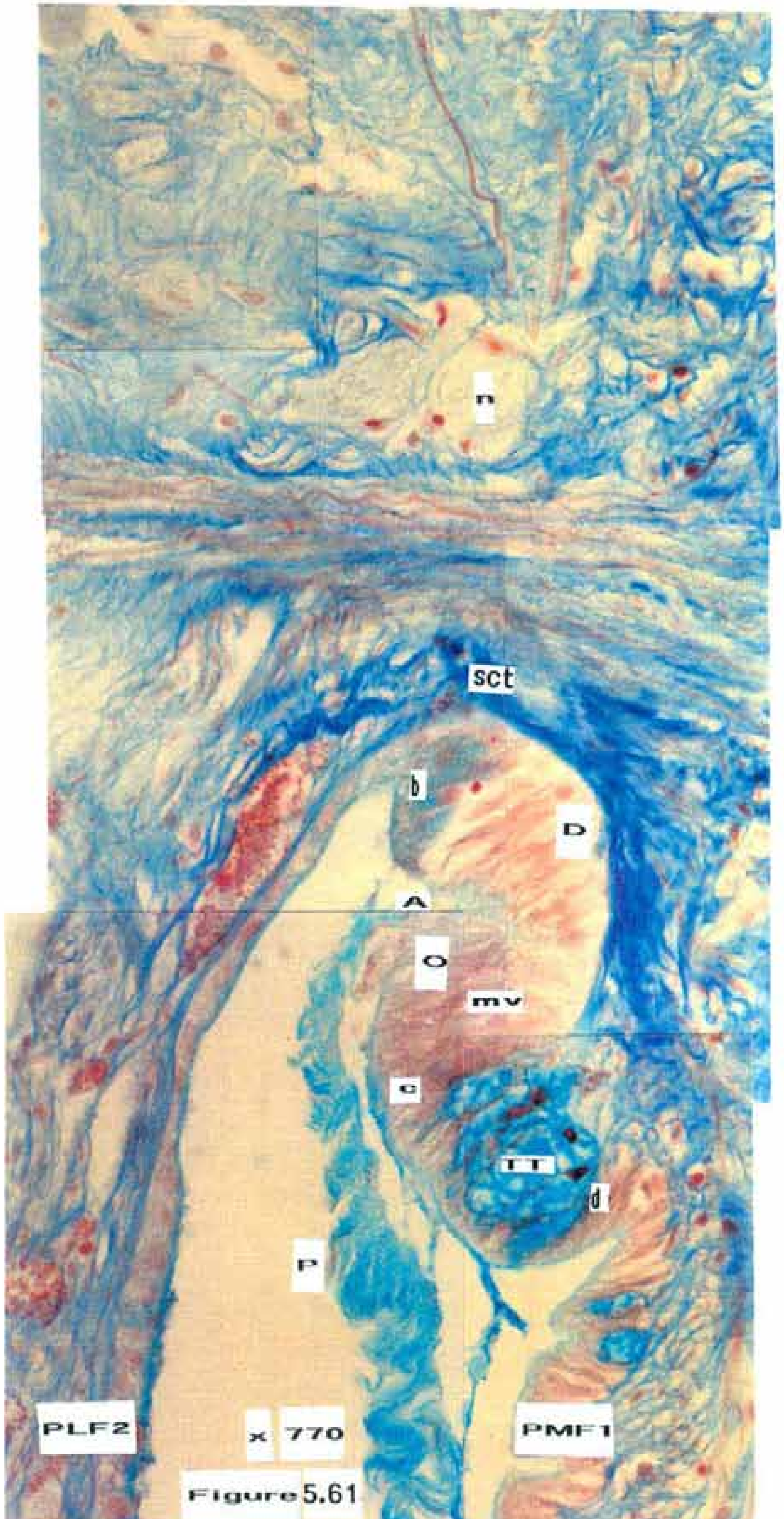

Figure 5.61

5.5.1.9.6. Apical Groove F1F2., Circum-pallial Nerve, Circum-pallial Sinus.

The cells of Apical Groove F1F2. may be further differentiated by Azan staining.

Here the Celtic Scroll Cells (c in Figure 5.62.) have an amber nucleus with a vacuolar and greenish tinged cytoplasm whereas the Multivesiculate Cells have purple staining nuclei and amber cytoplasm (mv in Figure 5.62.).

Similarly, the amber staining Dactylocytes are clearly differentiated from the purple staining Black Granule Secretory Cells (D and b in Figure 5.62. respectively.

Branches of the Circum-pallial Nerve innervate the secretory structures of the entire Mantle Margin. Nucleated cells occur in the body of this nerve (n in Figure 5.62. b) as well as the sheath cells around the periphery. (s in Figure 5.62. b).

The Circum-pallial Sinus. (cs in Figure 5.62. c), although it appears to directly connect with at least some other sinus in the Mantle Margin, is the only sinus where haemocytes have been seen. Illustrated in Figure 5.62. are at least three distinct types of Haemocytes labelled a, b and c.

FIGURE 5.62. *Pinctada maxima* Apical Groove F1F2. Circum-pallial Nerve and Sinus.

a. L.M. x 770. Azan. Apical Groove F1F2.

b. L.M. x 770. Azan. Circum-pallial Nerve.

c. L.M. x 770. Azan. Circum-pallial Sinus.

a

× 770

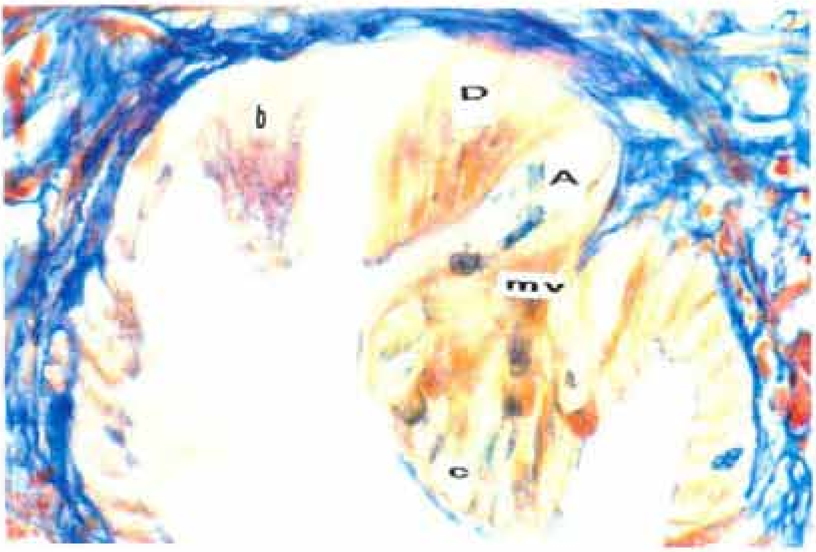

b

× 770

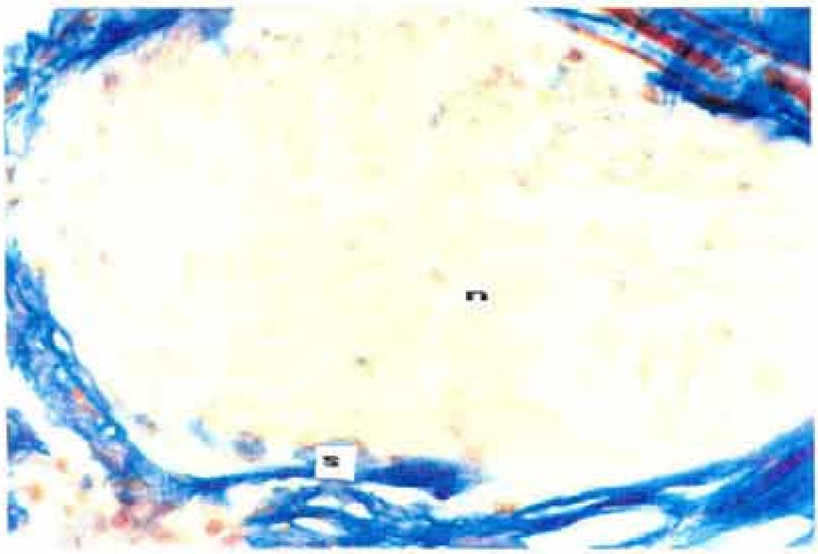

c

×770

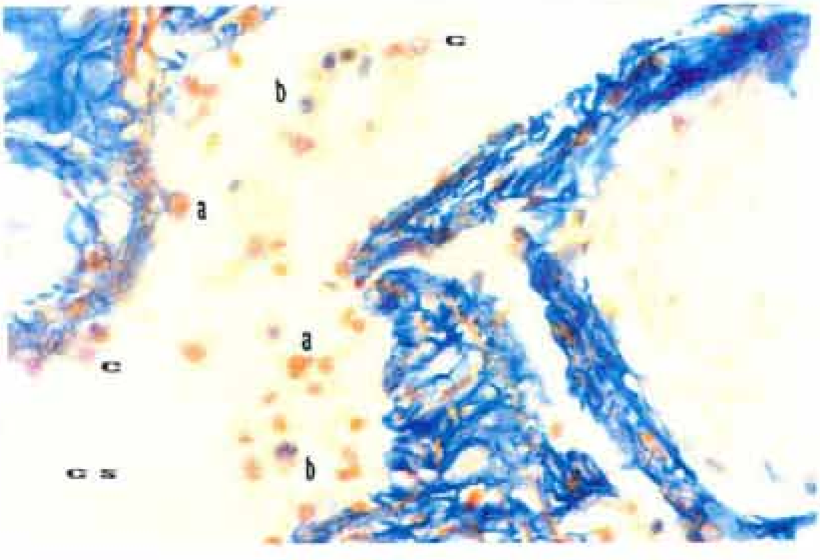

Figure
5.62 c s

5.5.1.9.7. T.E.M. Apical Groove F1F2..

Folding of the tissues of the Apical Groove F1F2. allows one section to display two rows of Dactylocytes bordering twin sectioning of the Apical Channel (D, D and A, A respectively in Figure 5.63.). Between the two Apical Channels are the Celtic Scroll Cells of the Omega Gland (c to c in Figure 5.63.). The Pleated Secretion of Groove F1F2., (P in Figure 5.63.), emanates from the Apical Channel and is a continuation of the sheet of secreted material (S in Figure 5.63.) lying across the distal extremities of the Dactylocytes' apical microvilli.

The basal nuclei of the Black Granule Secretory Cells (b in Figure 5.63.) are just above the Subapical Connective Tissue (s a c in Figure 5.63.).

The Amorphous Secretion (as in Figure 5.63.) is material bounded by a single membrane which appears to be produced by the deep cells of the Omega Gland.

FIGURE 5.63. *Pinctada maxima* Apical Groove F1F2..

T.E.M. x 1800 Cells of Apical Groove F1F2. which generate the Pleated Secretion of groove F1F2.


D
C
V
P
A
C
P
s
as
A
D
b
b
sac
Figure
5.63
x1800

5.5.1.9.8. T.E.M. Origin of Pleated Secretion of Groove F1F2. and Black Granule Secretory Cells.

The Pleated Secretion of Groove F1F2. (P in Figure 5.64. a) lies in the Groove from the Anterior Mantle Symphysis to the Posterior Mantle Symphysis. It originates at or about the asterisk in Figure 5.64. b., the proximal end of the Apical Channel of Groove F1F2.. The secretion lies across the ends of the microvilli of the Dactylocytes (D in Figure 5.64. a), between these and the Celtic Scroll Cells (CS in Figure 5.64. a), which form the superficial layer of the proximal part of the Omega Gland. Proximal to the initial point of appearance of the Pleated Secretion lies an Amorphous Secretion inside a single membranous boundary (a in Figure 5.64. c). This Amorphous Secretion appears to be generated by the Fenestrated Cells. (f in Figure 5.64. b). This Amorphous Secretion plus vesicles from the Multivesiculate Cells (mv in Figure 5.64. b), appear to take part in the formation of the Pleated Secretion of Groove F1F2.

The Black Granules (bg in Figure 5.64. d). of the Black Granule Secretory Cells originate in vesicles adjacent to multilayered membranous structures (m in Figure 5.64. d). There are numerous mitochondria in the vicinity of the origin of the visicles containing the Black Granules (mi in Figure 5.64. d).

FIGURE 5.64. *Pinctada maxima* Origin of Pleated Secretion of Groove F1F2. and Black Granule Secretory Cells.

a. T.E.M. x 7000 Celtic Scroll Cells, Apical Channel and Dactylocytes.

b. T.E.M. x 7000 Proximal end of Apical Channel.

c. T.E.M. x 7000 Amorphous Secretion.

d. T.E.M. x 15000 Black Granule Secretory Cells.

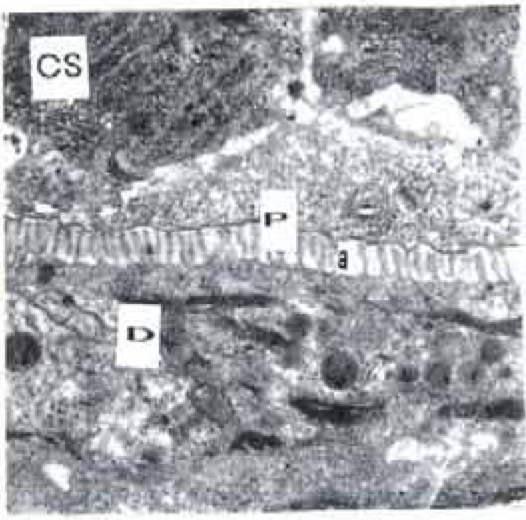

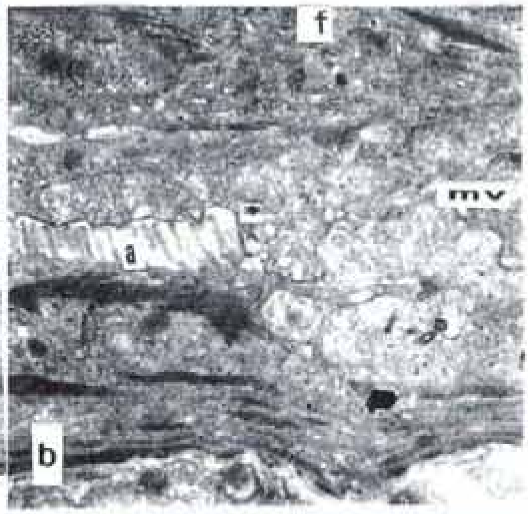

a

c

Figure 5.64

d

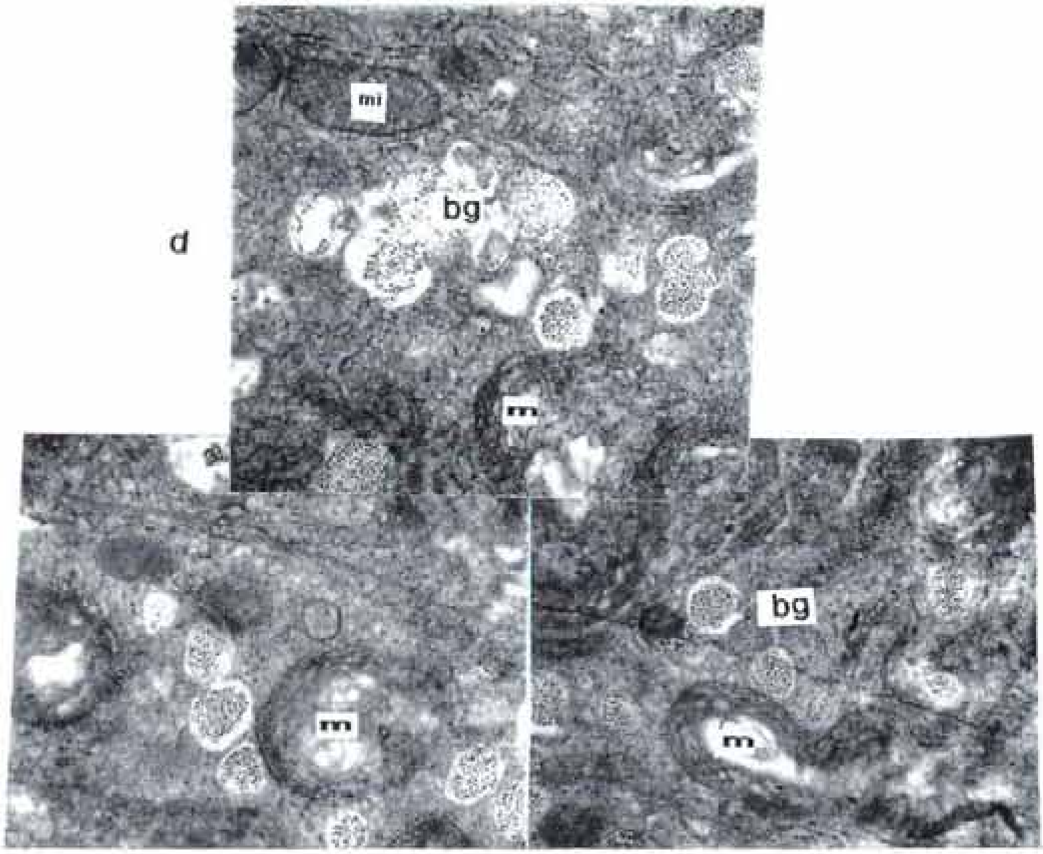

5.5.1.9.9. T.E.M. Black Granule Secretory Cells and Pleated Secretion of Groove F1F2..

The Black Granules first appear in light grey vesicles (b in Figure 5.65. c), located near recurved multimembranous structures (m in Figure 5.65. c), in the vicinity of mitochondria (mi in Figure 5.65., c), near the basal nuclei of the Black Granule Secretory Cells. The Vesicles nearest the apices of the cells carry granules which are increasingly electron dense, (b in Figure 5.65. a). The Vesicles carrying the Black Granules swell and rupture (r in Figure 5.65. a and b), and the released granules attach to the medial surface of the Pleated Secretion of Groove F1F2. as electron dense nodules (n on P in Figure 5.65. a and b), and on the opposing lateral surface of the Vesiculate Secretion of Groove F1F2..

FIGURE 5.65. *Pinctada maxima* T.E.M. of Black Granule Secretory Cells and Pleated Secretin of Groove F1F2..

a. T.E.M. x 9100

b. T.E.M. x 9100

c. T.E.M. x 9100

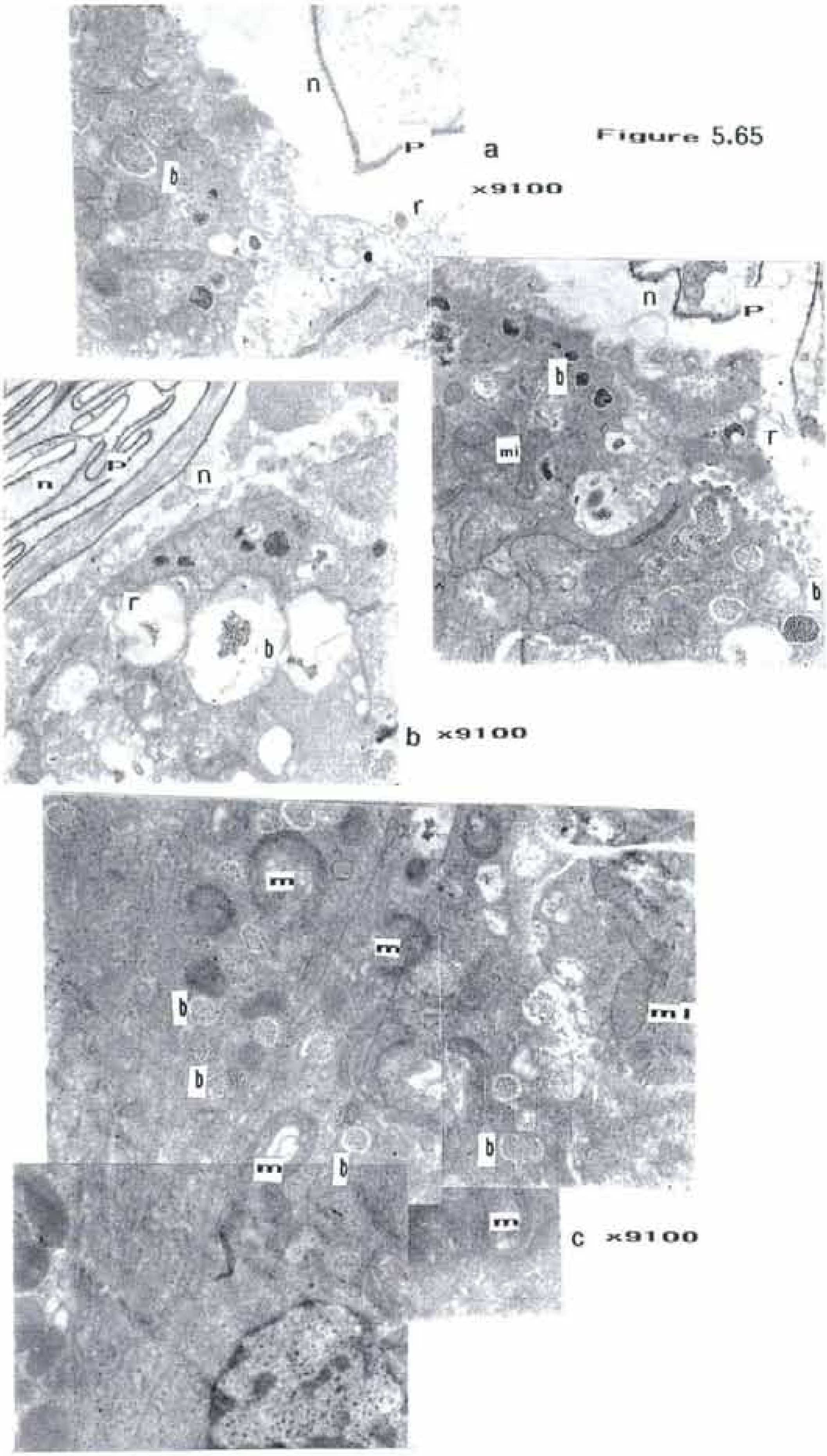

Figure 5.65

a ×9100

b ×9100

c ×9100

5.5.1.9.10. Omega Gland Epithelial Cells.

The Celtic Scroll Cells (Figure 5.66. c) produce large secretory vesicles which are discharged into the proximal Groove F1F2. underneath the Pleated Secretion of Groove F1F2. (Figure 5.63. V). They also form the lateral boundary to the distal part of the Apical Channel (A in Figure 5.66). ,and contribute secretory vesicles to the forming Pleated Secretion of Groove F1F2.. They are characterised by a cytoplasm with densely packed membranous structures and numerous mitrochondria (mi in Figure 5.66.).

The membrane bound Amorphous Secretion (as in Figure 5.66). just proximal to the origin of the Pleated Secretion of Groove F1F2. in Figure 5.66. is thought to combine with vesicles from the Multivesiculate Cell (mv in Figure 5.66.). in the initial formation of the forming Pleated Secretion of Groove F1F2..

The forming Pleated Secretion lies across the distal ends of the Dactylocytes' apical microvilli (D in Figure 5.66.) which contribute electron dense granular material to it via the microvilli.

FIGURE 5.66. *Pinctada maxima* Omega Gland Epithelial Cells.
T.E.M. x 9100.

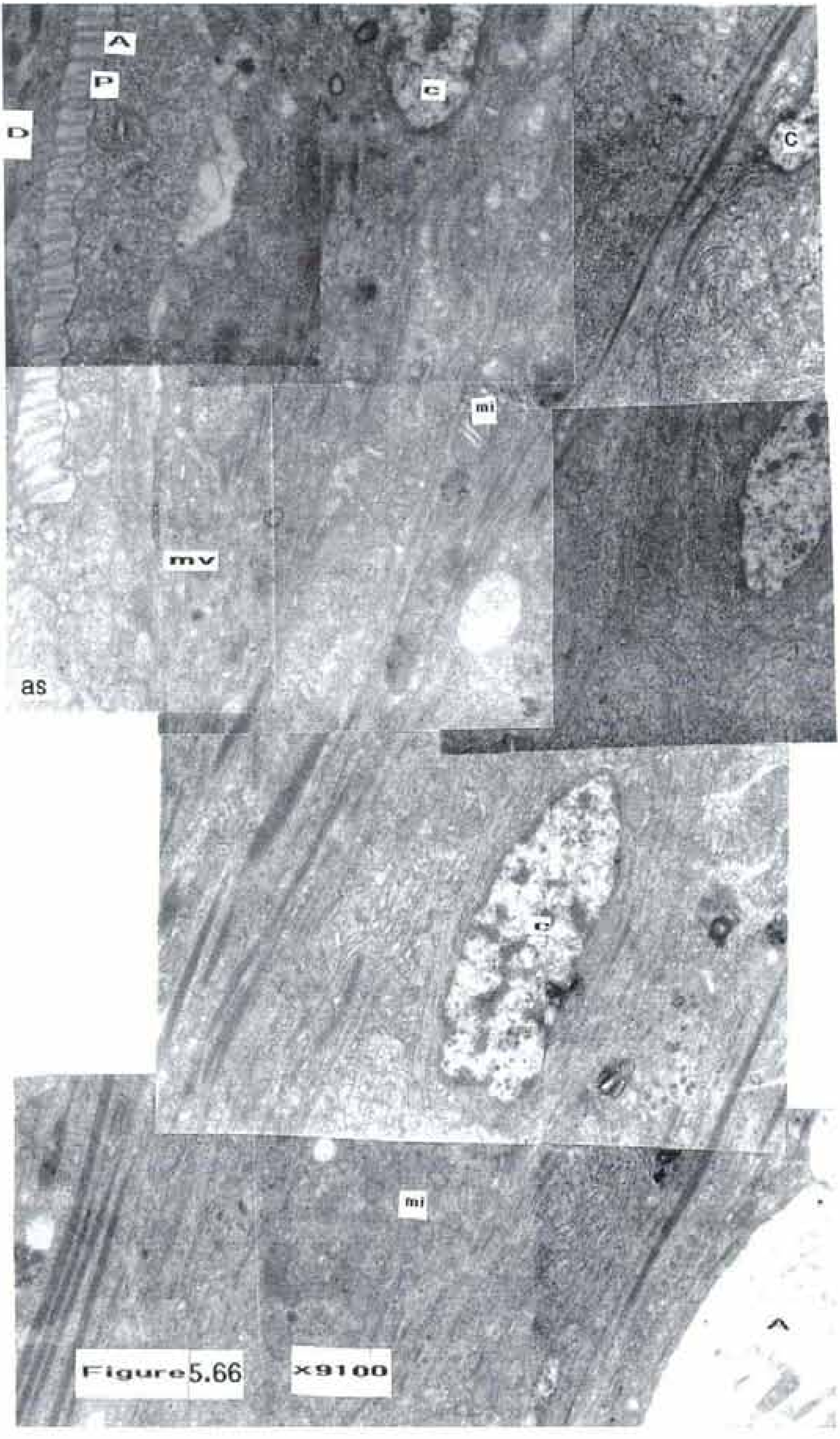

Figure 5.66 x9100

5.5.1.9.11. Secretory Tissues and Their Secretions of Proximal Groove F1F2..

The Pleated Secretion of Groove F1F2. (ps in Figure 5.67.) which issues from the Apical Channel acts as a physical barrier dividing the secretory products of MedF1. lateral to it from those of LatF2. which are medial to it (Figure 5.67.). In Figure 5.67. a and b, P is proximal, D is distal.

The secretory products of Proximal Med ~~Lat~~F1. include the vesiculate secretions (v in Figure 5.67. a and b) of the Celtic Scroll Cells (c in Figure 5.67. a) and the amorphous material (a in Figure 5.67. a and b) secreted by the Glands between the proximal and distal parts of the Omega Gland and the other secretory products of Proximal MedF1. (PMF!. in Figure 5.67.).

Cellular organelles are frequently seen in the secretions of Proximal LatF2. Three mitochondria are illustrated in this secretion in Figure 5.67. e.

The Secretions of Proximal LatF2. (PLF2 in Figure 5.67.) here are amorphous and not organised.

FIGURE 5.67. *Pinctada maxima* Proximal Groove F1F2..

a. T.E.M. x 1800 Pleated Secretion of Groove F1F2., Proximal F1. and its secretions.

b. T.E.M. x 7000 Secretios of Proximal F1. in a above at higher magnification.

c. T.E.M. x 7000 Secretions of Proximal Lat.F2.

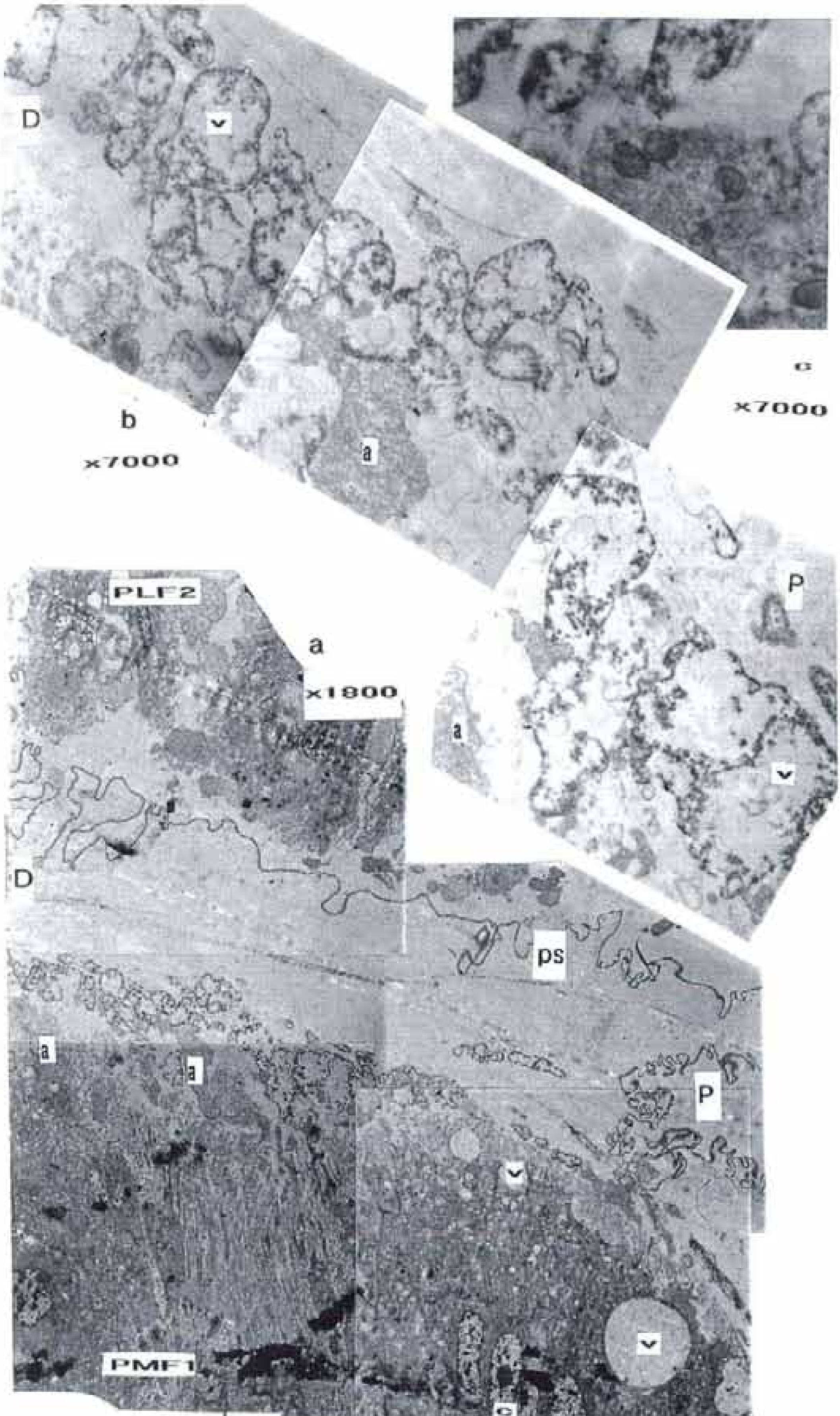

Figure 5.67

5.5.1.9.12. L.M. Proximal LatF2..

Ventral Proximal LatF2. under L.M. has a columnar epithelium, (e in Figure 5.68. a and b), which is covered by a secretory material which stains turquoise/pink with A.B./M.S.B. (a in Figure 5.68. a and b).

There is a fairly dense population of subepithelial unicellular glands including a variety of Granular Cytoplasm Secretory Glands (G in Figure 5.68. a and b) and the F2.-LatF3. type of Trabecular Turquoise Gland which occurs partly in the subepithelium and partly in the epithelium (TT in Figure 5.68. a and b).

In Figure 5.68. P is proximal, D, distal, and the distal end of Figure 5.68. a joins the proximal end of Figure 5.68. b.

Both the height of the Columnar epithelium and the amount of surface secretion (e and a in Figure 5.68. a and b) increase going distally.

FIGURE 5.68. *Pinctada maxima* Proximal LatF2..

a. L.M. x 770 Prtoximal part of Proximal LatF2..

b. L.M. x 770 Distal part of Proximal LatF2.

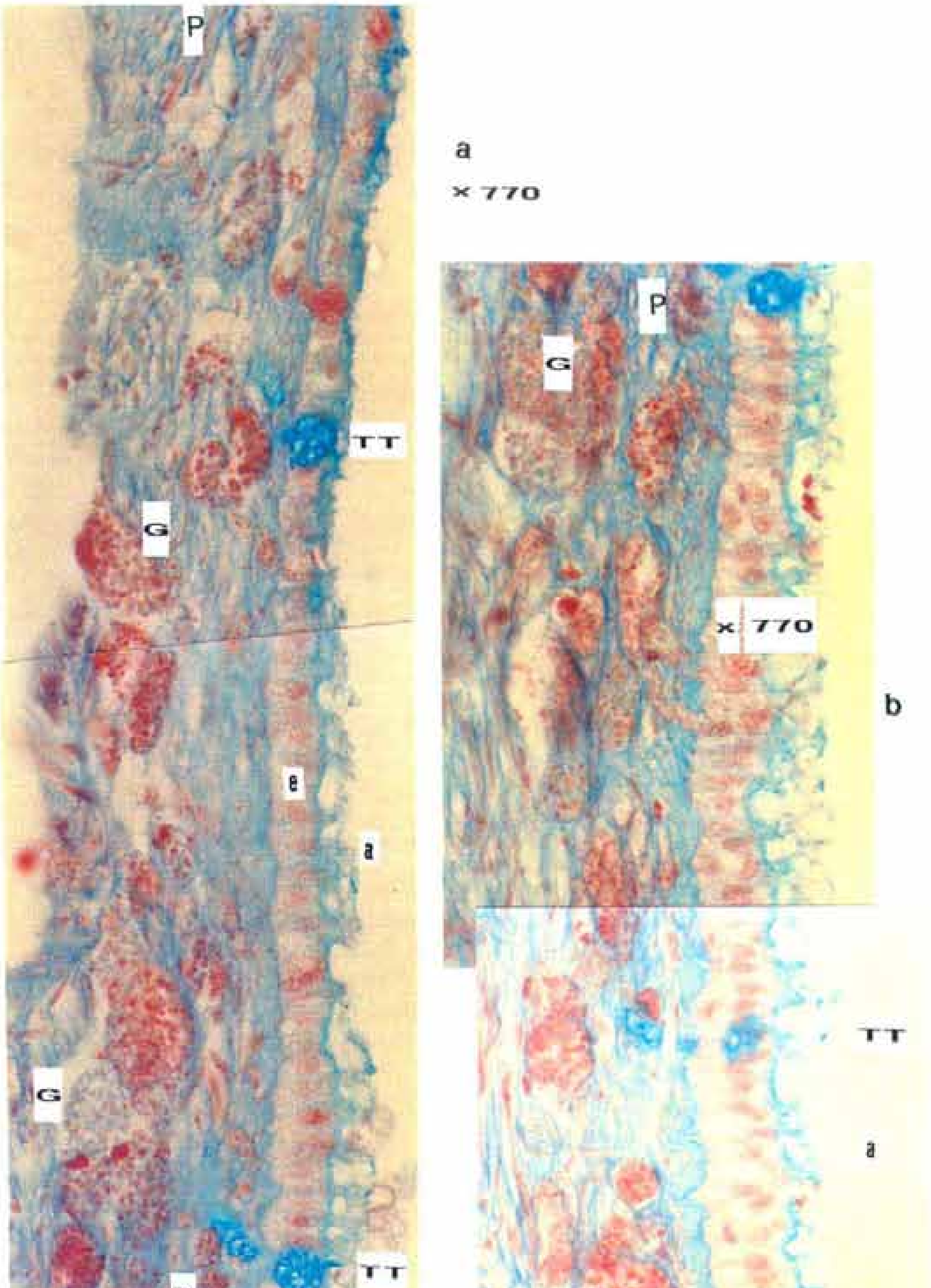

Figure 5.68

5.5.1.9.13. T.E.M. Proximal LatF2..

This region contributes to the Vesiculate Secretion of Grooe F1F2. (s in Figure 5.69. a) which lies between the surface epithelium (e in Figure 5.69. a) and the Pleated Secretion of Groove F1F2. (P in Figure 5.69. a).

The subepithelial glands secrete their cytoplasmic granules into Receptacle Glands (r in Figure 5.69. a and c) which are surrounded by specialised epithelial cells with elongate nuclei (n in Figure 5.69. a and c), cytoplasm rich in endoplasmic reticulum (er in Figure 5.69. c) and apical ctyoplasm containing numerous mitochondria (c in Figure 5.69. a and d).

The epithelial apical membrane bears a dense mass of secretory microvilli (to the right of c in Figure 5.69. d).

Fairly amorphous secretory bodies are produced in the epithelium and secreted into Groove F1F2. (b in Figure 5.69. a and b).

FIGURE 5.69. *Pinctada maxima* Proximal LatF2..

a. T.E.M. x 1800 LatF2. secretory structures and secretions.

b. T.E.M. x 7000 Higher magnification of part of a above.

c. T.E.M. x 7000 As for b above.

d. T.E.M. x 18000 As for b and c above.

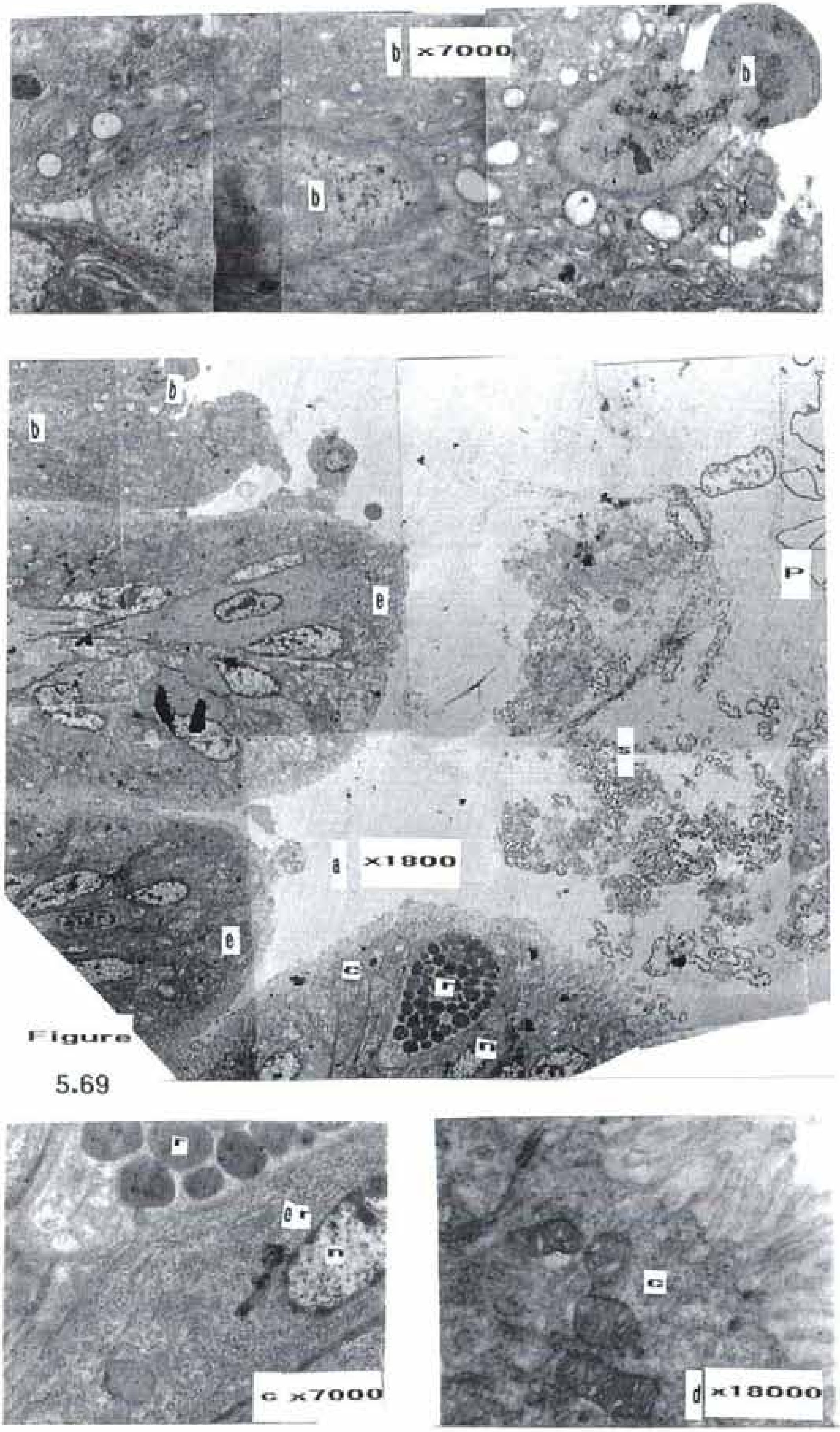

Figure 5.69

5.5.1.9.14. T.E.M. Junction of Proximal and Middle LatF2..

The surface epithelium of Proximal LatF2. (PLF2. in Figure 5.70. a) has a dense mat of apical microvilli (mv in Figure 5.70. a); that of Middle LatF2. (MLF2 in Figure 5.70. a), has conspicuous elongate cilia plus a mat of apical microvilli (c + mv in Figure 5.70. a). These are shown in higher magnification in Figure 5.70. c.

The subepithelium bears a gland unique to this location, the Light Blue Glands (b in Figure 5.70. b and d) which have evely sized and spaced spherical granules about 2um in diameter and which are usually closely associated with branches of the F2. ramis of the Circum-pallial Nerve bearing relatively large ovoid neurosecretory granules (n in Figure 5.70. d).

FIGURE 5.70. *Pinctada maxima* Junction of Proximal and Middle LatF2..

a. T.E.M. x 1800 Junction of Peoximal LatF2. and Middle LatF2..

b. T.E.M. x 1800 Light Blue Glands of Middle LatF2.

c. T.E.M. x 3500 Higher Magnification of surface epithelium of Middle LatF2.

d. T.E.M. x 7000 Nerve supply to a Light Blue Gland

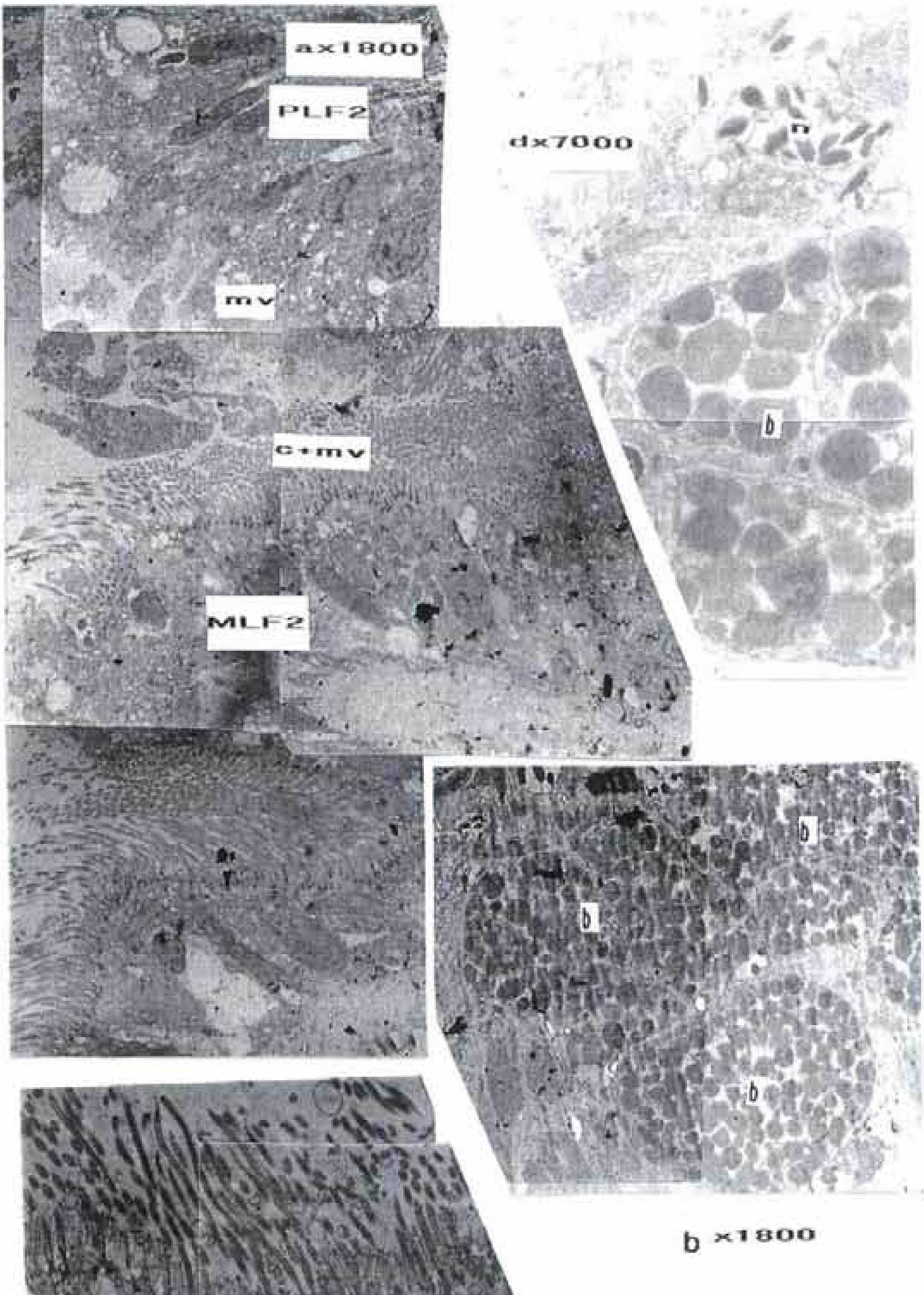

Figure 5.70

5.5.1.9.15. L.M. Middle LatF2..

The radial length of the Middle LatF2. Region is up to about 1.5mm, (d in Figure 5.71. adjoins p in Figure 5.72. and d in Figure 5.72. is only slightly proximal to p in Figure 5.73.). The elongate columnar external epithelium. of Middle LatF2. (e in Figures 5.71., 5.72. and 5.73.) rise from less than 50 μm near their proximal limits (p in Figure 5.71.) to 100 μm towards the middle of their radial distribution. (e in Figure 5.72.), before falling to about 20 μm at their distal limits (d in Figure 5.73.). The columnar epithelium bears elongate apical cilia (c in Figure 5.71.. 5.72. and 5.73.). The Vesiculate Secretion (s in Figure 5.71. and 5.72.) lies across the distal end of the cilia. With Azan it stains a similar purple (at s in Figure 5.71. b) to that of the Black Granule Secretory Cells of Apical Groove F1F2. (b in Figure 5.62). Similarly, with A.B./M.S.B. the staining affinity of the Vesiculate secretion is the same as that of these cells (s in Figure 5.72. and b in Figure 5.61 respectively). The subepithelial Unicellular Glands are of Three types. The Trabecular Turquoise Glands appear regularly spaced and of the standard appearance of F2.-LatF3. type having a relatively small subepithelial cell body immediately beneath the epithelial Basement Membrane, which discharges via a tubule into a Receptacle Gland like space in the surface epithelium (TT in Figure 5.71. and 5.72.). This is the same morphology as the Trabecular Turquoise Glands in Proximal LatF2. (Figure 5.68. a and b). There are a variety of Granular Cytoplasm Secretory Glands which stain a variety of shades of red, orange and purple with all stains used (G in Figure 5.71. a and b and Figure 5.72.). However far more numerous in this Region are the Light Blude Glands which are fairly refractory but stain faint blue with all stains used except for A.B./M.S.B. with which they stain a faint blue to fain pink (b in Figure 5.71., 5.72. and 5.73.). These glands are unique to the subepithelium of LatF2..

FIGURE 5.71. *P. maxima* Proximal part of Middlle LatF2..

a. x 770 A.B./M.S.B

b. x 770 Azan.

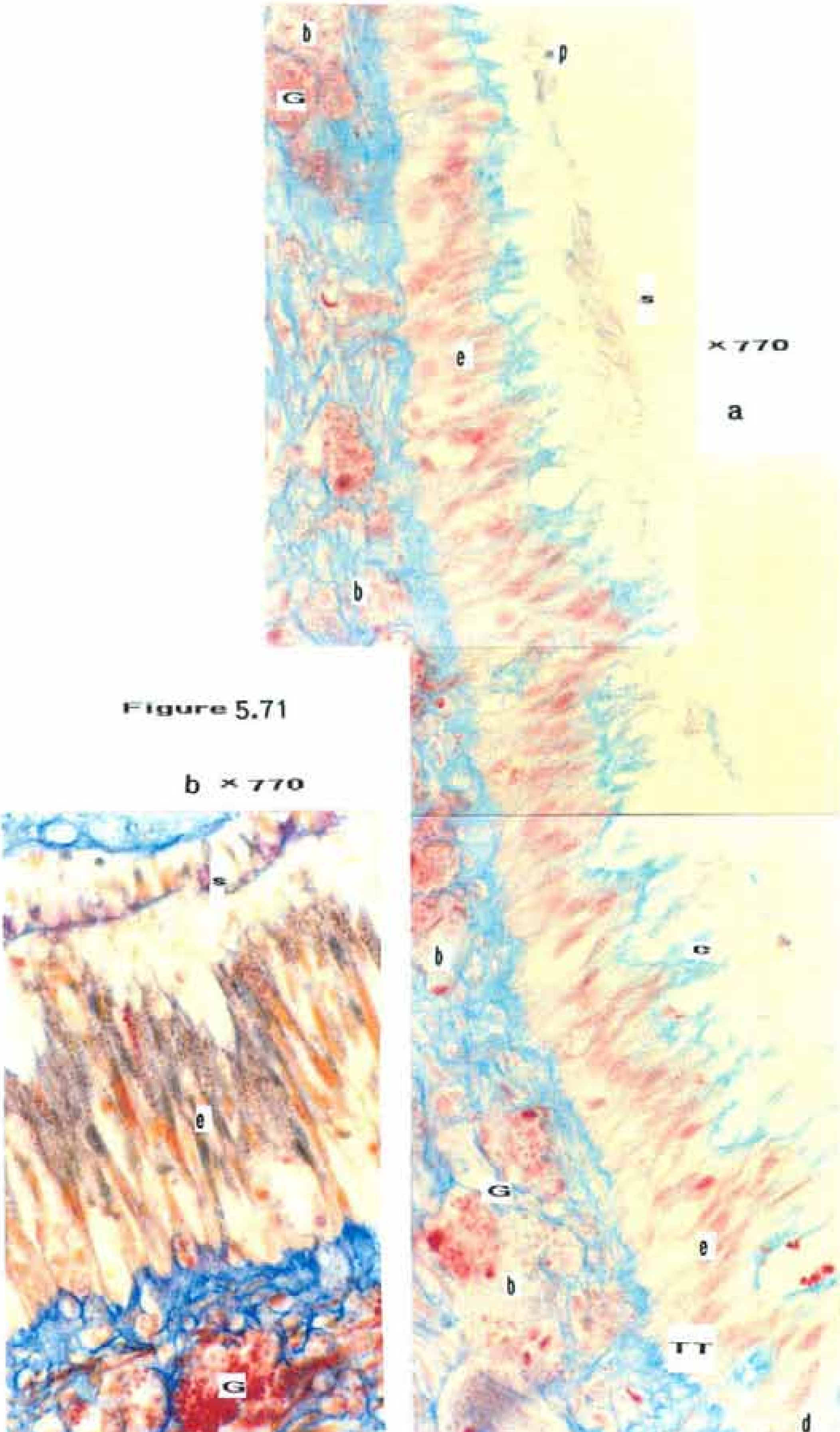

Figure 5.71

5.5.1.9.16. Middle LatF2. (Continued).

In Figure 5.72, p is proximal, d, distal, b marks the Light Blue Glands, G the Granular Cytoplasm Secretory Glands, e the surface epithelium, TT the Trabecular Turquoise Glands, c the apical cilia and s, the = Vesiculate Secretion.

FIGURE 5.72. *Pinctada maxima* Middle Part of Middle LatF2.
L.M. x 770 A.B./M.S.B.

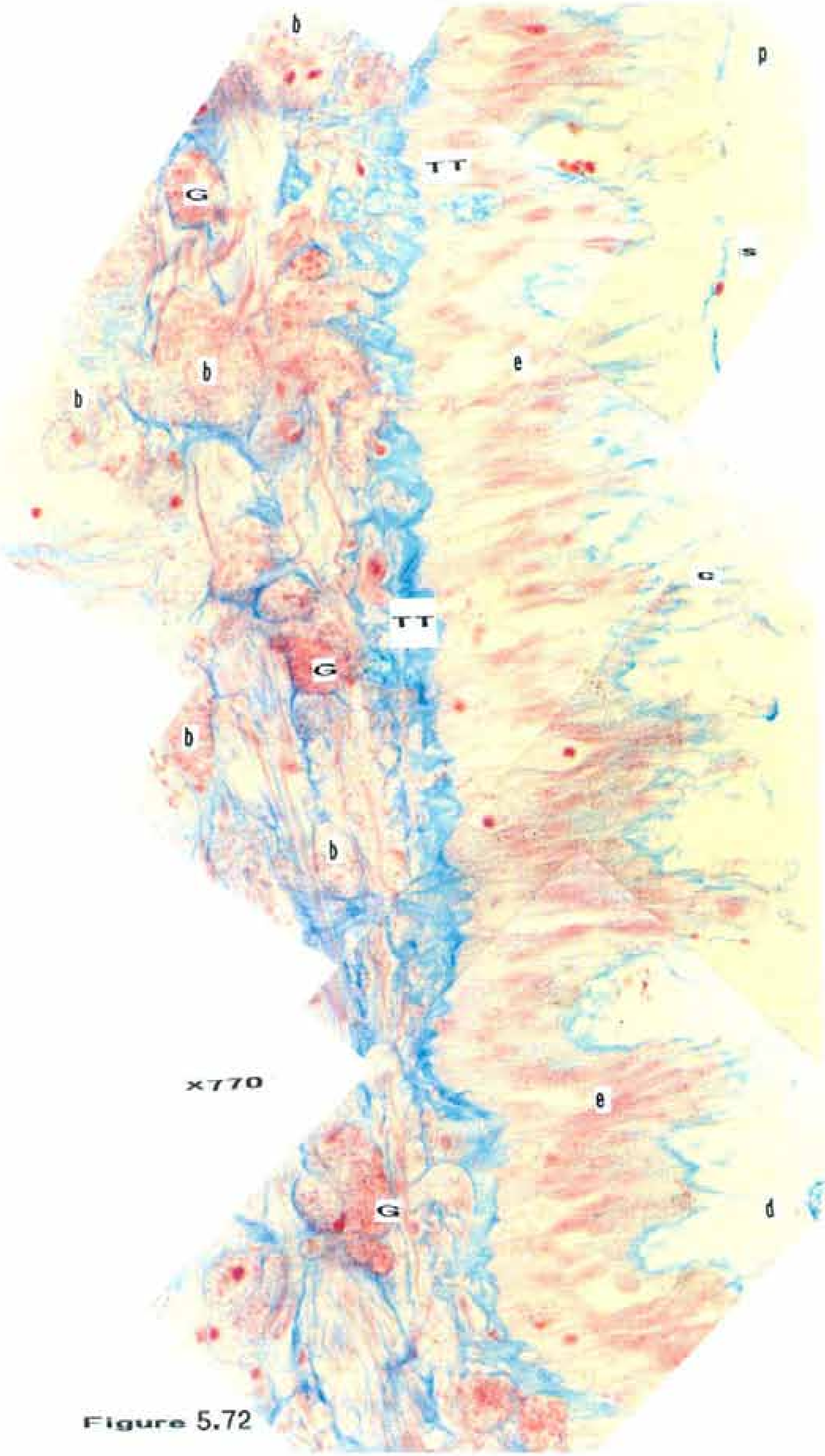

Figure 5.72

5.5.1.9.17. Middle LatF2. (Continued).

In Figure 5.73. p is proximal, d, distal, e marks the epithelium, b the Light Blue Glands, TT the Trabecular Turquoise Glands, and c the apical cilia.

FIGURE 5.73. *Pinctada maxima* Distal part of Middle LatF2.
L.M. x 770 A.B./M.S.B.

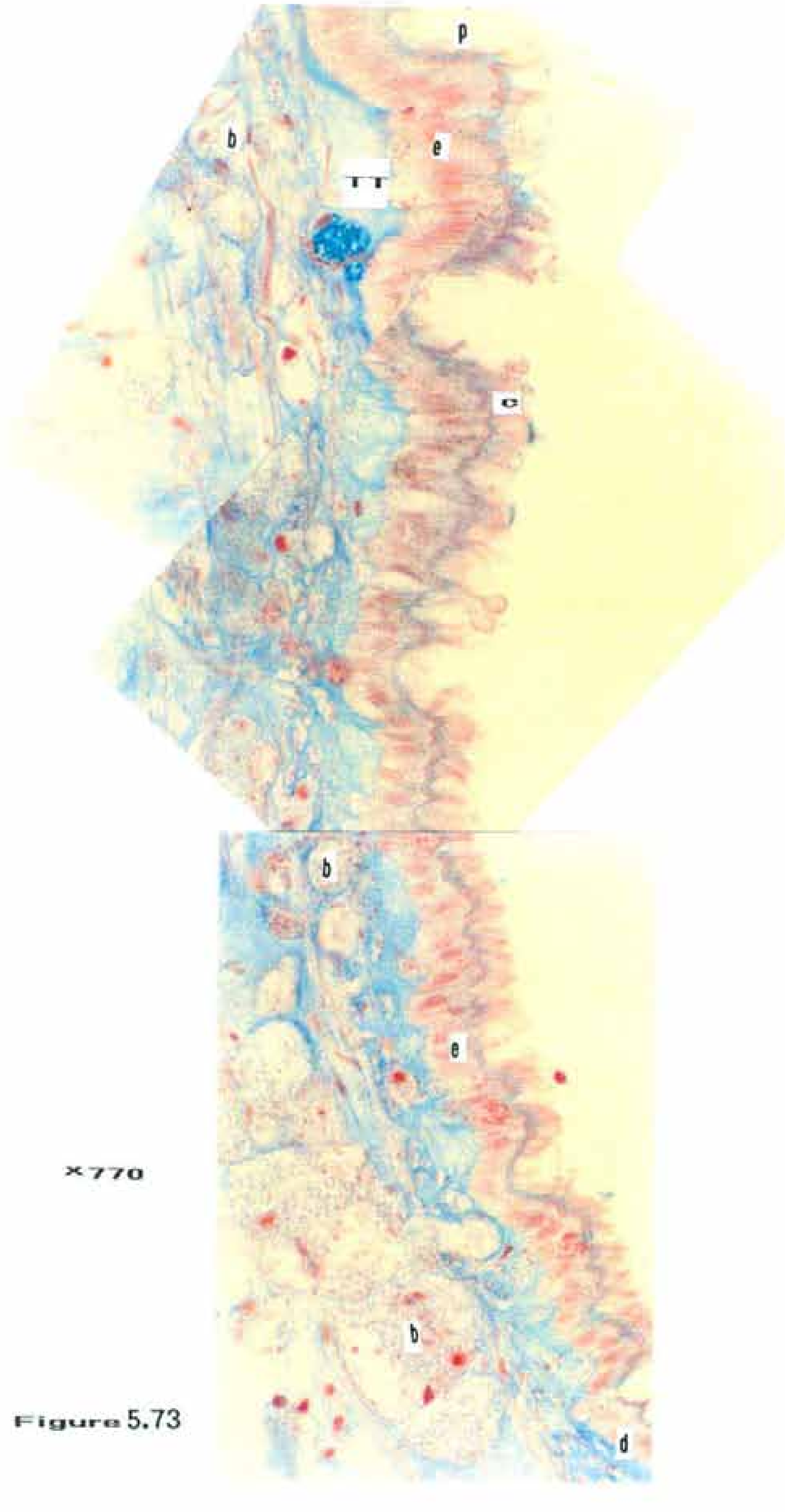

x770

Figure 5.73

5.5.1.9.18. Specialised Histological Features of Middle LatF2.

The bodies of the Trabecular Turquoise Glands of this Region lie immediately beneath the epithelial Basement Membane. The cytoplasmic trabeculae are less noticeable in these glands than in those of the External Mantle (Figure 5.56. a). The Light Blue Glands (b in Figure 5.74.) discharge through the surface epithelium.

The elongate surface cilia (c in Figure 5.74. a) have distinct Basal Bodies (bb in Figure 5.74. a) in the apical cytoplasm.

In the parenchyma of F2. and F3. are large glands with small ovoid nuclei (n in Figure 5.74. b) with numerous very small granules (m in Figure 5.74. b). - the Microgranular Glands. They appear to secrete into the sinus of Folds F2. and F3..

FIGURE 5.74. *Pinctada maxima* - Specialised histological features of Middle LatF2.

a. T.E.M. x 1800 Surface epithelium and secretory structures.

b. T.E.M. x 4800 Microgranular Gland

Figure 5.74

5.5.1.9.19. Distal LatF2. Region.

This region as a relatively low columnar epithelium whose apical membrane bears both microvilli (mv in Figure 5.75. a) and elongate cilia (c in Figure 5.75. b). The terminal epithelium has numerous melanin like pigment granules (m in Figure 5.75. b and c).

FIGURE 5.75. *Pinctada maxima* Distal LatF2.

a. T.E.M. x 1800 Distal LatF2. epithelium.

b. T.E.M. x 1800 Terminal F2.

c. T.E.M. x 7000 Pigment Granules in surface epithelium of b above.

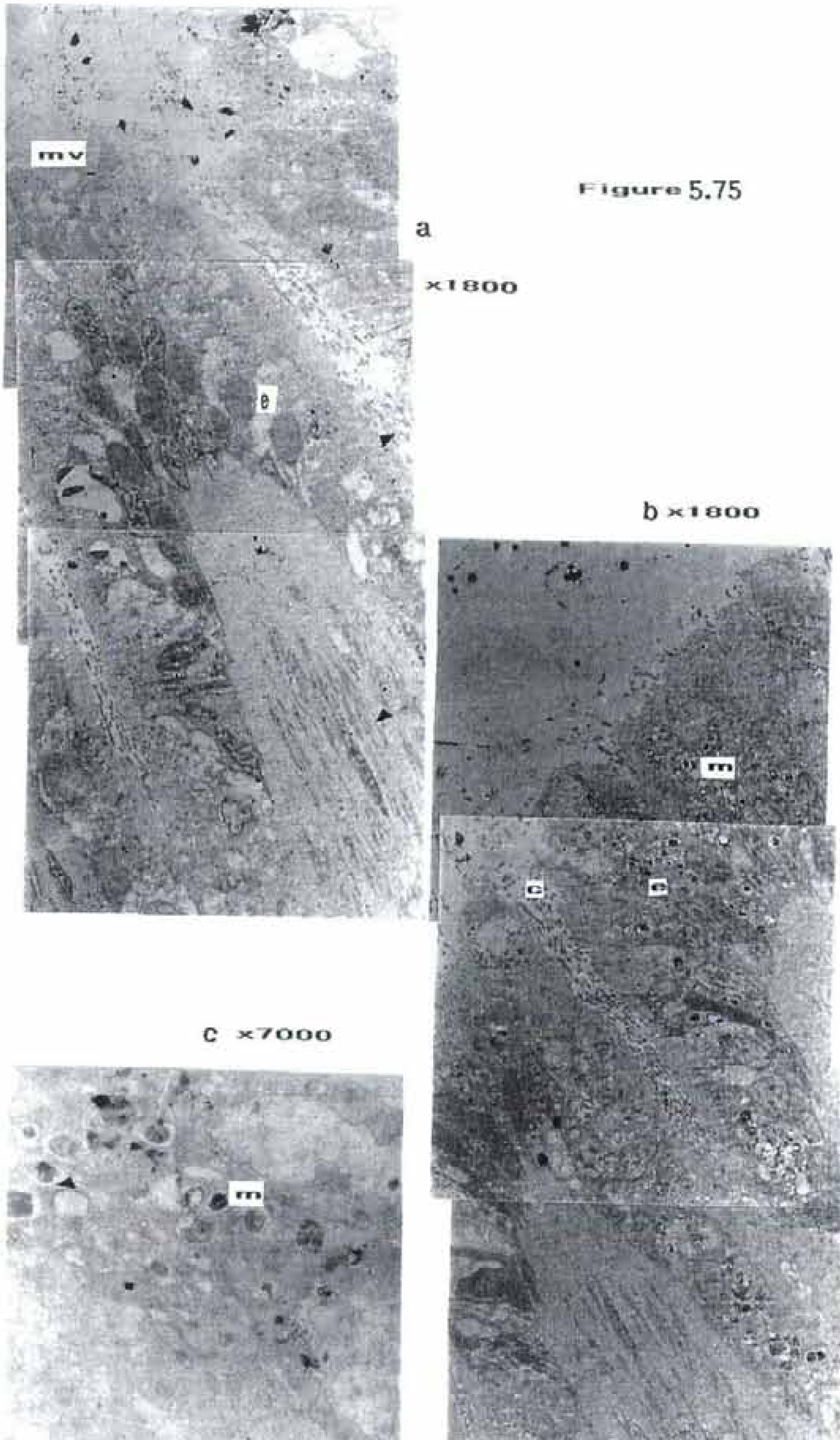

Figure 5.75

a ×1800

b ×1800

c ×7000

5.5.1.9.20. Terminal F2. and Distal and Proximal MedF2..

The surface epithelium of Distal LatF2. is markedly different from that of Distal MedF2.. The former is more elongate than the latter, the nuclei are basal rather than central, the apical regions of the cells stain more strongly turquoise with A.B./M.S.B. than is the case with the latter and they are more strongly ciliate than them, (el and c respectively in Figure 5.76. a, where c indicates cilia, L is lateral, M is medial, and dd, a Distal Diffuse Gland). The Distal Diffuse Gland is very unusual in this location.

The Distal MedF2. subepithelium has apparently evely spaced Trabecular Turquoise Glands (TT in Figure 5.76. b) but relatively few other unicellular glands. The Trabecular Turquoise Glands persist in the Proximal MedF2. subepithelium and there is an increase in several types of Granular Cytoplasm Secretory Glands (TT and G respectively in Figure 5.76. d and e). The pigmentation of the Proximal MedF2. surface epithelium (e in Figure 5.76.. d and e) stains well with Azan but not with A.B./M.S.B.

Branches of the F2. Ramis of the Circum-pallial Nerve run throughout the parenchyma of F2. and appear to innervate the Microgranular Glands (n and m respectively in Figure 5.76. c) and other secretory and muscular structures.

FIGURE 5.76. *Pinctada maxima* Terminal F2. and Distal and Proximal MedF2..

a. L.M. x 770 A.B./M.S.B. Terminal F2..

b. L.M. x 770 A.B./M.S.B. Distal MedF2..

c. L.M. x 1200 Azan. Parenchyma of F2. sinus nerve and Microgranular Gland.

d. L.M. x 1200 Azan. Proximal Med F2..

e. L.M. x 770 A.B./M.S.B. Proximal MedF2..

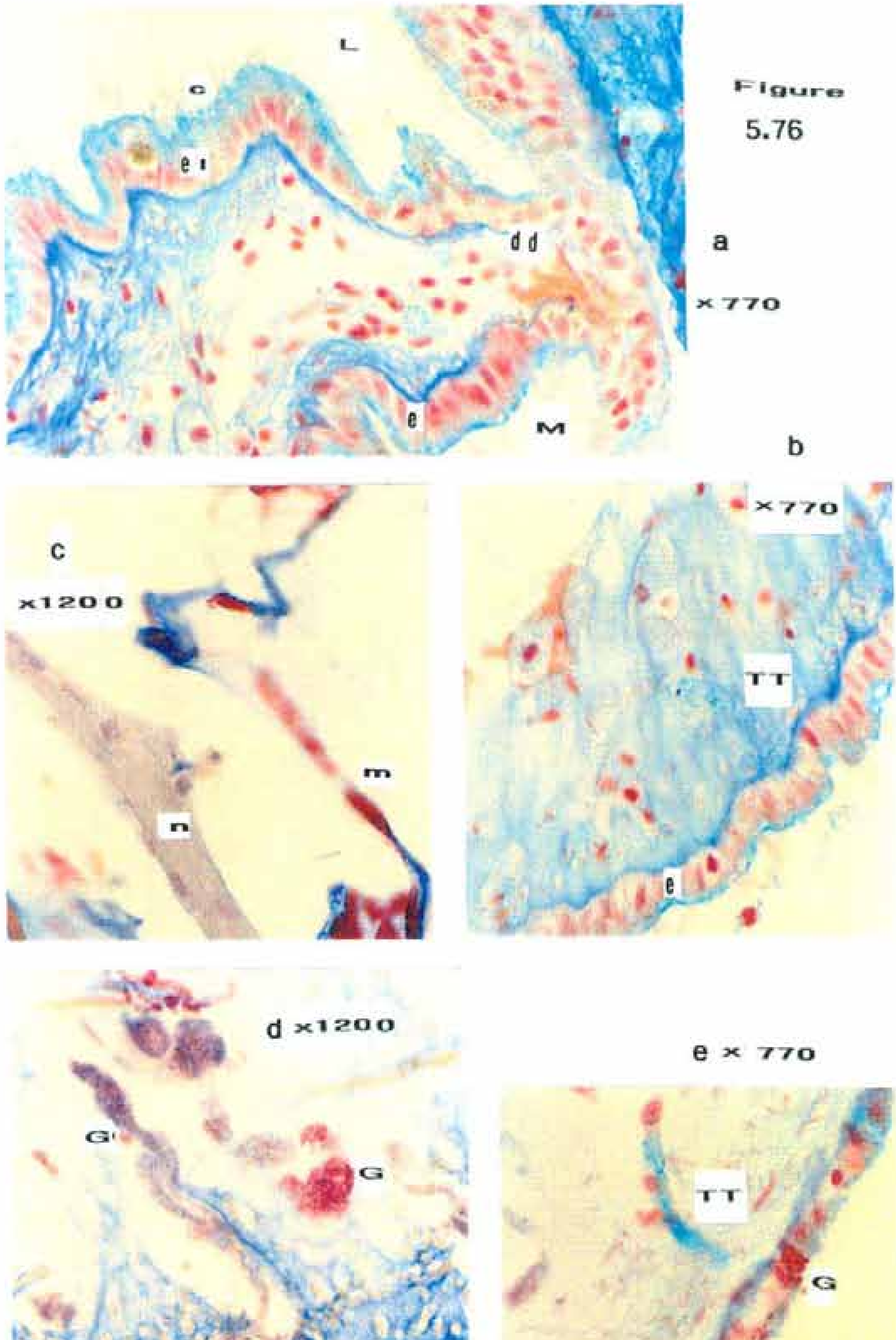

Figure 5.76

5.5.1.9.21. Proximal and Distal LatF3..

Proximal LatF3. has a columnar external epithelium (e in Figure 5.77. a). Trabecular Turquoise Glands of a type similar to those seen in LatF2. and MedF2. occur scattered throughout the subepithelium and epithelium of LatF3. (TT in Figure 5.77. a and c). (Trabecular Turquoise Glands stain poorly with Azan, TT in Figure 5.77. c). Microgranular Glands (m in Figure 5.77. a and d) occur throughout the parenchyma of F3., associated with sinus. With Azan they are distinguished from other similarly staining glands by location, lack of a secretory tubule to the Marginal Mantle Groove, and lack of granules in the cytoplasm at this magnification).

Granular Cytoplasm Secretory Glands (G in Figure 5.77. b, c and d) occur in localised concentration especially near Apical Groove F2F3., (a in Figure 5.77. c).

The surface epithelium (e in Figure 5.77. d) changes dramatically from that on the lateral surface of F3. (L in Figure 5.77. d) to that on the medial surfaces of F3. (M in Figure 5.77. d), as does its pigmentation MedF3. is not considered further as it is not thought to be involved in Shell Organic Matrix secretion.

FIGURE 5.77. *Pinctada maxima* Proximal and Distal LatF3..

a. L.M. x 770 A.B./M.S.B. Proximal LatF3..

b. L.M. x 1200 Azan. Proximal LatF3..

c. L.M. x 1200 Azan. Apical Groove F2F3..

d. L.M. x 1200 Azan. Distal LatF3 and Terminal F3..

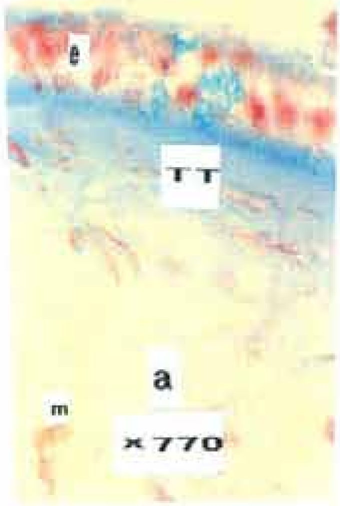

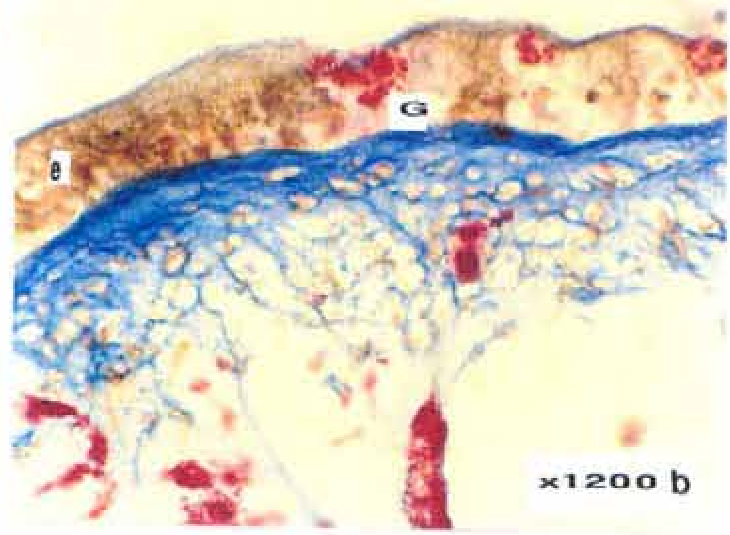

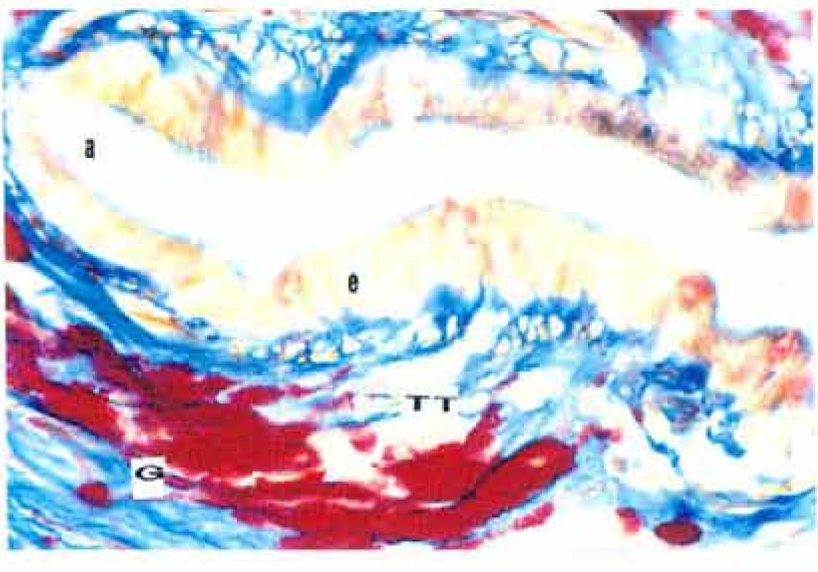

c
x1200

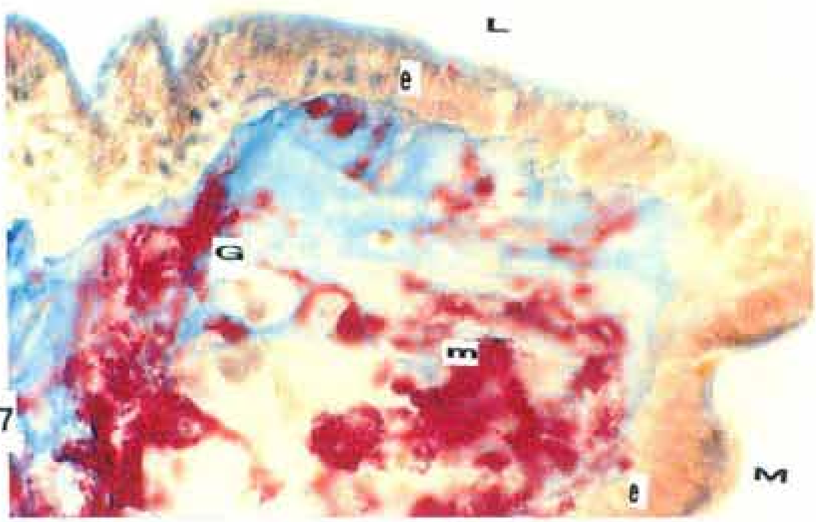

d
x1200

Figure 5.77

5.5.1.9.22. Apical Groove F1F2. of the Antero Dorsal Periphery.

While some of the associated unicellular glands may be locus-specific, the histological species of the Omega Gland are the same here as on the Ventral Mantle Margin, (c.f. Figures 5.61 - 5.64).

In Figure 5.78. L is lateral and M medial, p proximal and d distal.

The simple columnar epithelium of the Proximal MedF1. (e in Figure 5.78.) joins at j in Figure 5.78. the pseudostratified columnar epithelium of the Distal Omega Gland (dog in Figure 5.78.). Intraepithelial and subepithelial Granular Cytoplasm Secretory Glands and Trabecular Turquoise Glands (B and TT in Figure 5.78.) commonly evacuate their secretions into Groove F1F2. (GF1F2. in Figure 5.78.) on either side of the Distal Omega Gland. The proximal part of the Omega Gland is a two layered epithelial structure. Superficially the Celtic Scroll Cells (nuclei marked cs in Figure 5.78.) secrete large vesicles into Groove F1F2. which come to form a considerable proportion of the secretory material lying under the Pleated Secretion of Groove F1F2., (P in Figure 5.78.), in this location.

Deep to the Celtic Scroll Cells are the Multivesiculate Cells, (nuclei marked mv in Figure 5.78). Vesicles from these and the Amorphous Secretion, (as in Figure 5.78.), invest the proximal and lateral origin of the Pleated Secretion of Groove F1F2. at the apex of the Apical Channel (a in Figure 5.78.).

The most proximal Dactylocyte, (D in Figure 5.78.), is medial to the apex of the Apical Channel.

The Sub-apical Connective Tissue underlies the structures of Apical Groove F1F2.. Lodged in this, in this location are Spherular Cytoplasm Turquoise Glands and the branches of the Circum-pallial Nerve which innervate the structures of Apical Groove F1F2. (ST and n respectively in Figure 5.78.).

FIGURE 5.78. *Pinctada maxima* Apical Groove F1F2. Anterior Periphery. T.E.M. x 1800.

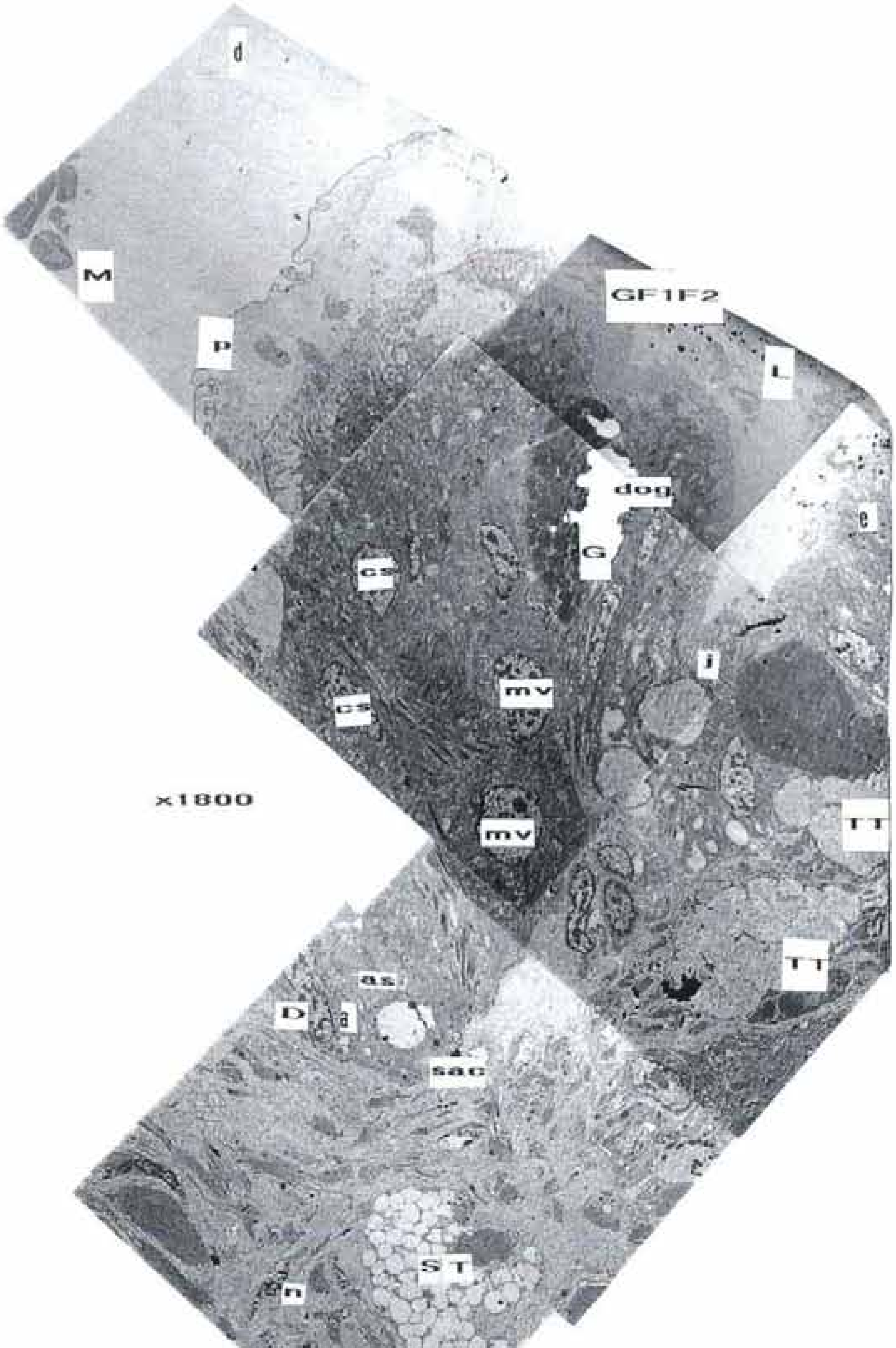

x1800

Figure 5.78

5.5.1.9.23. T.E.M. Medial Apical Groove F1F2. and Proximal LatF2. Antero-Dorsal Periphery.

In Figure 5.79. p is proximal, d, distal, L, lateral and M, medial.

The Subepithelial secretory Glands and the associated Receptacle Glands are far more numerous in the anterior periphery than ventrally or posteriorly (G and R respectively in Figure 5.79, c.f. Figures 5.67,5.68).

The F2. Ramis of the Circum-pallial Nerve (N in Figure 5.79.) distributes numerous branches throughout the subepithelial secretory glands (n in Figure 5.79.). These include Spherular Cytoplasm Turquoise Glands, (ST in Figure 5.79).

Secretory material (s in Figure 5.79.) from the Receptacle Glands lies between the surface epithelium and the Pleated Secretion of Groove F1F2. (gF1F2 in Figure 5.79).

FIGURE 5.79. *Pinctada maxima* Proximal part of Proximal LatF2., Subepithelial Glands, Receptacle Glands and F2. Ramis of Circum-pallial Nerve.

a. T.E.M. x 1800.

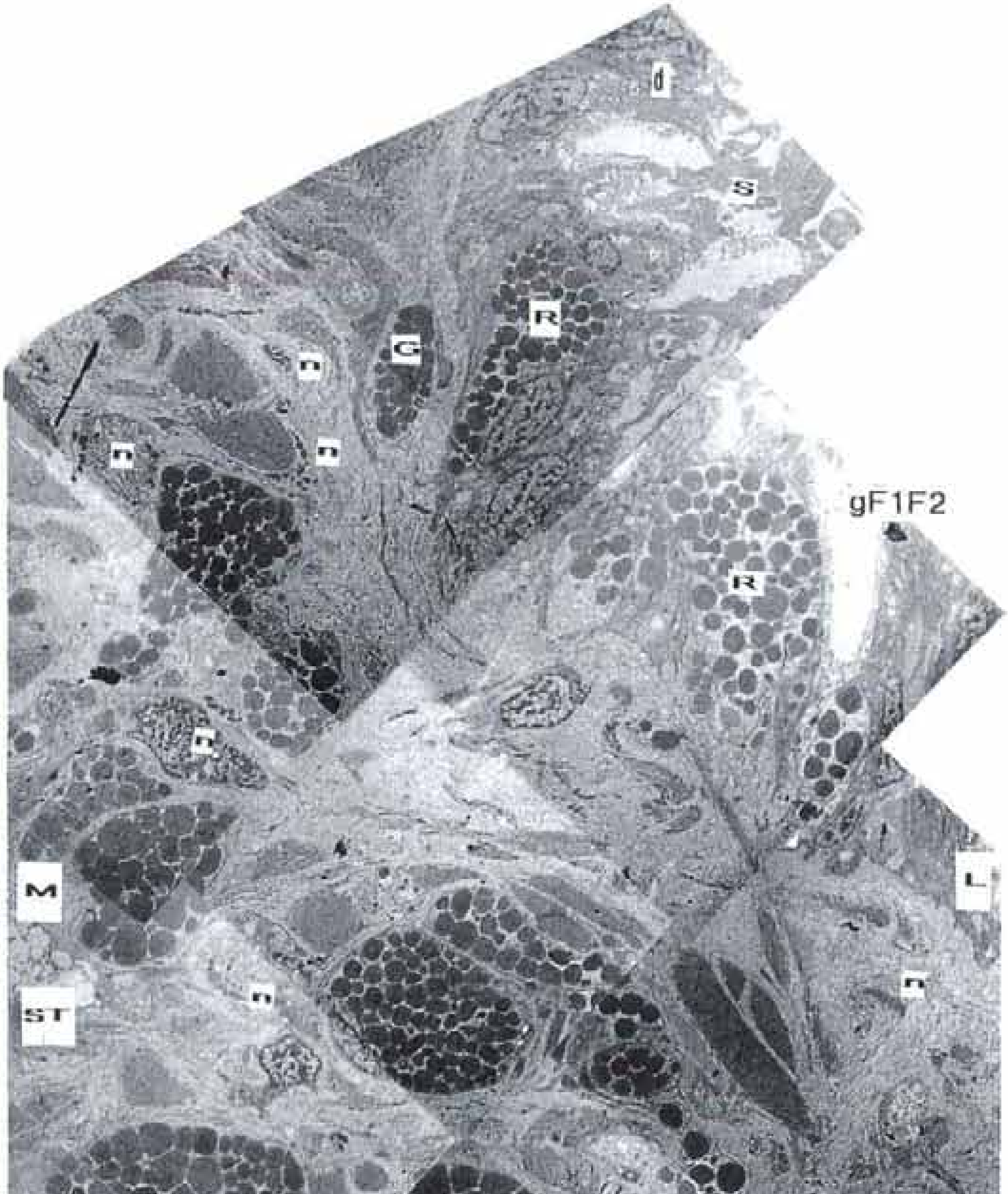

x1800

Figure 5.79

5.5.1.9.24. Proximal Lat F2. Antero-dorsal Periphery.

Here the arrangement of subepithelial unicellular glands discharging into Receptacle Glands (G in Figure 5.80. b, and R in Figure 5.80. c respectively), alters in some areas to intra-epithelial Granular Cytoplasm Secretory Glands (I in Figure 5.80, a), and Spherular Cytoplasm Turquoise Glands both of which appear to secrete by disintegration of the entire cell. D in Figure 5.80, a, appears to be a disintegrating Spherular Cytoplasm Turquoise Gland (ST in Figure 5.80. a), and S in Figure 5.80. a, appears to be a secreted disintegrated one.

Similarly granules from the intraepithelial Unicellular Glands appear to be secreted still attached to the nuclei of their cells (nu in Figure 5.80. a). The Granular Cytoplasm Secretory Glands, whether subepithelial as in 5.80. b, or intraepithelial as in Figure 5.80. a, are innervated by branches of the F2. Ramis of the Circum-pallial Nerve (n in Figure 5.80. a and b).

FIGURE 5.80. *Pinctada maxima* Proximal LatF2. Anterior Periphery.

a. T.E.M. x 1800 Intra-epithelial and sub-epithelial unicellular glands.

b. T.E.M. x 1800 Sub-epithelial Glands and their innervation.

c. T.E.M. x 1800 Recepticle Glands and secretions in proximal medial Groove F1F2..

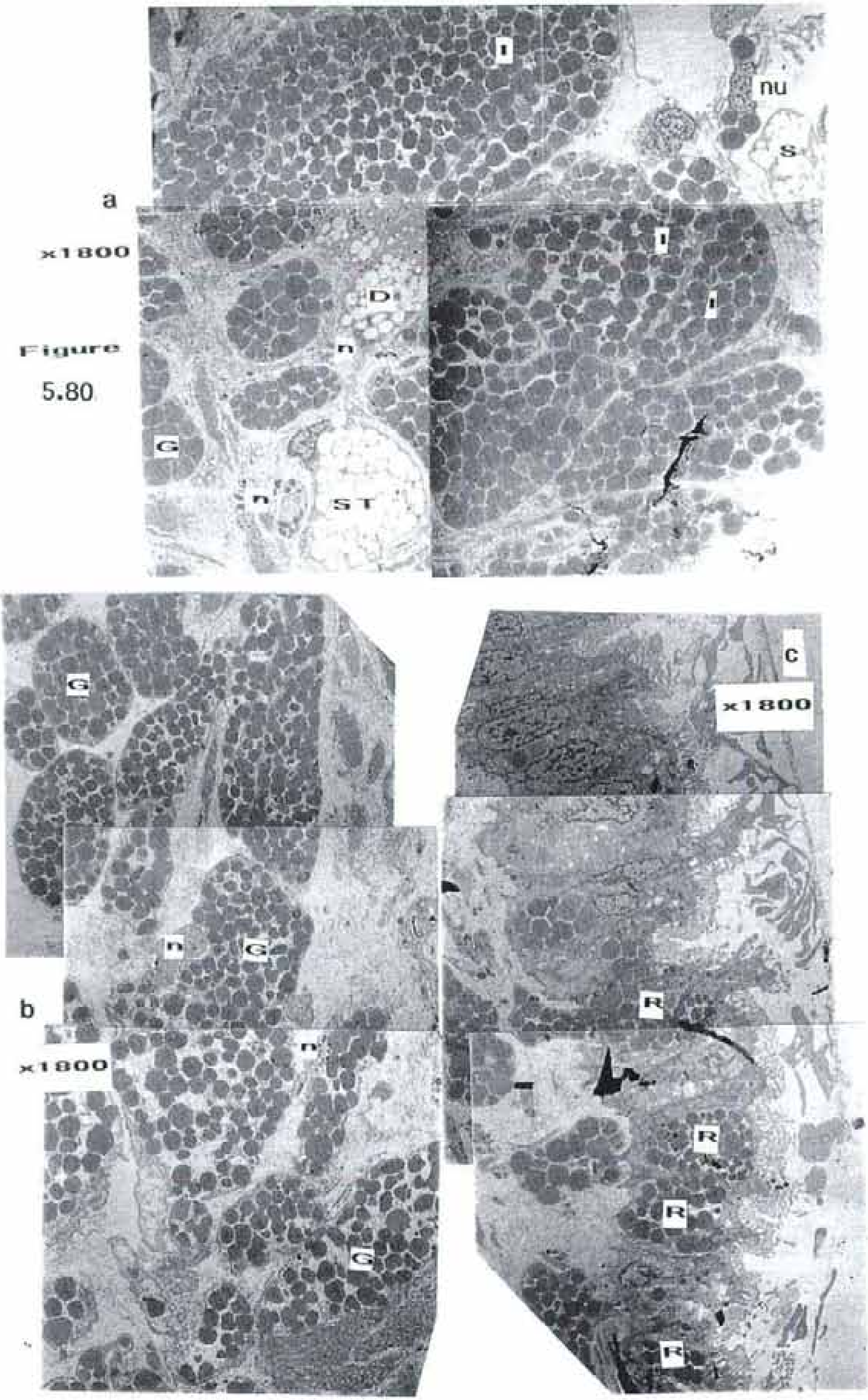
a
x1800
Figure
5.80
I
nu
S
I
I
D
n
G
n
ST
G
n
G
b
x1800
n
G
c
x1800
R
R
R
R

5.5.1.9.25. The F2. Ramis of the Circum-pallial Nerve.

The F2. Ramis of the Circum-pallial Nerve sends branches to the secretory structures themselves as well as the musculature of Fold F2.. Branches of the nerve lie contiguous with the plasmalemma of the secretory Glands (Figure 5.81. a).

There are three distinct types of neurosecretory granules seen in these nerves. The rounded neuro-secretory granules (R in Figure 5.81. a and b) appear to be concentrated in nerves associated with Granular Cytoplasm Secretory Glands (G in Figure 5.81. a).

Concentrations of very small granules. (s in Figure 5.81. c). and ovoid granules. (0 in Figure 5.81. c). occur in discrete bundles of nerve fibres in the main trunk of the F2. Ramis. (Figure 5.81. c).

FIGURE 5.81. *Pinctada maxima* F2. Ramis of Circum-pallial Nerve. Anterior Periphery.

a. T.E.M. x 7000 Nerve and secretory gland.

b. T.E.M. x 7000 Neurosecretory granules in a discrete. membrane bound part of the F2. Ramis.

c. T.E.M. x 7000 Morphologically different neurosecretory granules in separate discrete bundles of nerve fibres in the F2. Ramis.

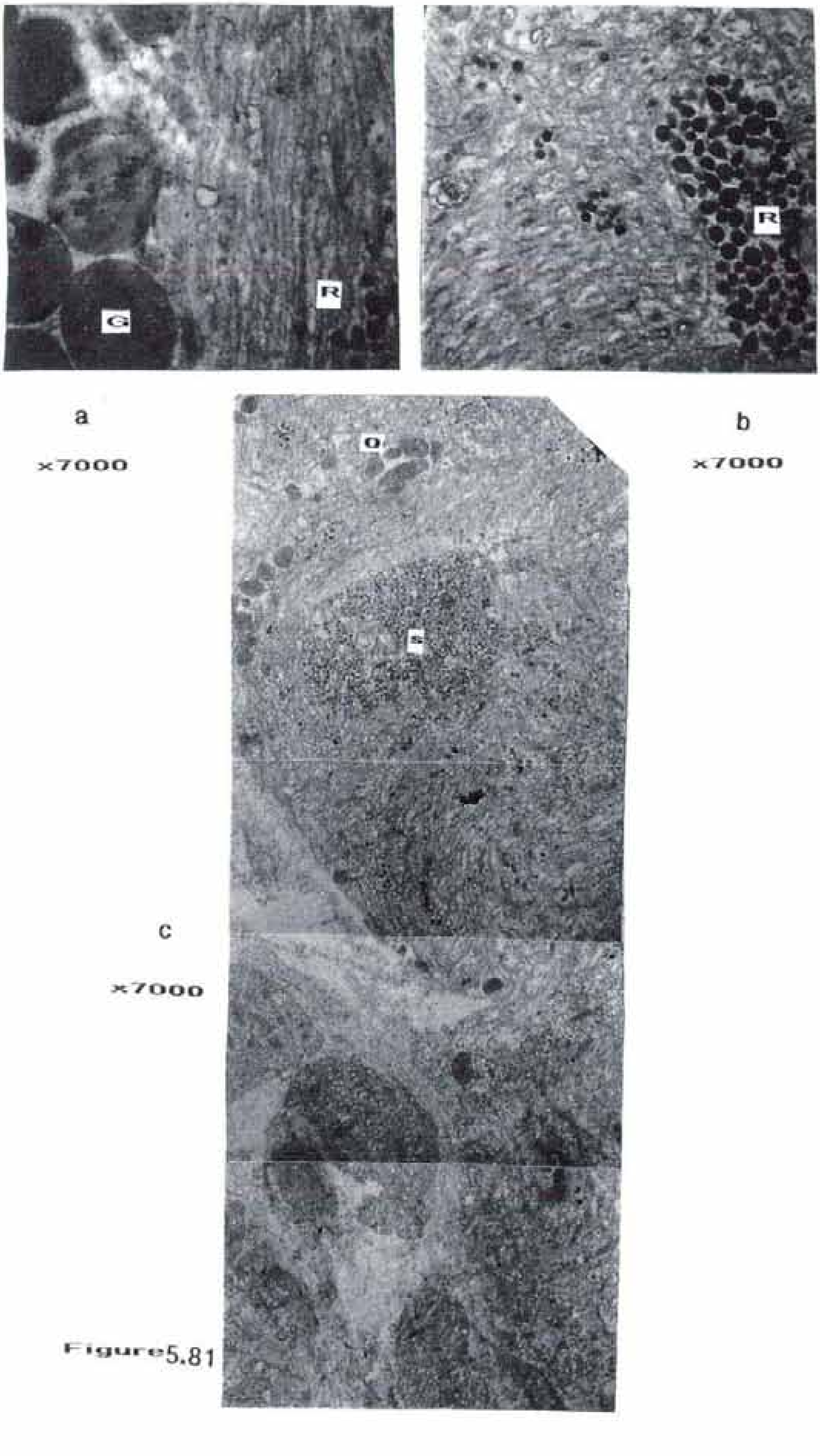

a ×7000

b ×7000

c ×7000

Figure5.81